

Mechanisms determining species succession and
dominance during an iron-induced phytoplankton bloom
in the Southern Ocean (LOHAFEX)

DISSERTATION

zur Erlangung des akademischen Grades
eines Doktors der Naturwissenschaften

(Dr. rer. nat.)

am Fachbereich Biologie/Chemie
der Universität Bremen

vorgelegt von

Isabelle Katharina Schulz

Bremen, September 2013



1. Gutachter: Prof. Dr. Victor Smetacek, Alfred Wegener Institut Helmholtz Zentrum für Polar- und Meeresforschung, Bremerhaven
2. Gutachter: Prof. Dr. Kai Bischof, Universität Bremen

“Das Prinzip aller Dinge ist Wasser, aus Wasser ist alles, und ins Wasser kehrt alles zurück.”

Thales von Milet

Abstract

To improve the understanding of population dynamics of organisms, it is necessary to examine organisms under natural conditions. Only at such conditions, knowledge about their *in situ* use of resources, predator-prey interactions and loss rates can be obtained. It is possible to examine and understand these processes with controlled ocean iron fertilization experiments, which stimulate the growth of unicellular algae. This thesis provides a comprehensive description of the reactions and vertical distribution of the main components of the pelagic ecosystem and highlights the food-web interactions of individual organisms, which characterize this habitat.

The response of the plankton community to iron addition was successfully observed during the Indo-German iron fertilisation experiment LOHAFEX (LOHA is hindi and means iron, FEX stands for fertilisation experiment) carried out in the Southern Ocean from January to March in 2009 lasting for 38 days. The iron-induced bloom was achieved in the closed core of a mesoscale eddy. The aim of the experiment was to study the growth and demise of the phytoplankton bloom and to examine whether the biomass is retained in the surface layers through recycling processes or whether biomass sinks out to the deep ocean.

The fertilized patch was characterized by low silicic acid concentrations, which is an essential nutrient for diatoms, hence a flagellate-bloom developed with cells $< 20 \mu\text{m}$ in size. The bloom remained stable over the course of the experiment. This was verified by microscopic analysis and molecular methods. The main reason for the lack of large scale biomass increase, was the strong grazing pressure by the large copepod population, consisting primarily of *Calanus simillimus* and *Oithona similis*. Incubation experiments proved that copepods increased their grazing rates and fecal pellet production within the patch. Neutrally buoyant PELAGRA traps were deployed to quantify the export fluxes. These contained a few diatoms and fecal pellets and were dominated by unicellular plankton like dinoflagellates, flagellates and coccoid cells. Hence fertilizing this type of plankton community did not increase the vertical flux. This lead to the hypothesis that the system was influenced by recycling processes in surface layers.

The protozoan community and its vertical distribution was an important part of this work and was studied by focussing on key heterotrophic organisms. These included

thecate dinoflagellates, loricate and aloricate ciliates, foraminifera, radiolarians, and juvenile and adult copepods. Again, the high grazing pressure by the copepods controlled the development of the protozoan community, and the copepod fecal pellets contained large amounts of damaged and empty loricae, but also foraminifera, which are usually not a preferred food item for copepods. This indicated that the copepods were food limited and resorted to large, armoured protozoans which they might have otherwise avoided. Dinoflagellates were mainly abundant at depths below 100 m, possibly this distribution pattern was caused by an escape response in order to avoid predators and to feed on the flux of larger particles which generally peaks at those depths.

In conclusion, the plankton community during LOHAFEX was top-down controlled whereby a highly efficient retention type system prevailed, which resulted in low particle export fluxes.

Zusammenfassung

Um das Verständnis der Populationsdynamik von Organismen zu vertiefen, ist es erforderlich Organismen unter natürlichen Bedingungen zu untersuchen. Nur unter diesen Bedingungen kann Kenntnis über ihre *in situ* Ressourcennutzung, die Räuber-Beute Beziehungen und über Verlustraten gewonnen werden. Mittels kontrollierter Eisendüngungsexperimente im Ozean, die das Wachstum von einzelligen Algen anregt, ist es möglich diese Prozesse im Meer zu untersuchen und besser zu verstehen. Diese Dissertation liefert eine umfassende Beschreibung der Reaktionen und Vertikalverteilung der Hauptkomponenten des pelagischen Ökosystems und hebt die Nahrungsnetzinteraktionen der einzelnen Organismen hervor, die diesen Lebensraum charakterisieren.

Während des indisch-deutschen Eisendüngungsexperimentes LOHAFEX, („LOHA“ ist das Hindi-Wort für Eisen und „Fex“ ist englisch und steht für ‚fertilization experiment‘) wurde die Reaktion der Planktongemeinschaft auf Eisendüngung erfolgreich über 38 Tage von Januar-März 2009 im südlichen Ozean verfolgt. Die eiseninduzierte Blüte wurde im Kern eines stabilen mesoskaligen Ozeanwirbels hervorgerufen. Das Ziel des Experiments war es, das Wachstum und den Niedergang der Phytoplanktonblüte zu studieren und zu prüfen, ob die Biomasse in den Oberflächenschichten durch Recyclingprozesse erhalten bleibt oder ob Biomasse in die Tiefsee herabsinkt.

Der gedüngte Fleck war charakterisiert durch geringe Kieselsäure Konzentrationen, ein essentieller Nährstoff für Diatomeen, somit entwickelte sich eine Flagellaten-Blüte mit Zellen $< 20 \mu\text{m}$, die über den Verlauf des Experimentes, sowohl qualitativ als auch quantitativ konstant blieb. Dies wurde mittels mikroskopischer Analysen und molekularer Methoden verifiziert. Es konnte keine Biomasse im größerem Umfang aufgebaut werden. Der Hauptgrund dafür lag an dem starken Fraßdruck der großen Copepoden-Population, vorrangig bestehend aus *Calanus simillimus* und *Oithona similis*. Inkubations-Experimente zeigten, dass die Copepoden ihre Fraß- und Kotballenproduktionsraten innerhalb des Flecks erhöhten. Dichte-neutrale PELAGRA-Fallen wurden ausgesetzt, um den Exportfluss zu bestimmen. Diese enthielten wenige Diatomeen und Kotballen auf, stattdessen dominierte unizelluläres Plankton wie Dinoflagellaten, Flagellaten und coccoiden Zellen. Folglich erhöhte die

Düngung dieser Planktongesellschaft nicht den Vertikalfluss. Dies führte zu der Hypothese, dass das System durch Recyclingprozesse in der Oberflächenschicht bestimmt wurde.

Die Protozoengemeinschaft und deren Vertikalverteilung war ein weiterer wichtiger Bestandteil dieser Arbeit und wurde anhand wichtiger heterotropher Organismengruppen untersucht. Dazu gehörten thekate and athekate Dinoflagellaten, loricate and aloricate Ciliaten, Foraminiferen, Radiolarien sowie juvenile und adulte Copepoden kleiner Arten. Auch hier kontrollierte der hohe Fraßdruck der Copepoden die Protozoengemeinschaft, denn in deren Kotballen wurden viele zerdrückte leere Tintinnen gesehen, aber auch Foraminiferen, die eigentlich keine bevorzugte Beute von Copepoden darstellen. Dies deutete darauf hin, dass Copepoden nahrungsimitiert waren und auf die großen Protozoen als Nahrungsquelle zurückgreifen mussten, welche sie normalerweise gemieden hätten. Dinoflagellaten waren hauptsächlich in den Tiefen ab 100 m zu finden, um ihren Prädatoren zu entkommen und um sich von herabsinkenden Partikeln zu ernähren, welche allgemein in diesen Tiefen ihren Höchstwert erreichen.

Zusammenfassend lässt sich sagen, dass die Planktongemeinschaft während LOHAFEX von Prädatoren kontrolliert wurde und eng gekoppelt war mit dem mikrobiellen Kreislauf, welcher den partikulären Export reduziert hat.

Abbreviations

^{234}Th	Isotope of Thorium
AABW	Antarctic Bottom Water
ACC	Antarctic Circumpolar Current
Ba	Barium
BF	Broken Frustules
C	Carbon
CaCO_3	Calcium Carbonate
CDW	Circumpolar Deep Water
CH_4	Methane
Chl <i>a</i>	Chlorophyll a
CIW	Central Intermediate Water
CO_2	Carbon Dioxide
CTD	Conductivity, Temperature, Depth
DIC	Dissolved Inorganic Carbon
DMS	Dimethylsulfide
DMSP	Dimethylsulfoniopropionate
DOM	Dissolved Organic Matter
DOM C	Dome Concordia
EIFEX	European Iron Fertilization Experiment
EisenEx	Eisen' is the German word for iron, Experiment
EPICA	European Project for Ice Corring in Antarctica
Fe	Iron
FeeP	Iron and Phosphate fertilization experiment
FeSO_4	Iron (II) Sulphate
Fm	Maximum Fluorescence
Fv	Variable Fluorescence
GPS	Global Positioning System
Gt	Gigatonne
H_2O	Water
HNLC	High-Nutrients-Low-Chlorophyll
IronEx I+II	Iron Experiment I+II
kyr	Thousand years
LGM	Last Glacial Maximum
LOHAFEX	LOHA (hindi) = Iron fertilization Experiment
N	Nitrogen
N_2O	Nitrous Oxide
$\text{Na}_2\text{S}_2\text{O}_3$	Sodium Thiosulphate
NADW	North Atlantic Deep Water
NBST's	Neutrally Buoyant Sediment Traps
OIF	Ocean Iron Fertilization
OM	Organic Matter
P	Phosphate
PA	Polyacrylamide

Abbreviations

pCO ₂	Partial Pressure Carbon Dioxide
PF	Polar Front
Pg	Petagram
pH	negative logarithm of the activity of the hydronium ion
POC	Particulate Organic Carbon
POM	Particulate Organic Matter
ppm	Parts per million
ppmv	Parts per million volume
SACCF	Southern Antarctic Circumpolar Current Front
SAF	Subantarctic Front
SEEDS I+II	Subarctic Pacific Iron Experiment for Ecosystem Dynamics Study
SERIES	Subarctic Ecosystem Response Iron enrichment Study
SF ₆	Sulfurhexafluoride
Si	Silica
SO	Southern Ocean
SOFEX-N/S	Southern Ocean Iron Experiment North and South
SOIREE	Southern Ocean Iron Release Experiment
SOLAS - SAGE	Surface-Ocean Lower-Atmosphere Studies Sea-Air Gas Exchange
Sr	Strontium
SrCl ₂	Strontium Chloride
SrSO ₄	Strontium Sulfate
TEP	Transparent Exopolymeric Particles
WML	Wind Mixed Layer
yr	Year
δD	Delta Deuterium

Index

Abstract.....	VII
Zusammenfassung	IX
Abbreviations	XI
1. Introduction.....	10
1.1 Setting the Scene	10
1.2 The Marine Carbon Cycle	12
1.3 Hydrography of the Southern Ocean	15
1.4 Southern Ocean Ecology	17
1.5 Marine Protist Plankton	20
1.6 Ocean Iron Fertilization	28
1.6.1 Importance of OIF experiments.....	28
1.6.2 OIF experiments.....	28
1.6.3 Natural Iron Fertilization.....	35
2. Objectives	36
3. Methods.....	38
3.1 Sampling site.....	38
3.2. Plankton sampling.....	39
3.3. Quantitative plankton analyses.....	40
3.4. Counting procedure.....	41
3.5. Biomass determination	41
4. Manuscripts	43
4.1 Manuscript Outline	43
Manuscript I	46
Manuscript II.....	102
Manuscript III	138
Manuscript IV.....	186
Manuscript V	224
6. Synthesis	270
7. Conclusions	274
8. Outlook.....	275
References	276
Acknowledgements	289

1. Introduction

1.1 Setting the Scene

Ice cores have been used to measure past atmospheric carbon dioxide (CO_2) concentrations. This led to the important realization that present global atmospheric CO_2 levels of 400 parts per million (ppm) are higher than during the last 650 thousand years (kyr). Furthermore, it was revealed that during this time period, atmospheric CO_2 concentrations showed cyclic changes between two extremes: they were lowest during glacial periods (180 ppm) and highest during interglacial periods (280 ppm) (Petit et al, 1999).

Two collaborative Antarctic drilling projects have contributed most to the understanding of past climate cycles. One of them was drilled in 1998 at the Russian research station “Vostock” providing a record of past environmental conditions over the last 420,000 years, revealing 4 glacial cycles (Petit et al., 1997, 1999). In 2004 the second major core, EPICA (European Project for Ice Coring in Antarctica) was drilled at Dome Concordia (Dome C), revealing 8 previous glacial cycles.

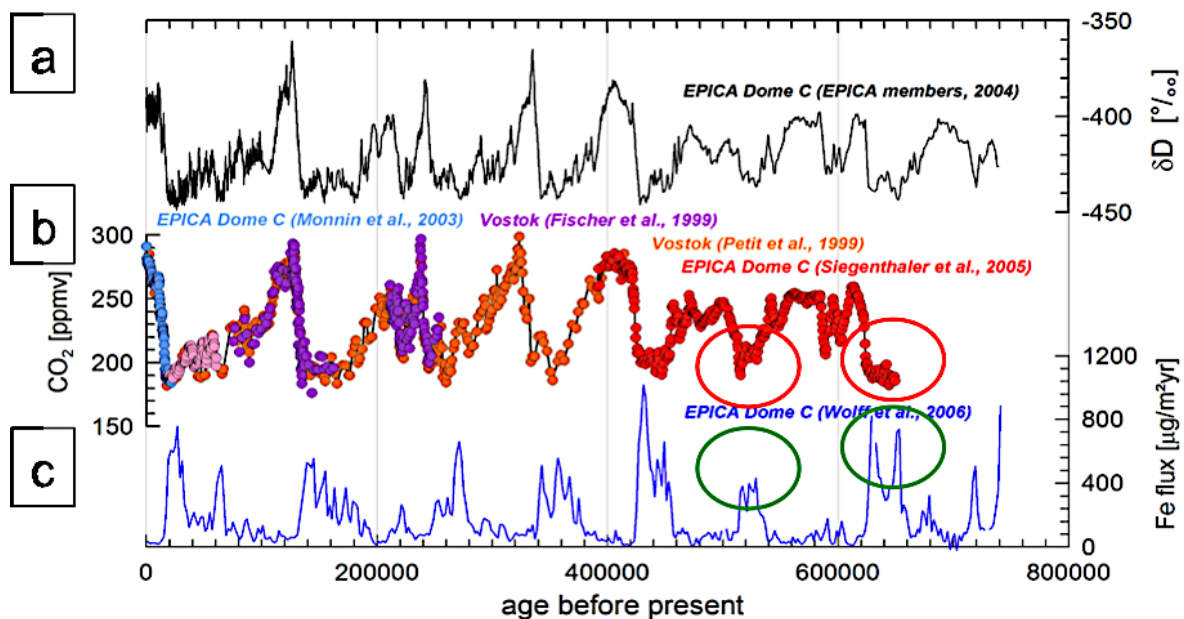


Fig. 1: Vostok and EPICA ice core measurements of **a.** Deuterium profile (δD ‰), a proxy for temperature, (high δD values indicate high temperature) **b.** atmospheric concentrations of Carbon dioxide in parts per million by volume (ppmv) and **c.** iron flux ($\mu\text{g}/\text{m}^2/\text{yr}$) indicating the clear correlation of carbon dioxide and temperature and anticorrelation of iron flux (green circles) and carbon dioxide (red circles), (with permission to use the graph: © Dr. Hubertus Fischer).

1. Introduction

The results of the ice core analyses demonstrate clearly the relationship between climate and CO₂ (Siegenthaler et al., 2005). As can be seen in Figure 1, past changes in atmospheric CO₂ concentration were accompanied by changes in mineral aerosols (dust) composition (De Angelis et al., 1987). It can be generalized, that during high dust fluxes (Fig. 1 depicts iron (Fe) in blue), atmospheric CO₂ concentrations were lower (view red and green circles in Fig. 1). Mineral dust plays a key role in marine ecosystems (Hutchins and Bruland et al., 1998) as it provides essential nutrients like Fe, which are often the limiting factor for marine primary producers (Martin and Fitzwater, 1988). During the last glacial maximum (LGM) the dust input was enhanced (Fig. 1 green circles), which reflects the enhanced dustiness of the atmosphere. The primary cause for this was an increase in arid areas accompanied by higher wind speeds (Petit et al. 1999; Sarinthein, 1987). Martin (1990) argued that the higher input of iron-rich dust to iron limited oceanic regions during glacial times must have stimulated photosynthesis of algae, which led to the drawdown of atmospheric CO₂ levels. This effect is defined as natural iron fertilization. Today's atmosphere is more humid, has more vegetation on land and weaker winds, which in sum, prevents dust-input into the ocean.

1.2 The Marine Carbon Cycle

Carbon dioxide is exchanged among the biosphere, geosphere, hydrosphere and atmosphere of the Earth. The carbon cycle describes the exchange of carbon, the incomes and losses, the recycling and re-use throughout the biosphere. Various chemical, physical, geological and biological processes are the driving forces of the cycle.

The ocean covers 71 % of the Earth's surface and plays an integral role in the Earth's climate and weather. With a total volume of about 1.3 billion cubic kilometres, the ocean has a great carbon and heat storage capacity. Approximately 38400 Gt of carbon are stored in the ocean (Falkowski et al., 2000), which is about 16 times more than in the terrestrial biosphere and 50 fold higher than in the atmosphere. Consequently the oceans play a prominent role in the global carbon cycle. The exchange of carbon between the surface and the deep ocean is controlled by the physical and biological carbon pumps (Volk and Hoffert, 1985).

The physical carbon pump describes the vertical carbon flux resulting from differences in CO₂ solubility at warm and cold temperatures. At high latitudes, surface water is cooled and salinity increases due to sea-ice formation. The high density of these water masses leads to sinking of cold-water masses, mainly in the North Atlantic and around Antarctica. These cold and dense water masses are rich in carbon and carry it into the deep ocean, because solubility of CO₂ is higher at low temperatures. In upwelling regions at lower latitudes, where dense, cooler, and usually nutrient-rich water moves towards the ocean surface, water is warming up and CO₂ is released again (Fig. 2) (Volk and Hoffert, 1985).

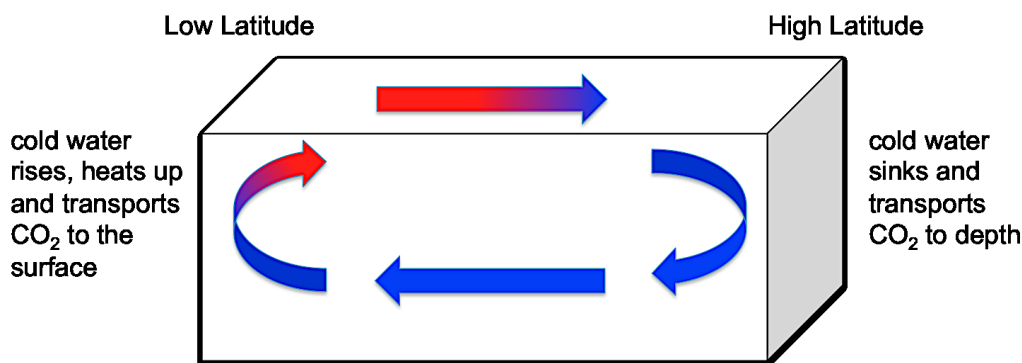


Fig. 2: Schematic drawing of the concept of vertical deep mixing. Warm surface water is advected to high latitudes, where it cools and sinks as North Atlantic Deep Water (NADW) in the North Atlantic and Antarctic Bottom Water (AABW) in the Southern Ocean. (adapted from: source: http://earthguide.ucsd.edu/virtualmuseum/climatechange1/06_1.shtml)

1. Introduction

The biological carbon pump, differentiated into the organic and carbonate pump, comprises a complex set of biologically mediated processes, including fixation of dissolved inorganic carbon (DIC) into biogenic matter, its subsequent sinking, remineralisation and/or dissolution (Volk & Hoffert, 1985).

The main driver of the biological pump is phytoplankton representing the marine photosynthetic community of protists, which fix DIC and convert it into biogenic compounds, causing a drawdown of CO₂ from the atmosphere into the ocean. The produced biomass can either be fed into the marine food web to higher trophic levels or forms aggregates, which sink out (Fig. 3). The organic material is then part of the production and recycling system of carbon in the water column. It can be converted into dissolved organic or particulate organic matter (DOM or POM) by excretion of transparent exopolymeric particles (TEP), viral lysis, bacterial interactions, sloppy feeding by zooplankton or faecal pellets. Zooplankton and microorganisms remineralize the majority of the particulate organic carbon (POC). Only a small amount of POC is exported to depth (1-3 %; De La Rocha and Passow, 2007). These interactions cause a vertical depth gradient of DIC and promote a continuous CO₂ uptake from the atmosphere (Broecker and Peng, 1982). The biological pumps are responsible for 75 % of the vertical DIC gradient (Sarmiento et al., 1995).

However, while the biological carbon pump tends to decrease CO₂ in surface water, the carbonate pump has the opposite effect. The carbonate pump, also termed carbonate counter pump, describes the production and sinking of calcium carbonate (CaCO₃) by calcifying organisms and releases CO₂ into the water. This counterintuitive effect is caused by the consumption of DIC as well as total alkalinity during the process of calcification (Zeebe and Wolf-Gladrow, 2007). The relative strengths of the two biological pumps is expressed in the rain ratio (POC export: CaCO₃ export) which determines the flux of CO₂ between surface ocean and atmosphere. According to a model study, switching off all biological production in the ocean would double atmospheric CO₂ (Maier-Reimer et al., 1996). This emphasises the role of the biological carbon pumps in influencing atmospheric CO₂ levels. Biological activity influences the climate by driving many of the global elemental cycles. Lovelock (1979, 2003) suggested in his Gaia-hypothesis that feedback-effects might mitigate, amplify or contribute to stabilize the climate. Therefore it is essential to gain a better understanding of the regulating factors of the biological pump and to study its interactions. Ocean Iron Fertilization (OIF) experiments provide a powerful tool to deepen our understanding of the biological carbon pump and will be further described in introduction-chapter No. 1.6.

1. Introduction

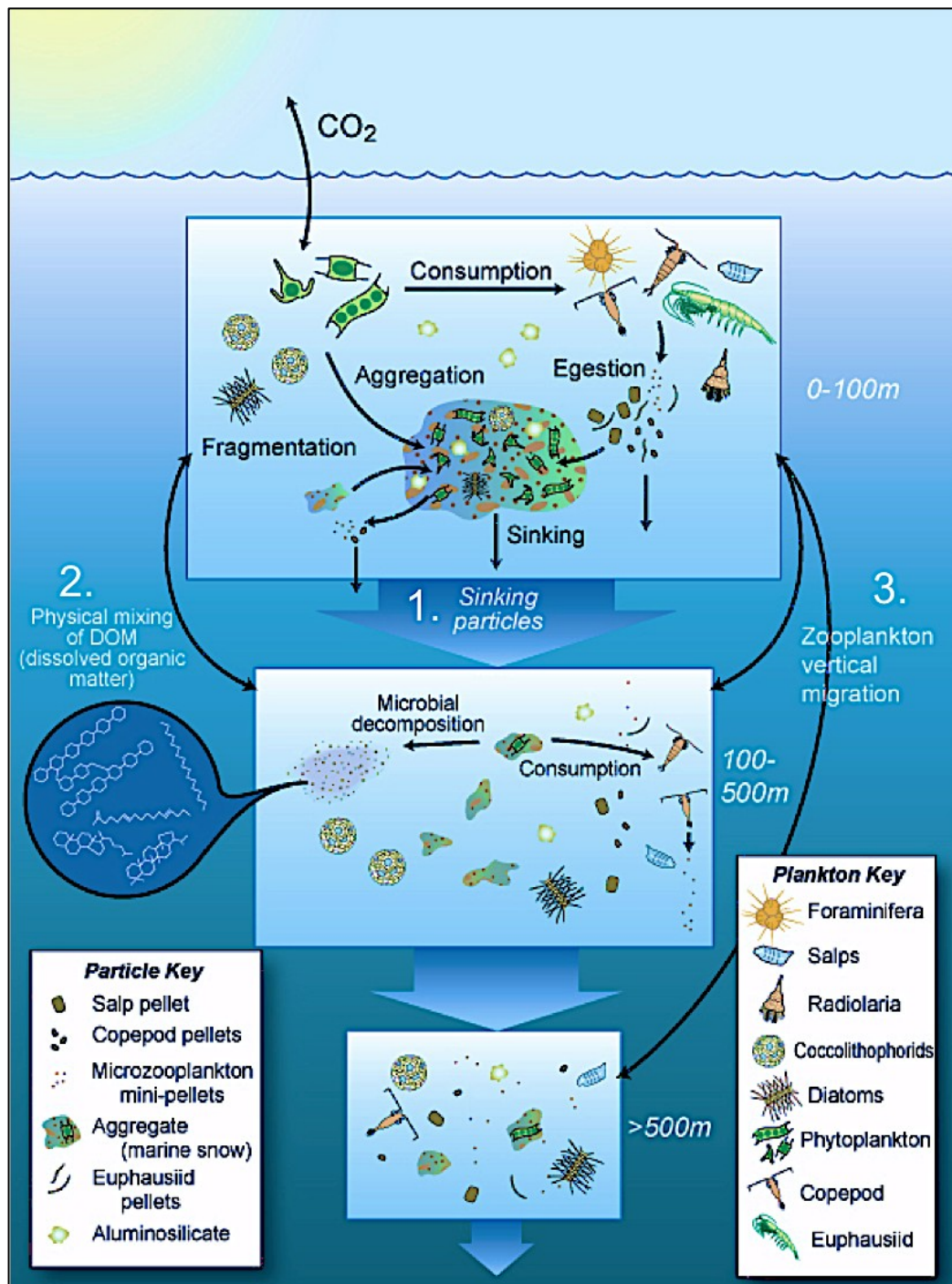


Fig. 3: A simplified view of the biological pump: carbon dioxide is fixed by phytoplankton in the surface mixed layer and transported via three major processes: 1. Passive sinking of particulate and dissolved organic matter (POM & DOM), 2. Physical mixing of POM and DOM 3. Active transport by zooplankton vertical migration and their subsequent decomposition by bacteria or consumption by detritophages in deeper layers. (source: K. Busseler & J. Cook; <http://cafethorium.who.edu/website/projects/tzex.html>, with permission to use)

1.3 Hydrography of the Southern Ocean

The Southern Ocean (SO), surrounding the Antarctic continent, extends from the coast to 50 degrees southern latitude. It contains the strongest ocean flow, the Antarctic Circumpolar Current (ACC), which combines the southern sectors of the Atlantic, Indian and Pacific Ocean. The ACC flows eastward around the Antarctica and is driven by westerly winds (Whitworth, 1983; Whitworth and Peterson, 1985). Most of its transport is concentrated in frontal jets (Orsi et al., 1995). The number, strength and latitudinal locations of these jets are influenced by the bathymetry (Pollard et al., 2002). From north to south, the main frontal systems in the Southern Ocean are the Subantarctic Front (SAF), the Polar Front (PF), the Southern ACC Front (SACCF) and the southern boundary of the ACC all extending from the surface to the sea floor (Orsi et al., 1995).

The Polar front (also Antarctic Convergence), forms the borderline between the SAF and SACCF, where cold waters of the ACC mix with warmer waters form the Sub-Antarctic. The Antarctic divergence is a region of upwelling and is formed where surface waters diverge between westward-flowing surface waters near the Antarctic continent and eastward-flowing waters, further away from the continent (e.g Orsi et al., 1995). The Weddell Gyre and the Ross Gyre south of the ACC are two upwelling regions with Circumpolar Deep Water (CDW) as predominant water mass. The subsurface of the Weddell Gyre is formed by the Central Intermediate Water (CIW), which is characterised by a depletion of oxygen, enrichment of nutrients and a maximum in DIC resulting from shallow remineralisation of export production (Whitworth and Nowlin, 1987; Hoppema et al., 1997; Hoppema, 2004) (Fig. 4). Natural carbon sequestration happens when the CIW leaves the Weddell Gyre to the north, carrying DIC to abyssal depths (Hoppema, 2004). Antarctic Bottom Water (AABW) is formed when dense shelf water, formed by heat loss and brine rejection during sea-ice formation, moves down the continental slope into the abyssal sea. This process occurs only in few shelf regions in the Southern Ocean, including the western Weddell Sea, Ross Sea and off Adélie Land (e.g Huhn et al., 2008; Foldvik, 2004; Rintoul, 1998; Gordon et al., 2009) and transports carbon to abyssal depths and sequesters it for the time scale of the ocean's overturning circulation.

The development of stable eddies is another characteristic of the ACC. Due to meanders and waves, which form and propagate along the ACC (Legechi, 1977, Sciermammano 1989), cold or warm eddies (Joyce & Patterson 1977), variable in size and duration can evolve. These eddies are characterised by a vertically coherent water mass from the surface to the bottom and are 30-100 km wide with approximate surface velocities of 30 cm s^{-1} . The closed core of

1. Introduction

a mesoscale eddy was chosen as the experimental site for LOHAFEX and two previous artificial OIF experiments (EisenEx and EIFEX, view section 1.6.2) because it provides vertical coherence between surface and deeper water layers.

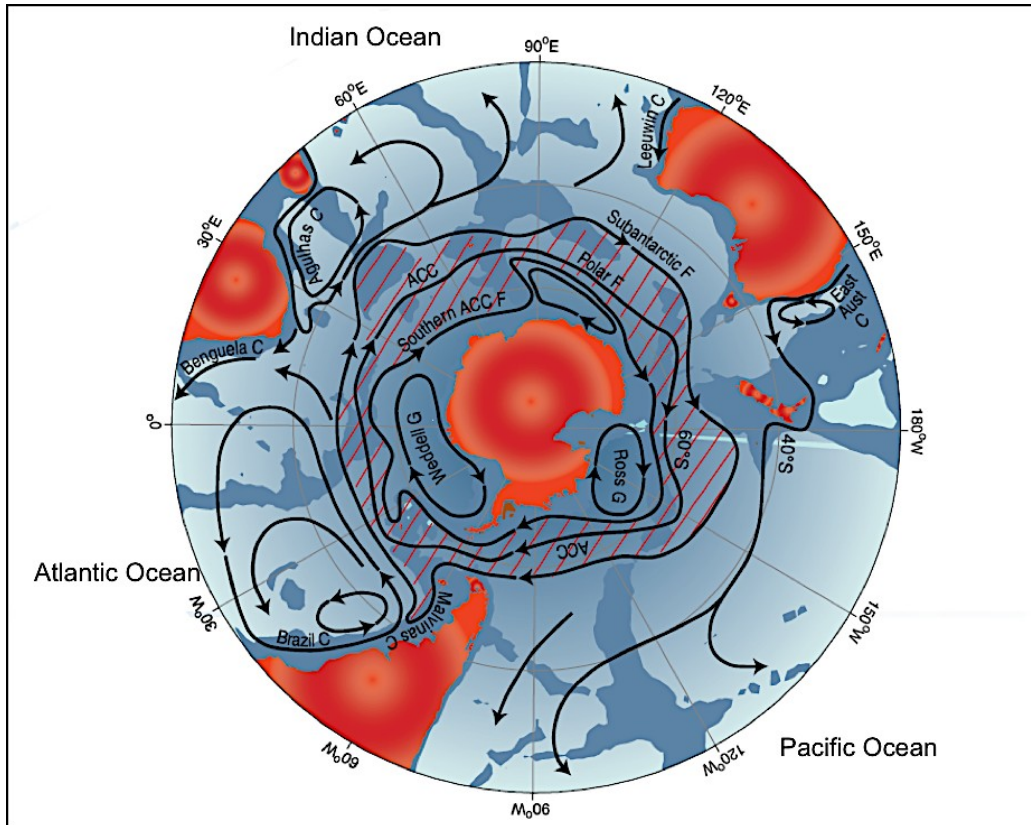


Fig. 4: The Southern Ocean currents: Antarctic circumpolar current (ACC), the Polar Front (PolarF or PF), the Subantarctic Front (Subantarctic F or SAF) and the Weddell and Ross Gyre (Weddel G, Ross G). (source: <http://takvera.blogspot.de/2011/12/ocean-acidification-warning-to-climate.html>)

1.4 Southern Ocean Ecology

Phytoplankton production in the SO is relatively low even though surface nutrients (nitrogen (N), phosphate (P) and silicate (Si)) concentrations are high (Chisholm and Morel, 1991). The inefficient utilisation of N and P is due to the low productivity of phytoplankton. These regions are defined as High-Nutrients-Low-Chlorophyll (HNLC) areas. They cover 25 % of the world's ocean and beside the SO, which is the largest, they can be found in the Equatorial Pacific and in the subarctic North East Pacific off the coast of Alaska (Chavez and Barber 1987; Martin et al., 1994; Chavez et al., 1996; Boyd et al., 1998; 2000). In these areas, the phytoplankton community is numerically dominated by pico- and nanoplankton. Several factors have been discussed to explain the low productivity. One explanation is based on the top-down control by zooplankton. It is proposed that zooplankton and protozoan grazing prevents the build up of phytoplankton biomass. Smetacek et al., (1990) described the Antarctic ecosystem as a “retention type system” in which relatively high abundances of zooplankton are sustained in an ecosystem despite low phytoplankton biomass. The key factor is that the bulk of zooplankton faeces are recycled in the surface layer, despite their relatively high sinking rates, hence providing the essential nutrients for phytoplankton growth (Gonzalez, 1992).

Another explanation is the bottom-up controlled system, in which phytoplankton growth is governed by resource availability. Iron for example is indispensable in many key enzyme systems e.g chlorophyll synthesis, nitrate utilisation, redox systems, which are involved in the biochemical processes of photosynthesis and carbon fixation (Geider and LaRoche, 1994). It is considered the most important trace metal for algal growth (Scharek et al., 1997). Iron concentrations in open oceans are orders of magnitude lower than levels in coastal waters hence representing the limiting nutrient for phytoplankton growth (Sunda & Huntsman, 1995). It has been suggested that low iron concentrations and other trace elements might affect mainly larger phytoplankton species, especially diatoms, explaining the predominance of smaller cells (nanoplankton), which preferentially take up regenerated nitrogen (Martin et al., 1991; Buma et al., 1991). Another prerequisite for photosynthesis is light. Deep mixing reduces the amount of light available for phytoplankton growth and hence limits phytoplankton productivity. To sum up, while grazing may exert an effect on biomass accumulation, iron and light limitation controls phytoplankton growth.

However, some regions in the SO e.g. near the ice-edge, where iron is released e.g. through ice-berg melting, support phytoplankton blooms and promote productivity of higher trophic

1. Introduction

levels (Sullivan et al., 1993; Holm-Hansen et al., 2004). If sedimentation rates exceed remineralisation rates, the end of a bloom can result in transport of organic matter (OM) to deeper water masses and even carbon export to the deep sea (Smetacek, 1985; Smetacek et al., 2012).

Another characteristic of the SO is the occurrence of large robust diatom species, albeit at low concentrations. These species of the iron-depleted system are, compared to the species in productive coastal waters, larger and have thicker frustules or robust spines (Hasle & Syverstsen, 1996). The silica to nitrogen (Si:N) ratio in iron-deficient diatoms is above 2 as compared to iron-sufficient diatoms which is around 1 (Takeda, 1998; Hutchins & Bruland, 1998). Once the diatom perished, the silica frustule either dissolves while sinking out enriching silicate concentrations in the deep ocean, or accumulate as diatom ooze in the sediments underlying the Southern Ocean. The latter process is responsible for the opal belt, the largest single silica sink, surrounding the Antarctic continent (Falkowski et al., 1998; Tréguer et al., 1995). Diatoms of the ACC are highly dependent on the recycling efficiency of the microbial community making iron bioavailable to them. However adequate iron supply may also result from wind-blown dust (Gao et al., 2001; Erickson et al., 2003) and from snow-deposited dust released by ice-berg melting (Raiswell et al., 2008). The influence of Patagonian dust (view circle in Fig. 5) can be seen in satellite images showing increased Chlorophyll *a* (Chl *a*) values, which are a measure for phytoplankton productivity.

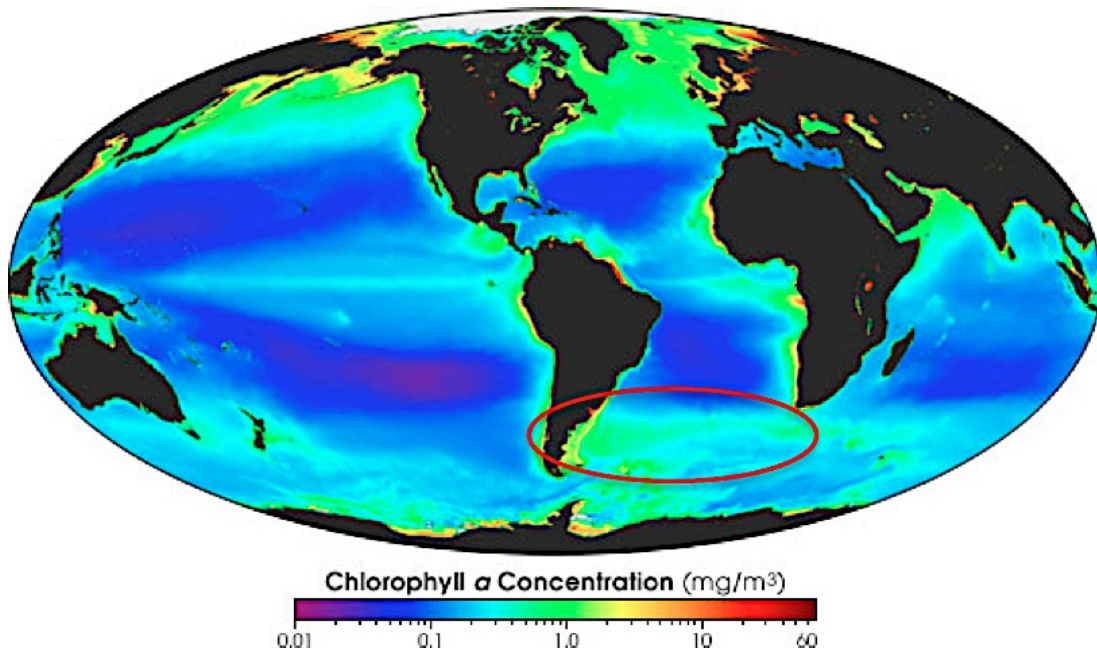


Fig. 5: Average global ocean chlorophyll (Chl *a*) concentration, a measure of productivity, in milligrams per cubic meter of seawater, measured by SeaWiFS (Sea-viewing Wide Field-of-View Sensor). Chl *a* concentrations are higher in coastal areas compared to the open ocean. Note the increased Chl *a* concentrations from South America (encircled) along the ACC, most likely due to Patagonian dust input.
(source: <http://earthobservatory.nasa.gov/IOTD/view.php?id=4097>).

1.5 Marine Protist Plankton

Marine primary productivity contributes 45 to 50 Petagram (Pg) Carbon (C) a⁻¹ to the global primary productivity (Falkowski et al., 1998; Field et al., 1998) and rivals the contribution of terrestrial primary production (56.4 Pg C a⁻¹) (Field et al., 1998). However, phytoplankton account for less than 1 % of plant biomass on earth, illustrating the much higher turn-over rates in planktonic as compared to terrestrial ecosystems (Field et al., 1998). Indeed, for most of the year heterotrophic biomass exceeds that of autotrophs in the plankton, except during blooms. These blooms occur when growth rates exceed mortality rates and are generally dominated by a single or a few phytoplankton species of the following taxa: diatoms, dinoflagellates, the coccolithophore *Emiliana huxleyi* or colony-forming species of the haptophyte *Phaeocystis* (Irigoyen et al., 2004). During these blooms, cells accumulate in the water column until a limiting factor usually the limiting nutrient or increased grazing pressure suppresses further biomass

built-up. Another important component of planktonic ecosystems is the microbial loop or network. In 1983 Azam et al., introduced the concept of the microbial loop referring to the trophic interactions between pico-, nano- and microplankton. On a seasonal basis the microbial network is more persistent compared to bloom-forming species. The microbial network comprises procaryotes, small autotrophic and heterotrophic flagellates (< 20 μm), larger protozoa (in particular ciliates and dinoflagellates) and their crustacean grazers (in

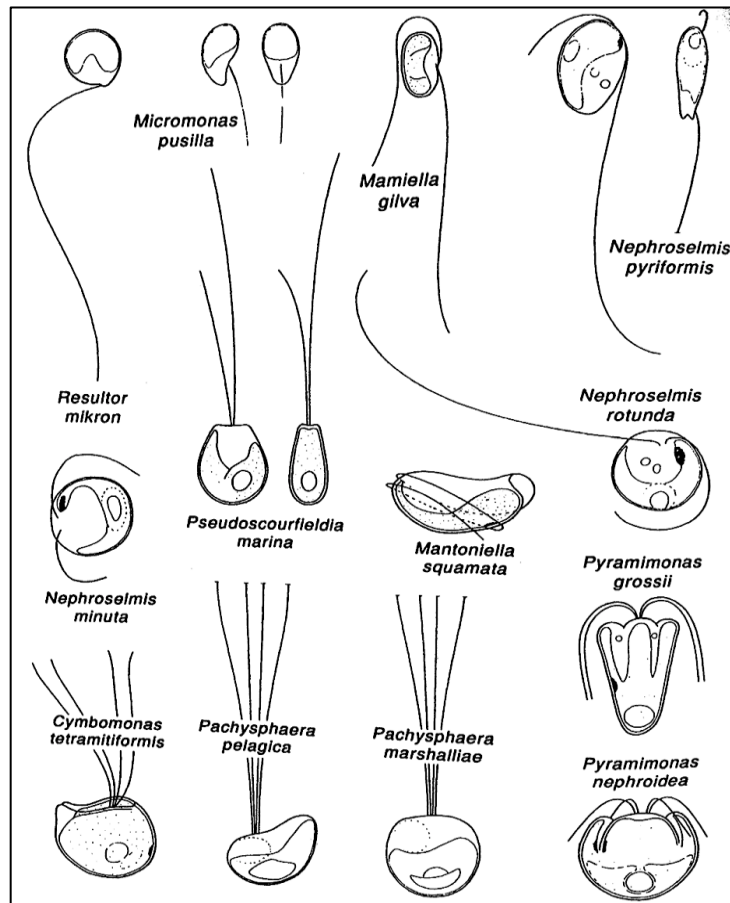


Fig. 6: Schematic drawing of flagellates adopted from Carmelo R. Tomas "Identifying marine Phytoplankton" (1997). © Elsevier B.V.

particular copepods). Within the Antarctic food web, autotrophic pico- and nanoplankton are

1. Introduction

of basic importance because heterotrophic protozoans or larger grazers such as salps, prey on these organisms and make them accessible to higher trophic levels. Several studies have shown that cells $< 20 \mu\text{m}$ dominate the Southern Ocean and contribute the bulk of chlorophyll biomass in the ACC (e.g Detmer and Bathmann, 1997). The classes, prymnesiophyceae, prasinophyceae, cryptophyceae and dinophyceae include flagellate stages, which are either dominant or play an important part in the life cycle of the species. Within the frame of this study the term flagellates has been used referring to species $< 20 \mu\text{m}$ excluding dinoflagellates.

Vaulot et al., (2008) reviewed the existing molecular data of small eukaryotic phytoplankton $< 3 \mu\text{m}$ and the result suggests the following order of dominance: green algae, more specifically prasinophytes, followed by dinoflagellates, cryptophytes, haptophytes, and stramenopiles. Among the prasinophytes most sequences recovered so far belong to the order Mamiellales. *Micromonas pusilla* (Fig. 6) was one of the first mamiellales species described and is abundant in coastal temperate waters and near-polar waters (Manton & Parke, 1960; Thronson & Kristiansen, 1991). The species can account on average for 45 % of the picoeukaryotes in the English Channel coastal waters (Not et al., 2004) and for 32 % in late summer Arctic waters off Spitzbergen with maximum concentrations of up to $10000 \text{ cells mL}^{-1}$ (Not et al., 2005).

Emiliana huxleyi (5-10 μm in diameter) and *Phaeocystis antarctica* (solitary cell 4-6 μm in diameter) constitute two prominent representatives of the prymnesiophytes. *P. antarctica* can additionally form large colonies consisting of hundreds of cells (Fig. 7). Blooms of *P. antarctica* in the Ross Sea have been shown to sequester a significant amount of CO_2 in the deep sea (DiTullio et al., 2000) and can produce a substantial amount of dimethylsulfoniopropionate (DMSP). DMSP is

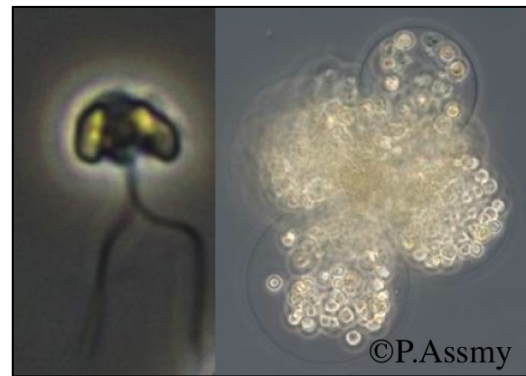


Fig. 7: Pictures taken during LOHAFEX, showing solitary cell (left) and colonies (right) of *Phaeocystis antarctica* (© P.Assmy).

known to be the biological precursor of the important trace gas dimethylsulfide (DMS) (Stefels, 2000; Arrigo, 1999; Verity and Smetacek, 1996).

The coccolithophore *Emiliana huxleyi* is globally distributed from the tropics to subarctic waters. It is a single-celled phytoplankton species and its cells are covered with uniquely

1. Introduction

ornamented calcite disks, called coccoliths. Blooms of *E. huxleyi* can be seen from space because their coccoliths reflect the incoming sunlight. *E. huxleyi* is an excellent competitor under many environmental conditions hence they are ecologically very successful. This is due to some physiological key traits, including tolerance for high irradiances and nitrogen-deprivation (Löbl et al., 2010) and an efficient phosphate uptake system (Riegman et al., 2000; Xu et al., 2010).

Cryptophytes have asymmetrical cell shapes of 10-50 μm in size with two unequal flagella and have red, olive, brown, blue or blue-green H-shaped plastids. These characteristics make them easy to identify by light microscopy (Fig. 8). They are common in freshwater, brackish and marine habitats and serve as important prey for diverse protozoan and metazoan grazers and are used as food in fish farming (Pedrós-Alió et al., 1995; Brown et al., 1997; Pastoureaud et al., 2003; Tirok and Gaedke, 2007). Cryptophytes acquired photosynthesis by secondary endosymbiosis through engulfment and assimilation of a red algal endosymbiont in their evolutionary past (Archibald and Keeling, 2002; Bhattacharya et al., 2003; Gould et al., 2008). Two types of light harvesting complexes are found in the cryptophyte plastid, a chlorophyll *a/c2* complex and a modified biliprotein (Gantt et al., 1971; Vesik et al., 1992), which enables them to photosynthesize in low light conditions (Gervais 1997; Hammer et al., 2002).

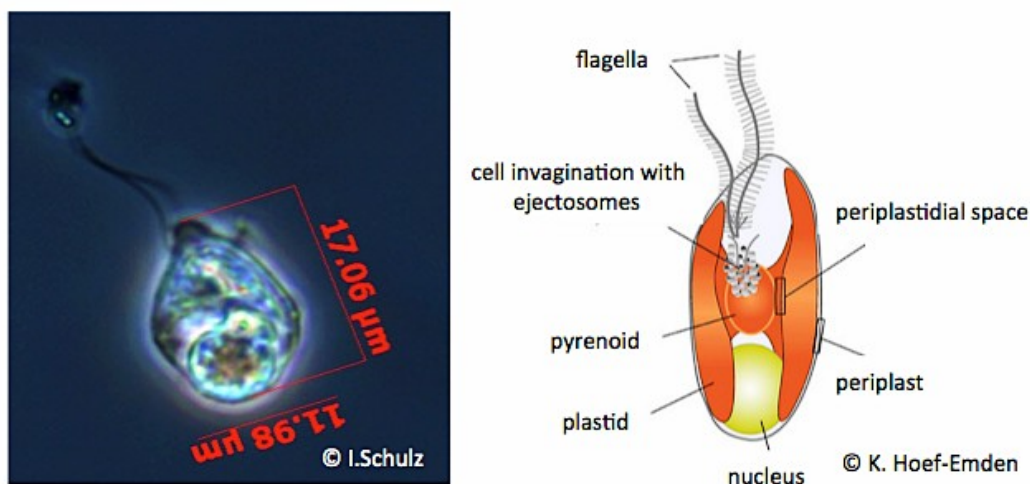


Fig. 8: To the left: cryptophyte species *Telonema* sp. (© I. Schulz) and to the right: a schematic drawing of a cryptophyte cell (© K. Hoef-Emden)
(source: <http://tolweb.org/Cryptomonads>)

Major grazers of phytoplankton are found within the group of **microzooplankton** (e.g. Sherr and Sherr, 2002; Calbet and Landry, 2004), which include loricate (tintinnids) and aloricate

1. Introduction

(naked) ciliates, heterotrophic athecate and thecate dinoflagellates, foraminifera, radiolarians, acantharians, heliozoans as well as small metazoans (copepod nauplii, copepods and meroplanktonic larvae). These groups are phylogenetically and functionally very diverse with different nutritional modes, species can be either autotrophic, heterotrophic or mixotrophic. However, the systematic study of these has lagged behind the study of bacteria, phytoplankton, heterotrophic protists and metazoan. Still, their role in structuring pelagic ecosystems is important (Burkill et al., 1993; 1995; Becquevort 1997; Klaas, 1997; Caron et al., 2000) because they can occasionally build up large stocks during winter, spring and summer (Gowing 1989; Alder and Boltovskoy, 1993; Abelmann and Gowing, 1996; Klaas, 2001). Microprotozoa constitute a major link between primary production and metazoans and are believed to be primarily responsible for the regeneration of inorganic nutrients and providing these nutrients again to phytoplankton (Azam et al., 1983; Caron and Goldmann, 1990).

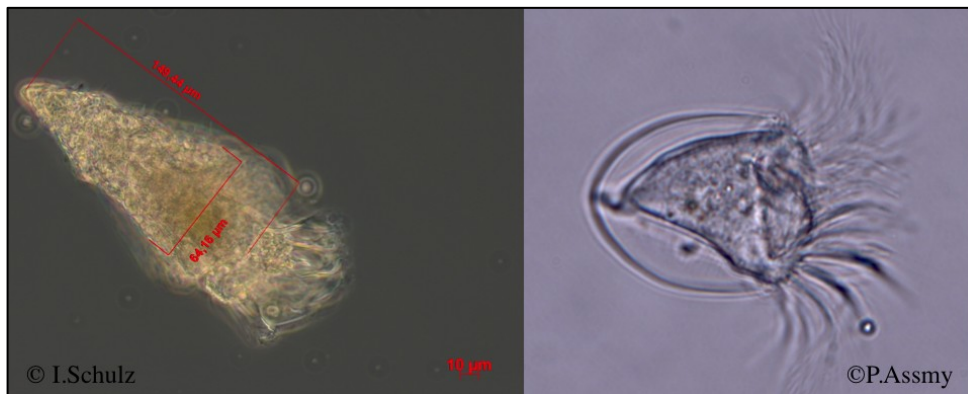


Fig. 9: Picture of *Laboea strobila* (left; © I. Schulz) and of *Cymatocylis norvegica* (right; © P. Assmy) under light microscope.

Ciliat include aloricate (naked) and loricate (tintinnids) species. The tintinnid lorica constitutes a stiff house, providing protection against grazers (Fig. 9). Some tintinnids attach biogenic particles (e.g. coccoliths, diatom frustules) and/or non-biogenic particles (e.g. sand grains, mineral flakes) to their loricae, this behaviour is commonly referred to as agglutination (Gold and Morales, 1976). Henjes and Assmy (2008) compared agglutination in the tintinnid genus *Stenosemella* spp. Jørgensen between the OIF experiments EisenEx and EIFEX and could show that particle availability seems to be the driving mechanism in the agglutination of Southern Ocean tintinnids. Tintinnids during EisenEx agglutinated almost exclusively coccoliths of the species *E. huxleyi*, despite available fragments of diatoms, whereas during EIFEX mainly broken diatom frustules (BF) were agglutinated. This was due to the fact that

1. Introduction

initial BF-abundances during EIFEX were as high as the final abundances during EisenEx (Henjes and Assmy, 2008). It has been suggested that tintinnids might ingest their prey organisms before utilising them in loricae construction (Gold and Morales, 1977; Takahashi & Ling, 1984, Gowing & Garrison, 1992; Wasik et al., 1996). In general tintinnids in the SO prey on small flagellates but also on bacteria, diatoms and dinoflagellates (Gowing, 1989; Gowing and Garrison, 1992). They have few to many cilia or compound ciliary organelles, which are used for locomotion and for creating currents, which bring food particles to their mouth. Some species contain chlorophyll and are phototrophic like e.g. *Myrionectra rubra* (= *Mesodinium rubrum*, Krainer and Foissner, 1990). It is a cosmopolitan ciliate, which feeds on cryptophytes and keeps their chloroplast and nucleus (Gustafson et al., 2000), known as kleptoplasty. This species carries out vertical migration and can form blooms, hence may be a link to upper trophic levels, through consumption by copepod nauplii (Irigoién et al., 2003) and fish larvae (Figueiredo, Nash, and Montagnes, 2005).

Dinoflagellates are found in the nano- and microplankton size fraction and are composed of two groups: thecate (armoured) and athecate (non-armoured or naked) species. They have evolved different feeding modes and are capable of feeding on a considerable size range of organisms from bacteria to crustacean larvae (e.g., prey can be an order of magnitude larger than the predator) and have quite diverse mechanisms to capture and ingest their prey. Several dinoflagellates e.g. *Protoperidinium cf. antarcticum* (Fig. 10) can extrude a large feeding veil,



Fig. 10: Picture of *Protoperidinium cf. antarcticum* under light microscope (©P.Assmy).

a pseudopod called the pallium, to capture prey, which is subsequently digested extracellular (pallium-feeding) (Smetacek, 1981). In the SO more than 35 species of *Protoperidinium* have been reported (Dodge and Priddle, 1987). Other species use a feeding tube, a peduncle, to suck up the cytoplasm from their prey (Hansen, 1991; Jeong et al., 2010). The effect of microzooplankton can even be larger than copepods in controlling phytoplankton biomass and might even be able to control diatom blooms (Irigoién et al., 2005). Many dinoflagellate species are known to form blooms (Taylor et al., 2008). Some bloom genera have species that produce toxins, which can cause fish and invertebrate mortality (Burkholder et al., 1995). But

1. Introduction

also if they do not produce toxins, the increased biomass may result in low oxygen waters and subsequent fish mortality (Kudela et al., 2005).

Rhizaria, including foraminifera, acantharia, radiolarian, taxopodida and cercozoa, belong to the larger protozoa (micro- to meso-size), which are less well studied due to the requirement of different sampling methods. However, several studies have shown that they are quite abundant in the SO and have relatively rapid reproductive rates (Caron and Swanberg, 1990, Gowing and Garrison, 1992, Abelman and Gowing 1996, Klaas, 2001, Henjes et al. 2007). They feed on particles ranging from bacteria to relatively large metazooplankton (Gowing, 1989, Caron and Swanberg, 1990, Gowing and Garrison 1991; Nöthig and Gowing, 1991; Gowing and Garrison, 1992; Gowing et al., 2001).

Acantharia (Fig. 11) are cosmopolitan, exclusively marine protozoa ranging in size from 0.05-5 mm in diameter. Like several other radiolarian, acantharia have axopodia, long radiating processes used to capture prey. They feed on all kinds of particulate materials, including bacteria micro- and picoplanktonic algae, tintinnids and other ciliates and sarcodines, dinoflagellates, copepod nauplii, copepodids and adults and pelagic molluscs (Caron and Swanberg, 1990). They are mostly found in surface waters and several species host autotrophic symbionts located either in the endoplasm or the ectoplasm. Their distinguishing features are: a skeleton of strontium sulfate (SrSO_4), or celestite, based on a general plan of 10 diametral or 20 radial spicules arranged in a regular pattern called Müller's law (Müller, 1859); a cell body covered with an outer pellicle, the periplasmic cortex and the myonemes, contractile filaments grouped around the spicules. Due to the solubility of the celestite skeletons, they do not preserve in sediments. Hence evidence of the origin and geologic history on this group is scarce. However acantharia contribute, due to the formation of seed-like cysts, mainly consisting of barium (Ba) and strontium (Sr), which sink out from the surface layer, to downward POC flux and play an important role in the biological carbon pump but also in the marine chemistry of Sr and Ba (Bernstein et al., 1987; Lampitt et al., 2009; Martin et al., 2010; Decelle et al., 2013). Barite can be used as proxy in several ways because it is an authigenic (generated from where it is found) marine mineral for instance past and modern ocean productivity can be reconstructed through the accumulation rate of marine barite in oxic-pelagic sediments (Griffith and Paytan, 2012).

1. Introduction

Foraminifera are also important index fossils for past environmental conditions because they have mineralized tests and are widely distributed and abundant (Fig. 11). Past seawater parameters, such as temperature (Lea, 2003) salinity (Rohling, 2000), pH (measure of hydronium ion concentration) (Spero et al., 1997; Spivack et al., 1993) and nutrients can be estimated from the (trace) element and stable isotope compositions of their calcite shells. Some species host unicellular endosymbionts from several lineages like e.g. diatoms or dinoflagellates and others retain chloroplasts from ingested algae to conduct photosynthesis (Hemleben et al., 1989; Bernhard & Bowser, 1999). The major pelagic producers of calcium carbonate are coccolithophores and foraminifera (Baumann et al., 2004), which are the driving forces of the carbonate pump.

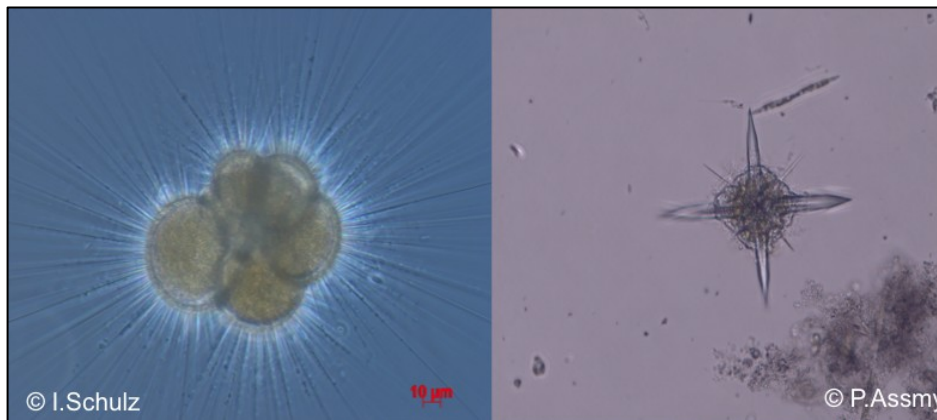


Fig. 11: To the left a picture of *Turborotalita quinquiloba* (foraminifera) and to the right of *Acanthostaurus sp.* (acantharia) (© I. Schulz & P. Assmy)

Radiolaria are important components of epipelagic communities in oligotrophic oceans because they prey on algae and other planktonic organisms. Many surface-dwelling species possess symbiotic algae, predominantly dinoflagellates, which are photosymbiotically active and contribute significantly to the nutrition of the host (Caron et al., 1995). Radiolaria form colonies of individuals by extending their cytoplasm to form a big net of pseudopodia enclosed within a gelatinous matrix. These colonies vary in size and form and many lack siliceous skeletons (Swanberg, 1983). Others have skeletons consisting of opaline silica that preserve in the sediment record and are widely used as microfossils (Takahashi et al., 1983; Gersonde and Wefer, 1987). A recent study proved the reliability of polycystine radiolaria as proxy for past SO conditions (Morley et al., 2013).

Plankton plays a key role in marine ecosystems because they form the basis of marine food webs and are important in biogeochemical processes. Changes in plankton abundance,

1. Introduction

diversity, and distribution could have cascading effects through the ecosystem. However plankton composition is still not fully understood and we lack a basic understanding of the spatial and temporal variation in plankton community and therefore it is essential to investigate in plankton ecology research through long-term monitoring, mesocosm experiments and perturbation experiments like LOHAFEX to understand the complex structure underlying pelagic ecosystems.

1.6 Ocean Iron Fertilization

1.6.1 Importance of OIF experiments

The approach of OIF experiments is to induce a phytoplankton bloom and enhance biological productivity through artificial iron addition. These experiments are the equivalent of perturbation experiments, which are carried out by all disciplines of science and enable to study the structure and functioning of systems too complex to be analysed by observation alone. Artificial OIF simulates natural processes (chapter 1.6.2) by adding iron to iron-limited land-remote ocean waters. With OIF experiments it is possible to deepen the understanding of how open ocean ecosystem function and how the organisms of the plankton interact with one another and with the environment to drive biogeochemical cycles and sinking of particulate matter to the deep sea (Smetacek & Naqvi, 2008). It is a holistic approach to study the plankton community and represents a useful tool to understand and make comparisons to naturally occurring blooms, which are less well understood (Boyd et al., 2007).

So far only small scale experiments were carried out and these were and still are necessary to increase our understanding of OIF effects on the ocean environment, including possible negative side effects such as oxygen depletion, stimulation of toxic species or production of potent greenhouse gases such as nitrous oxide (N₂O) and methane (CH₄). The ideal conditions to perform such an experiment are found in the closed core of a mesoscale eddy formed by a frontal jet. The fertilized patch is retained within it for the lifetime of the eddy, generally several months, and provides vertical coherence between surface and subsurface layers (Smetacek & Naqvi, 2008).

1.6.2 OIF experiments

Martin et al., (1990) formulated a two part “Iron-Hypothesis”. Firstly he hypothesized that iron is the limiting nutrient in HNLC regions for phytoplankton productivity and secondly that the greater supply of iron bearing dust to these regions during the dry glacials, stimulated phytoplankton blooms, which sank out and sequestered CO₂ in the deep ocean, hence lowering atmospheric CO₂ concentrations.

Shipboard incubations experiments using HNLC water, showed evidence that phytoplankton growth was limited by Fe availability. However due to artefacts in these experiments, Martin (1990) proposed mesoscale in situ ocean iron fertilization experiments.

1. Introduction

In 1993 the first experiment **IronEx I** was carried out in HNLC-waters of the Equatorial Pacific, near the Galápagos Islands (Martin et al., 1994, Coale et al., 1996, 1998). During IronEx I a significant increase in the photosynthetic quantum efficiency (Fv/Fm) from 0.3-0.6 within 24 hours could be observed (Kolber et al., 1994). Primary productivity increased from initially 10-15 mg C m⁻³ to 48 mg C m⁻³ d⁻¹ and Chl *a* from 0.24 to 0.65 mg m⁻³. Unfortunately the patch (62 km² in size) was subducted to 30-35 m depth after five days, preventing further bloom development (Watson et al., 1994). During the follow-up experiment **IronEx II** in May 1995 to the same region the patch (72 km² in size) was fertilized three times over the course of one week and Fv/Fm increased rapidly from 0.25 to 0.5 (Behrenfeld et al., 1996). All phytoplankton species responded to the Fe addition. The increased cellular photopigment concentration, observed in all phytoplankton species, was an indicator for previous Fe limitation (Cavender-Bares et al., 1999). At the end of the bloom *Pseudo-nitzschia*, a pennate diatom, dominated in terms of biomass and smaller pico- and nanoplankton were kept in check by grazers (Cavender-Bares et al., 1999; Landry et al., 2000a, 2000b). During this experiment the ²³⁴Th (Thorium) deficiency method provided first insights about iron-induced POC export, which reached nearly 50 mmol m⁻² d⁻¹ during days 8-14 (Bidigare et al., 1999).

The results of IronEx II motivated the scientific community to focus now, with respect to OIF, on the low productivity area of the Southern Ocean. The emphasis was on longer duration experiments to be able to track particle export, remineralisation and trophic interactions (De Baar et al., 2005). The Southern Ocean Iron Release Experiment (SOIREE), EisenEx (Eisen is the German word for iron), Southern Ocean Iron Experiment north and south (SOFeX-North/South), European Iron Fertilization Experiment (EIFEX), Surface-Ocean Lower-Atmosphere Studies Sea-Air Gas Exchange experiment (SOLAS-SAGE) and LOHAFEX were conducted between 1999 and 2009 (Fig. 12).

The first experiment **SOIREE** (1999), lasting for 13-days was conducted south of the Polar Front with four Fe infusions. The initial patch of SOIREE increased from 50 km² to about 250 km² hence the patch dilution was strong (Abraham et al., 2000). However 5 days after the release a significant increase in algal photosynthetic efficiency and a species shift from haptophytes to diatoms was observed. *Fragilariopsis kerguelensis*, *Rhizosolenia* sp. and *Pseudo-nitzschia* sp. were the dominant diatom species and were mainly responsible for the increased biomass (Gall et al., 2001). No increase in carbon export was observed (Boyd et al., 2000; Trull and Armand 2001; Trull et al., 2001; Waite and Nodder, 2001). The response of

the biota to iron fertilisation was slow in comparison to IronEx I and II in the equatorial Pacific Ocean, possibly due to the strong lateral dilution and far lower temperatures and a deeper wind mixed layer (WML) (Boyd et al., 1999).

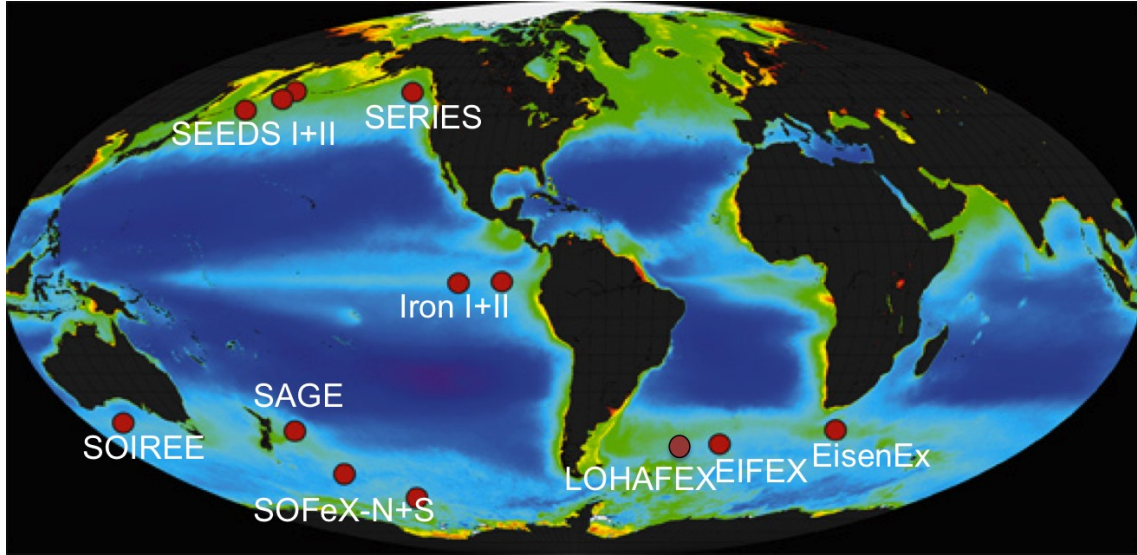


Fig. 12: Red dots indicate the location of the OIF experiments carried out from 1999-2009 (picture adapted from Philipp Boyd, 2008; source: <http://www.whoi.edu/oceanus/feature/will-ocean-iron-fertilization-work>)

EisenEx took place in the austral spring in November 2000, in a cold core Antarctic eddy originating from the Polar Frontal jet. During the 21-day experiment major storms and strong winds diluted the initial patch of 50 km² and caused an increase in patch size to 950 km² and the WML increased from initially 40-50 m to almost 100 m (Turner et al., 2004). Fv/Fm increased steadily from 0.3 to 0.52 at the end of the experiment, indicating Fe limitation (Gervais et al., 2002). Chlorophyll *a* measurements of the pico-, nano-, and microplankton community showed that Chl *a* of picoplankton remained constant after day 2, while nanoplankton steadily and microplankton exponentially increased and the latter finally dominated the bloom after day 16 (Gervais et al., 2002). Microplankton was firstly dominated by the species *Fragilariopsis kerguelensis* and in the second part of the experiment by *Pseudo-nitzschia lineola*, which accounted for 53 % of the total diatom cells and 25 % of total diatom biomass (Assmy et al., 2007). The fate of the bloom remains uncertain as the experimental site had to be abandoned while the bloom was still building up (Assmy et al., 2007).

During **SOFeX** (2002) two patches with different initial silicate concentrations were fertilized simultaneously and followed for 30 days. **SOFeX-north** was conducted in sub-Antarctic waters with low-silicate (< 3 mmol m⁻³) and high nitrate (20 mmol m⁻³) concentrations while

1. Introduction

SOFeX south was conducted in Antarctic waters with high Si (60 mmol m^{-3}) and high N (28 mmol m^{-3}) concentrations. During SOFeX-north the initial WML was 45 m and increased to 55 m at the end of the experiment (Coale et al., 2004). The whole patch evolved into a 7 km-wide and at least 340-km-long filament and was characterized by an approximately 20-fold increase in Chl *a* (2.6 mg m^{-3}), a fourfold increase in phytoplankton carbon biomass and increase in Fv/Fm from 0.2 to 0.5 (Coale et al., 2004). During the first two weeks the phytoplankton community was dominated by prymnesiophytes, pelagophytes and dinoflagellates. However, despite low Si-concentrations diatoms $> 20 \mu\text{m}$ increased from 5-38 % of total phytoplankton biomass (Coale et al., 2004). The experiment showed also that despite low Si concentrations, iron promotes non-silicious phytoplankton growth and the uptake of carbon dioxide (Coale et al., 2004). During **SOFeX-south** the WML stayed constant (35 m) and a significant shift from smaller to intermediate and large-sized cells and more diatoms could be observed. Fv/Fm was a little bit higher compared to SOFeX-N and increased from 0.25 to 0.65 (Coale et al., 2004). SOFeX-south showed the first convincing export of POC and Si, using the ^{234}Th deficiency technique (Buesseler et al., 2004, 2005).

EIFEX (2004) was conducted to evaluate the carbon export response and community shift in an artificial bloom (Hoffmann et al., 2006). The 35-day experiment was carried out in a clockwise-rotating core of an eddy, 60 km in diameter, formed by a meander of the APF. The area increased from 167 km^2 to 798 km^2 on day 19. Initial Si concentrations ranged between $14\text{-}19 \text{ mmol m}^{-3}$. The bloom was dominated by large, spiny, heavily silicified diatoms (Assmy et al., in review), which peaked in the fourth week after fertilization and reached $286 \text{ mg Chl } a \text{ m}^{-2}$. So far this is the highest chlorophyll stock recorded in an OIF experiment. After the peak a mass mortality event of several diatom species followed. These formed mucilaginous aggregates containing cells and chains that rapidly sank out and resulted in deep carbon export. So far, only during this experiment enhanced deep carbon export could be observed (Smetacek et al., 2012) thus providing support for the second condition of the iron hypothesis.

SAGE (2004) was conducted to investigate the influence of Fe-fertilization on sea-air gas exchange, particularly DMS. DMS plays a role in cloud formation and hence plays a role in climatic regulation and potentially in increasing Earth's albedo (Charlson et al., 1987). However in the experiment the DMS precursor DMSP was kept in check through grazing activity and in contrast to most OIF experiments dissolved DMS concentration declined (Harvey et al., 2011). The patch, which was located in the Pacific sector of the Southern Ocean was characterized by low Si concentrations (0.9 mmol m^{-3}) and low Fv/Fm (0.43),

1. Introduction

which increased after Fe addition to 0.61 (Peloquin et al., 2011). During this 16-day experiment the enhancement of chlorophyll *a* and primary production was twofold by the end of patch occupation (Peloquin et al., 2011). Initial diatom stocks were low (< 1%) and did not change over the course of the experiment. Instead small flagellates in the size class of 2-20 μm contributed most to standing stocks. High winds caused the patch to stretch into a thin filament around an eddy and patch dilution and mixing of water masses caused an increase in Si but a loss of Fe (Law et al., 2011).

Four additional experiments; Subarctic Pacific Iron Experiment for Ecosystem Dynamics Study (SEEDS I+II 2001/2004), Subarctic Ecosystem Response Iron enrichment Study (SERIES, 2002) and a combined Iron and Phosphate fertilization experiment (FeeP.), the former three were carried out in the Subarctic Pacific and the latter in the low nutrient low chlorophyll area of the Sub-tropical Northeast Atlantic.

SEEDS I (2001) generated high accumulation of surface phytoplankton biomass (18 mg Chl m^{-3}), which was accompanied by a floristic shift from oceanic diatoms to neritic diatoms (Tsuda et al., 2003). Due to the short observation period the fate of the bloom could not be determined. Hence three years later **SEEDS II** (2004) was conducted nearly at the same location and season to characterize the evolution of the fertilized patch over the time scale of one month and to measure a greater range of parameters. In contrast to SEEDS I, the surface Chl *a* accumulation during SEEDS II was lower (0.8–2.5 mg m^{-3}) and with no prominent diatom bloom (Tsuda et al., 2007).

SERIES (2004) was conducted over a month in a 77 km^2 patch, which enlarged to 1000 km^3 . The phytoplankton responded immediately to iron addition and Fv/Fm increased from 0.2 to 0.4. Flagellates were predominant and reached maximum abundance on days 6–9, before diatoms dominated on days 16–19. The majority of fixed carbon was remineralized by bacteria and zooplankton grazing in the surface layer (Timothy et al., 2006; de Baar et al., 2005).

To conclude these experiments taught us a lot about initial phytoplankton community and response to iron fertilization. They differ not only in length, season, and depth of the WML but also and especially in the response of the phytoplankton community. However, all experiments confirmed iron limitation of productivity in HNLC regions. Even though the results were highly variable, they have substantially increased our understanding of ecological and biogeochemical dynamics. Still more research needs to be done as many questions remain unsolved. *In situ* fertilization experiments represent the ideal tool to improve our

1. Introduction

understanding of oceanic plankton ecology. The major facts of the previous experiments are summarized in table 1.

The following chapters will describe the results and findings of LOHAFEX (2009).

Table 1: Overview of the main characteristics of all iron fertilization experiment carried out from 1993-2009.

Acronym (reference)	Year (season)	Duration (days)	Location	bloom composition (dominating species)	patch size and shape (km ²)	Important Characteristics	WML depth (m)	Fv/Fm (initial and max.)	Chl <i>a</i> t=0 (mg m ⁻³)	Chl <i>a</i> max. (mg m ⁻³)
IronEx I (Martin et al., 1994)	1993 (fall)	5	Pacific Ocean (east equatorial)	mixed	64 km ²	patch subsided	35	0.3→0.6	7	21
IronEx II (Coale et al., 1996)	1995 (summer)	17	Pacific Ocean (east equatorial)	diatom (<i>Pseudo-nitzschia</i> spp.)	72 km ² , patch	first assessment of POC export (7 → 50 mmol m ⁻² d ⁻¹)	40	0.25→0.5	8	132
SOIREE (Boyd et al., 2000)	1999 (summer)	13	Southern Ocean (Australian sector)	diatom (<i>F. kerg.</i> , <i>Rhipidolesmia</i> , <i>Pseudo-nitzschia</i>)	elongated patch 50-250 km ²	silicate conc. 10 mmol m ⁻³	65	0.2→0.6	13	150
EisenEx (Gervais et al., 2002)	2000 (spring)	21	Southern Ocean (Atlantic sector)	diatom (<i>F. kerg.</i> , <i>Pseudo-nitzschia kerkela</i>)	eddy, round (50-1000km ²)	low-silicate (dilution of patch by major storms)	80	0.3→0.52	40	224
SEEDS I (Tunda et al., 2005)	2001 (summer)	10	Pacific Ocean (northwest)	diatom, (<i>Chaetoceros debilis</i>)	8 x 10 km patch	shallow WML,	13	0.2→0.3	12	234
SOFeX-North (Coale et al., 2004)	2002 (summer)	27	Southern Ocean (Pacific sector)	mixed (<i>Pseudo-nitzschia</i> spp.)	7 x 340 km	low-silicate (< 3 mmol m ⁻³); long filament	45	0.2→0.5	14	108
SOFeX-South (Bluessteiner et al., 2004)	2002 (summer)	28	Southern Ocean (Pacific sector)	various large diatom species	225 km ²	high-silicate (60 mmol m ⁻³)	35	0.25→0.65	7	88
SERIES (Boyd et al., 2004)	2002 (summer)	25	Pacific Ocean (northwest)	flagellates + diatom (<i>Pseudo-nitzschia</i> spp.)	77-200 km ² up to 1000km ²	strong bloom development	30	0.2→0.4	12	165
EIPLEX (Smayda et al., 2012)	2004 (summer)	37	Southern Ocean (Atlantic sector)	very diverse, 21 diatom species contribute >85% of bloom biomass	eddy, round (167-740 km ²)	deep carbon export	100	0.28 → 0.4	60	300
SAGE (Harvey et al., 2011; Pelouquin et al., 2011)	2004 (fall)	17	Southern Ocean (Pacific sector)	flagellates (< 20 μm)	6 x 6 km ²	low-silicate (0.9-9.6 mmol m ⁻³) patch stretched into a long thin filament	70	0.27→0.61	42	91
SEEDS II (Tunda et al., 2007)	2004 (summer)	25	Pacific Ocean (northwest)	diatoms+ prymnesio-prasinophytes	80 km ²	broad range of diatoms, but did not bloom despite adequate Si conc.	30	n.a.	24	75
LOHAFEX (Martin et al., 2013)	2009 (spring)	37	Southern Ocean (Atlantic sector)	flagellates (< 20 μm)	eddy, round (150-300 km ²)	low-silicate (< 2 μmol L ⁻¹)	80	0.33→0.40	40	96

1.6.3 Natural Iron Fertilization

Events of iron fertilization can also occur naturally. A major iron source is aeolian dust, e.g. from the Saharan desert, which causes enhanced primary production in the southern North Atlantic or Patagonian dust, which causes enhanced productivity along the ACC (view Fig.4) (Gao et al., 2001, Erickson et al., 2003, Duce and Tindale 1991, Jickells et al., 2005). In coastal areas, upwelling of iron rich sediment particles or riverine flux can be another iron source (Bruland et al., 2001, Figuères et al, 1978). Adequate iron supply may also result from snow deposited dust released by ice-berg melting (Raiswell et al., 2008) or through volcanic ash. Hamme et al. (2010) documented by the eruption of Mt. Kasatoshi in 2008, where the ash covered a large portion of the Gulf of Alaska. Parsons and Whitney (2012) hypothesized that the volcanic emission of iron rich dust, which caused a massive late summer bloom of diatoms, may even have led to improved recruitment of young sockeye salmon.

So far two natural iron fertilization studies were carried out near Crozet Island and Kerguelen Island, respectively (Pollard et al. 2009; Blain et al. 2007). The bloom north of the Crozet Islands and Plateau (Crozet) was surveyed and compared with a HNLC region south of Crozet. The CROZet natural iron bloom and EXport experiment (**CROZEX**), took place from November 2004 to January 2005 (Pollard et al., 2007). It could be confirmed that iron from Crozet fertilised the bloom and caused enhanced phytoplankton production and most export flux estimates were much larger in the bloom area than in the HNLC control area (Pollard et al., 2007).

The KERguelen Ocean and Plateau compared study (**KEOPS**) was conducted in austral summer 2005 and showed that a persistent iron fertilisation caused the bloom. However, the supply of macronutrients from surrounding waters determined the duration of the bloom (Blain et al., 2007). Blain et al. (2007) concluded, due to the findings of KEOPS that the impact of natural iron fertilization in the Southern Ocean is significantly different from the artificial OIF.

2. Objectives

Several in-situ iron fertilization experiments have been carried out in the Southern Ocean in order to investigate the role of iron limitation in explaining the low productivity of this HNLC area. The outcome of previous experiments, all resulting in the development of diatom blooms, have demonstrated unequivocally that iron is indeed the main factor limiting phytoplankton growth rates in the silicic acid rich regions of the ACC. Understanding the effect of changes in iron supply to the Southern Ocean through dust deposition or changes in the ACC circulation on carbon export and atmospheric pCO₂ over past climatic cycles and in the future is, however, still lacking. The main reason is the poor understanding of the effect of iron fertilization on the composition and temporal dynamics of plankton communities as well as a quantitative understanding of the relationship between plankton community characteristics and the efficiency of the biological carbon pump. Artificial iron fertilization experiments provide unique conditions to follow the development of a plankton bloom under in-situ but controlled conditions in a coherent water mass, allowing the study of processes determining plankton community composition and vertical particle export under conditions and at scales relevant to the understanding of the global carbon cycle.

Although high concentrations of nitrogen and phosphate are present all year round in the ACC, waters north of the APF, show very low silicic acid concentrations during the productive growth season. To date, only two experiments (SOFEX-north patch, Coale et al., 2004 and SAGE, Harvey et al., 2011) investigated the effect of iron fertilization in this silicic acid poor region. During SOFEX-N a significant response of diatoms to iron addition could still be observed despite the low silicic acid concentrations ($\sim 4 \mu\text{M}$) but this applies not to SAGE. LOHAFEX is the third iron fertilization experiment carried out in this silicic acid poor region of the northern ACC. In contrast to SOFEX-north, silicic acid concentrations during LOHAFEX were close to the detection limit as the experiment took place later in the growth season.

The **overall aim** of this PhD was to gain a quantitative and qualitative understanding of factors driving the temporal dynamics of the plankton community and ultimately the fate of the produced biomass under iron-replete conditions in the silicic acid poor region of the ACC. The project focused on the study of phytoplankton with special emphasis on biogeochemical relevant phytoplankton taxa by assessing the temporal dynamics of the phytoplankton

2. Objectives

community over the course of the experiment. The temporal trends of the relevant taxa have been interpreted in the light of the growth (bottom-up control) and mortality (top-down control) environment.

The major questions addressed in this thesis were:

1. How will plankton species composition differ in an iron fertilized bloom induced in a Si-limited region of the polar frontal zone of the Atlantic sector of the ACC to previous experiments carried out in high-Si waters? (Manuscript **I+II+III**)
2. What are the effects of iron fertilization on higher trophic levels? (Manuscript **III+IV**)
3. What is the fate, surface retention versus vertical export, of the iron-induced bloom? (Manuscript **V**)

3. Methods

3.1 Sampling site

The joint Indo-German iron fertilisation experiment LOHAFEX, was carried out in the productive south-western Atlantic sector of the Antarctic Circumpolar Current during RV *Polarstern* cruise ANT-XXV/3 from 7 January to 17 March 2009. The term LOHAFEX is derived from the hindi word LOHA which means iron and FEX stands for fertilisation experiment.

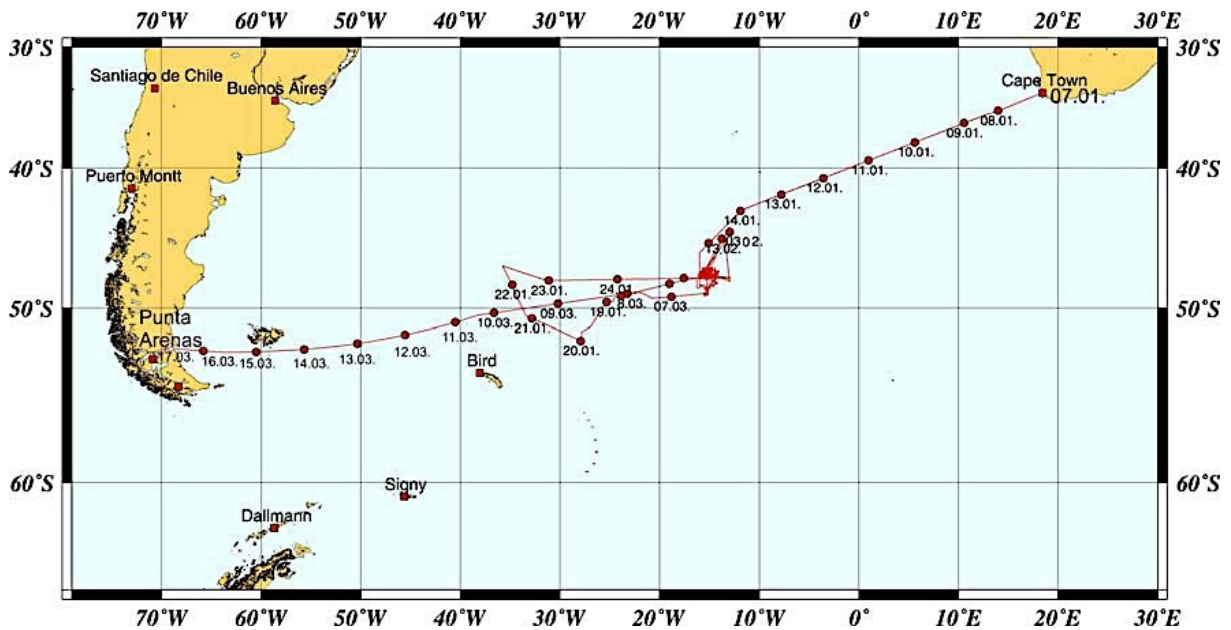


Fig. 13: Cruise track of *RV Polarstern* between Cape Town and Punta Arenas with corresponding date of sampling. (source: Smetacek & Naqvi et al., 2010)

The closed core of a mesoscale eddy represents the best condition to perform such an experiment because the fertilized patch is retained within it for the lifetime of the eddy, which is generally several months. LOHAFEX was carried out in low Si ($< 2 \mu\text{M}$) waters in a cold core eddy originating from the PFZ located at $48^\circ\text{S } 16^\circ\text{W}$ (Fig. 14).

An area of 300 km^2 was fertilized with 10t of dissolved iron (II) sulphate (FeSO_4) in the core of the eddy (the patch). To prevent further phytoplankton Fe deficiency a second fertilization was carried out on day 18 with the same amount of dissolved FeSO_4 .

Four different ways of tracking the patch were used:

1. Trajectories of GPS drifters,

2. Labelling with the inert tracer sulfurhexafluoride (SF_6) released together with the FeSO_4 solution,
3. Online measurements of photosynthetic efficiency (F_v/F_m),
4. Underway Chl *a* sampling and continuous pCO_2 measurements.

IN-patch stations were distinguished according to highest and OUT-patch stations according to lowest SF_6 concentrations and F_v/F_m ratios. The WML ranged between 60-80 m. The station taken on day -0.6, before fertilisation, represents the starting point of the experiment and was included in the IN and OUT patch trends.

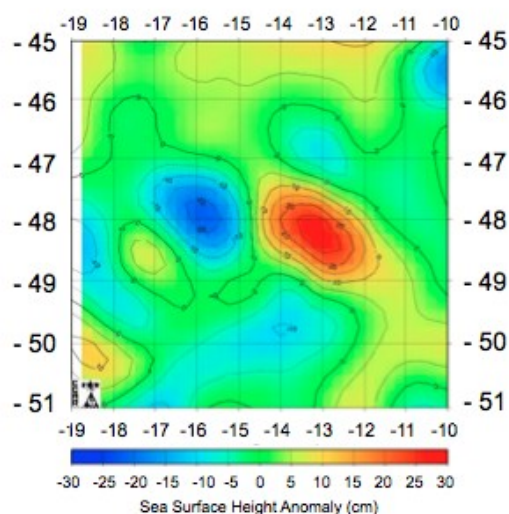


Fig. 14: Image of the Sea Surface Height Anomaly (SSHA) of the selected cyclonic cold (blue) and adjacent warm (red) core eddy (25.01.2009). It was selected at 16°W and 48°S in the central South Atlantic. (Source: Smetacek & Naqvi et al., 2010)

3.2. Plankton sampling

The main analyses for this Dissertation were done via microscopy. Therefore the focus of the method part is on this technique. Additional methods applied within the context of this dissertation are given at the end of this chapter.

Phyto- and microzooplankton samples were collected at 5 discrete depths (10, 20, 40, 60, 80 m) in the WML with Niskin bottles attached to a CTD (conductivity, temperature, depth) rosette (SeaBird Electronics, USA). One set of samples was fixed with hexamethylenetetramine-buffered formaldehyde (2 % final concentration) and another set with Lugol solution (5 % final concentration). Samples were stored dark at 4°C to prevent the degradation of Lugol's iodine in light.

For estimating the species composition and abundance of large protozooplankton and copepods <1 mm, the content of one Niskin bottle (12 L) was gently passed over 20 μm mesh sized gauze for samples taken from 10-150 m and two Niskin-Volumes for depth intervals from 200-500 m. In addition to hexamethylenetetramine-buffered formaldehyde (2 % final concentration), strontium chloride (SrCl_2) was added to prevent dissolution of acantharian skeletons. The final sample volume was 50 ml and stored dark at 4°C.

For grazing experiments copepods >1 mm were gently collected by slow vertical hauls in the upper 100 m water column with a WP2 net (60 cm mouth diameter, 200 µm mesh) equipped with a 10 L plastic bucket as non-filtering cod-end to prevent damaging the organisms. The samples were diluted in 25 L coolers that had been previously half filled with water pumped from the surface and immediately transported to laboratory, where grazing experiments were performed.

3.3. Quantitative plankton analyses

Cells were identified and enumerated using inverted light and epifluorescence microscopy (Axiovert 200, Axio Observer 1,0, Oberkochen, Germany) according to the methods of Utermöhl (1958) and Thronson (1995).

Sedimentation chambers consisted of cylinders (Utermöhl chamber) of different volume (10 ml, 25 ml or 50 ml) and a bottom plate with a small well in which the sedimented cells were collected (Fig. 15 a). Settling time was dependent on the height of the cylinder and the preservative used (Lund et al., 1958; Nauwerck, 1963). Samples fixed with Lugol's iodine solution and settled in 25 ml cylinders, were settled for 24 hours. Formaldehyde preserved samples were settled in 50 ml cylinders for 48 hours. After sedimentation the cylinder was emptied through the hole in the chamber (Fig.15 b (3.)) and the chamber was sealed with a cover glass.

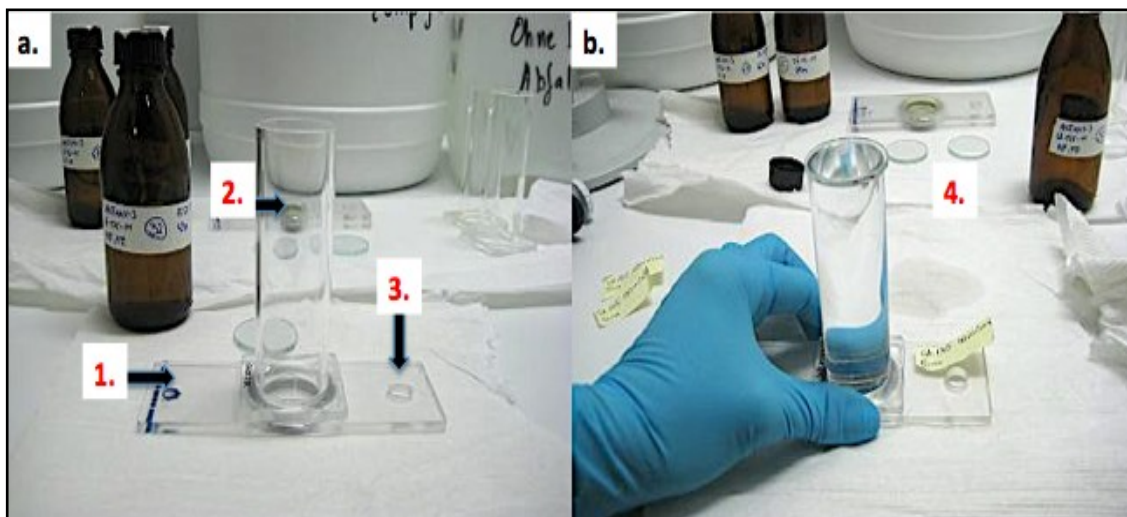


Fig. 15: **a.** showing the base plate (1.) with Utermöhl chamber and a 50 mL cylinder (2.) and the releasing hole (3.) **b.** showing the filled cylinder with cover glass (4.)

© S.Wolzenburg

Due to the effect of discolouration by Lugol's iodine fixative, the identification of some phytoplankton species was difficult. The surplus of iodine was chemically reduced to iodide by dissolving a small amount of sodium thiosulphate ($\text{Na}_2\text{S}_2\text{O}_3 \cdot 5 \text{H}_2\text{O}$) in the sedimented aliquot and thereby discolouring the sample.

3.4. Counting procedure

Cells have been counted according to their abundance and size in transects, half or complete chamber at low or high magnification. Flagellates, naked ciliates and dinoflagellates were counted in Lugol preserved samples at high magnification (400x). Diatoms and thecate dinoflagellates were counted in formaldehyde preserved samples in either high or low magnification, depending on cell size (200x or 400x). Epifluorescence microscopy allowed counting and identification of heterotrophic and autotrophic organisms. At least 50 counting units of each dominating taxon was counted, and the total count exceeded 500 cells. The transformation of the microscopic counts to the concentration of phytoplankton of desired water volume, was achieved using the following equation (1):

$$\text{Cells } L^{-1} = N * \left(\frac{A_t}{A_c} \right) * \frac{1000}{V} \quad (1)$$

V: volume of counting chamber (mL)

A_t : total area of the counting chamber (mm^2)

A_c : counted area of counting chamber (mm^2)

N: number of units (cells) of specific species counted

3.5. Biomass determination

To estimate phytoplankton biomass, cell size of each species/category was measured on 20 randomly picked cells and their biovolume calculated from equivalent geometrical formulas (Hillebrand et al., 1999). Menden-Deuer and Lessard, (2000) recommend carbon conversion factors for specific plankton groups to calculate cellular carbon content. Abundance and biomass of all species described in this study are trapezoidal depth-integrated values for the WML 0-80 m. Abundance values were back calculated to litre according to equation (2):

$$N_t = \left(\int_{80}^0 N dz \right) / z \quad (2)$$

N_t : is the average abundance at time t

$\int_{80}^0 N$: the depth integral and

z: depth

A brief overview of the additional methods employed is given below:

Manuscript II

- C. Wolf used Roche/454 GS FLX Titanium technology (Ronaghi et al., 1996)
- B. Fuchs used a FACScalibur flow cytometer to determine total cell numbers
- S. Thiele used manual and automated cell enumeration via an automated counting machine using the macro MPISYS (Zeder unpublished) and the analyses program ACMEtool 0.76 (Zeder unpublished)

Manuscript V

- F. Ebersbach collected sinking particles using:
 - i) bulk samples of neutrally buoyant sediment traps (NBSTs) for biogeochemical fluxes and microscopic investigations, and
 - ii) polyacrylamide (PA) gel equipped NBSTs in order to preserve the shape and structure of intact particles.
 - iii) transparent exopolymer particles (TEP) were analysed in the water column and in trap samples.

4. Manuscripts

4.1 Manuscript Outline

Manuscript I: Response of a flagellate-dominated plankton community to artificial iron fertilization in the Southern Ocean

Isabelle Katharina Schulz, Philipp Assmy, Friederike Ebersbach, Mangesh Gauns, Christine Klaas, Grazia Mazzocchi, Marina Montresor, Rajdeep Roy, Amit Sakar, Stefan Thiele, Christian Wolf, Sina Wolzenburg, Victor Smetacek

(30.09.2013 – to be submitted to PLOS ONE)

P. Assmy collected water samples during the Southern Ocean iron fertilization experiment LOHAFEX. I.K. Schulz analysed the phytoplankton community at the home laboratory at the Alfred Wegener Institute in Bremerhaven, Germany. Samples for flow cytometric analysis were collected and analysed by R. Roy at the National Institute of Oceanography in Goa, India. S. Thiele analysed bacteria data and C. Wolff did the 454-pyrosequencing analyses. S. Wolzenburg collected data of protozooplankton abundance and biomass. I.K. Schulz wrote the paper with input from all co-authors.

Manuscript II: Investigation of the nano- and picoplankton community during the iron fertilization experiment LOHAFEX

Stefan Thiele, Christian Wolf, Isabelle Katharina Schulz, Philipp Assmy, Katja Metfies, Bernhard Fuchs, Rudolf Amann

(30.09.2013 – to be submitted to PLOS ONE as companion paper to Chapter I)

P. Assmy, S. Thiele, B. Fuchs, K. Metfies and I.K. Schulz derived the concept of this publication. P. Assmy and B. Fuchs took the samples. C. Wolf and S. Thiele analysed the samples at the home laboratory and wrote the manuscript with contribution and input from all co-authors.

Manuscript III: Investigation of the protist plankton (>20µm) during the iron fertilization experiment LOHAFEX in the Southern Ocean

Isabelle Katharina Schulz, Sina Wolzenburg, Philipp Assmy, Victor Smetacek

(30.09.2013 – to be submitted to *Deep Sea Research I*)

P. Assmy took the samples. S. Wolzenburg analysed the samples. I.K. Schulz wrote the manuscript with contribution from all co-authors.

Manuscript IV: Copepod grazing during the LOHAFEX Experiment: natural diets and impact on phytoplankton communities (preliminary title)

Maria Grazia Mazzocchi, Isabelle Katharina Schulz, Humberto González, Ines Borrione, Mangesh Gauns, Marina Montresor, Diana Sarno

(30.09.2013 – in preparation)

M. Mazzocchi derived the concept of this publication. M. Mazzocchi performed experiments on board of *RV Polarstern* and took the samples. I.K. Schulz did the microscopic quantification of plankton composition. M. Mazzocchi wrote the manuscript with contribution from all co-authors.

Manuscript V: Sedimentation patterns of phyto- and protozooplankton and sinking particle assemblage during the iron fertilisation experiment LOHAFEX in the Southern Ocean

Friederike Ebersbach, Philipp Assmy, Patrick Martin, Isabelle Katharina Schulz, Sina Wolzenburg, Eva-Maria Nöthig

(30.09.2013 – submitted to Deep Sea Research I)

F. Ebersbach did the microscopic analysis of sediment trap samples. P. Assmy did the supervision during microscopic examination. P. Martin did the biogeochemical analysis of bulk sediment trap samples. I. Schulz contributed microscopic analysis of surface phytoplankton samples. S. Wolzenburg analysed surface protozooplankton samples. F. Ebersbach wrote the manuscript with contribution from all co-authors.

4. Manuscripts

Manuscript I

Response of a flagellate-dominated plankton community to artificial iron fertilization in the Southern Ocean

Isabelle Schulz^{1,2,#}, Philipp Assmy³, Marina Montresor⁴, Friederike Ebersbach¹, Mangesh Gauns⁵, Christine Klaas¹, Grazia Mazzocchi⁴, Rajdeep Roy⁵, Amit Sarkar⁵, Stefan Thiele⁶, Christian Wolf^d, Sina Wolzenburg¹, Victor Smetacek^{1,5, #}

To be submitted to PLOS ONE

¹ Alfred Wegener Institute Helmholtz Center for Polar and Marine Research, 27570 Bremerhaven, Germany,

² MARUM – Center for Marine Environmental Sciences, University of Bremen, Leobener Str., 28359 Bremen

³ Norwegian Polar Institute, Fram Centre, Hjalmar Johansens gt. 14, 9296 Tromsø, Norway

⁴ Stazione Zoologica Anton Dohrn, Villa Comunale, 80121 Naples, Italy

⁵ National Institute of Oceanography, Dona Paula-Goa, 403 004 India

⁶ Max Planck Institute for Marine Microbiology, Celsiusstr. 1, 28359 Bremen, Germany

corresponding authors

contact: Alfred Wegener Institute Helmholtz Center for Polar and Marine Research, 27570 Bremerhaven, Germany

e-mail: Isabelle.Schulz@awi.de

e-mail: Victor.Smetacek@awi.de

Acknowledgements

We are indebted to the captain and crew of RV *Polarstern*. We thank the co-chief scientist S.W.A. Naqvi for making LOHAFEX a successful experiment. The Council of Scientific and Industrial Research (CSIR), India and the Helmholtz Foundation, Germany equally shared the costs of the experiment. This work was funded through DFG- Research Center / Cluster of Excellence „The Ocean in the Earth System“.

We thank Gandi Forlani, Diana Sarno and Adriana Zingone from the Stazione Zoologica Anton Dohrn, Naples, Italy, for preparation of samples for SEM and support in species identification.

Abstract

Ocean iron fertilization (OIF) experiments carried out in the Southern Ocean (SO) have all induced phytoplankton blooms dominated by diatoms, because silicon required by diatoms was in sufficient supply. However, silicate (dissolved silicon) concentrations are below the biomass accumulation threshold for diatoms over the northern half of the SO where a different response of non-diatom phytoplankton to OIF can be expected. The Indo-German OIF experiment LOHAFEX, lasting over 39 days, was conducted during austral summer 2009 in the core of an oceanic eddy (150-300 km² in size) with low silicic acid concentrations (<2 μM). The objective was to study the temporal developments of a plankton bloom in the natural ecosystem under in situ conditions and allow comparisons between the experimental patch and the unperturbed surrounding waters. Two iron (Fe) infusions on day 0 and 18 applied to the 80 m wind mixed layer (WML) caused a three-fold increase in chlorophyll concentrations from initially 0.5 to 1.5 mg Chl *a* m⁻³ and stabilized thereafter, although rates of primary production remained high (> 1.0 g C m⁻² d⁻¹). Photochemical efficiency (Fv/Fm), measured with a fast repetition rate fluorometer (FRRF), increased within the first six days, reaching its maximum of 0.5 on day 14 indicating that phytoplankton was relieved from iron stress. Despite low silicic acid concentrations some diatom species increased, however their contribution to total standing stocks over the WML was < 5 %. Instead nanoflagellates contributed most (70-90 %) to total standing stocks. Investigation of the nanoflagellate community was based on microscopic counts and HPLC-pigment analyses. Due to the difficulties in distinguishing nanoflagellate species under light microscopy, size categories were the main classification tool. Biomass of bacteria, nanoflagellates but also microphyto- and protozooplankton stayed stable over the course of the experiment due to strong top-down control by larger grazers which resulted in the low particle export below the permanent pycnocline.

1. Introduction

Pelagic ecosystems can be grouped into two broad categories: a) blooms of large-celled phytoplankton generally dominated by diatoms and characterized by new production based on nitrate, and, b) microbial communities based on regenerated production recycled between autotrophic, mixotrophic and heterotrophic nanoflagellates and bacteria that are preyed upon by larger protists, mainly ciliates and dinoflagellates (Pomeroy, 1974, Cushing, 1989; Smetacek et al. 1990). These categories represent successional stages in which the initial phytoplankton bloom accumulates biomass by outstripping mortality by pathogens (viruses), parasitoids (small cells preying on larger ones) and predators (grazers) and grows until a nutrient becomes limiting after which the accumulated biomass, together with the limiting nutrient, sinks out of the surface mixed layer. The second pelagic ecosystem category is then established in the nutrient impoverished, stratified surface layer and maintains itself by recycling the limiting nutrient which is gradually depleted by particles sinking out of the surface layer with the final oligotrophic state being reached in the centres of the subtropical gyres (Karl, 2002).

The limiting nutrient varies between ocean regions: it is nitrogen and/or phosphate along the ocean margins, in the North Atlantic and in the subtropical gyres, but in the open ocean upwelling regions along the Equatorial Pacific, in the Subarctic Pacific and in the entire Southern Ocean, the limiting nutrient is iron. The regions are characterized by high nutrient but low chlorophyll (HNLC) concentrations (Chavez and Barber 1987; Martin et al., 1994; Chavez et al., 1996; Boyd et al., 1998; 2000). Interestingly, the recycling communities inhabiting the nitrate- and iron-limited ocean regions are similar in as much as they both fall into the second category of pelagic ecosystem characterized above (Landry, 2002; Smetacek et al., 2004). Given the high phylogenetic diversity of planktonic protists and the variety of shapes and range of sizes represented in the various phyla, it is surprising that the same superficial structure of the pelagic ecosystem prevails over most of the ocean. In contrast, there is much more variety in terms of shape and size amongst the contributors to plankton blooms that arise when resources (light and nutrients) are not limiting. No doubt, diatoms tend to dominate blooms, but it should be remembered that this is a vast group that evolved at about the same time as the angiosperms, and is speciating at about equal rates, implying that genetic distances amongst the diatom groups will be as much as that between grasses and trees (Armbrust, 2009). At least in terms of shape, the two ends of the geometric spectrum:

spheres and needles are occupied by diatom species that have been observed to dominate blooms, with many variations in between (Smetacek, 1999). Hence, treating the diatoms as a homogeneous group is like treating the bulk of the terrestrial vegetation as “angiosperms” and expecting to make sense of their ecology. Besides, there are other groups such as dinoflagellates and prymnesiophytes which contribute substantially to, or even dominate, bloom biomass, particularly along continental margins but also well offshore. Their respective impacts on ecology and biogeochemistry of the occupied water mass will differ widely. The point we are making is that blooms exhibit much more variability than the apparently uniform microbial communities.

As mentioned above, there is a much higher phylogenetic diversity within the functional groups lumped under the terms nanoflagellates or picoplankton than there is within groups of the microplankton, e.g. dinoflagellates, diatoms, etc. (Fenchel, 2002). Thus amongst the (phyla) represented amongst the nanoflagellates are groups that are ancient (e.g. kinetoplastids) and others that are recent arrivals (e.g. choanoflagellates); besides, all the groups represented within the bloom-forming microplankton are also present in the microbial community. This diversity within superficially similar (to the human eye) components of a tightly-knit network of interaction between auto- and heterotrophs is remarkable given the comparative homogeneity of the well-mixed surface layer and raises a number of questions pertaining to the structure and functioning of the microbial network at the species or at least genus level (Hutchinson, 1961). Thus, the limiting nutrient will be available at very low concentrations, which implies that the uptake efficiency of all the autotrophs present is likely to be at similar levels, since competitive exclusion (Hardin, 1960) does not seem to take place. Furthermore, the survival ability of the various species involved in the face of heavy grazing pressure is apparently also comparable.

We studied the dynamics of a microbial community during the course of a 39-day iron fertilization experiment (LOHAFEX) located in an eddy encircled by a meander of the Polar Front in the Atlantic Sector of the Antarctic Circumpolar Current (ACC). Ocean iron fertilization (OIF) experiments were conceived to test the iron hypothesis (Martin 1990) but they also lend themselves to the study of temporal developments in natural ecosystems under in situ conditions and allow comparisons between the experimental patch and the unperturbed surrounding waters. LOHAFEX was carried out in late summer in a region of the ACC where silicate concentrations reach very low levels and the pelagic ecosystem is dominated by the microbial community. The dynamics of the microbial community was studied using

microscopy (Thronsen, 1995) and HPLC pigment analysis (Uitz et al., 2006). Our study was part of a comprehensive interdisciplinary investigation including 1.) the evolution of the patch (Martin et al., 2013), 2.) the export flux (Martin et al., 2013 and Ebersbach et al., in revision), 3.) the bacterioplankton composition and abundance (Thiele et al., 2012), 4.) the protozooplankton composition and abundance (Schulz et al., in preparation, Manuscript III), and 5.) the structural (composition and abundance) and functional (grazing) responses of mesozooplankton to the evolution of the bloom (Mazzocchi et al., in preparation (Manuscript IV); González et al., in preparation).

2. Materials and Methods

2.1. Study site and tracking of the fertilized patch

LOHAFEX was carried out in the Atlantic sector of the Southern Ocean during RV Polarstern cruise ANT-XXV/3 from 27 January to 6 March 2009 (Fig. 1). A stable cyclonic eddy, located at approximately 48° S 16°W and originating from the Polar Frontal Zone (PFZ), was chosen as the experimental site. The chosen eddy provided a coherent water mass over the course of the experiment, and the wind mixed layer (WML) depth was initially at 50 m but deepened to 70 - 90 m during the last two weeks (Martin et al, 2013).

With 39 days, LOHAFEX was the longest OIF experiment carried out so far. During the first fertilization, 10t of dissolved iron (II) sulphate (FeSO_4) were applied to a 300 km² patch, resulting in a final concentration of $\sim 1.2 \text{ nmol L}^{-1}$. A second fertilization, releasing an additional 10t of dissolved FeSO_4 , was conducted 18 days later.

Four different ways of tracking the patch were used: 1. Trajectories of GPS drifters, 2. Labeling with the inert tracer sulfurhexafluoride (SF_6) released together with the FeSO_4 solution, 3. Online measurements of photosynthetic efficiency (Fv/Fm), 4. Underway Chl *a* sampling and continuous pCO₂ measurements.

2.2. Sampling

For phytoplankton pigment analyses 1.5 - 3 L and for fluorometric chlorophyll *a* measurements 1 L of seawater was filtered at all stations onto 0.7 μm Whatman glass fibre filters (GF/F). Phyto- and microzooplankton samples were collected at 5 discrete depths (10, 20, 40, 60, 80 m) in the WML (table 1) with Niskin bottles attached to a CTD (conductivity, temperature, depth) rosette (SeaBird Electronics, USA). One set of samples was fixed with hexamethylenetetramine-buffered formaldehyde (2% final concentration) and another set with Lugol's iodine solution (5% final concentration). Phytoplankton pigment samples were stored at -80°C and phyto and microzooplankton samples dark at 4°C.

For estimating the species composition and abundance of large protozooplankton and copepods <1 mm (including nauplii, early copepodites, and adults of small cyclopoids), the whole content of one Niskin bottle (12 L) was gently passed over 20 μm mesh sized gauze and concentrated to a final volume of 50 ml. In addition to hexamethylenetetramine-buffered formaldehyde (2% final concentration), strontium chloride (SrCl_2) was added to prevent dissolution of acantharian skeletons. Copepods >1 mm were collected with multi-nets (200 μm mesh) tows in the upper 200 m of the water column. To determine bacterial and archaeal

abundance formaldehyde (1% final concentration) fixed seawater samples (20-100 ml) from each station (table 1) were filtered onto 0.22 μm pore size polycarbonate filters (Millipore, Eschborn, Germany) (Thiele et al., 2012) and stored at -20°C .

2.3. Bacterial and Archea

Total cell counts were taken from Thiele et al., (2012). In order to calculate the total biomass of bacterial and archaeal cells, we calculated total cell volume (TCV) from total cell counts (TCC, in cells mL^{-1}) and the average biovolume of the cells (V , in μm^3) following the equation $\text{TCV} = \text{TCC} \times V$. Pictures for the biovolume analyses were taken using a Zeiss Axio Imager.Z2 (Zeiss, Jena, Germany) microscope and the software package AxioVision Release 7.6 (Zeiss, Jena, Germany) with the automated imaging routine MPISYS (Zeder, unpublished). The average biovolume was calculated from measurements of 1000 to 11000 cells per station using the YABBA software (Zeder et al., 2011). Cell volumes lower than 18 pixel and higher than 600 pixel were not taken into account. The biomass was then obtained by calculating the cell dry weight according to Loferer-Kröbber, using the total biovolume, and assuming 50% of the dry weight comprises carbon (Loferer-Kröbber et al., 1998).

2.4. Nano- and microplankton

Cells were identified and enumerated using inverted light and epifluorescence microscopy (Axiovert 200 and Axio Observer 1.0, Oberkochen, Germany) according to Thronson (1995).

To determine nanoplankton abundance and biomass, Lugol preserved water samples, were settled in 10 mL sedimentation chambers (Hydrobios, Kiel, Germany) for 24 hours. Due to the lack of distinctive morphological features size differentiation was the main classification tool for most flagellates and small round, in the following termed as coccoid, cells. They were classified in three size categories: $< 3 \mu\text{m}$, $3-6 \mu\text{m}$ and $6-20 \mu\text{m}$. The prymnesiophyte *Phaeocystis antarctica* has been classified in two size categories $2-4 \mu\text{m}$ and $4-6 \mu\text{m}$ and *Emiliana huxleyi* only in one size category ($5-10 \mu\text{m}$). More distinct flagellates could be identified to species level (e.g. *Leucocryptos marina*, *Telonema* sp., *Plagioselmis* sp., *Halosphaera viridis*) using scanning electron microscopy (SEM). SEM preparations were made at the Stazione Zoologica in Naples, Italy, following the methods illustrated by D. Sarno (Sarno et al., 2005) and observed using a JEOL JSM-6700 SE Filter SEM (JEOL-USA Inc., Peabody, MA, USA).

To determine microplankton, hexamethylenetetramine-buffered formaldehyde fixed water samples were settled in 50 ml sedimentation chambers for 48 hours. Diatoms, dinoflagellates (< 20 µm) and ciliates were counted according to their abundance in transects, in half or the whole chamber.

To estimate phytoplankton biomass, cell size of each species/category was measured on 20 randomly picked cells and their biovolume calculated from equivalent geometrical formulas (Hillebrand et al., 1999). The biovolumes were then converted into cellular carbon contents using carbon conversion factors for specific plankton groups after Menden-Deuer and Lessard (2000). Abundance and biomass of all species described in this study are trapezoidal depth-integrated values for the WML, $N_t = \left(\int_0^{80} N dz \right) / z$ where N_t is the average abundance at time t , $\int_0^{80} N$ the depth integral and z the depth (80 m).

2.5. Autotrophic and heterotrophic nanoflagellate investigation through epifluorescence counting technique

Hundred milliliter samples were preserved with glutaraldehyde at the final concentration of 0.3% and stored at 40 °C for up to 24 hours before slides for nanoflagellate enumeration were prepared. Subsamples of 40 mL or 60 mL were stained with DAPI and proflavin (Porter and Feig, 1980; Haas, 1982), filtered onto 0.8 µm black nucleopore filters and mounted in type- F immersion oil on glass slides. Slides were stored frozen at -200 °C until analyses. Autotrophic and heterotrophic nanoflagellates were counted on an Olympus BH2 epifluorescence microscope at 1000x magnification. Red or orange-red auto-fluorescing cells were counted as autotrophic nanoflagellates whereas only green fluorescing (proflavin) cells were counted as heterotrophic nanoflagellates. Flagellates were further categorized into four major size classes- upto 2 µm, 2-5 µm, 5-10 µm and 10-20 µm.

2.6. Large protists and copepods

Large shell-bearing protists (>20 µm) and copepods < 1 mm were enumerated according to the method of Thronson (1995). All samples were settled in 50 mL sedimentation chambers (Hydrobios, Kiel, Germany) at 4°C for 48 hours. Depending on their size and abundance, organisms were counted at 50-200 magnification in transects (1-4), a quarter, half or complete Utermöhl chamber. In order to obtain a statistically robust result from the quantitative analysis, samples were analyzed until at least 50 cells of the most abundant species and in total 500 cells were counted. In total 10 functional groups could be distinguished: aloricate and loricate (tintinnid) ciliates, athecate (naked) and thecate (armoured) dinoflagellates,

foraminifera, acantharia, the taxopodidan *Sticholonche zanclea*, radiolaria, silikoflagellates and copepods. Naked ciliates were not retained quantitatively by the 20 μm gaze and therefore counted in Lugol fixed samples (see above). Large protist biomass was calculated as described above. The carbon content of the most abundant copepod species >1 mm, including *Calanus simillimus*, *Calanoides* sp., *Ctenocalanus citer*, *Clausocalanus laticeps*, *Pleuromamma*, *Oithona similis* and *Oithona atlantica*, was measured with a Carbon-Hydrogen-Nitrogen- (CHN) analyzer (Thermo CHN Flash EA112).

2.7 HPLC-Pigment Analyses

Extraction of pigments was done in 3 ml of 100% acetone for 1 min in a sonic dismembrator (Fisher Scientific, Model 100) with an output of 40 W submerged in a beaker of ice to prevent heat accumulation. The extracts were then stored approximately 8 hours (hrs) at -20°C for High Performance Liquid Chromatography (HPLC) analysis. These were passed through a Teflon syringe cartridge (Millipore) having a glass fiber pre acrodisc filter (pore size 0.45 μm , diameter 25 mm) to remove the cellular debris before analysis. The clear sample was then collected in a 2 mL glass vial and placed directly into the temperature controlled (5°C) auto-sampler tray for HPLC analysis. Entire extraction procedure was carried out in dim light and at low temperature to minimize degradation of pigments. Pigments were separated following a slight modification of the procedure of Bidigare et al., (2002), which provides quantitative analysis of 20 pigments and qualitative analysis of several others. The HPLC system was equipped with an Agilent 1100 pump together with online degasser, an Agilent diode array detector connected via guard column to an Eclipse XDB C8 HPLC column (4.6 X150 mm) manufactured by Agilent Technologies. The column was maintained at 60°C . Elution at a rate of 1.1 ml/minute was performed using a linear gradient program over 22 min with 5/95% and 95/5% of solvents B/A being the initial and final compositions of the eluant, where solvent B was methanol and solvent A was (70:30) methanol and 28 mM Tetra Butyl Ammonium acetate (pH 6.8). An isocratic hold on 95% B was necessary from 22 to 27 min for the elution of the last pigment (a- or b-carotene) at approximately 27 min. After returning to the initial condition (5% solvent B) by 31 min, the column was equilibrated for 5 min prior to next analysis. The eluting pigments were detected at 450 and 665 nm (excitation and emission) by the diode array detector. All chemicals used were of HPLC-grade, procured from E. Merck (Germany) and pigments standards were purchased from DHI (Denmark).

In order to retrieve the taxonomic composition of phytoplankton from some marker pigments, the HPLC approach has been analyzed using the CHEMTAX program (Mackey et al., 1996).

Seven taxa were chosen based on the previous published data available from the region (Wright et al., 1996).

2.8 Statistical data analysis

Mann-Whitney U-test was applied to test differences between in-patch and out-patch station data sets. All data were tested for equality of variances via Levene's test.

3. Results

3.1 Environmental setting

In the first three weeks the fertilized patch completed two rotations within the eddy core, before moving southward (Martin et al., 2013). Maximal wind speeds of 11 m s^{-1} were recorded and the mixed layer depth varied between 50-80 m (Martin et al., 2013). Over the course of the experiment nitrate decreased from initially 20 to $17 \text{ }\mu\text{M}$ and phosphate from 1.3 to $1.1 \text{ }\mu\text{M}$. Silicic acid concentrations were low and ranged from 0.5 to $1.4 \text{ }\mu\text{M}$.

Chl *a* standing stocks doubled from initially 36 mg m^{-2} to 77 mg m^{-2} on day 13. The second fertilization caused a further increase with a maximum Chl *a* standing stock of 94 mg m^{-2} on day 23. The six OUT stations showed a mean Chl *a* value of 44 mg m^{-2} (± 8.0). The temporal trend of phytoplankton carbon (PPC) and corrected PPC is in good agreement with the temporal trend of Chl *a* (Fig. 2). This validates the accuracy of the biomass data obtained by microscopy. Primary productivity based on ^{14}C bottle incubations increased within the patch to a maximum of $1600 \text{ mg C m}^{-2} \text{ d}^{-1}$ and remained below $1000 \text{ mg C m}^{-2} \text{ d}^{-1}$ outside the patch. The second fertilization caused no further increase, but values remained high at $1300 \text{ mg C m}^{-2} \text{ d}^{-1}$ (M.Gauns, personal communication). Prior to fertilization photochemical efficiency (F_v/F_m), measured with a fast repetition rate fluorometer (FRRF), was low (~ 0.33) and increased within the first six days, reaching its maximum of 0.5 on day 14 (Martin et al., 2013). Particulate organic carbon (POC) increased from initially 6 g C m^{-2} to its maximum on day 14 with 11 g C m^{-2} (Fig. 3 A, black stars). The mean out-patch value was 7.6 g m^{-2} (± 0.94) (Fig. 3 B, black stars). These results show that the first fertilization produced a notable increase in biomass. The majority (60-90 %) of the size-fractionated biomass was allocated in the $< 20 \text{ }\mu\text{m}$ phytoplankton fraction.

3.2 Plankton community and standing stocks

Although plankton standing stocks generally exceeded POC stocks there was a good agreement between the two (Fig. 3 A & B). Note that copepods >1 mm are not included in POC stocks because larger copepods were hand-picked from POC filters when encountered. Total plankton standing stocks inside the patch increased from initially 8.4 g C m⁻² to 11.5 g C m⁻² on day 24.6 (Fig. 3 A). Standing stocks outside the patch remained stable at 8.7 g C m⁻² (\pm 0.5) (Fig. 3 B). Diatoms contributed < 5 % and < 4 % to total phytoplankton biomass inside and outside the patch, respectively. Non-diatom phytoplankton, dominated by unidentified flagellates and coccoid cells accounted for the largest fraction of total plankton and > 48% and 29% of phytoplankton standing stocks, respectively. The bacterial and archaean community stayed stable over the course of the experiment, at 0.48 (\pm 0.03) g C m⁻² for inside and 0.43 g C m⁻² (\pm 0.08) outside the patch, only members of the SAR11 clade showed a significant increase in abundance towards the end of the experiment (Thiele et al., 2012). Stocks of protozooplankton and copepods <1 mm remained relatively stable at 0.84 g C m⁻² (\pm 0.16) and 0.25 g C m⁻² (\pm 0.06) inside the patch, respectively and declined outside the patch. Standing stocks of copepods > 1 mm showed a considerable variability both inside and outside the patch.

3.2.1 Phytoplankton community composition

Although accounting for a minor fraction (4-5 %) of phytoplankton standing stocks diatoms showed a biomass increase inside the patch from initially 344 mg C m⁻² to 457 mg C m⁻² on day 9.5 and declined thereafter to initial values (Fig. 4 A). Stocks outside the patch increased slightly from 344 to 389 mg C m⁻². Ten species/genera (*Thalassionema nitzschioides*, *Corethron pennatum*, *Haslea trompii*, *Navicula* sp., *Lennoxia flaveolata*, *Thalassiosira* spp. < and >20 μ m, *Fragilariopsis kerguelensis*, *Pseudo-nitzschia* spp. and *Ephemera* sp.) accounted for the bulk (95 %) of diatom biomass while the remaining seven species occurred at background levels. Four response patterns could be discerned among the ten dominant species inside the patch: (i) declining stocks from the beginning, (ii) more or less constant stocks throughout the experiment, (iii) stocks that initially increased and declined thereafter, and (iv) stocks with a continuous increase. *T. nitzschioides* belonged to the first category with a steep initial and a more continuous decline thereafter and stocks outside the patch declined from initially 163 mg C m⁻² to 51 mg C m⁻² by the end of the experiment (Fig. 4 B). Stocks of *Navicula* sp. and *C. pennatum* showed no consistent trend inside the patch while stocks outside increased both 2-fold (Figs. 4 C & D). Stocks of *F. kerguelensis*, *Ephemera* sp. and

Pseudo-nitzschia spp. initially increased 2.4-fold, 7.5-fold and 3.4-fold until days 9.5, 13.9 and 9.5 respectively, while stocks outside stayed rather constant in the former two species and increased 2-fold in the latter species (Figs. 4 E & F; 5 A). *L. flaveolata* and *Thalassiosira* species < 20 and > 20 μm exhibited a continuous increase inside the patch (Figs. 5 B-D). While a similar increase outside the patch was observed for the former species the latter two categories showed a significantly steeper increase inside compared to outside the patch (T-test, $p < 0.05$).

Phytoplankton other than diatoms accounted for the bulk (95%) of phytoplankton biomass. Stocks of non-diatom phytoplankton were higher inside than outside the patch and were dominated by unidentified flagellates and coccoid cells with a mean contribution of 3890 mg C m^{-2} (± 790) and 2190 mg C m^{-2} (± 628) respectively (Fig. 6 A & B). Two prymnesiophytes, the haptophyte flagellate *Phaeocystis antarctica* and the coccolithophore *Emiliana huxleyi*, accounted for 11 % and 4 % of phytoplankton standing stocks. While the former showed a 2.6-fold increase the latter species declined from initially 484 mg C m^{-2} to 137 mg C m^{-2} at the end of LOHAFEX (Fig. 7 A & B). However, there was no significant difference between stocks inside and outside the patch in both species. Within the prasinophytes, stocks of Mamiellales and *Halosphaera viridis* initially increased and declined thereafter while stocks outside the patch stayed relatively constant (Fig. 8 A & B).

Heterotrophic nanoflagellates (HNF), differentiated from autotrophic nanoflagellates (ANF) by epifluorescence microscopy, accounted for 10 – 30% of total nanoflagellate abundances (Fig. 9 A). The heterotrophic taxa identified under light microscopy, including the three cryptophytes *Leucocryptos marina*, *Plagioselmis* sp. and *Telonema* sp., choanoflagellates and heterotrophic dinoflagellates < 20 μm , accounted together for only 3 % of total nanoflagellates cell counts (Fig. 9 B).

During our study the phytoplankton carbon (PPC) to chlorophyll ratio was exceptionally high reaching a ratio of 89.6 and intercept of 43 mg C m^{-2} (Fig. 10). Counts through inverted light microscopy led to an overestimation of autotrophic flagellates (< 20 μm). Instead most of the cells were mixotrophic flagellates. These have higher carbon to chlorophyll ratios. Hence during our study we ‘corrected’ the PC by subtraction of 3,4 g C m^{-2} at each station (Fig. 2, 3, 14). This value was derived from the y-intercept (43 $\mu\text{g C L}^{-1}$) integrated over 80 m.

3.2.2 Protozooplankton microscopy

Standing carbon stocks of protozooplankton prior the fertilization (day -0,6) amounted to 1276 mg C m^{-2} , decreased to 765 mg C m^{-2} on day 5 and thereafter increased again to 1112

mg C m⁻² on day 14 inside the patch. Values decreased after the peak on day 14 and remained stable until the end of the experiment with a mean value of 813 mg C m⁻² (\pm 111 mg C m⁻²). Protozooplankton standing carbon stocks for were only investigated at two out-stations (day 16 and 35) but with 877 mg C m⁻² and 655 mg C m⁻² on days 16 and 35, respectively, fell within the range reported for the in-patch stations. The bulk of protozooplankton biomass was contributed by tintinnid ciliates (mean: 410 mg C m⁻² \pm 154 mg C m⁻²) and heterotrophic dinoflagellates (mean 185 mg C m⁻² \pm 35 mg C m⁻²). Autotrophic dinoflagellates contributed 449 mg C m⁻² \pm 169 mg C m⁻² and are grouped under non-diatom-phytoplankton in Figure 1. The contribution of rhizaria, including acantharia, foraminifera, radiolaria and the taxopodidan *Sticholonche zancelea*, to total protozooplankton standing stocks was minor. Acantharia contributed 4% within the patch and 6% out of the patch and foraminifera 4% within and 3% out of the patch. The contribution of radiolaria was less than 0.1% both inside and outside the patch. The detailed response of the protozooplankton assemblage over 500 m depth, will be described in a separately paper Schulz et al. (in preparation/ Manuscript III).

4. Discussion

Over a dozen iron fertilization experiments have been carried out since 1993 (IronEx I, Martin et al., 1994) in iron-limited oceanic waters to test the iron hypothesis proposed by Martin (1990). The first condition of his hypothesis, that phytoplankton growth rates are limited by iron deficiency in the HNLC regions of the ocean, was confirmed by all experiments as indicated by the increase in photosynthetic efficiency (F_v/F_m) of phytoplankton upon iron addition (Boyd et al., 2007). In most of the experiments, alleviation of iron deficiency resulted in a several-fold increase of chlorophyll concentrations and a subsequent, significant increase in biomass and particulate organic carbon (de Baar et al., 2005). In all cases where a bloom developed, diatoms contributed the bulk of the biomass, particularly where silicate concentrations were sufficiently high. In one case, the SOFEX-north patch, silicate concentrations in the region were low ($< 3 \text{ mmol m}^{-3}$; Coale et al. 2004) but did not reach limiting concentrations within the patch presumably due to replenishment of this element by admixture from the surroundings (Coale et al, 2004; Bishop et al., 2004). This was possible because the patch was stretched into a streak 340 km long but only 7 km broad patch, which facilitated dilution of the patch with surrounding waters along its breadth. Although detailed monitoring of the SOFEX south bloom composition was not carried out, it was estimated that diatoms dominated bloom biomass (Coale et al., 2004), the remainder was contributed by various flagellate groups.

In the two experiments where biomass increase was less marked, one was located in the Subantarctic zone with very low silicate concentrations (SAGE); however, the patch here was also pulled into a narrow streak within the 2 week experiment, so it is possible that an increase in biomass was hampered by strong dilution with outside water (Peloquin et al., 2011). The other experiment, SEEDS II, with a minor biomass increase (Suzuki et al., 2009) was carried out in the same region and under much the same conditions as SEEDS where a massive, almost mono-specific diatom bloom of *Chaetoceros debilis* occurred in the 10-day long experiment (Tsuda et al., 2003). However, during SEEDS II a broad range of diatom species was present, but they did not bloom despite adequate silicate availability. Instead the 2.5-fold increase in chlorophyll by the end of the second week was due to nanoflagellates comprising prymnesiophytes and prasinophytes initially, followed by cryptophytes a week later (Sato et al., 2009). By the end of the fourth week phytoplankton pigments were lower than the initial values.

4.1.1 The LOHAFEX experiment

The LOHAFEX patch was fertilized in the centre of the closed core of a mesoscale eddy, and the initial patch size of 300 km² was much larger than that of previous experiments, hence the effects of dilution in the centre of the patch during the first 3 weeks will have been negligible. At the time of the second fertilization (Day 18), the eddy started collapsing which led to subsequent elongation, hence promoted dilution along the length of the patch, and its eventual expulsion to the south. Thereafter, the patch, or rather the portion not advected to the east, reached a stable position by Day 32 and remained stationary until the end of the experiment. Dilution is likely to have been low during this final phase as well (Martin et al., 2013).

The experiment was located in the productive SW Atlantic sector of the Antarctic Zone (AZ, the band of the ACC between the winter ice edge and the Polar Front), which receives more iron from various sources than the more remote, less productive SE Atlantic sector where EisenEx and EIFEX were located. The sources of iron are from Patagonian dust, from sediments and runoff from the Antarctic Peninsula and its associated islands as well as South Georgia and from “fossil” dust released from melting ice bergs (Raiswell et al., 2008). This sector has a particularly high density of ice-bergs in the AZ that emanate from the Bellingshausen and Weddell Seas and drift north-eastwards from the Peninsula tip, to break up and melt by the time they reach the latitude of the Polar Front (Borrione et al., 2013). The substantial effect of ice-berg fertilization has been verified in several studies (Smetacek et al., 1997; Smith et al., 2007; Raiswell et al., 2008; Schwarz et al., 2009; Smith et al., 2011; Verneta et al., 2011). As a result of the higher productivity, Si concentrations in the surface layer of the AZ are depleted to very low levels by the end of the austral summer by a succession of diatom populations stimulated by various sources of natural iron input over the course of the growth season. Silicate concentrations in the eddy core (0.5 to 1.4 μM) were at the limit of detection of the method and nitrate concentrations declined from 20 μM to 17 μM at the end of LOHAFEX. In contrast, EIFEX was also conducted at the same latitude and in late summer but in the less-productive SE Atlantic Sector; thus, silicate concentrations in the eddy core pinched off from the AZ by a meander of the Polar Front were initially >15 μM m⁻³ and were reduced by about half by the end of the experiment on 20 March 2004. Nitrate concentrations declined from > 25 to 23.5 μM from beginning to end of the experiment.

A pre-experimental site survey of the AZ, carried out to the west of the LOHAFEX eddy, from the Polar Front due north of South Georgia to as far south as 52°S, revealed that surface layer silicate concentrations were extremely low: < 3 μmol m⁻³ and diatom populations at low biomass levels throughout the region traversed by the ship (Smetacek and Naqvi et al., 2010).

Nevertheless, the composite satellite image of the LOHAFEX bloom taken on days 14-16 clearly shows patches and streaks of chlorophyll concentrations of similar, or even higher levels in the surroundings (Fig. 1), most likely triggered by local dust outfall (Cassar et al., 2007) or by melting ice-bergs of which some were very large, with extending melt-water plumes (Wolf-Gladrow, personal communication). The higher productivity of the southwestern compared to the southeastern Atlantic sector of the ACC can be seen from the distribution of green, yellow and orange shades in Fig. 1. It is highly unlikely that diatoms contributed to the biomass of these natural blooms, in particular the large, intense bloom to the northeast of the LOHAFEX eddy whose provenance is mysterious. Hence it is likely that the composition of the LOHAFEX bloom was basically similar to those of the natural blooms. The zooplankton community of the LOHAFEX eddy, but also the area that was surveyed, was dominated by three copepod species: the large *Calanus simillimus*, the medium-sized *Ctenocalanus citer* and the small *Oithona similis* (H. Gonzalez, personal communication). Euphausiids were present in very low numbers and salps were not recorded in the multinet samples collected in the epipelagic layer. The macroplankton was dominated by the hyperiid amphipod *Themisto gaudichaudii* which is a voracious, visually-oriented predator occurring in mobile swarms. Smetacek et al. (2004) have argued that, in addition to feeding on copepods and pteropods, *Themisto*, with its large eyes, is also equipped to feed on transparent chaetognaths and salps. Since the composition of the phytoplankton was of the ideal size for filter-feeding salps, *Themisto* predation is the most likely reason for the absence of salps in the epipelagic layer. An interesting question arising here is whether higher salp abundances, often found in the ACC (Atkinson et al., 2004), would have had an effect on the nanoplankton bloom.

4.1.2 Processes within the patch

The phytoplankton of the LOHAFEX region was iron limited as indicated by the increase in Fv/Fm following fertilization, which rose from 0.33 initially to a maximum of 0.5 on day 14 (Martin et al., 2013). Chlorophyll stocks also increased steadily inside the patch (Fig. 2) from 36 to 94 mg Chl m⁻² (0.5 to a maximum of 1.2 mg m⁻³). The peak was reached on Day 22.6 after which stocks decreased at first fairly abruptly and then levelled off at values only slightly, but significantly, above outside values, which remained more or less constant throughout the experiment. We suspect that the first abrupt decline between Days 22.6 and 24.6 was primarily due to dilution with outside water as it occurred concomitantly with the elongation and rapid movement of the patch within the collapsing eddy. Thereafter dilution

rates decreased and chlorophyll concentrations stabilised. Phytoplankton biomass stocks increased in parallel with chlorophyll and contributed about half of the total plankton biomass estimated from microscope counts of all organisms groups (Fig. 3 A). Particulate organic carbon (POC) stocks measured with a Carbon-Nitrogen (CN) analyzer correlated remarkably well with total biomass stocks ($y = 0,9866x + 51,057$, $r^2 = 0,75673$) (Fig.11) as was also the case in the diatom-dominated EIFEX bloom (Assmy et al., in revision). The large copepods were not included in the comparison because they were removed from the filters prior to measurements. Copepod stocks in terms of carbon in the top 200 m layer varied 5-fold between stations without significant differences between inside and outside the fertilized patch, presumably due to small-scale patchiness. Copepod diel vertical migration, followed with an Underwater Video Profiler, was pronounced in the upper 200 m layer, likely in response to feeding activities or escaping visual predators, which can only have been *Themisto* sp. (Mazzocchi et al., 2009).

By far the bulk of the phytoplankton biomass throughout the experiment both inside and outside the patch was in the size fraction 3 – 20 μm . This is an exceptional finding because as a rule blooms are dominated by large cells (Cullen, 1991). It needs to be pointed out that the peak chlorophyll concentration attained by the LOHAFEX bloom of 1.2 mg m^{-3} would not qualify for bloom status over most of the ocean, where mixed layer depths are much shallower than in the ACC. But it is the size of the total stock integrated over the surface mixed layer that is relevant both for the carbon cycle and the food supply to higher trophic levels and the benthos. Thus, the peak chlorophyll stock recorded on Day 22.6, if condensed into a 10 m surface layer typical of coastal regions, but also found in SEEDS I, would be equivalent to $9.4 \text{ mg Chl m}^{-3}$ which would be considered a bloom by any standard. In the ACC, chlorophyll concentrations $>1 \text{ mg m}^{-3}$ require a recent input of iron hence qualify as “blooms” against the barren HNLC ocean. Hence, the fact that the LOHAFEX bloom only doubled the initial biomass does not detract from its status of a bloom but highlights the high background productivity of the region where the experiment was carried out compared to most of the ACC.

Another unusual feature of the LOHAFEX bloom is its exceptionally high phytoplankton carbon (PPC) to chlorophyll ratio of 89.6 and intercept of 43 mg C m^{-2} (Fig. 10 A). In contrast, PPC/Chl ratios of 19 and 24 with an intercept close to zero were found in the diatom-dominated EisenEx and EIFEX patches (Assmy et al., 2007; Smetacek et al., 2012). There are several explanations for the discrepancy. The slightly higher PC than POC values are clearly due to a methodological error resulting in overestimation of biomass of the

nanoflagellate size classes. Because biomass increases by the cube of the length, a slight bias in assigning cells to the size classes chosen can lead to over- or under-estimation of total biomass. However, the size spectrum of the plankton did not change significantly over the duration of the experiment, both inside and outside the patch. The main reason for the high PPC/Chl ratio is most probably due to the fact that the bulk of the “phytoplankton” cells were actually mixotrophic flagellates, which inherently have higher ratios than the purely autotrophic diatoms where chloroplasts constitute most of the biomass. Hence during our study we ‘corrected’ the PC by subtraction of 3,4 g C m⁻² at each station. This value was derived from the y-intercept (43 µg C L⁻¹) integrated over 80 m (Fig. 10 A). The lower POC/PON ratio of the LOHAFEX (4.9 ± 0.1) (Fig. 12) as compared to the EIFEX bloom (5.3 ± 0.8) could be explained by the larger amount of structural lipids in the chloroplasts as compared to the phagotrophic apparatus, which presumably consists of structural proteins, as also the flagella that are extremely large relative to cell size in many taxa.

Since many of the chlorophyll-bearing cells were also practising phagotrophy, a strict separation of phytoplankton from the truly heterotrophic protists does not make much sense. We have accordingly inserted a “gray zone” between the obligate heterotrophic protists and the facultative phagotrophs that also carry chloroplasts (Fig. 3 A & B). Many of the mixotrophic flagellates will, together with the “classic” bacterivorous heterotrophic nanoflagellates, choanoflagellates and kinetoplastids (Fenchel, 1982), have ingested bacteria. A detailed study of bacterial production rates, abundance and biomass as well as taxonomic composition revealed higher thymidine and leucine uptake rates inside the patch but otherwise only minor differences in abundance, biomass and taxonomic composition between inside and outside the patch (Thiele et al., 2012). A remarkable feature of the bacterial assemblage was the lack of trends over time in biomass and composition. The rather low biomass levels were attributed to the heavy grazing pressure exerted by the large flagellate assemblage. Indeed, the only significant, albeit minor, increase in any of the bacterial taxa was the clade SAR11, which is reputed to be grazer protected by its small size (Morris et al., 2002; Thiele et al., 2012).

Summing up, iron addition promoted chlorophyll synthesis, which led to an increase in cellular chlorophyll levels indicated by the initial decrease in the PPC/Chl and POC/Chl ratios. However, since POC increased concomitantly, a significant amount of the chlorophyll increase was due to an increase in chloroplast biomass. The high, but also highly significant PPC/Chl ratios of 89 (Fig. 10) indicate that there was also a significant increase in heterotrophic biomass fuelled by primary production. When mixotrophic flagellates dominate

plankton biomass, it will be necessary to differentiate the carbon in the autotrophic from that in the phagotrophic apparatus of the same cell as the latter is functioning as a part of the heterotrophic assemblage. This broadening of the concept of heterotrophic biomass will be necessary when assessing the balance between net autotrophy and heterotrophy in ecosystems run by mixotrophs (Flynn et al., 2012). Thus, the ratio of autotrophic/heterotrophic biomass in the diatom-dominated EIFEX bloom increased from 0.7 (day 9) to 1.2 (day 28) and declined thereafter to 0.8 (day 36) and stayed always higher than outside (Assmy et al, in revision). In LOHAFEX the ratio was much higher, even after correcting autotrophic biomass for the systematic errors. Interestingly, levels of primary production estimated with the ^{14}C -method in LOHAFEX in the first 3 weeks were quite similar to those of EIFEX ($\sim 1.5 \text{ g C m}^{-2} \text{ d}^{-1}$), despite the twofold higher Chl stocks in EIFEX. We attribute the discrepancy to grazer protection of the accumulating diatom biomass in the latter experiment in contrast to the less efficient accumulation rate of mixotrophic biomass in the former. This difference between diatom and nanoflagellate based ecosystems thus has profound implications for carbon cycling within the mixed layer and export from it by the biological carbon pump.

4.1.3 Species composition of the LOHAFEX bloom

As can be seen from Fig. 13 A & B only about one quarter of the cells counted for in- and out-patch could be identified at least to group level, the bulk, comprising both coccoid and flagellated cells, were grouped only according to size. A striking feature of the identified biomass is the constancy of the relative proportions contributed by the various groups during the 39 days. The implication is that the assemblage under study was operating at a steady state, hence stable. Since the unidentified pool contributed the bulk of biomass, the 36 % increase in total plankton carbon from Day -1 to Day 24 was most obvious in this category. However, visual examination of the cells assigned here did not indicate that a single taxon was responsible for most of the increase or that there was a significant difference in the relative composition of the entire assemblage inside and outside the patch. This conclusion is corroborated by the results of the pigment measurements, which showed close similarity in relative contributions of the various groups from Day -1 to Day 18.6, the period of biomass increase (Fig. 14 A & B). We conclude that no single taxon was stimulated to a much greater extent than the others and that the response was distributed fairly evenly across the nanoflagellate groups.

The results of the pigment analysis indicate that around two-thirds of the chlorophyll was located in prymnesiophytes with about equal proportions in the coccolithophore and

Phaeocystis subgroups. Prasinophytes contributed most of the remaining one-third with peridinin-containing autotrophic dinoflagellates and diatoms comprising less than 2 % (Fig. 14 A & B).

Microplankton

The stable steady state maintained by the smaller size classes of the classic microbial food web contrasted with the dynamics of the populations of larger species, in particular the diatoms. These variations in the microplankton had little effect on the LOHAFEX bloom stock because their contribution to total phytoplankton biomass verged on the negligible (~ 5 %). Nevertheless, it is worthwhile examining the distinct differences in response patterns of those species that were present in significant numbers, as they shed light on the behaviour of microplankton in general and diatoms under silicate-limiting conditions in particular. Another interesting question arising from these results is why other large phytoplankton species such as *Phaeocystis* colonies, *Ceratium pentagonum* or other species present, did not increase their biomass significantly. In this connection it is worth pointing out that the size categories pico-, nano- and microplankton, arbitrarily fixed at < 2, 2-20, 20-200 µm respectively (Sieburth et al., 1978) and now common currency, are not adequate to differentiate the nanoflagellates of the classic microbial food web from the smaller “microplankton” that regularly form blooms. To the latter belong coccolithophores such as *Emiliana huxleyi* and many dinoflagellates of ~10 µm such as *Prorocentrum* cf. *balticum* whose ecological behaviour is closer to that of larger bloom-forming species than to the classic nanoflagellates. Both were present during LOHAFEX and are dealt with in this section.

Diatoms

Previous OIF experiments have stimulated growth of a broad range of species representing all the major groups of diatoms with wide variation in the species composition of each experiment. In all cases, the species involved belonged to the common diatoms of the respective region, implying that iron fertilization does not favour growth of atypical species and that artificial blooms do not differ from natural blooms caused by local iron input. This also applies to the diatoms of the LOHAFEX experiment. Thus, various common species belonging to pennate and centric groups responded to iron fertilization by increasing their population size. Some of these reached a peak within the first 2-3 weeks and declined thereafter (Fig. 4 E & F), others continued accumulating biomass until the end (Fig. 5 B-D). Other common species behaved like the nanoflagellates and maintained the same levels

throughout (Fig. 4 B & D). During the EisenEx and EIFEX blooms, similar response patterns amongst the diatom assemblages present were recorded, albeit at an order of magnitude higher population sizes (Assmy et al. 2007, Assmy et al., in revision).

Given the fact that silicate concentrations were extremely low, one would expect intense competition for this nutrient and a competitive advantage for thinner-shelled species, i.e. with a Si/N ratio below the average diatom ratio of 1/1 (Takeda, 1998; Hutchins & Bruland, 1998). This was indeed the case for the weakly silicified genera *Ephemera* and *Pseudo-nitzschia*, but larger species (> 20 µm) of the thicker-shelled genus *Thalassiosira* steadily built up their biomass more than fourfold over the course of the experiment (notwithstanding dilution) and also about doubled outside the patch. An alternative strategy would be to drastically decrease the cell size of the species as was observed in the case of *Corethron pennatum* and *Fragilariopsis kerguelensis*. In both cases the average cell length found in LOHAFEX was at the lower end of those reported in the literature (Hasle and Syvertsen, 1996) The dynamics of the diatom species indicate that biomass build-up but not growth rates were limited by the very low Si concentrations (0.5 to 1.4 µM) and the significant increase following fertilization further indicates that they were initially iron-limited. In five cases, the weakly silicified, small *Lennoxia*, *Corethron pennatum*, *Navicula* sp, *Pseudo-nitzschia* spp. and *Thalassiosira* spp., a significant increase in accumulation rates was found in the surrounding waters.

Other bloom-forming phytoplankton species

According to the ecumenical hypothesis (Morel et al., 1991; Cullen, 1995) only large cells dominate blooms because nano- and picoplankton biomass is kept in check by grazing. The LOHAFEX results not only show that this is not a hard and fast rule but they also raise the question as to why large phytoplankton other than diatoms did not build up more biomass. Thus, intense blooms of *Phaeocystis* colonies that can reach individual sizes of >1 mm are a regular feature in the Ross Sea (Arrigo, 2003) and parts of the Arctic (Reigstad and Wassmann, 2007) and have also been observed sporadically in the Weddell Gyre (Smetacek et al., 2004). Although most commonly found in coastal waters, *Phaeocystis* blooms have also been recorded in oceanic waters but to our knowledge have not been reported yet in the region of the Polar Front. This is surprising because the solitary form of the species is one of the dominant constituents of ACC nanoflagellates and colonies are not rare but do not reach bloom proportions. Smetacek et al. (2004) have argued that colony formation is the transition from the vulnerable nanoflagellate to a more secure microplankton stage in the life history of the relevant species. Since the early stages of colony formation are even more vulnerable than

the active nanoflagellate stage, they are often located on diatom spines. During the second week of LOHAFEX a marked increase in *Phaeocystis* epiphytes on various diatom species but largely on spines of *Corethron pennatum* (Fig. 15) and a subsequent increase in free-floating colonies was observed but both declined to very low levels thereafter (Fig. 16). The first increase in epiphytic colonies was likely enabled by protection through their diatom “host” until epiphytic colonies reached a critical size at which they detached from their diatom “host” reflected in the sudden appearance of free-floating colonies and decline in epiphytic colonies (Fig. 16). We attribute the subsequent decline in free-floating colonies to selective grazing by copepods as the colonies had not yet reached the critical size to escape predation by the dominant large copepod species. On-board experiments in which surface water was incubated for 50 hours in 500 mL glass bottles under in situ light and temperature conditions showed a dramatic increase in *Phaeocystis* colonies illustrating the bloom-forming capabilities of this species when grazing copepods are excluded.

Similarly, the other potentially bloom-forming plankton species, *Emiliania huxleyi*, declined during the experiment. In this species the decline occurred simultaneously inside and outside the patch suggesting that iron was not involved. The contribution of this species to the total flagellate biomass of its size class (3 – 6 μm) was 8 % initially and sank to 2 % by the end of the experiment. Similar declines in the populations of this species were also found in EisenEx and EIFEX (Assmy et al, 2007, Assmy et al in revision). Indeed we know of no experiment where coccolithophore populations increased significantly following iron addition. It is well established that coccolithophores are grazed by copepods and that their fecal pellets can be packed with calcite liths (Harris, 1994). However cells can survive gut passage and Smetacek et al. (2004) argued this strategy is selected for by the evolutionary arms race. On board we incubated copepod fecal pellets in growth medium for 19 days and estimated a growth rate range of 0.14 d^{-1} for *E. huxleyi* by counting the cells that had grown out of the fecal pellet and assuming two cells as the inoculum size within the fecal pellet (Fig.17).

E. huxleyi is known to have a complex life cycle in which the coccolith-bearing form is only one of several stages; so it is possible that the decline during LOHAFEX was due to a life cycle transition to the motile, non-calcite stage which escaped identification by light microscopy. The alternative explanation is that cells were killed by viruses or ingested by grazing copepods. Our anecdotal observations raise interesting questions pertaining to the ecology of this biogeochemically important species that are worth pursuing.

Blooms of the genus *Ceratium* sp. are a regular feature of the autumn in the North Atlantic (Hinder et al., 2012), including the Arctic, from coastal seas to the open ocean but have not

been reported from the Southern Ocean although the species *C. pentagonum* can be quite common north of the Polar Front. It was present during LOHAFEX but at low levels. Their crushed cell walls were occasionally observed in fecal pellets, implying that although grazing pressure is likely to have been low, it was enough to suppress a possible response to fertilization. Another species known to reach high abundances in other oceans is the prasinophyte *Halosphaera viridis* (Schmitz, 1878; Bérard-Therriault, 1999). The large phycoma stage, up to 800 μm in diameter, was occasionally observed in zooplankton net samples while the motile quadriflagellate stage (15-20 μm in length) constituted the bulk of biomass. The large phycoma stage was likely an adaptation to the high grazing pressure exerted on the flagellate stage illustrated by the initial iron-induced increase in *H. viridis* standing stocks but its subsequent collapse below out-patch values. This also likely limited the built-up of the phycoma stage because recruitment from the flagellate stage was constrained by grazing.

5. Conclusions

A major finding of this study of a nanoflagellate-dominated pelagic ecosystem is the maintenance of the relative proportions of its component taxa over 39 days, which is remarkable given the fact that the turnover rate of the participating organisms is on the order of days (Giavannoni and Vergin, 2012). A similar structural stability in the assemblage was found in the bacteria, albeit at levels below the average ocean cell concentration (Thiele et al., 2012). The initial biomass of the microbial community in the study area was exceptionally high – about threefold above average ACC levels - due to a combination of natural iron input to the region and the absence of salps. Alleviation of iron limitation resulted in an elevation of biomass of the entire eukaryote community to bloom proportions but the peak biomass attained was well below that achieved by the “classic” phytoplankton generally dominated by larger-celled or armoured phytoplankton. The observations imply that the classical microbial food web based on a network of tight interactions between bacteria and a phylogenetically diverse assemblage of nanoflagellates comprising obligate heterotrophic, mixotrophic and possibly obligate autotrophic species (Strom, 2008) is stabilized by feedback loops within the network that buffer the effects of perturbation by nutrient addition. It follows that microbial networks sensu Smetacek et al. (1990) can be surprisingly resilient.

Diatom accumulation was clearly limited by silicate availability and we attribute the absence of population build-up by other, larger species such as *Phaeocystis* colonies or dinoflagellates to selective grazing exerted by copepods on seed stocks. An explanation for why blooms are “nipped in the bud” in the silicate-limited ACC but not elsewhere is provided by the “merry-go-round” hypothesis of the ACC ecosystems enabling long residence time of the water masses comprising the zonal branches of the ACC within the same climate zone. This allows for maintenance of large copepod populations with differing life cycle strategies ranging from year-round presence in the surface layer to diapausing stages in the deep water column (Smetacek et al., 2004). It is generally accepted that microbial communities are retention systems that lose only a small percentage of organic matter by sinking particles. Nevertheless, vertical flux measured by Thorium measurements indicated loss rates of $\sim 6.3 \text{ mmol POC m}^{-2} \text{ d}^{-1}$ in the patch which amounts to about 13 % of primary production. Richardson and Jackson (2007) argue that loss rates from regenerating systems can be appreciable. However, there was no difference between the magnitude of vertical flux from inside and outside the patch, indicating that loss rates were not necessarily a function of the biomass in the surface layer (Martin et al., 2013). Further detailed observations of the same water column employing

metagenomic approaches, will reveal the degree of specialization and possible niche partitioning within the community that enable resilience to perturbation.

References

- Armbrust, E. V., 2009, The life of diatoms in the world's oceans: *Nature*, v. 459, no. 7244, p. 185-192.
- Arrigo, K. R., Worthen, D. L., and Robinson, D. H., 2003, A coupled ocean-ecosystem model of the Ross Sea: 2. Iron regulation of phytoplankton taxonomic variability and primary production: *J. Geophys. Res.*, v. 108, no. C7, p. 3231-3248.
- Assmy, P., Henjes, J., Klaas, C., and Smetacek, V., 2007, Mechanisms determining species dominance in a phytoplankton bloom induced by the iron fertilization experiment EisenEx in the Southern Ocean: *Deep Sea Research Part I*, v. 54, no. 3, p. 340-362.
- Assmy, P., Smetacek, V., Montresor, M., Klaas, C., Henjes, J., Strass, V. H., Arrieta, J. M., Bathmann, U., Berg, M. G., Breitbarth, E., Cisewski, B., Friedrichs, L., Fuchs, N., Herndl, G. J., Jansen, S., , Krägefsky, S., Latasa, N., Passow, U., Peeken, I., Röttgers, R., Scharek, R., Schüller, S. E., Steigenberger, S., and Webb, A., IN REVISION, 2013, Grazer-protected diatoms decouple ocean carbon and silicon cycles around Antarctica: *PNAS*.
- Atkinson, A., Siegel, V., Pakhomov, E. A., and Rothery, P., 2004, Long-term decline in krill stock and increase in salps within the Southern Ocean: *Nature*, v. 432, no. 02996, p. 100-103.
- Bérard-Therriault, L., Poulin, M., and Bossé, L., 1999, Guide d'identification du phytoplancton marin de l'estuaire et du Golfe du Saint-Laurent incluant également certains protozoaires. : Publication Spéciale Canadienne des Sciences Halieutiques et Aquatiques v. 128, p. 1-387.
- Bidigare, R. R., Van Heukelem., L., and Trees, C. C., 2002, HPLC phytoplankton pigments: Sampling, laboratory methods, and quality assurance procedures.: In: Mueller, J., and Fargion, G., (Eds.), *Ocean Optics Protocols for Satellite Ocean Color Sensor, Revision 3*, v. 2, no. 16, p. 258-268.
- Bishop, J. K. B., Wood, T. J., Davis, R. E., and Sherman, J. T., 2004, Robotic Observations of Enhanced Carbon Biomass and Export at 55 {degrees}S During SOFeX 10.1126/science.1087717: *Science*, v. 304, no. 5669, p. 417-420.
- Borrione, I., Aumont, O., Nielsdóttir, M. C., , and Schlitzer, R., 2013, Sedimentary and atmospheric sources of iron around South Georgia, Southern Ocean: a modelling perspective: *Biogeosciences*, v. 10, p. 10811-10858.
- Boyd, P., Berges, J. A., and Harrison, P. J., 1998, In vitro iron enrichment experiments at iron-rich and -poor sites in the NE subarctic Pacific: *Journal of Experimental Marine Biology and Ecology [J. Exp. Mar. Biol. Ecol.]*. v. 227, no. 1, p. 133-151.
- Boyd, P. W., Jickells, T., Law, C. S., Blain, S., Boyle, E. A., Buesseler, K. O., Coale, K. H., Cullen, J. J., de Baar, H. J. W., Follows, M., Harvey, M., Lancelot, C., Levasseur, M., Owens, N. P. J., Pollard, R., Rivkin, R. B., Sarmiento, J., Schoemann, V., Smetacek, V., Takeda, S., Tsuda, A., Turner, S., and Watson, A. J., 2007, Mesoscale iron enrichment experiments 1993-2005: Synthesis and future directions: *Science*, v. 315, no. 5812, p. 612-617.
- Boyd, P. W., Watson, A. J., Law, C. S., Abraham, E. R., Trull, T., Murdoch, R., Bakker, D. C. E., Bowie, A. R., Buesseler, K. O., Chang, H., Charette, M., Croot, P., Downing, K., Frew, R., Gall, M., Hadfield, M., Hall, J. A., Harvey, M., Jameson, G., LaRoche, J., Liddicoat, M., Ling, R., Maldonado, M. T., McKay, R. M., Nodder, S. D., Pickmere, S., Pridmore, R., Rintoul, S., Safi, K. A., Sutton, P., Strzepak, R., Tanneberger, K., Turner, S., Waite, A., and Zeldies, J., 2000, A mesoscale phytoplankton bloom in the polar Southern Ocean stimulated by iron fertilization: *Nature*, v. 407, no. 6805, p. 695-702.

- Cassar, N., Bender, M. L., Barnett, B. A., Fan, S., Moxim, W. J., Levy, H., II, and Tilbrook, B., 2007, The Southern Ocean Biological Response to Aeolian Iron Deposition: *Science*, v. 317, no. 5841, p. 1067-1070.
- Chavez, F. P., and Barber, R. T., 1987, An estimate of new production in the equatorial Pacific: Deep Sea Research Part I: *Oceanographic Research Papers*, v. 34, p. 1229-1243.
- Chavez, F. P., Buck, K. R., Serivce, S. K., Newton, J., and Barber, R. T., 1996, Phytoplankton variability in the central and eastern tropical Pacific: Deep Sea Research Part II: *Topical Studies in Oceanography*, v. 43, p. 835-870.
- Coale, K. H., Johnson, K. S., Chavez, F. P., Buesseler, K. O., Barber, R. T., Brzezinski, M. A., Cochlan, W. P., Millero, F. J., Falkowski, P. G., Bauer, J. E., Wanninkhof, R. H., Kudela, R. M., Altabet, M. A., Hales, B. E., Takahashi, T., Landry, M. R., Bidigare, R. R., Wang, X. J., Chase, Z., Strutton, P. G., Friederich, G. E., Gorbunov, M. Y., Lance, V. P., Hilting, A. K., Hiscock, M. R., Demarest, M., Hiscock, W. T., Sullivan, K. F., Tanner, S. J., Gordon, R. M., Hunter, C. N., Elrod, V. A., Fitzwater, S. E., Jones, J. L., Tozzi, S., Koblizek, M., Roberts, A. E., Herndon, J., Brewster, J., Ladizinsky, N., Smith, G., Cooper, D., Timothy, D., Brown, S. L., Selph, K. E., Sheridan, C. C., Twining, B. S., and Johnson, Z. I., 2004, Southern ocean iron enrichment experiment: Carbon cycling in high- and low-Si waters: *Science*, v. 304, no. 5669, p. 408-414.
- Cullen, J. J., 1991, Hypotheses to explain high-nutrient conditions in the open sea: *Limnology and Oceanography* [LIMNOL. OCEANOGR.], v. 36, no. 8, p. 1578-1599.
- , 1995, Status of the iron hypothesis after the Open-Ocean Enrichment Experiment: *Limnology and Oceanography*, v. 40, no. 7, p. 1336-1343.
- Cushing, D. H., 1989, A difference in structure between ecosystems in strongly stratified waters and in those that are only weakly stratified: *Journal of Plankton Research*, v. 11, p. 1-13.
- de Baar, H. J. W., Boyd, P. W., Coale, K. H., Landry, M. R., Tsuda, A., Assmy, P., Bakker, D. C. E., Bozec, Y., Barber, R. T., Brzezinski, M. A., Buesseler, K. O., Boye, M., Croot, P. L., Gervais, F., Gorbunov, M. Y., Harrison, P. J., Hiscock, W. T., Laan, P., Lancelot, C., Law, C. S., Levasseur, M., Marchetti, A., Millero, F. J., Nishioka, J., Nojiri, Y., Oijen, T. v., Riebesell, U., Rijkenberg, M. J. A., Saito, H., Takeda, S., Timmermans, K. R., Marcel J. W. Veldhuis, Waite, A. M., and Wong, C.-S., 2005, Synthesis of iron fertilization experiments: From the Iron Age in the Age of Enlightenment: *Journal of Geophysical Research*, v. 110, p. C09S16.
- Ebersbach, F., Assmy, P., Martin, P., Schulz, I. K., Wolzenburg, S., and Nöthig, E.-M., IN REVISION, Sedimentation patterns of phyto- and protozooplankton and sinking particle assemblage during the iron fertilisation experiment LOHAFEX in the Southern Ocean: *Deep Sea Research Part I: Oceanographic Research Papers*.
- Fenchel, T., 1982, Ecology of Heterotrophic Microflagellates. IV. Quantitative Occurrence and Importance as Bacterial Consumers: *Marine ecology progress series*. Oldendorf, v. 9, no. 1, p. 35-42.
- , 2002, Microbial Behavior in a Heterogeneous World: *Science*, v. 296, no. 5570, p. 1068-1071.
- Flynn, K. J., Stoecker, D. K., Mitra, A., Raven, J. A., Glibert, P. M., Hansen, P. J., Granéli, E., and Burkholder, J. M., 2012, Misuse of the phytoplanktonzooplankton dichotomy: the need to assign organisms as mixotrophs within plankton functional types: *Journal of Plankton Research*, v. 35, no. 1, p. 3-11.
- Giovannoni, S. J., and Vergin, K. L., 2012, Seasonality in ocean microbial communities. : *Science*, v. 335 no. 6069, p. 671-676.

- Haas, L. W., 1982, Improved epifluorescence microscopy for observing planktonic microorganisms: *Annales De L Institut Oceanographique*, v. 58, p. 261-266.
- Hardin, G., 1960, The competitive exclusion principle: *Science*, v. 131, p. 1292-1298.
- Harris, R. P., 1994, Zooplankton grazing on the coccolithophore *Emiliania huxleyi* and its role in inorganic carbon flux: *Marine Biology*, v. 119, no. 3, p. 431-439.
- Hasle, G. R., and Syvertsen, E. E., 1996, Marine diatoms: IN: *Identifying Marine Phytoplankton.*, v. Tomas, C.R. Eds, San Diego: Academic Press., p. 5-385.
- Hillebrand, H., Duerksen, C. D., Kirschtel, D., Pollinger, U., and Zohary, T., 1999, Biovolume calculation for pelagic and benthic microalgae: *Journal of Phycology [J. Phycol.]*, v. 35, no. 2, p. 403-424.
- Hinder, S. L., Hays, G. C., Edwards, M., Roberts, E. C., Walne, A. W., and Gravenor, M. B., 2012, Changes in marine dinoflagellate and diatom abundance under climate change: *Nature Climate Change*, v. 2, p. 271-275.
- Hutchins, D. A., and Bruland, K. W., 1998, Iron-limited diatom growth and Si:N uptake ratios in a coastal upwelling regime: *Nature*, v. 393, no. 6685, p. 561-564.
- Hutchinson, G. E., 1961, The paradox of the plankton: *The American Naturalist*, v. 95, no. 882, p. 137-145.
- Karl, D. M., 2002, Hidden in a sea of microbes: *Nature*, v. 415, no. 6872, p. 590-591.
- Landry, M. R., 2002, Integrating classical and microbial food web concepts: evolving views from the open-ocean Tropical Pacific: *Hydrobiologia [Hydrobiologia]*, v. 480, p. 1-3.
- Loferer-Kröbber, M., Klima, J., and Psenner, R., 1998, Determination of Bacterial Cell Dry Mass by Transmission Electron Microscopy and Densitometric Image Analysis: *Applied Environmental Microbiology*, v. 64, no. 2, p. 688-694.
- Mackey, M. D., Mackey, D. J., Higgins, H. W., and Wright, S. W., 1996, CHEMTAX - a program for estimating class abundances from chemical markers: application to HPLC measurements of phytoplankton: *Marine Ecology Progress Series*, v. 144, p. 265-283
- Martin, J. H., 1990, Glacial-interglacial CO₂ change: The iron hypothesis: *Paleoceanography*, v. 5, no. 1, p. 1-13.
- Martin, J. H., Coale, K. H., Johnson, K. S., Fitzwater, S. E., Gordon, R. M., Tanner, S. J., Hunter, C. N., Elrod, V. A., Nowicki, J. L., Coley, T. L., Barber, R. T., Lindley, S., Watson, A. J., Van Scoy, K., and Law, C. S., 1994, Testing the iron hypothesis in ecosystems of the Equatorial Pacific Ocean: *Nature*, v. 371, no. 6493, p. 123-129.
- Martin, P., Rutgers van der Loeff, M., Cassar, N., Vandromme, P., d'Ovidio, F., Stemmann, L., Rengarajan, R., Soares, M., González, H. E., Ebersbach, F., Lampitt, R. S., Sanders, R., Barnett, B. A., Smetacek, S., and Naqvi, S. W. A., 2013, Iron fertilization enhanced net community production but not downward particle flux during the Southern Ocean iron fertilization experiment LOHAFEX: *Global Biogeochemical Cycles*, v. 27.
- Mazzocchi, G. M., González, H. E., Vandromme, P., Borriore, I., Ribera d'Alcala, M., Gauns, M., Assmy, P., Fuchs, B. M., Klaas, C., Martin, P., Montresor, M., Ramaiah, N., Naqvi, S. W. A., and Smetacek, V., 2009, A non-diatom plankton bloom controlled by copepod grazing and amphipod predation: Preliminary results from the LOHAFEX iron-fertilisation experiment: *GLOBEC International Newsletter*, v. 15, no. 2, p. 3-6.
- Menden-Deuer, S., and Lessard, E. J., 2000, Carbon to volume relationships for dinoflagellates, diatoms and other protist plankton: *Limnology and Oceanography*, v. 45, no. 3, p. 569-579.
- Morel, F. M. M., Rueter, J. G., and Price, N. M., 1991, Iron nutrition of phytoplankton and its possible importance in the ecology of ocean regions with high nutrient low biomass: *Oceanography*, v. 4, p. 56-61.

- Morris, R. M., Rappe, M. S., Connon, S. A., Vergin, K. L., Siebold, W. A., Carlson, C. A., and Giovannoni, S. J., 2002, SAR11 clade dominates ocean surface bacterioplankton communities: *Nature* [Nature], v. 420, no. 6917, p. 806-810.
- Peloquin, J., Hall, J., Safi, K., Smith, W. O., Wright, S., and van den Enden, R., 2011, The response of phytoplankton to iron enrichment in Sub-Antarctic HNLCLSi waters: Results from the SAGE experiment: *Deep-Sea Research Part Ii-Topical Studies in Oceanography*, v. 58, no. 6, p. 808-823.
- Pomeroy, L. R., 1974, The oceans food web, a changing paradigm: *Biol. Sci.*, v. 24, no. 9, p. 499-504.
- Porter, K. G., and Feig, Y. S., 1980, The use of DAPI for identifying and counting aquatic microflora: *Limnology and Oceanography*, v. 25, p. 943-948.
- Raiswell, R., Benning, L. G., Tranter, M., and Tulaczyk, S., 2008, Bioavailable iron in the Southern Ocean: the significance of the iceberg conveyor belt: *Geochemical Transactions*, v. 9.
- Reigstad, M., and Wassmann, P., 2007, Does *Phaeocystis* spp. contribute significantly to vertical export of organic carbon?: *Biogeochemistry* [Biogeochemistry], v. 83, p. 1-3.
- Richardson, T. L., and Jackson, G. A., 2007, Small Phytoplankton and Carbon Export from the Surface Ocean: *Science*, v. 315, no. 5813, p. 838-840.
- Sarno, D., Kooistra, W. H. C. F., Medlin, L. K., Percopo, I., and Zingone, A., 2005, Diversity in the Genus *Skeletonema* (Bacillariophyceae). II. An Assessment of the Taxonomy of *S. costatum*-like Species with the Description of Four New Species: *Journal of Phycology* [J. Phycol.], v. 41, no. 1, p. 151-176.
- Sato, M., Takeda, S., and Furuya, K., 2009, Responses of pico- and nanophytoplankton to artificial iron infusions observed during the second iron enrichment experiment in the western subarctic Pacific (SEEDS II): *Deep-Sea Research Part Ii-Topical Studies in Oceanography*, v. 56, no. 26, p. 2745-2754.
- Schmitz, F., 1878, *Halosphaera*, eine neue Gattung grüner Algen aus dem Mittelmeer.: *Mittheilungen aus der Zoologischen Station zu Neapel*, v. 1, p. 273-286.
- Schulz, I. K., Assmy, P., Wolzenburg, S., Klaas, C., and Smetacek, V., TO BE SUBMITTED, Response of large protozooplankton (>20 μm) during the Southern Ocean iron fertilization experiment LOHAFEX Deep Sea Research Part I: *Oceanographic Research Papers*.
- Schwarz, J. N., and Schodlok, M. P., 2009, Impact of drifting icebergs on surface phytoplankton biomass in the Southern Ocean: Ocean colour remote sensing and in situ iceberg tracking: *Deep-Sea Research Part I-Oceanographic Research Papers*, v. 56, no. 10, p. 1727-1741.
- Sieburth, J. M., Smetacek, V., and Lenz, J., 1978, Pelagic ecosystem structure: Hetrotrophic compartments of the plankton and their relationship to plankton size fractions: *Limnol. and Oceanogr.*, v. 23, no. 6, p. 1256-1263.
- Smetacek, V., 1999, Diatoms and the Ocean Carbon Cycle: *Protist*, v. 150, p. 25-32.
- Smetacek, V., Assmy, P., and Henjes, J., 2004, The role of grazing in structuring Southern Ocean pelagic ecosystems and biogeochemical cycles: *Antarctic Science*, v. 16, no. 4, p. 541-558.
- Smetacek, V., de Baar, H. J. W., Bathmann, U. V., Lochte, K., and Rutgers van der Loeff, M. M., 1997, Ecology and biogeochemistry of the Antarctic Circumpolar Current during austral spring: a summary of Southern Ocean JGOFS cruise ANT X/6 of R.V. *Polarstern*: *Deep Sea Research Part II: Topical Studies in Oceanography*, v. 44, no. 1-2, p. 1-21.
- Smetacek, V., Klaas, C., Strass, V. H., Montesor, M., Cisewski, B., Savoye, N., Webb, A., d'Ovidio, F., Arrieta, J. M., Bathmann, U., Bellerby, R., Berg, M. G., Croot, P., Gonzalez, S., Henjes, J., Herndl, G. J., Hoffmann, L. J., Leach, H., Losch, M., Mills,

- M. M., Neill, C., Peeken, I., Röttgers, R., Sachs, O., Sauter, E., Schmidt, M. M., Schwarz, J., Terbrüggen, A., and Wolf-Gladrow, D., 2012, Deep carbon export from a Southern Ocean iron-fertilized diatom bloom: *Nature*, v. 487, p. 313–319.
- Smetacek, V., and Naqvi, S. W. A., 2010, The Expedition of the Research Vessel “Polarstern” to the Antarctic in 2009 (ANT-XXV/3-LOHAFEX): Reports on Polar and Marine Research, v. 613/2010.
- Smetacek, V., Scharek, R., and Nöthig, E.-M., 1990, Seasonal and regional variation in the pelagial and its relationship to the life history cycle of krill, *in* Kerry, K. R., and Hempel, G., eds., Antarctic ecosystems. Ecological change and conservation: Berlin Heidelberg, Springer-Verlag, p. 103-114.
- Smith Jr., K. L., Robison, B. H., Helly, J. J., Kaufmann, R. S., Ruhl, H. A., Shaw, T.J., Twining, B. S., and Vernet, M., 2007, Free-drifting icebergs: Hot spots of chemical and biological enrichment in the Weddell Sea: *Science*, v. 317, no. (5837), p. 478-482.
- Smith Jr., K. L., Sherman, A. D., Shaw, T. J., Murray, A.E., Vernet, M., and Cefarelli, A. O., 2011, Carbon export associated with free-drifting icebergs in the Southern Ocean: Deep Sea Research Part II: Topical Studies in Oceanography, v. 58, no. 11-12, p. 1485–1496.
- Strom, S. L., 2008, Microbial ecology of ocean biogeochemistry: A community perspective: *Science*, v. 320, no. 5879, p. 1043-1045.
- Suzuki, K., Saito, H., Isada, T., Hattori-Saito, A., Kiyosawa, H., Nishioka, J., McKay, R. M. L., Kuwata, A., and Tsuda, A., 2009, Community structure and photosynthetic physiology of phytoplankton in the northwest subarctic Pacific during an in situ iron fertilization experiment (SEEDS-II): Deep-Sea Research Part II-Topical Studies in Oceanography, v. 56, no. 26, p. 2733-2744.
- Takeda, S., 1998, Influence of iron availability on nutrient consumption ratio of diatoms in oceanic waters: *Nature*, v. 393, no. 6687, p. 774-777.
- Thiele, S., Fuchs, B. M., Ramaiah, N., and Amann, R., 2012, Microbial Community Response during the Iron Fertilization Experiment LOHAFEX: *Applied Environmental Microbiology*, v. 78, no. 24, p. 8803.
- Thronsen, J., 1995, Chapter “Estimating cell numbers: In: Manual on Harmful Marine Microalgae. (eds. Hallegraeff, G. M., Anderson, D. M. & Cembella, A. D.) v. 33, no. UNESCO, Paris,, p. 63–80.
- Tsuda, A., Takeda, S., Saito, H., Nishioka, J., Nojiri, Y., Kudo, I., Kiyosawa, H., Shiimoto, A., Imai, K., Ono, T., Shimamoto, A., Tsumune, D., Yoshimura, T., Aono, T., Hinuma, A., Kinugasa, M., Suzuki, K., Sohrin, Y., Noiri, Y., Tani, H., Deguchi, Y., Tsurushima, N., Ogawa, H., Fukami, K., Kuma, K., and Saino, T., 2003, A Mesoscale Iron Enrichment in the Western Subarctic Pacific Induces a Large Centric Diatom Bloom: *Science*, v. 300, no. 5621, p. 958-961.
- Uitz, J., Claustre, H., Morel, A., and Hooker, S. B., 2006, Vertical distribution of phytoplankton communities in open ocean: An Assessment based on surface chlorophyll. : *Journal of Geophysical Research*, v. 111, no. C08005.
- Verneta, M., Sinesb, K., Chakosc, D., Cefarellid, A. O., and Ekerne, L., 2011, Impacts on phytoplankton dynamics by free-drifting icebergs in the NW Weddell Sea: Deep Sea Research Part II: Topical Studies in Oceanography, v. 58, no. 11-12, p. 1422-1435.
- Wright, S. W., Thomas, D. P., Marchant, H. J., Higgins, H. W., Mackey, M. J., and Mackey, D. J., 1996, Analysis of phytoplankton of the Australian sector of the Southern Ocean: comparisons of microscopy and size frequency data with interpretations of pigment HPLC data using the 'CHEMTAX' matrix factorisation program: *Marine Ecology Progress Series*, v. 144, p. 285-298
- Zeder, M., Ellrott, A., and Amann, R., 2011, Automated sample area definition for highthroughput microscopy: *Cytometry*, v. 79A, p. 306-310.

Tables:

Table 1: Sampling overview. Stations taken during LOHAFEX for (1) Phytoplankton, (2) Microzooplankton, (3) Protozooplankton, (4) Bacteria and (5) HPLC-pigment analyses.

Figures:

Fig. 1: MODIS (Moderate Resolution Imaging Spectroradiometer) image of the LOHAFEX study area for the period 12-14 February 2009. The satellite image shows increased Chlorophyll *a* (mg m^{-3}) concentration in the fertilized patch (encircled). Note the higher background chlorophyll stocks in the southwestern quarter of the image compared to the southeastern, but also northwestern quarters. The warm-core eddy adjacent to the LOHAFEX one is impoverished compared to the latter. The large bloom dominating the northeastern quarter is mysterious. The Chlorophyll *a* data were downloaded from NASA website <http://oceancolor.gsfc.nasa.gov/>.

Fig. 2: Integrated chlorophyll *a* (mg m^{-2}) (red circles) and phytoplankton carbon stocks (g m^{-2}) (PPC; blue circles) in the 80 m surface layer, inside (open circles) and outside (full circles) of the fertilized patch (A). PPC values (B) corrected for the mixotrophic fraction (3,4 g) (B).

Fig. 3: Total plankton carbon stocks (bars) and POC (stars) (g C m^{-2}) inside (A) and outside (B) the patch, with contribution of diatom, non-diatom phytoplankton, mixotrophic fraction, bacteria, protozooplankton, small copepods $< 1\text{mm}$ and large copepodites and adult copepods $> 1\text{ mm}$). Copepod values are integrated values over 200 m, remaining categories are integrated over 80 m.

Fig. 4: Standing stocks (mg C m^{-2}) of total diatoms (A) and different species, including *Thalassionema nitzschioides* (B), *Navicula* sp. (C), and *Corethron pennatum* (D), *Fragilariospis kerguelensis* (E), *Ephemera* sp. (F) inside (black spheres) and outside (white spheres) the fertilized patch.

Fig. 5: Standing stocks (mg C m^{-2}) of different species, including *Pseudo-nitzschia* spp. (A), *Lennoxia faveolata* (B), *Thalassiosira* spp. $< 20\ \mu\text{m}$ (C) and *Thalassiosira* spp. $> 20\ \mu\text{m}$ (D) inside (black spheres) and outside (white spheres) the fertilized patch.

Fig. 6: Standing stocks (mg C m^{-2}) of unidentified flagellates (A) and unidentified coccoid cells (B) inside (black spheres) and outside (white spheres) the fertilized patch.

Fig. 7: Standing stocks (mg C m^{-2}) of the prymnesiophyte species *Phaeocystis antarctica* (A) and *Emiliania huxleyi* (B) inside (black spheres) and outside (white spheres) the fertilized patch.

Fig. 8: Standing stocks (mg C m^{-2}) of the prasinophyte species *Halosphaera viridis* (A) and *Mamiellales* sp. (B) inside (black spheres) and outside (white spheres) the fertilized patch.

Fig. 9: Relative contribution of heterotrophic nanoflagellates (HNF) and autotrophic nanoflagellates (ANF) determined by epifluorescence (A) and light (B) microscopy.

Fig. 10: Slope and intercept of linear regression between phytoplankton carbon and chlorophyll *a* (PPC:Chl *a*) (A) and plankton carbon and Chlorophyll *a* (PC:Chl *a*) (B) ($\mu\text{g L}^{-1}$).

Fig. 11: Slope and intercept of linear regression between plankton carbon and particulate organic carbon (PC:POC) ($\mu\text{g L}^{-1}$) (A) and temporal trends in PC:POC ratio (B).

Fig. 12: Slope and intercept of linear regression between particulate organic carbon and particulate organic nitrogen (POC:PON) ($\mu\text{g L}^{-1}$) (A) and temporal trends in POC:PON ratio (B).

Fig. 13: Total plankton carbon (mg C m^{-2}) stocks (bars) inside (A) and outside (B) the patch, with contribution of all plankton categories, except copepods.

Fig. 14: Comparison of plankton composition obtained by microscopic counts (left) with HPLC-analyses (right) at three IN stations (day -0.6, 9.5, 18.6) (A) and one OUT station (day 16.3) (B). Contribution of unidentified flagellates and coccoid cells are the corrected values, meaning heterotrophic fraction was subtracted proportionally.

Fig. 15: *Phaeocystis antarctica* cells growing on *Corethron* sp. spines (A) and overgrowing a small centric diatom (B). Colonies of *Phaeocystis antarctica* make blooms in coastal waters, but were suppressed by zooplankton during LOHAFEX.

Fig. 16: Biomass ($\mu\text{g C L}^{-1}$) of epiphytic *Phaeocystis* (A) and of ‘free’ *Phaeocystis* colonies (B) from samples at 20 m depth. Epiphytic *Phaeocystis* colonies peak on day10 and ‘free’ *Phaeocystis* colonies on day 14.

Fig. 17: Fecal pellet from a 19-day incubation experiment on board, encircled in red the coccolitophorid cells, (28 cells).

Date	Station	Day since first Fe-release	Latitude (Degree decimal)	Longitude (Degree decimal)	IN or OUT patch	Application
26.01.09	114	-0,6	-47,99793	-15,80336	IN/OUT	1,2,3,4,5
29.01.09	120	2,1	-47,86125	-15,79564	IN	1,2,4
31.01.09	132	4,6	-47,65656	-15,73177	IN	1,2,3,4,5
05.02.09	135	9,5	-47,69418	-15,09783	IN	1,2,3,4,5
09.02.09	139	13,9	-47,90817	-15,12972	IN	1,2,3,4,5
14.02.09	148	18,6	-47,94246	-15,29277	IN	1,2,3,4,5
18.02.09	159	22,6	-47,35282	-15,41548	IN	1,2,4,5
20.02.09	162	24,6	-47,35543	-14,7156	IN	1,2,3,4,5
01.03.09	192	33,1	-48,80416	-15,20391	IN	1,2,3,4,5
04.03.09	204	36,6	-48,97476	-15,23412	IN	1,2,3,4,5
30.01.09	127	3,8	-47,99718	-16,00048	OUT	1,2,4,5
12.02.09	146	16,3	-47,49086	-15,41995	OUT	1,2,3,4,5
25.02.09	174	29,5	-48,44292	-14,73347	OUT	1,2,4,5
03.03.09	199	35,0	-48,06129	-15,23194	OUT	1,2,3,4,5
06.03.09	212	38,7	-49,03491	-15,5135	OUT	1,2,4,5

Table 1: Sampling overview. Stations taken during LOHAFEX for (1) Phytoplankton, (2) Microzooplankton, (3) Protozooplankton, (4) Bacteria and (5) HPLC-pigment analyses.

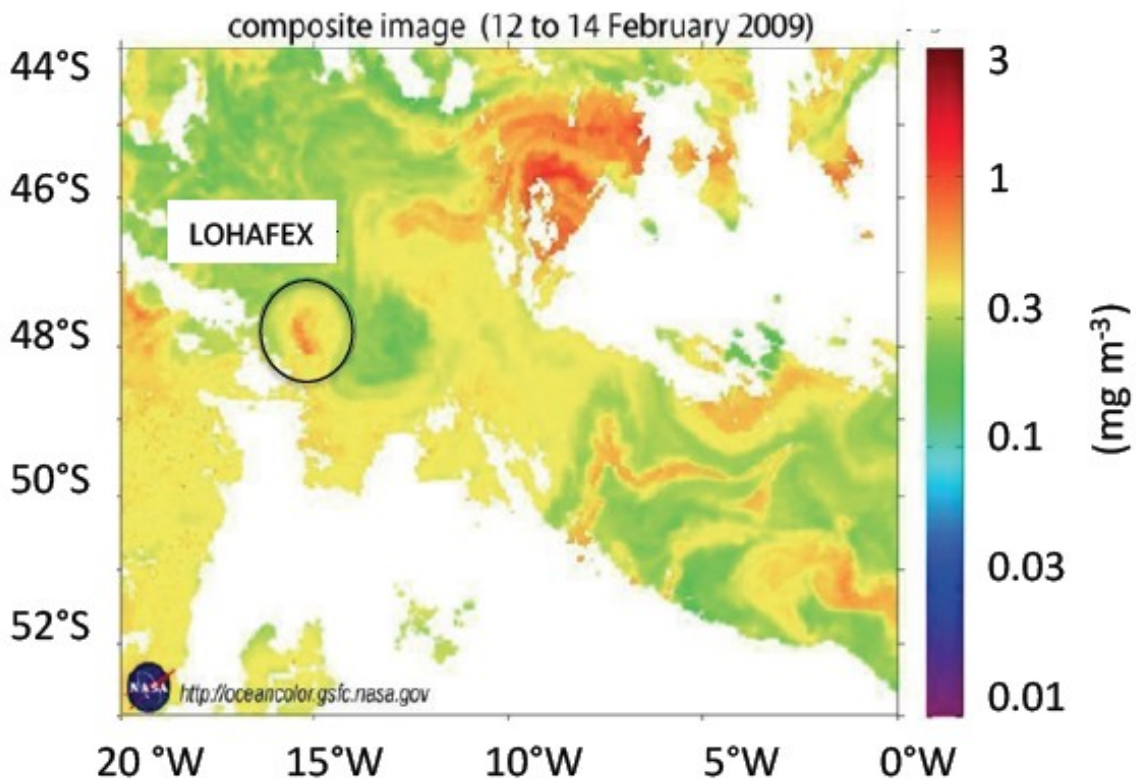


Fig. 1: MODIS (Moderate Resolution Imaging Spectroradiometer) image of the LOHAFEX study area for the period 12-14 February 2009. The satellite image shows increased Chlorophyll *a* (mg m^{-3}) concentration in the fertilized patch (encircled). Note the higher background chlorophyll stocks in the southwestern quarter of the image compared to the southeastern, but also northwestern quarters. The warm-core eddy adjacent to the LOHAFEX one is impoverished compared to the latter. The large bloom dominating the northeastern quarter is mysterious. The Chlorophyll *a* data were downloaded from NASA website <http://oceancolor.gsfc.nasa.gov/>.

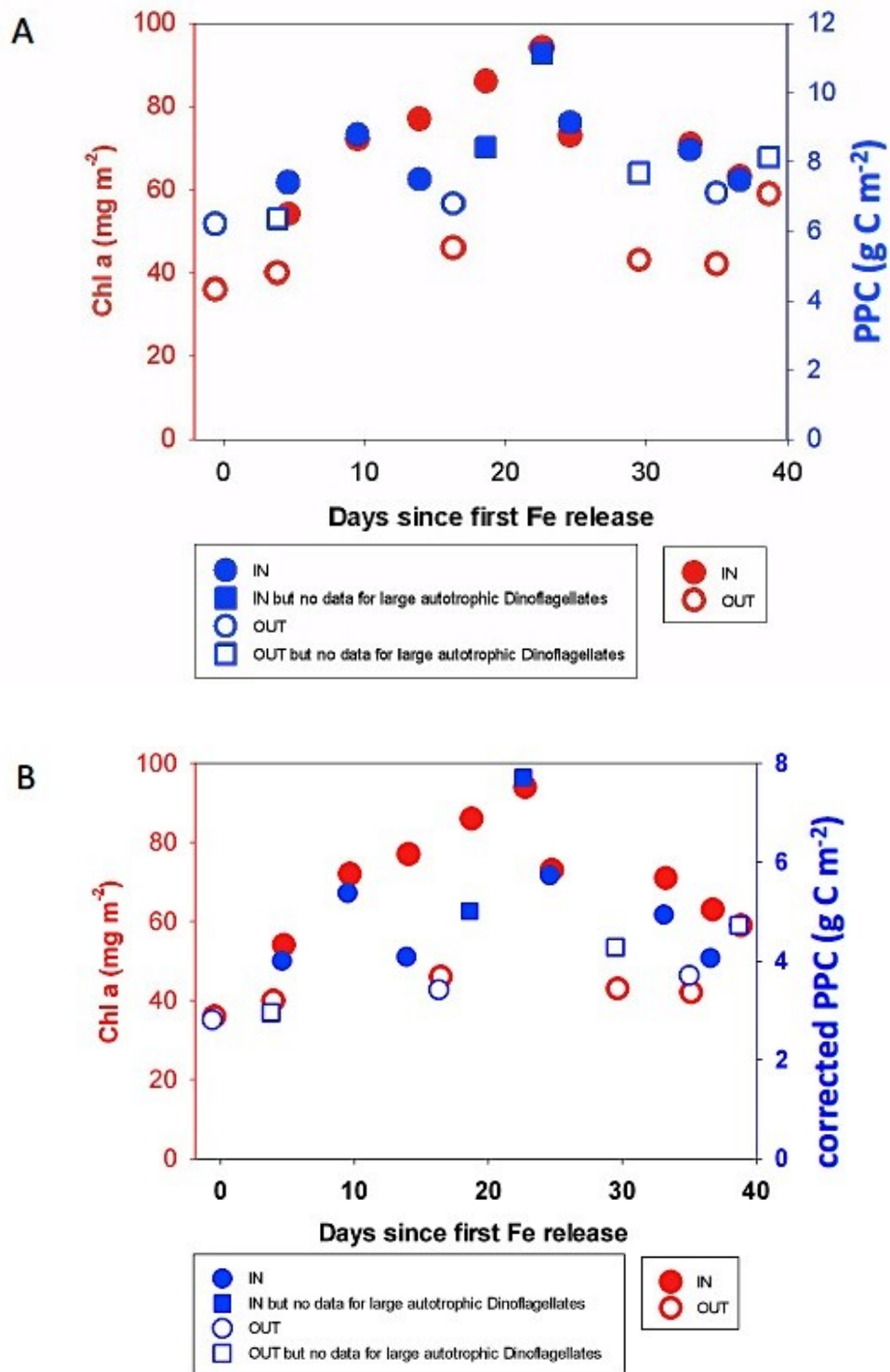


Fig. 2: Integrated chlorophyll *a* (mg m^{-2}) (red circles) and phytoplankton carbon stocks (g m^{-2}) (PPC; blue circles) in the 80 m surface layer, inside (open circles) and outside (full circles) of the fertilized patch (A). PPC values (B) corrected for the mixotrophic fraction (3,4 g) (B).

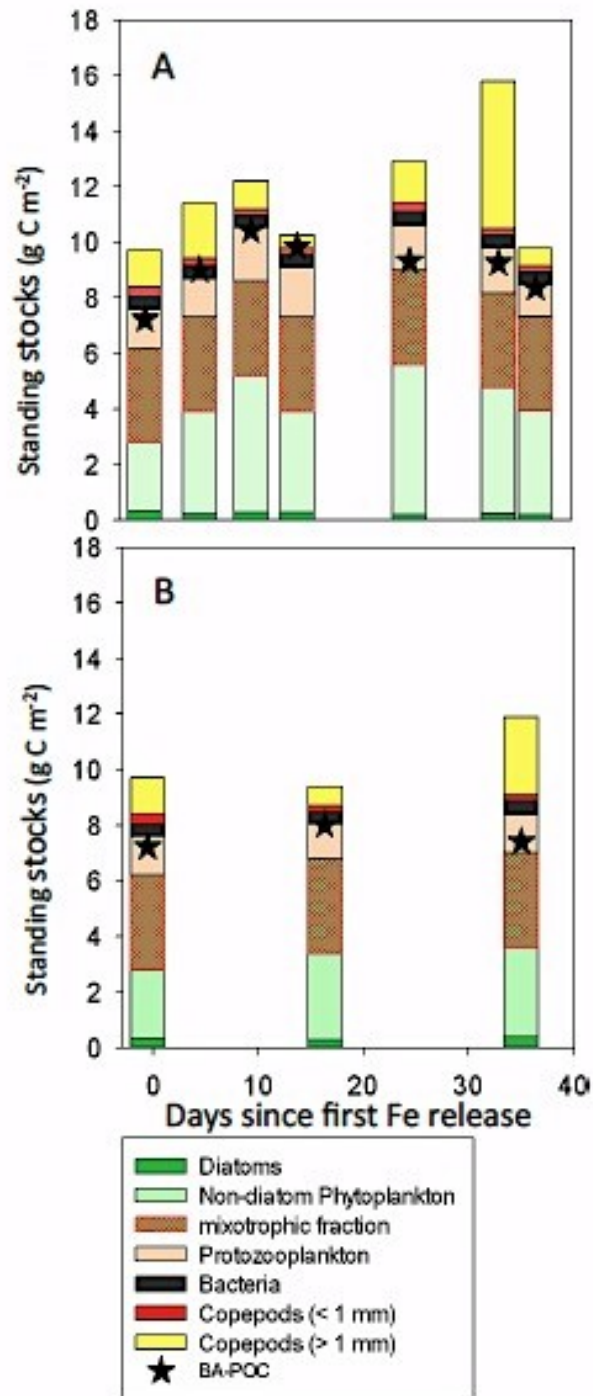


Fig. 3: Total plankton carbon stocks (bars) and POC (stars) (g C m^{-2}) inside (A) and outside (B) the patch, with contribution of diatom, non-diatom phytoplankton, mixotrophic fraction, bacteria, protozooplankton, small copepods < 1 mm and large copepodites and adult copepods > 1 mm). Copepod values are integrated values over 200 m, remaining categories are integrated over 80 m.

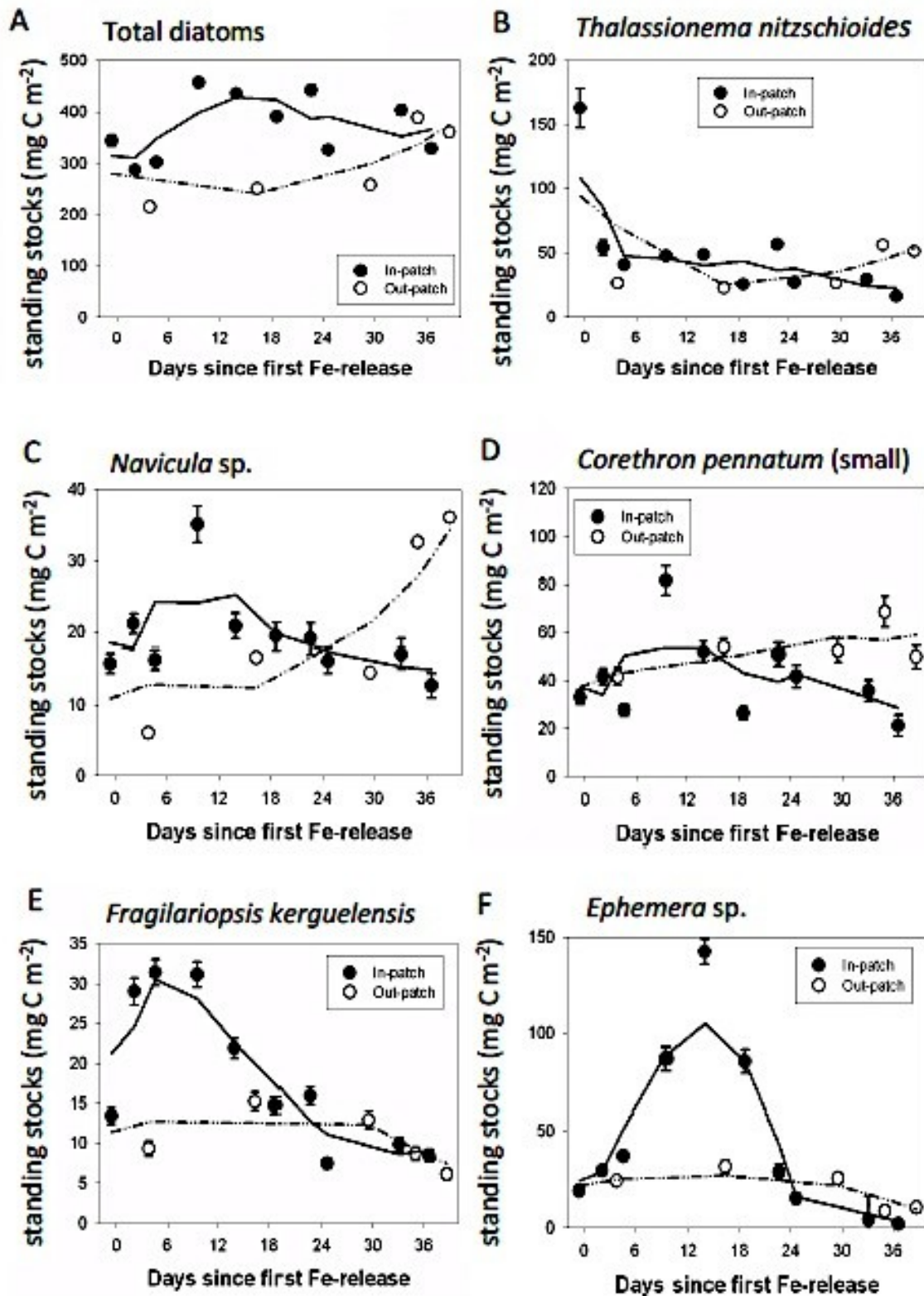


Fig. 4: Standing stocks (mg C m⁻²) of total diatoms (A) and different species, including *Thalassionema nitzschioides* (B), *Navicula* sp. (C), and *Corethron pennatum* (D), *Fragilariopsis kerguelensis* (E), *Ephemera* sp. (F) inside (black spheres) and outside (white spheres) the fertilized patch.

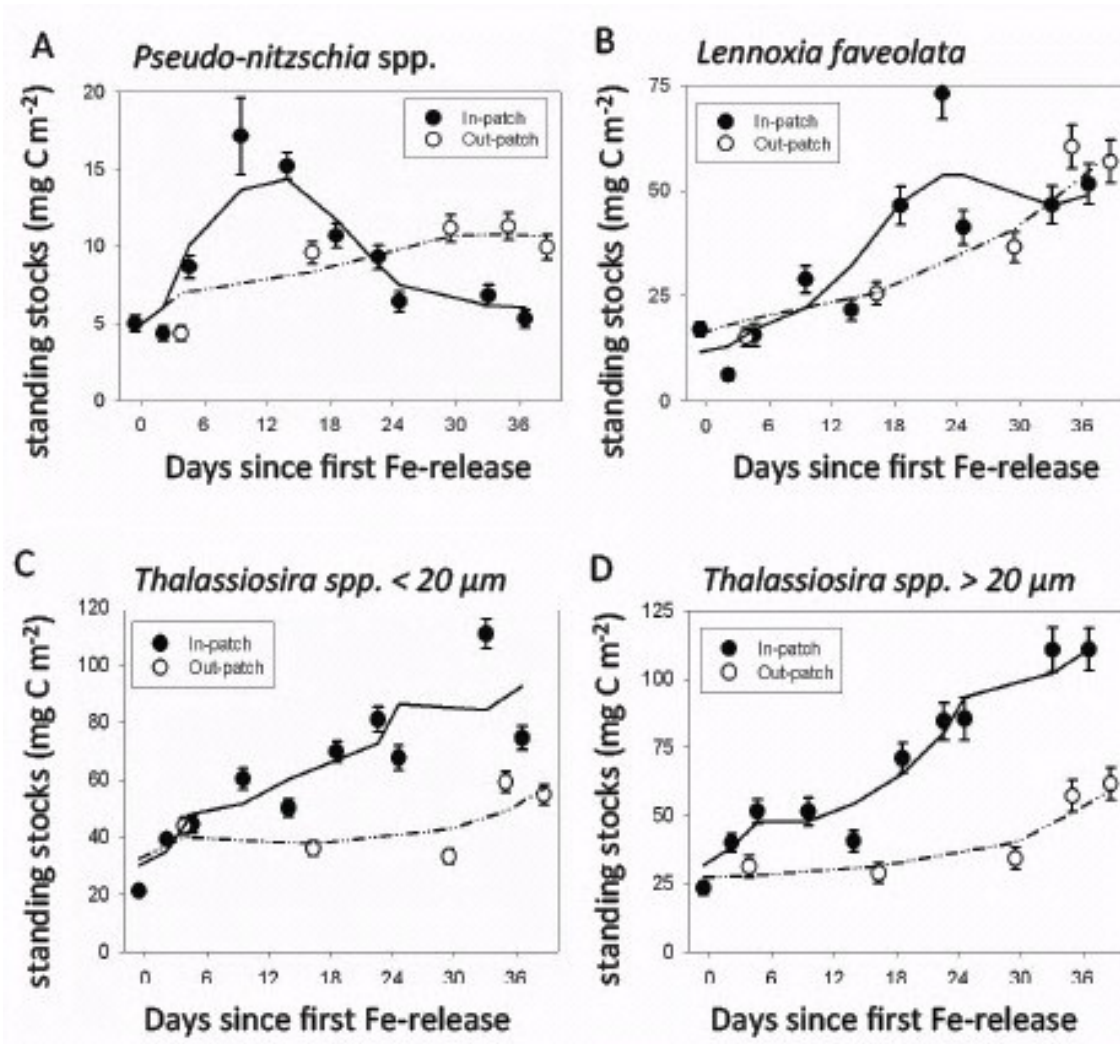


Fig. 5: Standing stocks (mg C m⁻²) of different species, including *Pseudo-nitzschia* spp. (A), *Lennoxia faveolata* (B), *Thalassiosira* spp. < 20 μm (C) and *Thalassiosira* spp. > 20 μm (D) inside (black spheres) and outside (white spheres) the fertilized patch.

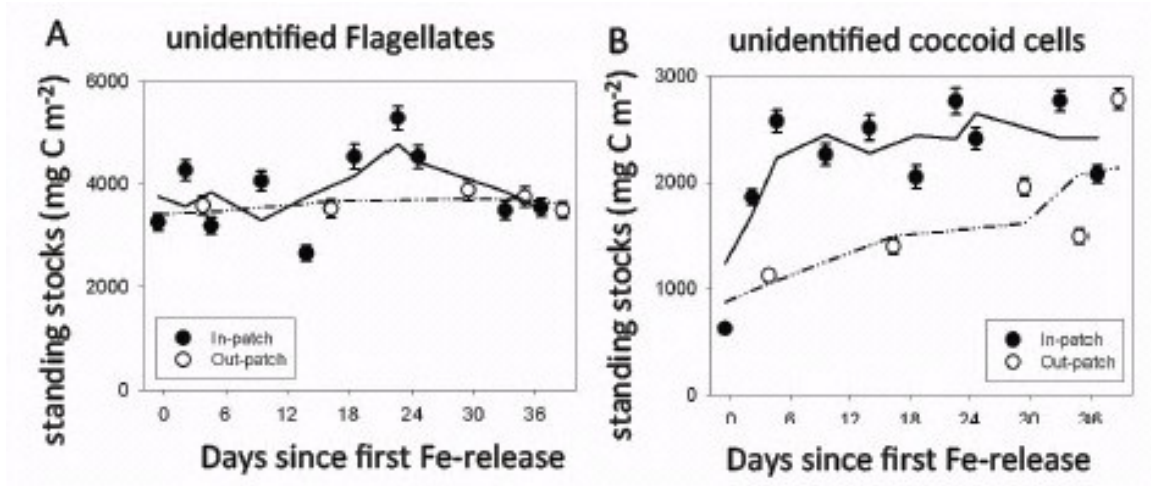


Fig. 6: Standing stocks (mg C m^{-2}) of unidentified flagellates (A) and unidentified coccoid cells (B) inside (black spheres) and outside (white spheres) the fertilized patch.

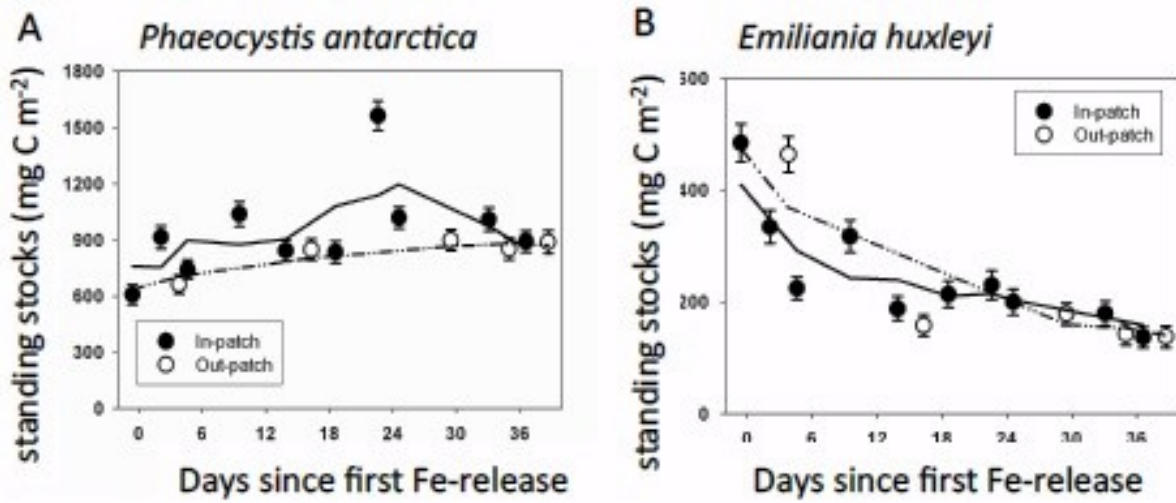


Fig. 7: Standing stocks (mg C m^{-2}) of the prymnesiophyte species *Phaeocystis antarctica* (A) and *Emiliana huxleyi* (B) inside (black spheres) and outside (white spheres) the fertilized patch.

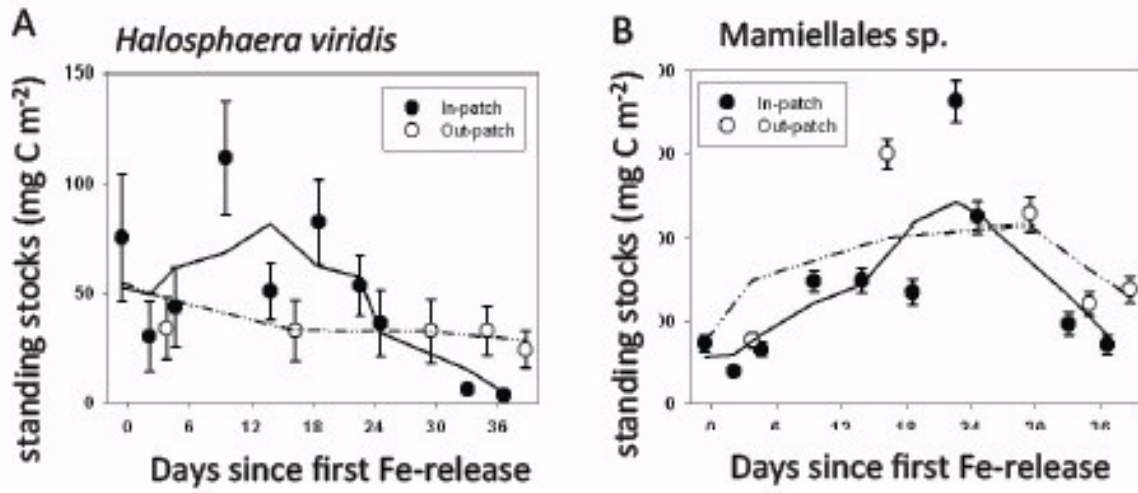


Fig. 8: Standing stocks (mg C m⁻²) of the prasinophyte species *Halosphaera viridis* (A) and *Mamiellales* sp. (B) inside (black spheres) and outside (white spheres) the fertilized patch.

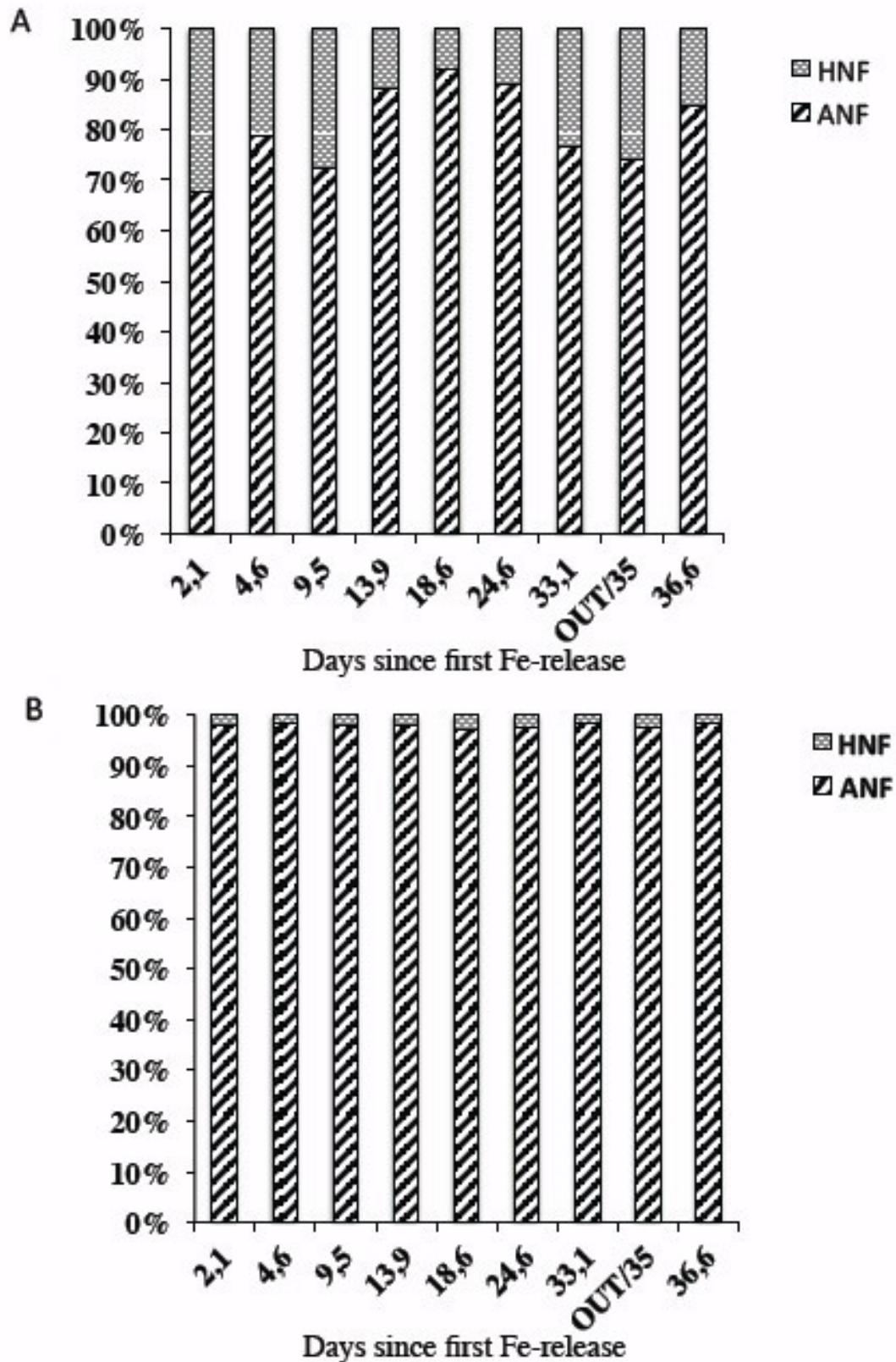


Fig. 9: Relative contribution of heterotrophic nanoflagellates (HNF) and autotrophic nanoflagellates (ANF) determined by epifluorescence (A) and light (B) microscopy.

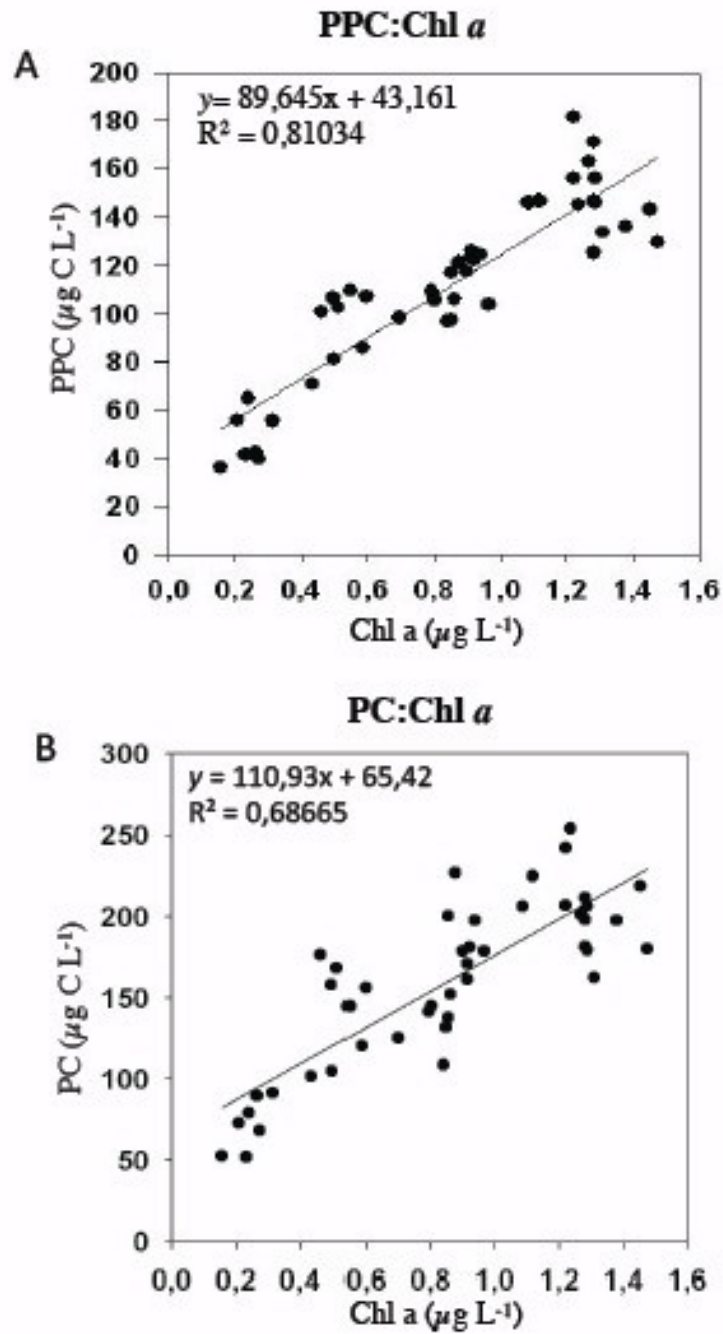


Fig. 10: Slope and intercept of linear regression between phytoplankton carbon and chlorophyll *a* (PPC:Chl *a*) (A) and plankton carbon and Chlorophyll *a* (PC:Chl *a*) (B) ($\mu\text{g L}^{-1}$).

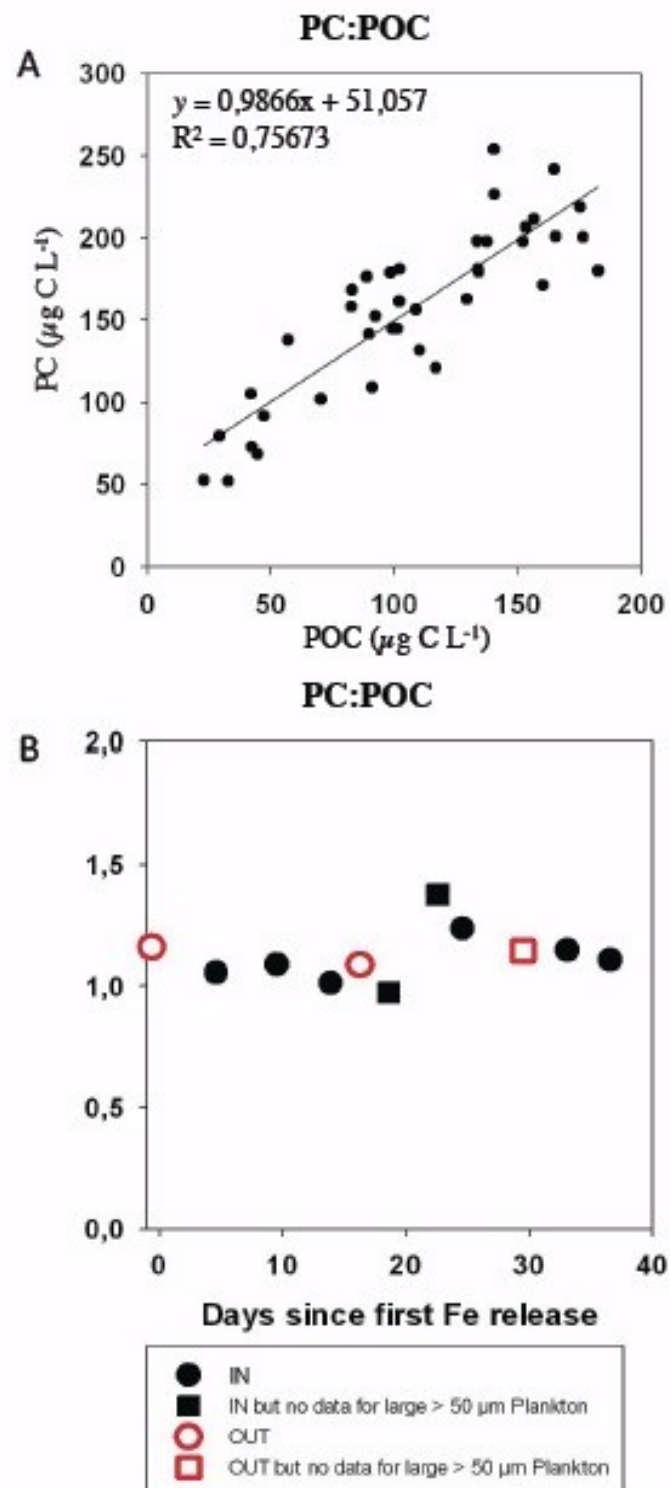


Fig. 11: Slope and intercept of linear regression between plankton carbon and particulate organic carbon (PC:POC) ($\mu\text{g L}^{-1}$) (A) and temporal trends in PC:POC ratio (B).

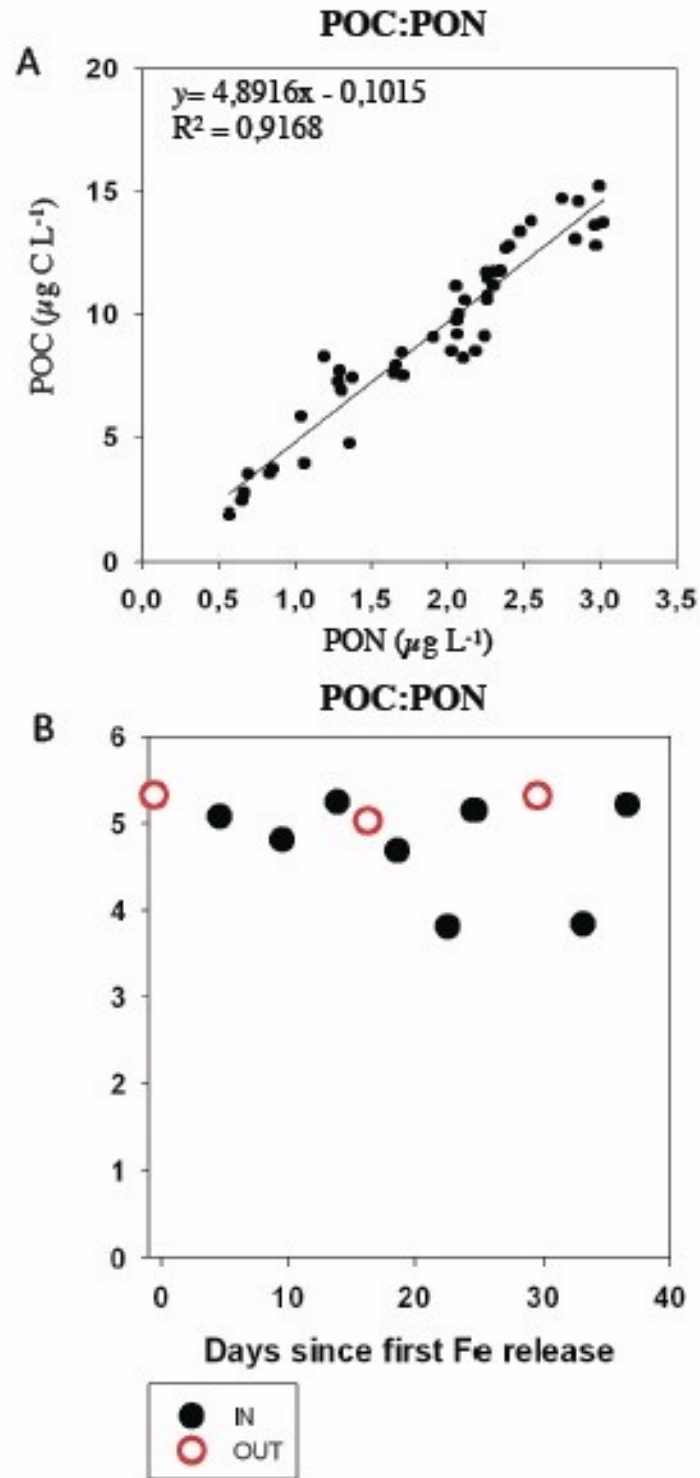


Fig. 12: Slope and intercept of linear regression between particulate organic carbon and particulate organic nitrogen (POC:PON) ($\mu\text{g L}^{-1}$) (A) and temporal trends in POC:PON ratio (B).

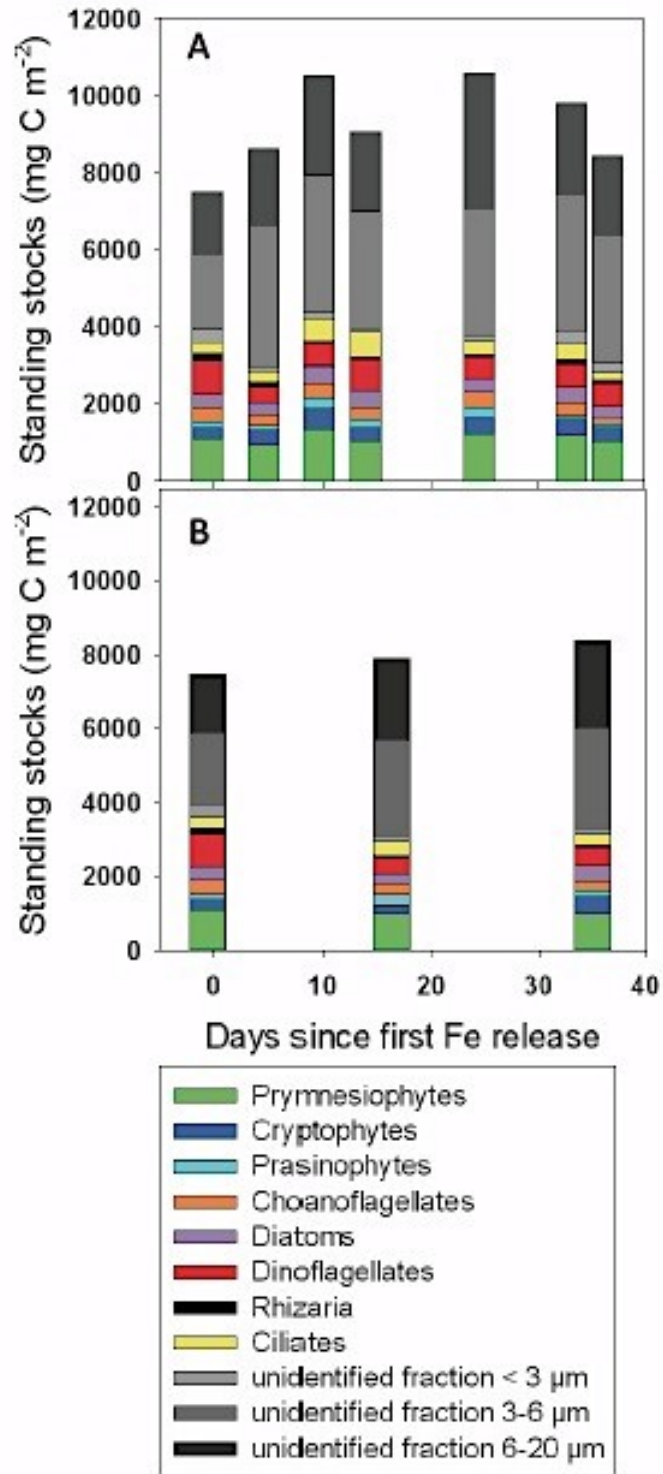
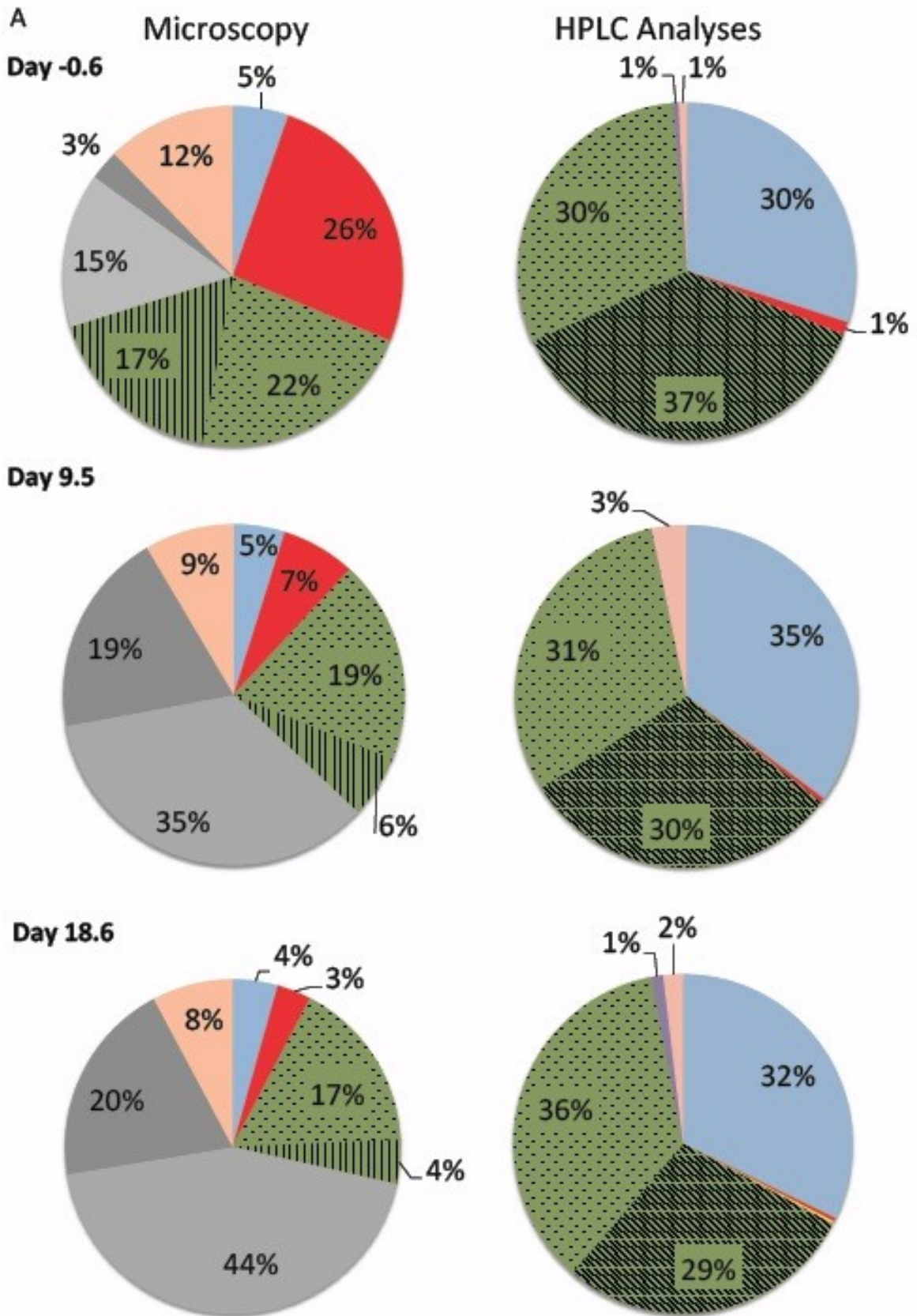


Fig. 13: Total plankton carbon (mg C m⁻²) stocks (bars) inside (A) and outside (B) the patch, with contribution of all plankton categories, except copepods.



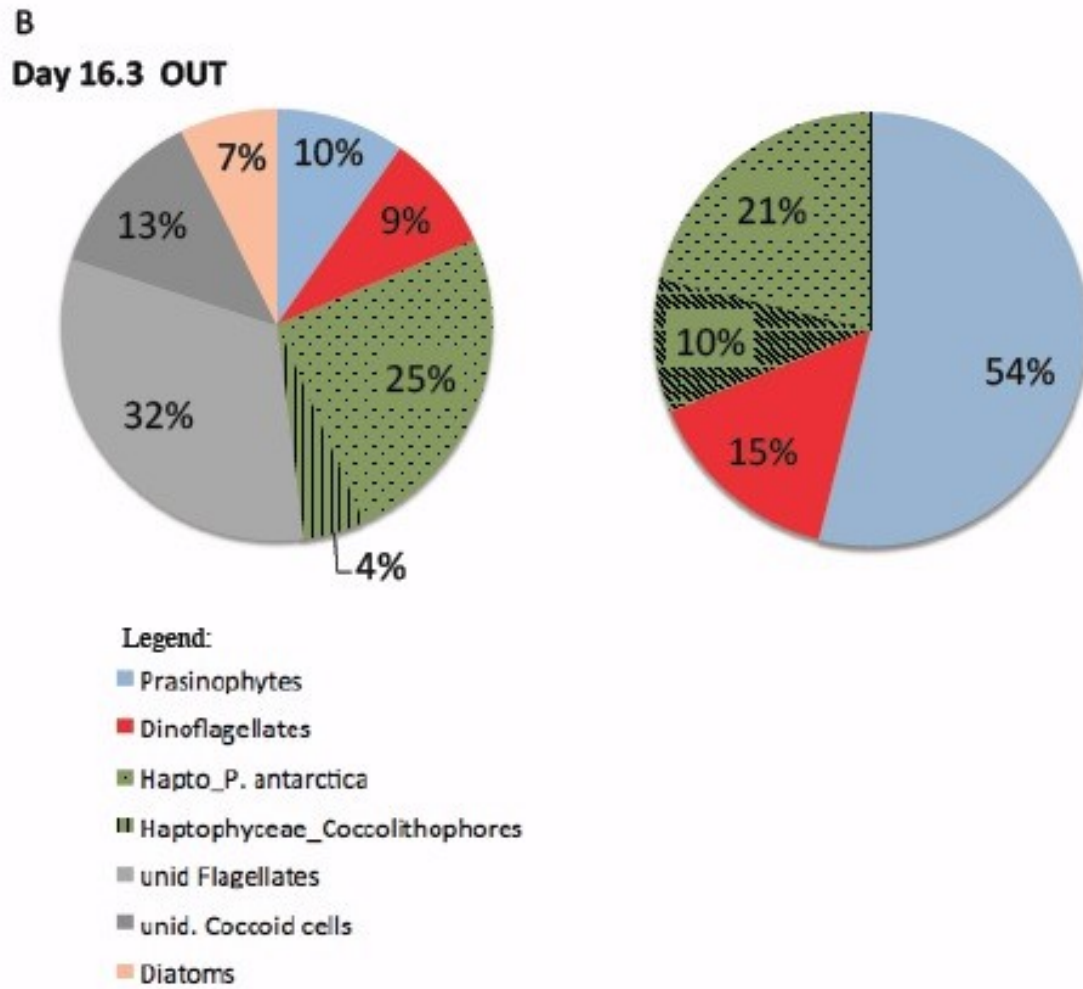


Fig. 14: Comparison of plankton composition obtained by microscopic counts (left) with HPLC-analyses (right) at three IN stations (day -0.6, 9.5, 18.6) (A) and one OUT station (day 16.3) (B). Contribution of unidentified flagellates and coccoid cells are the corrected values, meaning heterotrophic fraction was subtracted proportionally

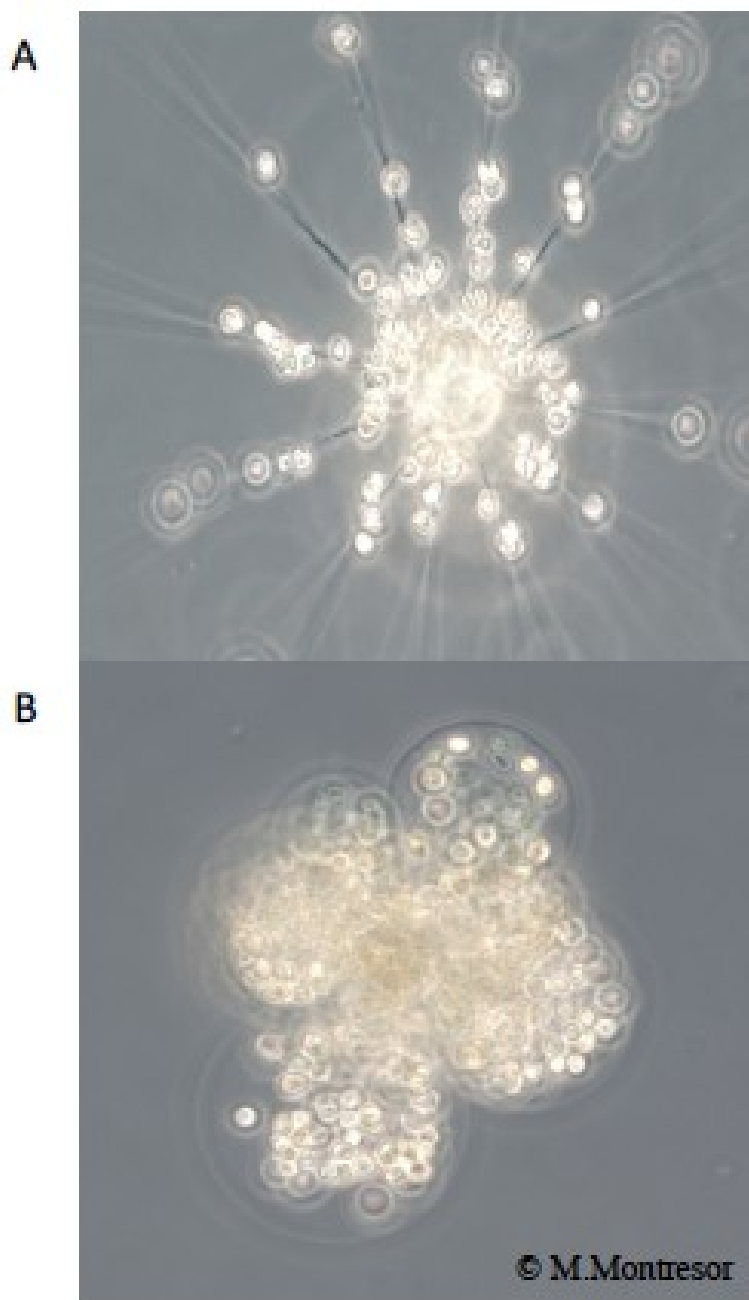


Fig. 15: *Phaeocystis antarctica* cells growing on *Corethron* sp. spines (A) and overgrowing a small centric diatom (B). Colonies of *Phaeocystis antarctica* make blooms in coastal waters, but were suppressed by zooplankton during LOHAFEX.

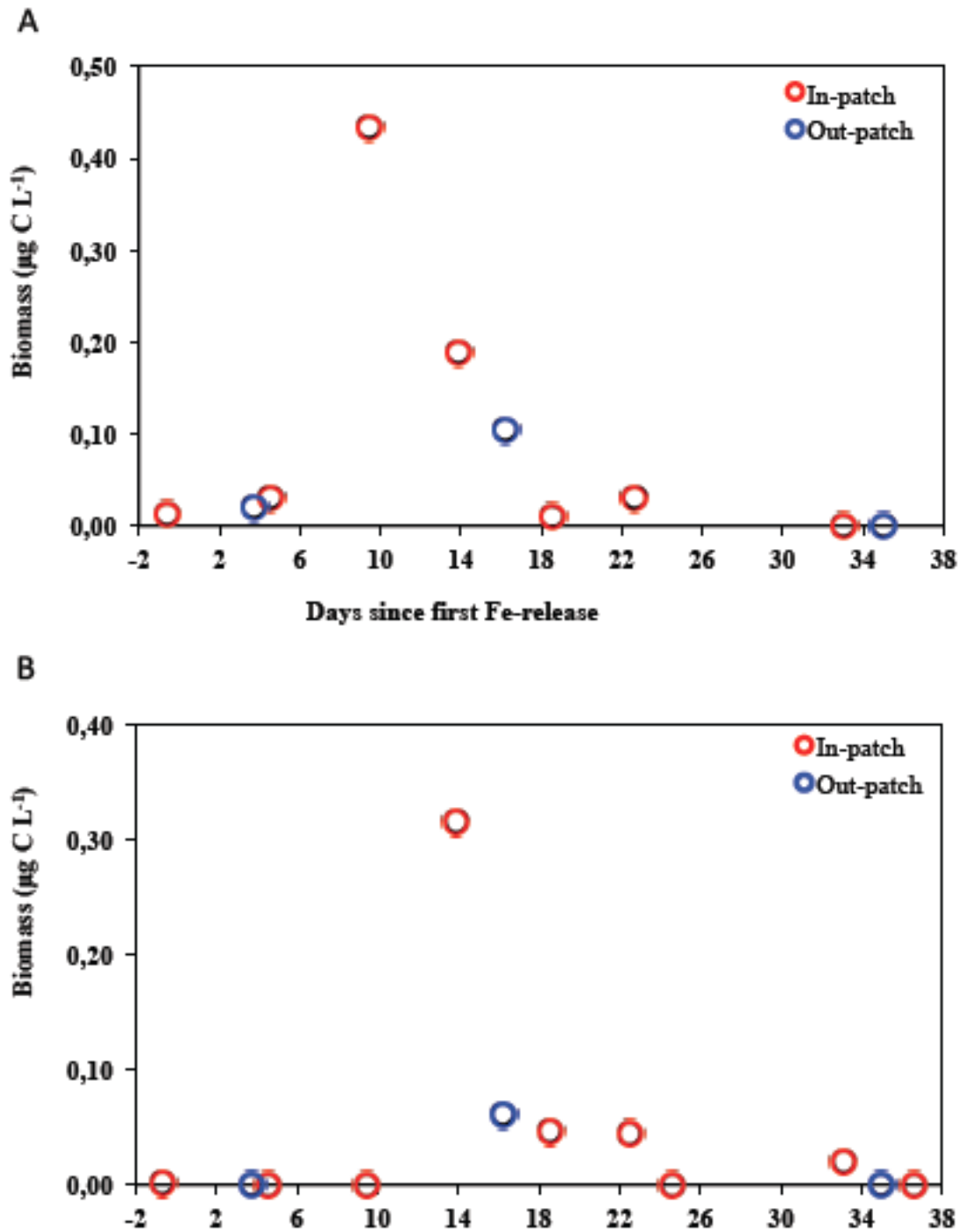


Fig. 16: Biomass ($\mu\text{g C L}^{-1}$) of epiphytic *Phaeocystis* (A) and of 'free' *Phaeocystis* colonies (B) from samples at 20 m depth. Epiphytic *Phaeocystis* colonies peak on day 10 and 'free' *Phaeocystis* colonies on day 14.



Fig. 17: Fecal pellet from a 19-day incubation experiment on board, encircled in red the coccolithophorid cells, (28 cells).

Manuscript II

Investigation of the nano- and picoplankton community during the iron fertilization experiment LOHAFEX

Stefan Thiele^{1}, Christian Wolf^{2*}, Isabelle Schulz^{2,3}, Philipp Assmy⁴, Katja
Metfies², Bernhard M. Fuchs^{1#}, Rudolf Amann¹*

to be submitted to PLOS ONE as companion paper to Manuscript I

¹Max Planck Institute for Marine Microbiology, Celsiusstr. 1, 28359 Bremen, Germany

²Alfred Wegener Institute for Polar and Marine Research, Am Handelshafen 12, 27570
Bremerhaven, Germany

³MARUM – Center for Marine Environmental Sciences, University of Bremen, Leobener
Str., 28359 Bremen

⁴Norwegian Polar Institute, Fram Centre, Hjalmar Johansens gt. 14, 9296 Tromsø, Norway

corresponding author

* these authors contributed equally

contact: Max Planck Institute for Marine Microbiology, Celsiusstr. 1, D-28359 Bremen,
Germany

email: bfuchs@mpi-bremen.de

phone: +49 421 2028-935

fax: +49 421 2028-790

Acknowledgements

We would like to thank the captain and crew of the RV Polarstern, the chief scientists of the LOHAFEX project, V. Smetacek and W. Naqui, and all collaborators within LOHAFEX. Furthermore we thank J. Köhler and E. Ruff for their help. This work was funded by the Max Planck Society and funds dedicated to the Young Investigator Group PLANKTOSENS (VH-NG-500) by the Initiative and Networking Fund of the Helmholtz Association.

Abstract

Iron fertilization experiments are known to induce phytoplankton blooms in ocean areas with low chlorophyll concentrations despite high nutrient concentrations. In silicate limited waters iron fertilization experiments often induce phytoplankton blooms, which consist mainly of nano- and picoplankton. We used flow cytometry, tag pyrosequencing and catalyzed reported deposition fluorescence in situ hybridization (CARD-FISH) to investigate the diversity and community structure of the nano- and picoplankton during the iron fertilization experiment LOHAFEX conducted in the Southern Atlantic Ocean. As previously shown for the bacterial community, the diversity and community structure of the nano- and picoplankton remained remarkably stable during the course of the experiment. Besides *Phaeocystis*, OTUs of the *Syndiniales* and *Micromonas* clades made up the main part of the tag sequences within the fertilized patch. By CARD-FISH only *Micromonas* showed a minor peak in numbers at day 22 of the experiment, while numbers of *Phaeocystis* and clades I and II of *Syndiniales* were almost constant throughout the experiment inside the fertilized patch. With the combination of tag pyrosequencing and fluorescence in situ hybridization with automated cell counting we were able to shed light into the “black box” of the nano- and picoplankton during the LOHAFEX experiment.

1. Introduction

Phytoplankton blooms thrive seasonally or continuously in large parts of the oceans, where nutrients are found in plenty. However, large areas of the oceans exhibit low chlorophyll *a* concentrations despite high nutrient levels, a paradox known as the high nutrient-low chlorophyll areas (HNLCs). For example, large parts of the Southern Ocean are iron limited and thus do not support extensive phytoplankton blooms (1). In several experiments it could be shown, that an artificial fertilization with iron-induced phytoplankton blooms. Although, these blooms were often dominated by diatoms (2–4), nano- and picoplankton can make up a substantial fraction of the induced phytoplankton blooms (5, 6). In areas with both iron and silicate limitations, nano- and picoplankton can even dominate the blooms as found for example during the SAGE iron fertilization experiment (7).

The iron fertilization experiment LOHAFEX ('loha' is Hindi for 'iron'; FEX for Fertilization EXperiment) was conducted in a cold core eddy in the Southern Atlantic to induce a phytoplankton bloom and investigate the effects on the biological carbon pump. A phytoplankton bloom, dominated by nano- and picoplankton, was induced and monitored over the course of the experiment (8). However, these small *Eukarya*, ranging from 2 – 20 μm (nanoplankton) and 0.2 – 2 μm (picoplankton), are rarely explored in detail and remain a "black box" in most studies.

In previous studies the identification of eukaryotic nano- and picoplankton was done by direct microscopic counting of Lugol-fixed samples by the Utermöhl method (9), scanning electron microscopy (SEM) (e.g. 61), and marker pigment analyzes (reviewed in 23). More recently molecular biological tools, like clone libraries, catalyzed reporter deposition fluorescence in situ hybridization (CARD FISH) and 454 tag pyrosequencing were established for the identification and quantification of nano- and picoplankton (12–18). Using the molecular techniques it was found that *Haptophyta* is one of the most abundant marine groups which include a high diversity of picoeukaryotes (19, 20) The most prominent members of this group comprise the genus *Phaeocystis*, which forms large blooms worldwide (21), *Chrysochromulina* (22), and members of the class *Prymnesiophyceae*. Recently a high diversity especially for *Phaeocystis* was found using a set of molecular biological tools (23). Within the *Chlorophyta*, the *Prasinophyceae* are highly diverse (20, 24, 25) and paraphyletic and thus need to be newly classified based on molecular data (26–29). Investigations of this group were so far focused mainly on few subgroups. For example, *Micromonas*, a genus within the *Mamiellophyceae* including the single species *M. pusilla*, was found in high numbers in the British Channel (16), in clone libraries of pacific coastal waters, in the

Sargasso Sea (25), and in Arctic waters (30). Ribosomal RNA, pigment and metagenomic studies showed, that members of the class *Pelagophyceae* (*Heterokonta*) are major contributors to marine nano- and picoplankton communities (30–33). Different clades of the Marine Stramenopiles (MAST) were abundant worldwide (15) and putatively parasitic *Syndiniales*, belonging to the marine Alveolates (MALV) II clade were found throughout the Mediterranean Sea (34).

In our earlier study, we could observe only little changes in the community composition and abundance of *Bacteria* and *Archaea* in response to the iron fertilization experiment LOHAFEX. We postulated a high grazing pressure onto this community exerted by nano- and picoplankton grazers (35). In this study we used cutting edge molecular methods, including flow cytometry, tag pyrosequencing (36) and CARD FISH (37) to investigate the diversity and community structure of the nano- and picoplankton community during LOHAFEX.

2. Material & Methods

2.1. Sampling

The iron fertilization experiment LOHAFEX was conducted during the RV “Polarstern” cruise ANT XXV/3 (12th January till 6th March, 2009) as described previously (35). Briefly, a cold core eddy in the South Atlantic was fertilized with 10 t Fe(II)SO₄ on day 0. Another fertilization step using 10 t Fe(II)SO₄ was done on day 18 to provide stable concentrations of bioavailable iron over the course of the experiment. As a consequence of the fertilization, chlorophyll a concentrations increased from 0.5 µg l⁻¹ to 1.25 µg l⁻¹ (8, 35). The fertilized patch was monitored for 38 days. Samples for CARD-FISH analyses were taken on day -1 prior to the start of the experiment, on days 5, 9, 14, 18, 22, 24, 33, 36 inside the fertilized patch (“IN” stations) and days 4, 16, 29, 35 (only 20 m), and 38 outside the fertilized patch (“OUT” stations, FIG. 1). Both IN and OUT stations were situated within the eddy. On each day, 190 ml of water from 20 m depth and 40 m depth were fixed with 10 ml acidic Lugol solution (5% final conc. v/v) and stored in brown glass bottles at 4°C in the dark for 3 years until CARD FISH analysis. For DNA extraction for tag pyrosequencing 90 l (day -1), 85 l (day 9), 75 l (day 16/ OUT), 67 l (day 18) were sampled from 20 m depth on 0.2 µm pore size cellulose acetate filters (Sartorius, Göttingen, Germany) after a prefiltration step over 5 µm. These samples were stored at -80°C.

2.2. Flow cytometric cell counting

Total nano- and picoplankton was counted after fixation of fresh samples from 20 m depth and 40 m depth with particle-free formaldehyde solution (final conc. 1% v/v) and staining with SYBR Green I (1:10,000 dilution of stock) using a FACScalibur flow cytometer (BD Biosciences, Heidelberg, Germany) as described previously (38, 39).

2.3. Tag-pyrosequencing

DNA extraction was done using the E.Z.N.A.TM SP Plant DNA Kit (Omega Bio-Tek, Norcross, USA). Initially, the filters were incubated in lysis buffer (provided in the kit) at 65°C for 10 min before performing all further steps as described in the manufacturer’s instructions. The eluted DNA was stored at -20°C until further analysis.

We amplified ~670 bp fragments of the 18S rRNA gene, containing the highly variable V4-region, using the primer-set 528F (5'-GCGGTAATTCCAGCTCCAA-3') and 1055R (5'-ACGGCCATGCACCACCACCCAT-3') modified after Elwood (40) as described by Wolf

(41). Pyrosequencing (single reads, forward direction) was performed on a Genome Sequencer FLX system (Roche, Penzberg, Germany) by GATC Biotech AG (Konstanz, Germany).

Raw sequence reads were processed to obtain high quality reads. Reads with a length below 300 bp, reads longer than >670 bp and reads with more than one uncertain base (N) were excluded from further analysis. Chimera sequences were excluded using the software UCHIME 4.2 (42). The high quality reads of all samples were clustered into operational taxonomic units (OTUs) at the 97% similarity level using the software Lasergene 10 (DNASTAR, Madison, USA). Subsequently, reads not starting with the forward primer were manually removed. Consensus sequences of each OTU were generated and used for further analyses. The 97% similarity level is conservative, but was found suitable to reproduce original eukaryotic diversity (43) and brace the sequencing errors (44). For the calculation of the Chao1 index and the Shannon index, the number of input reads for each sample was randomly re-sampled (in this case 11858 reads) to have the same number of reads from all samples. The diversity indices were calculated using the program R (R Development Core Team 2012).

OTUs comprised of only one sequence (singletons) were removed. The consensus sequences were aligned using the software HMMER 2.3.2 (45) and implemented into a reference tree, containing about 1,200 high quality sequences of *Eukarya* from the SILVA reference database (SSU Ref 108), using the software pplacer 1.0 (46). OTUs assigned to fungi and metazoans were excluded from further analysis. Rarefaction curves were computed using the freeware program Analytic Rarefaction 1.3. For the calculation of the Chao1 index and the Shannon index, the number of input reads for each sample was randomly re-sampled (in this case 11858 reads) to have the same number of reads from all samples. The diversity indices were calculated using the program R. The raw sequence data generated in this study has been deposited at GenBank's Short Read Archive (SRA) under Accession No SRA064723.

2.4. CARD FISH

Nano- and picoplankton abundances were quantified for all stations in samples from 20 m and 40 m depth by CARD FISH. In preliminary tests, a clear cell loss was detected for the Lugol-fixed samples after CARD FISH. Additionally, the margins of the remaining Lugol-fixed cells appeared disrupted, shrunken or shapeless. An additional fixation step with formaldehyde was necessary to stabilize the cells for CARD FISH and resulted in bright signals and stable cell counts. Hundred milliliter of the Lugol-fixed sample was fixed for 1 h with formaldehyde (1% final concentration), destained with 1 M sodium thiosulfate and filtered onto

polycarbonate filters with 0.8 μm pore size (Millipore, Tullagreen, Ireland). Due to limited sample amount, only 25 ml and 70 ml were filtered for samples of day -1 and day 38 (both 20 m depth). CARD FISH was done as described previously (37) modified after Thiele (47). Briefly, a permeabilization step was done with Proteinase K (5 $\mu\text{g}/\text{ml}$) for 15 minutes for samples which were hybridized with the probe PHAEO03, due to the enhanced length (34 bp) of this probe. Hybridization and amplification was done on glass slides using 50 ml tubes or in Petri dishes using 700 ml glass chambers as moisture chambers at 46°C. We used 14 horseradish peroxidase (HRP) labeled oligonucleotide probes (TAB. 1) including the probe NON338 (48) as a control. All other probes were chosen according to 454 tag sequencing results. For signal amplification, Alexa488 labeled tyramides (49) were used for all probes and samples were stained with DAPI after the CARD procedure (SUP 2).

Fluorescence signals from CARD FISH stained cells were counted manually on an Eclipse 50i microscope (Nikon, Amstelveen, Netherland), at 1000x magnification in 50 fields of view (FOV) per sample of duplicates. Since the wind mixed layer (WML) was 60 – 80 m deep during the experiment and rather stable chlorophyll a values throughout the WML were found (8) results from 20 m and 40 m depth were treated as replicates. Quantification of total cell numbers after CARD FISH was done with a Zeiss Axio Imager.Z2 microscope (Zeiss, Jena, Germany) with an automated stage. Image acquisition was done using the software package AxioVision Release 7.6 (Zeiss, Jena, Germany) and the macro MPISYS (Zeder unpublished) based on an automated focusing routine, sample area definition and image quality assessment (50–52). Only samples with a minimum of 15 picture triplets (SUP 3) were taken into account and evaluated using the software ACMETool 0.76 (Zeder unpublished) with an algorithm for nanoflagellate quantification. We used a combination of natural fluorescence of the cells, autofluorescence of cell pigments and probe signals which appeared to be clearly visible on pictures. DAPI signals were sometimes covered by strong autofluorescence, making a counting of the signals difficult. In addition, not all cells are autofluorescent or stained by the probe EUK516, thus making both signals insufficient for total cell counting. Therefore, we used the combination of all three signals to determine cells for total cell counts. Results from both depths were pooled and total cell numbers were calculated as a mean value of a minimum of 13 samples.

2.5. Probe design and re-evaluation

We designed two new probes for the subclades I and II of the *Syndiniales* clade (TAB. 1) using the ARB SILVA ref 108 database (53). SYNI 1161 targets 71% of the *Syndiniales* group I sequences, with 151 outgroup hits within the dinoflagellates and 220 outgroup hits in other *Eukarya*. SYNII 675 targets 58% of the *Syndiniales* group II with 28 outgroup hits within the dinoflagellates and 347 in other *Eukarya* (SUP. 4). Since no culture of *Syndiniales* was available, a melting curve was done on a sample from day 38 (20 m depth) of the experiment, resulting in a formamide concentration of 20% for both probes.

The probe PRAS04 (16) was designed for *Prasinophyceae*. Since the clade was recently found to be paraphyletic and thus phylogenetically reviewed, we evaluated the probe PRAS04 and found a coverage of 95% for the class *Mamiellophyceae* (29) with only one outgroup hit in the *Dinophyceae* and one in the *Chrysophyceae* and no other hits in the *Prasinophyceae*. Thus, we propose to use the probe only for *Mamiellophyceae*.

2.6. Statistics

The total cell numbers achieved by flow cytometry and automated counting of CARD FISH cells were compared using linear regressions. CARD FISH data were tested on normal distribution of the data using the Kolmogorov-Smirnov test and analyses of variance (ANOVA) were done accordingly. Normal distributed data were tested using one way ANOVAs including Holm-Sidak comparison and not-normal distributed data were tested using ANOVA on ranks. Differences between the IN and OUT stations were verified using t-tests. All analyses were done using SigmaStat 3.5 (Statcon, Witzenhausen, Germany).

3. Results

3.1. Nano- and picoplankton cell numbers

During LOHAFEX, the nano- and picoplankton cells were enumerated on freshly fixed samples inside and outside the fertilized patch by flow cytometry on board. Inside the patch nano- and picoplankton abundances increased significantly ($p < 0.001$) from 7.5×10^3 cells ml^{-1} on day 5 to 1.9×10^4 cells ml^{-1} on day 22 (FIG. 2 A). Outside the fertilized patch cell numbers were rather stable ($1.0 \times 10^4 \pm 1.2 \times 10^3$ cells ml^{-1}) but showed two maxima on day 29 (1.8×10^4 cells ml^{-1}) and day 38 (1.7×10^4 cells ml^{-1}) (FIG. 2 A).

Cell counts obtained with automated cell counting after CARD FISH of Lugol- and formaldehyde fixed samples were by a factor of ~ 2 (1.2- 3.1) lower compared to the flow cytometric direct counts. Similar to the flow cytometric counts, abundances peaked on day 22 with 9.3×10^3 cells ml^{-1} ($p < 0.001$), but otherwise cell numbers remained rather constant at $6.1 \pm 1.3 \times 10^3$ cells ml^{-1} (FIG. 2 B).

3.2. Community composition

The eukaryotic diversity in the 0.2 to 5 μm fraction was assessed in the eddy one day before the start of the experiment, during the experiment on days 9 and 18 inside the fertilized patch, and at day 16 outside the fertilized patch using tag pyrosequencing (FIG 3). The Shannon diversity index increased from 3.71 at day -1 to 4.1 at day 18 inside the patch and to 4.12 outside the patch. The chao1 index showed an increase from 660 (day -1) to 729 (day 9) and 697 (day 18), but showed numbers as high as 733 at the OUT station on day 16.

Although, the diversity increased over the course of the experiment, all four samples were similar in the major group composition (FIG 3). The most frequent tags in all samples originated from *Syndiniales* (~ 26 -33%), followed by *Chlorophyta* (24-29%) and *Haptophyceae* (~ 21 -28%). Some of the 21 abundant OTUs ($> 1\%$ of all sequences) showed some fluctuations in sequence abundance over the course of the experiment (FIG 3). The most abundant genus was *Phaeocystis* (*Haptophyta*) accounting for $\sim 14\%$ (day 18) to $\sim 23\%$ (day -1) of all sequences (FIG 3). This OTU showed a slight decrease inside the fertilized patch. Among the *Mamiellophyceae*, a class within the *Chlorophyta*, two different OTUs affiliated to the genus *Micromonas* were most dominant (17.3-18.5%) inside the patch. Within this genus we observed a shift from *Micromonas* OTU A to *Micromonas* OTU B inside the patch, while both OTUs decreased in the OUT station (FIG 3; SUP 5). A OTU of the *Monomastix* genus (8.5%) was dominating the *Mamiellophyceae* outside the fertilized patch. Only the

Pelagophyceae showed a distinct decrease in sequence abundance from 5.8% at day -1 to 2.0% at day 18 inside the patch. The two abundant OTUs within the *Pelagophyceae* were found in highest abundance at the OUT station on day 16, with ~5% (*Pelagomonas* sp.) and ~3% (uncultured *Pelagophyceae*) of total sequences (FIG 3). Inside the fertilized patch both were found only in low sequence abundances (~1-2% of total sequences). Only two abundant OTUs belonging to MAST (*Stramenopila*) were found, each with the highest sequence abundance of ~1.2% at day 18 (FIG 3). *Syndiniales* were present with seven different abundant unclassified OTUs which were labeled arbitrarily with letters from A to G (SUP 2). The OTU *Syndiniales* A (Dino-group II) was by far the most abundant one in all samples with a sequence abundance of ~11-15%, while other *Syndiniales* OTUs showed sequence abundances of ~1-3.5% or were absent in some samples (FIG 3).

3.3. Quantification of specific nano- and picoplankton clades

For eight of the dominant clades in tag pyrosequencing, specific probes were used to quantify their *in situ* abundance by CARD FISH. The EUK516 probe, specific for most *Eukarya* (48), showed abundances which were about 1.8-fold lower than the total cell numbers obtained by flow cytometric cell counting. The numbers of EUK516 stained cells were highest at day -1 with 5.8×10^3 cells ml⁻¹, decreasing to 1.9×10^3 cells ml⁻¹ on day 9, before a second peak of 4.7×10^3 cells ml⁻¹ and 4.8×10^3 cells ml⁻¹ on days 22 and 24 inside the fertilized patch (FIG. 4 A). EUK-positive cell numbers were relatively constant outside the patch, but were as high as 7.0×10^3 cells ml⁻¹ on day 38, which was significantly different from the comparable IN station on day 36 (p=0.045) (FIG. 4 B).

In order to investigate the nano- and picoplankton community, we used CARD FISH probes with a nested specificity with different taxonomic depths. The total cell counts obtained by the EUK516 probe were covered by the sum of non-overlapping clade specific probes (FIG. 4A, 4B). Within the nano- and picoplankton community inside the fertilized patch, *Haptophyta*, mainly from the genus *Phaeocystis* were contributors to the nano- and picoplankton community. However, abundances of both clades did not change significantly within the fertilized patch over the course of the experiment (FIG. 5 A + B). Values were constant at about 1.0×10^3 cells ml⁻¹ for *Haptophyta* and 5.0×10^2 cells ml⁻¹ for *Phaeocystis*, thus *Phaeocystis* accounted for about 50% of the *Haptophyta*. At the OUT station on day 16, higher numbers of *Phaeocystis* were found with 1.1×10^3 cells ml⁻¹, resulting also in significantly higher numbers of *Haptophyta* (1.5×10^3 cells ml⁻¹) (p=0.01). *Mamiellophyceae*, a second dominant clade in the tag sequences, showed a higher variation in cell numbers inside the fertilized patch, while cell numbers in the OUT stations remained rather constant.

After a rather dramatic initial decrease from 3.2×10^3 cells ml^{-1} to 5.9×10^2 cells ml^{-1} on day 9 inside the patch, cells increased again to 1.8×10^3 cells ml^{-1} on day 22. This abundance of *Mamiellophyceae* was significantly ($p=0.03$) higher compared to the OUT station on day 29 (FIG. 5 C). The dominant subgroup of *Mamiellophyceae*, namely *Micromonas*, mimicked these patterns, showing a decrease in cell numbers from 1.3×10^3 cells ml^{-1} on day -1 to numbers around 4.4×10^2 cells ml^{-1} on day 9. Again elevated numbers were found on day 22, which were as high as 1.2×10^3 cells ml^{-1} and thus significantly ($p=0.028$) higher than the following OUT station at day 29. On average *Micromonas* accounted for ~72% of the *Mamiellophyceae* (FIG. 5 D).

Pelagophyceae were also found rather stable in- and outside of the patch with numbers as high as 1.13×10^3 cells ml^{-1} outside the patch on day 16 (FIG 5 E). Abundances of Marine Stramenopiles (MAST) were low and never exceeded 1.7×10^2 cells ml^{-1} during the course of the experiment (FIG 5 F). Also the numbers of both *Syndiniales* clades were low and oscillated around 7.7×10^1 cells ml^{-1} (*Syndiniales* clade I) and around 1.8×10^2 cells ml^{-1} (*Syndiniales* clade II) within and outside of the fertilized patch (FIG. 5 G + H). For both *Syndiniales* clades no cells could be detected on day 29.

4. Discussion

During the 38 days of the LOHAFEX experiment a phytoplankton bloom was induced and the chlorophyll a concentration inside the fertilized patch more than doubled (35). On board analyses already indicated that diatoms were limited by silicate ($<2 \mu\text{M}$) and thus showed only a moderate response to iron addition. The major biomass of the bloom was constituted by the pico- and nanoflagellate community (8). The high abundance of nano- and picoplankton was postulated to exert grazing pressure on the bacterial and archaeal community (35). Consequently, we investigated the nano- and picoplankton community using a combination of flow cytometry, tag pyrosequencing, CARD FISH and automated cell counting. It turned out that the methods used had some technical challenges.

Shipboard flow cytometry revealed consistently higher cell numbers compared to automated microscopic cell counting. An overestimation of cell counts by flow cytometry was previously reported (54) and might originate from autofluorescent detritus as well as from the detection of large bacterial cells such as *Roseobacter* or *Gammaproteobacteria*. Both bacterial groups were abundant during the LOHAFEX experiment (35). In turn, fixation could lead to an underestimation of total cell counts due to cell shrinkage and cell disruption caused by the fixative (55). Formaldehyde fixation was used for flow cytometric analyses, while for automated cell counting and CARD FISH cell were first fixed with Lugol solution and subsequently with formaldehyde. Possibly the long-term storage the samples of >3 years might have caused cell loss which led to approximately 50% lower microscopic cell counts compared to flow cytometric counts. Another source of cell loss might be the filtration and washing steps necessary for CARD FISH. Small picoplankton cells might have passed the $0.8 \mu\text{m}$ size pores of the polycarbonate filter (56, 57) or might have been lost in washing steps during CARD FISH. However, we were able to successfully apply CARD FISH and automated cell counting on Lugol fixed samples even after the prolonged storage time.

With the probe EUK516, targeting *Eukarya*, about 50-70% of all nano- and pico eukaryotic cells showed a signal in our samples after CARD FISH. The sum of cells detected by all clade-specific probes was almost as high as the counts of the EUK516 probe ($\sim 90\%$) and resembled largely the representation of dominant clades found with tag pyrosequencing.

The high representation of *Syndiniales* sequences in the tag libraries somehow conflicted with low CARD FISH numbers. A possible explanation might be that members of the *Syndiniales* group have been described as parasites (58, 59). Cells residing inside dinoflagellates might be inaccessible for large HRP-labeled oligonucleotide probes. Furthermore, the detection of the

newly designed probes SYNI 1161 and SYNII 675 might remain insufficient for the detection of all cells of this group, since no *Syndiniales* culture was available and probe testing had to be done directly on the samples. Besides technical challenges, *Syndiniales* might have multiple chromosome copies, as it is known for the neighboring group of *Dinoflagellata* (60). Thus, the number of 18S rRNA gene copies might be elevated, resulting in high abundances in the tag sequences.

For the different MAST clades we used specific oligonucleotide probes and found a rather stable community structure. However, all clades were found in rather low numbers compared to the reported $>1.0 \times 10^2$ MAST 1 cells ml^{-1} in the Southern Ocean (15).

In several clades an initial decrease in abundance, though not statistically significant, was followed by a non-significant peak on day 22 inside the fertilized patch. This marginal pattern was especially pronounced for the *Mamiellophyceae* in general and for the clades *Micromonas* in particular. A possible explanation for the initial massive decrease in cell numbers might be an active grazer community, which developed during a bloom prior to the experiment and which immediately counteracted the response of the nano- and picoplankton community to the iron fertilization.

The subsequent increase of these clades towards day 22 might be caused by the highest bacterial and archaeal numbers on day 18, which could support growth of the hetero- and mixotroph nano- and picoplankton (35). Heterotrophic pico-eukaryotes like MAST (15) or mixotrophic *Micromonas* are known to feed on bacteria (61, 62) and might profit from higher prey numbers. Ultimately heterotrophic nano- and picoplankton could benefit from elevated food availability and started to out-compete the grazer community, which were found to be mainly dinoflagellates (8), and to increase in cell numbers (63). Another reason might be a release of grazing pressure on the nano- and picoplankton community by increased copepod numbers, which kept the dinoflagellate dominated grazer community under control.

The second decline in cell numbers after the maximum on day 22 could be the result of a reinforced grazing pressure on nano- and picoplankton by predators, which grew on the increased nano- and picoplankton numbers.

Our results show that tag pyrosequencing and CARD FISH are suitable tools to open the “black box” of the small marine *Eukarya*. While tag pyrosequencing provides valuable information about the diversity and community structure, it also provides guidance for the selection of oligonucleotide probes for CARD FISH quantifications. These enumerations have a profound taxonomic resolution compared to light microscopy and pigment analyses, and allow for faster sample analyses than electron microscopy. In addition, we were able to show that samples fixed with Lugol solution for light microscopy can be used for CARD FISH

analyses even after long storage times. Still not all nano- and picoplankton clades can be covered sufficiently on a high taxonomic level, showing the urgent need of further sequencing and probe design, in order to fully investigate these important mediators between the world of *Bacteria* and *Archaea* and the world of the microzooplankton.

References

1. **Martin JH.** 1990. Glacial-interglacial CO₂ change: The iron hypothesis. *Paleoceanography* **5**:1–13.
2. **Martin JH, Coale KH, Johnson KS, Fitzwater SE, Gordon RM, Tanner SJ, Hunter CN, Elrod VA, Nowicki JL, Coley TL, Barber RT, Lindley S, Watson AJ, Van Scoy K, Law CS, Liddicoat MI, Ling R, Stanton T, Stockel J, Collins C, Anderson A, Bidigare R, Ondrusek M, Latasa M, Millero FJ, Lee K, Yao W, Zhang JZ, Friederich G, Sakamoto C, Chavez F, Buck K, Kolber Z, Greene R, Falkowski P, Chisholm SW, Hoge F, Swift R, Yungel J, Turner S, Nightingale P, Hatton A, Liss P, Tindale NW.** 1994. Testing the iron hypothesis in ecosystems of the equatorial Pacific Ocean. *Nature* **371**:123–129.
3. **deBaar HJW, Boyd PW, Coale KH, Landry MR, Tsuda A, Assmy P, Bakker DCE, Bozec Y, Barber RT, Brzezinski MA, Buesseler KO, Boyé M, Croot PL, Gervais F, Gorbunov MY, Harrison PJ, Hiscock WT, Laan P, Lancelot C, Law CS, Levasseur M, Marchetti A, Millero FJ, Nishioka J, Nojiri Y, Oijen T van, Riebesell U, Rijkenberg MJA, Saito H, Takeda S, Timmermans KR, Veldhuis MJW, Waite AM, Wong C.** 2005. Synthesis of iron fertilization experiments: From the iron age in the age of enlightenment. *J. Geophys. Res.* **110**:1–24.
4. **Smetacek V, Klaas C, Strass VH, Assmy P, Montresor M, Cisewski B, Savoye N, Webb A, D' Ovidio F, Arrieta JM, Bathmann U, Bellerby R, Berg GM, Croot P, Gonzalez S, Henjes J, Herndl GJ, Hoffmann LJ, Leach H, Losch M, Mills MM, Neill C, Peeken I, Röttgers R, Sachs O, Sauter E, Schmidt MM, Schwarz J, Terbrüggen A, Wolf-Gladrow D.** 2012. Deep carbon export from a Southern Ocean iron-fertilized diatom bloom. *Nature* **487**:313–319.
5. **Hall JA, Safi K.** 2001. The impact of in situ Fe fertilisation on the microbial food web in the Southern Ocean. *Deep-Sea Res. Pt. II* **48**:2591–2613.
6. **Coale KH, Johnson KS, Chavez FP, Buesseler KO, Barber RT, Brzezinski MA, Cochlan WP, Millero FJ, Falkowski PG, Bauer JE, Wanninkhof RH, Kudela RM, Altabet MA, Hales BE, Takahashi T, Landry MR, Bidigare RR, Wang X, Chase Z, Strutton PG, Friederich GE, Gorbunov MY, Lance VP, Hilting AK, Hiscock MR, Demarest M, Hiscock WT, Sullivan KF, Tanner SJ, Gordon RM, Hunter CN, Elrod VA, Fitzwater SE, Jones JL, Tozzi S, Koblizek M, Roberts AE, Herndon J, Brewster J, Ladizinsky N, Smith G, Cooper D, Timothy D, Brown SL, Selph KE, Sheridan CC, Twining BS, Johnson ZI.** 2004. Southern Ocean iron enrichment experiment: Carbon cycling in high- and low-Si waters. *Science* **304**:408–414.
7. **Peloquin J, Hall J, Safi K, Ellwood M, Law CS, Thompson K, Kuparinen J, Harvey M, Pickmere S.** 2011. Control of the phytoplankton response during the SAGE experiment: A synthesis. *Deep Sea Res. Part II: Topical Studies in Oceanography* **58**:824–838.
8. **Schulz I, Assmy P, Rajdeep R, Gauns M, Sakar A, Thiele S, Wolf C, Wolzenburg S, Klaas C, Smetacek V.** 2013. Response of a flagellate dominated plankton community to artificial iron fertilization in the Southern Ocean. In preparation.
9. **Utermöhl H.** 1958. Zur Vervollkommnung der quantitativen Phytoplankton-Methodik. *Mitt. int. Ver. theor. angew. Limnol.* **9**:1–38.

10. **Zingone A, Chretiennot-Dinet M-J, Lange M, Medlin L.** 1999. Morphological and genetic characterization of *Phaeocystis cordata* and *P. jahnii* (Prymnesiophyceae), two new species from the Mediterranean Sea. *J. Phycol.* 1322–1337.
11. **Jeffrey S, Wright S.** 2006. Photosynthetic pigments in marine microalgae: insights from cultures and the sea, p. 33–90. *In* Rao, DVS (ed.), *Algal cultures, Analogues of blooms and applications*. Science Publisher, Enfield (UK).
12. **Not F, Simon N, Biegala IC, Vaultot D.** 2002. Application of fluorescent in situ hybridization coupled with tyramide signal amplification (FISH-TSA) to assess eukaryotic picoplankton composition. *Aquat. Microb. Ecol.* **28**:157–166.
13. **Cheung MK, Au CH, Chu KH, Kwan HS, Wong CK.** 2010. Composition and genetic diversity of picoeukaryotes in subtropical coastal waters as revealed by 454 pyrosequencing. *ISME J.* **4**:1053–1059.
14. **Massana R, Guillou L, Díez B, Pedrós-Alió C.** 2002. Unveiling the Organisms behind Novel Eukaryotic Ribosomal DNA Sequences from the Ocean. *Appl. Environ. Microbiol.* **68**:4554–4558.
15. **Massana R, Terrado R, Forn I, Lovejoy C, Pedrós-Alió C.** 2006. Distribution and abundance of uncultured heterotrophic flagellates in the world oceans. *Environ. Microbiol.* **8**:1515–1522.
16. **Not F, Latasa M, Marie D, Cariou T, Vaultot D, Simon N.** 2004. A single species, *Micromonas pusilla* (Prasinophyceae), dominates the eukaryotic picoplankton in the western English Channel. *Appl. Environ. Microbiol.* **70**:4064–4072.
17. **Stoeck T, Bass D, Nebel M, Christen R, Jones MDM, Breiner H-W, Richards TA.** 2010. Multiple marker parallel tag environmental DNA sequencing reveals a highly complex eukaryotic community in marine anoxic water. *Mol. Ecol.* **19**:21–31.
18. **Medlin LK, Metfies K, Mehl H, Wiltshire K, Valentin K.** 2006. Picoeukaryotic Plankton Diversity at the Helgoland Time Series Site as Assessed by Three Molecular Methods. *Microb. Ecol.* **52**:53–71.
19. **Moon-van der Staay SY, Van der Staay GWM, Guillou L, Vaultot D, Claustre H, Medlin LK.** 2000. Abundance and Diversity of Prymnesiophytes in the Picoplankton Community from the Equatorial Pacific Ocean Inferred from 18S rDNA Sequences. *Limnol. Oceanogr.* **45**:98–109.
20. **Cuvelier ML, Allen AE, Monier A, McCrow JP, Messié M, Tringe SG, Woyke T, Welsh RM, Ishoey T, Lee J-H, Binder BJ, DuPont CL, Latasa M, Guigand C, Buck KR, Hilton J, Thiagarajan M, Caler E, Read B, Lasken RS, Chavez FP, Worden AZ.** 2010. Targeted Metagenomics and Ecology of Globally Important Uncultured Eukaryotic Phytoplankton. *PNAS* **107**:14679–14684.
21. **Schoemann V, Becquevort S, Stefels J, Rousseau V, Lancelot C.** 2005. *Phaeocystis* blooms in the global ocean and their controlling mechanisms: a review. *J. Sea Res.* **53**:43–66.
22. **Liu H, Probert I, Uitz J, Claustre H, Aris-Brosou S, Frada M, Not F, Vargas C de.** 2009. Extreme diversity in noncalcifying haptophytes explains a major pigment paradox in open oceans. *PNAS* **106**:12803–12808.
23. **Medlin L, Zingone A.** 2007. A Taxonomic Review of the Genus *Phaeocystis*. *Biogeochemistry* **83**:3–18.

24. **Guillou L, Eikrem W, Chrétiennot-Dinet M-J, Le Gall F, Massana R, Romari K, Pedrós-Alió C, Vaultot D.** 2004. Diversity of Picoplanktonic Prasinophytes Assessed by Direct Nuclear SSU rDNA Sequencing of Environmental Samples and Novel Isolates Retrieved from Oceanic and Coastal Marine Ecosystems. *Protist* **155**:193–214.
25. **Worden AZ.** 2006. Picoeukaryote diversity in coastal waters of the Pacific Ocean. *Aquat. Microb. Ecol.* **43**:165–175.
26. **Lewis LA, McCourt RM.** 2004. Green Algae and the Origin of Land Plants. *Am. J. Bot.* **91**:1535–1556.
27. **Adl SM, Simpson AGB, Farmer MA, Andersen RA, Anderson OR, Barta JR, Bowser SS, Brugerolle G, Fensome RA, Fredericq S, James TY, Karpov S, Kugrens P, Krug J, Lane CE, Lewis LA, Lodge J, Lynn DH, Mann DG, McCourt RM, Mendoza L, Moestrup Ø, Mozley-Standridge SE, Nerad TA, Shearer CA, Smirnov AV, Spiegel FW, Taylor MFJR.** 2005. The New Higher Level Classification of Eukaryotes with Emphasis on the Taxonomy of Protists. *J. Euk. Microbiol.* **52**:399–451.
28. **Shi XL, Lepère C, Scanlan DJ, Vaultot D.** 2011. Plastid 16S rRNA Gene Diversity among Eukaryotic Picophytoplankton Sorted by Flow Cytometry from the South Pacific Ocean. *PLoS ONE* **6**:e18979.
29. **Marin B, Melkonian M.** 2010. Molecular Phylogeny and Classification of the Mamiellophyceae class. nov. (Chlorophyta) based on Sequence Comparisons of the Nuclear- and Plastid-encoded rRNA Operons. *Protist* **161**:304–336.
30. **Balzano S, Marie D, Gourvil P, Vaultot D.** 2012. Composition of the summer photosynthetic pico and nanoplankton communities in the Beaufort Sea assessed by T-RFLP and sequences of the 18S rRNA gene from flow cytometry sorted samples. *ISME J.* **6**:1480–1498.
31. **Andersen RA, Sounders GW, Paskind MP, Sexton JP.** 1993. Ultrastructure and 18S rRNA gene sequence for *Pelagomonas Calceolata* Gen. et Sp. Nov. and the Description of a new algal class, the Pelagophyceae Classis Nov. *J. Phycol.* **29**:701–715.
32. **Not F, Latasa M, Scharek R, Viprey M, Karleskind P, Balagué V, Ontoria-Oviedo I, Cumino A, Goetze E, Vaultot D, Massana R.** 2008. Protistan assemblages across the Indian Ocean, with a specific emphasis on the picoeukaryotes. *Deep Sea Res. Pt. I* **55**:1456–1473.
33. **Worden AZ, Janouskovec J, McRose D, Engman A, Welsh RM, Malfatti S, Tringe SG, Keeling PJ.** 2012. Global distribution of a wild alga revealed by targeted metagenomics. *Curr. Biol.* **22**:R675–R677.
34. **Siano R, Alves-de-Souza C, Foulon E, Bendif EM, Simon N, Guillou L, Not F.** 2011. Distribution and host diversity of Amoebophryidae parasites across oligotrophic waters of the Mediterranean Sea. *Biogeosciences* **8**:267–278.
35. **Thiele S, Fuchs BM, Ramaiah N, Amann R.** 2012. Microbial community response during the iron fertilization experiment LOHAFEX. *Appl. Environ. Microbiol.* **78**:8803–8812.
36. **Ronaghi M, Karamohamed S, Pettersson B, Uhlén M, Nyrén P.** 1996. Real-Time DNA sequencing using Detection of pyrophosphate release. *Analyt. Biochem.* **242**:84–89.

37. **Pernthaler A, Pernthaler J, Amann R.** 2002. Fluorescence in situ hybridization and catalyzed reporter deposition for the identification of marine bacteria. *Appl. Environ. Microbiol.* **68**:3094–3101.
38. **Marie D, Partensky F, Jacquet S, Vaulot D.** 1997. Enumeration and Cell Cycle Analysis of Natural Populations of Marine Picoplankton by Flow Cytometry Using the Nucleic Acid Stain SYBR Green I. *Appl. Environ. Microbiol.* **63**:186–193.
39. **Tarran GA, Heywood JL, Zubkov MV.** 2006. Latitudinal changes in the standing stocks of nano- and picoeukaryotic phytoplankton in the Atlantic Ocean. *Deep Sea Res. Part II: Topical Studies in Oceanography* **53**:1516–1529.
40. **Elwood HJ, Olsen GJ, Sogin ML.** 1985. The small-subunit ribosomal RNA gene sequences from the hypotrichous ciliates *Oxytricha nova* and *Stylonychia pustulata*. *Mol. Biol. Evol.* **2**:399–410.
41. **Wolf C, Frickenhaus S, Kiliyas ES, Peecken I, Metfies K.** published online. Regional variability in eukaryotic protist communities in the Amundsen Sea. *Antarctic Science* DOI:10.1017/S0954102013000229.
42. **Edgar RC, Haas BJ, Clemente JC, Quince C, Knight R.** 2011. UCHIME Improves Sensitivity and Speed of Chimera Detection. *Bioinformatics* **27**:2194–2200.
43. **Behnke A, Engel M, Christen R, Nebel M, Klein RR, Stoeck T.** 2011. Depicting more accurate pictures of protistan community complexity using pyrosequencing of hypervariable SSU rRNA gene regions. *Environ. Microbiol.* **13**:340–349.
44. **Kunin V, Engelbrektson A, Ochman H, Hugenholtz P.** 2009. Wrinkles in the rare biosphere: pyrosequencing errors can lead to artificial inflation of diversity estimates. *Environ. Microbiol.* **12**:118–123.
45. **Eddy SR.** 2011. Accelerated Profile HMM Searches. *PLoS Comput Biol* **7**:e1002195.
46. **Matsen FA, Kodner RB, Armbrust EV.** 2010. pplacer: linear time maximum-likelihood and Bayesian phylogenetic placement of sequences onto a fixed reference tree. *BMC Bioinformatics* **11**:538.
47. **Thiele S, Fuchs B, Amann R.** 2011. Identification of microorganisms using the ribosomal RNA approach and fluorescence in situ hybridization, p. 171–189. *In* Wilderer, P (ed.), *Treatise on Water Science* Wilderer, P. Academic Press, Oxford.
48. **Amann RI, Binder BJ, Olson RJ, Chisholm SW, Devereux R, Stahl DA.** 1990. Combination of 16S rRNA-targeted oligonucleotide probes with flow cytometry for analyzing mixed microbial populations. *Appl. Environ. Microbiol.* **56**:1919–1925.
49. **Pernthaler J, Amann R.** 2004. Sensitive multi-color fluorescence in situ hybridization for the identification of environmental microorganisms. *Molecular Microbial Ecology Manual* **3**:711–726.
50. **Zeder M, Kohler E, Pernthaler J.** 2009. Automated quality assessment of autonomously acquired microscopic images of fluorescently stained bacteria. *Cytometry* **9999A**:NA–NA.
51. **Zeder M, Ellrott A, Amann R.** 2011. Automated sample area definition for high-throughput microscopy. *Cytometry A*:306–310.
52. **Zeder M, Pernthaler J.** 2009. Multispot live-image autofocusing for high-throughput microscopy of fluorescently stained bacteria. *Cytometry* **75A**:781–788.

53. **Pruesse E, Quast C, Knittel K, Fuchs BM, Ludwig W, Peplies J, Glöckner FG.** 2007. SILVA: a comprehensive online resource for quality checked and aligned ribosomal RNA sequence data compatible with ARB. *Nucl. Acids Res.* **35**:7188–7196.
54. **Li WKW, Wood AM.** 1988. Vertical distribution of North Atlantic ultraphytoplankton: analysis by flow cytometry and epifluorescence microscopy. *Deep Sea Res. Part I: Oceanograph. Res. Papers* **35**:1615–1638.
55. **Choi JW, Stoecker DK.** 1989. Effects of fixation on cell volume of marine planktonic protozoa. *Appl. Environ. Microbiol.* **55**:1761–1765.
56. **Cynar FJ, Estep KW, Sieburth JM.** 1985. The detection and characterization of bacteria-sized protists in “protist-free” filtrates and their potential impact on experimental marine ecology. *Microbial Ecol.* **11**:281–288.
57. **Gasol JM, Morn XAG.** 1999. Effects of filtration on bacterial activity and picoplankton community structure as assessed by flow cytometry. *Aquat. Microb. Ecol.* **16**:251–264.
58. **Coats DW, Bockstahler KR.** 1994. Occurrence of the Parasitic Dinoflagellate *Amoebophrya ceratii* in Chesapeake Bay Populations of *Gymnodinium sanguineum*. *J. Euk. Microbiol.* **41**:586–593.
59. **Coats DW, Adam EJ, Gallegos CL, Hedrick S.** 1996. Parasitism of Photosynthetic Dinoflagellates in a Shallow Subestuary of Chesapeake Bay, USA. *Aquat. Microb. Ecol.* **11**:1–9.
60. **Spector DL.** 1984. Dinoflagellate nuclei, p. 107–147. *In* *Dinoflagellates*, D. L. Spector [ed.]. Academic Press, Inc., Orlando, Florida, USA.
61. **Gonzalez JM, Sherr BF, Sherr E.** 1993. Digestive enzyme activity as a quantitative measure of protistan grazing: the acid lysozyme assay for bacterivory. *Mar. Ecol. Prog. Ser.* **100**:197–206.
62. **Sanders RW, Gast RJ.** 2012. Bacterivory by phototrophic picoplankton and nanoplankton in Arctic waters. *FEMS Microbiol. Ecol.* **82**:242–253.
63. **Rokkan Iversen K, Seuthe L.** 2010. Seasonal microbial processes in a high-latitude fjord (Kongsfjorden, Svalbard): I. Heterotrophic bacteria, picoplankton and nanoflagellates. *Polar Biol.* **34**:731–749.
64. **Wallner G, Amann R, Beisker W.** 1993. Optimizing fluorescent in situ hybridization with rRNA-targeted oligonucleotide probes for flow cytometric identification of microorganisms. *Cytometry* **14**:136–143.
65. **Simon N, Campbell L, Ornlófsdóttir E, Groben R, Guillou L, Lange M, Medlin LK.** 2000. Oligonucleotide probes for the identification of three algal groups by dot blot and fluorescent whole-cell hybridization. *J. Eukaryot. Microbiol.* **47**:76–84.

Tables

Tab. 1: List of oligonucleotides used in this study. ^a Formamide concentration in the CARD FISH hybridization buffer.

Figures

Fig. 1: Map of the fertilized area. The chlorophyll *a* picture shows the LOHAFEX bloom (encircled). Stations and experiment days of both the IN (black) and OUT stations (white) are shown in the small map. The X marks day -1 before the experiment. The globe and the inset map were generated with the M_Map package for Matlab (version 7.12.0.635; MathWorks, Natick, MA). The chlorophyll *a* data were downloaded from the NASA website <http://oceancolor.gsfc.nasa.gov/>.

Fig. 2: Total cell counts of all stations inside the fertilized patch achieved by using flow cytometric (FCM) counting and automated microscopic counting after CARD FISH staining. Black spheres with straight lines represent stations inside while white spheres with dashed lines represent stations outside the fertilized patch.

Fig. 3: Relative 18S rRNA gene amplicon frequency revealed by tag pyrosequencing at 20 m depth.

Fig. 4: Total cell numbers of cells stained with the EUK516 probe of the IN (black, A) and OUT (white, B) stations. Bar charts represent the coverage of the EUK516 probe by all other probes used in this study.

Fig. 5: Total cell numbers of different groups counted using CARD FISH for the IN (black spheres, straight lines) and OUT (white spheres, dashed lines) stations. Please note different scales.

Tab. 1: List of oligonucleotides used in this study. ^a Formamide concentration in the CARD FISH hybridization buffer.

Probe	Target organism	Sequence (5' → 3')	FA (%) ^a	Reference
EUK516	<i>Eukarya</i>	ACCAGACTTGCCCTCC	0	(48)
NON338	Control	ACTCTACGGGAGGCAGC	35	(65)
PRAS04	<i>Mammielophyceae</i>	CGTAAGCCCGCTTTGAAC	40	(16)
PRYM02	<i>Haptophyta</i>	GGAATACGAGTGCCCTGAC	40	(66)
MICRO01	<i>Micromonas pusilla</i>	AATGGAACACCCCGGGCG	40	(16)
PHAE03B	<i>Phaeocystis</i>	GAGTAGCCCGGTCTCCGGAAAGAAGGCCGGCC	20	(10)
PELA01	<i>Pelagophyceae</i>	GCAACAATCAATCCCAATC	20	(66)
MAST1A	MAST1 clade	ATTACCTCGATCCGCAAA	30	(15)
MAST1B	MAST1 clade	AACGCAAGTCTCCCGCG	30	(15)
MAST1C	MAST1 clade	GTTGTTCCCTAACCCCGAC	30	(15)
MAST3	MAST3	ATTACCTTGGCCTCCAAC	30	(14)
MAST4	MAST4	TACTTCGGTCTGCAAACC	30	(14)
SYNI1161	<i>Syndiniales</i> group I	TCCTCGCGTTAGACACGC	20	This study
SYNI1675	<i>Syndiniales</i> group II	CACCTCTGACGGGTTAAT	20	This study

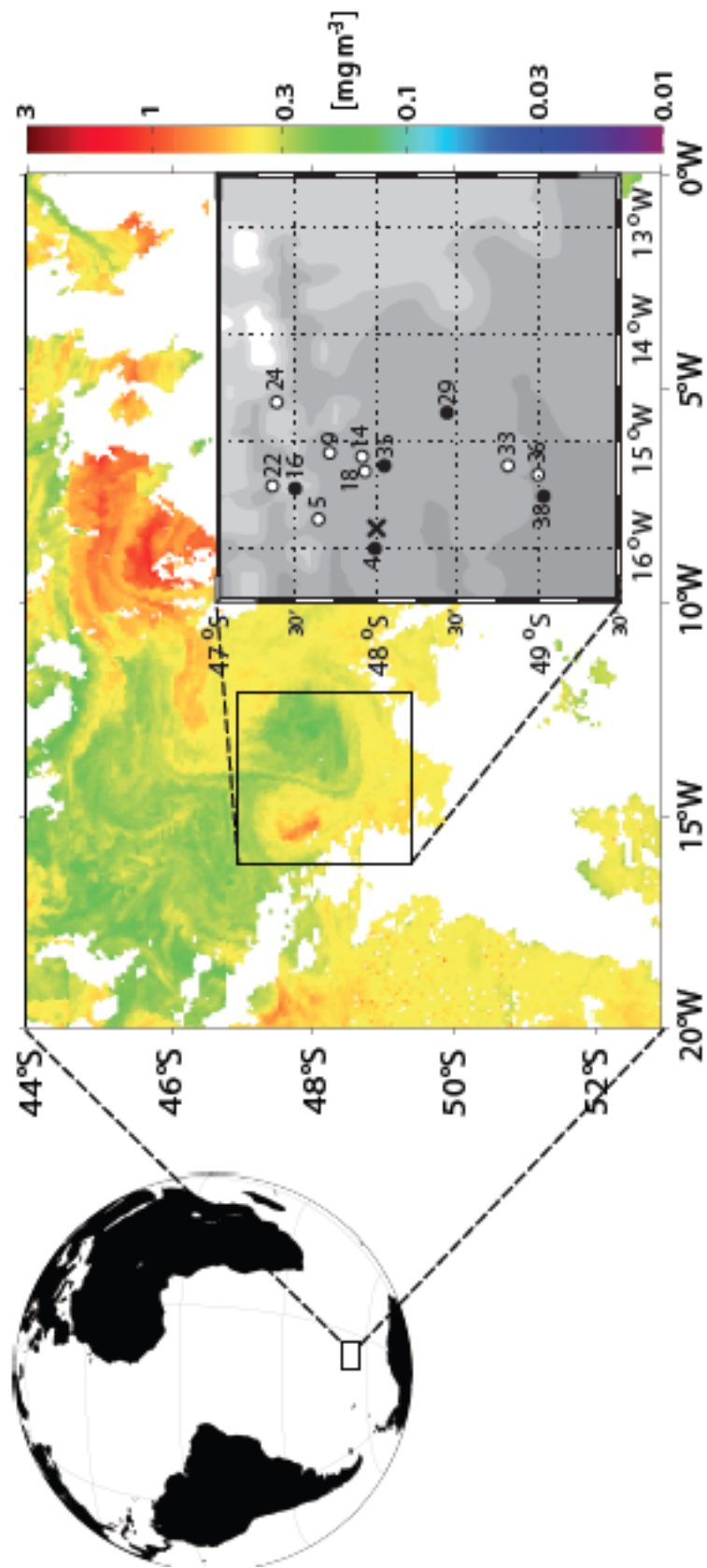


Fig. 1: Map of the fertilized area. The chlorophyll a picture shows the LOHAFEX bloom (encircled). Stations and experiment days of both the IN (black) and OUT stations (white) are shown in the small map. The X marks day -1 before the experiment. The globe and the inset map were generated with the M_Map package for Matlab (version 7.12.0.635; MathWorks, Natick, MA). The chlorophyll a data were downloaded from the NASA website <http://oceancolor.gsfc.nasa.gov/>.

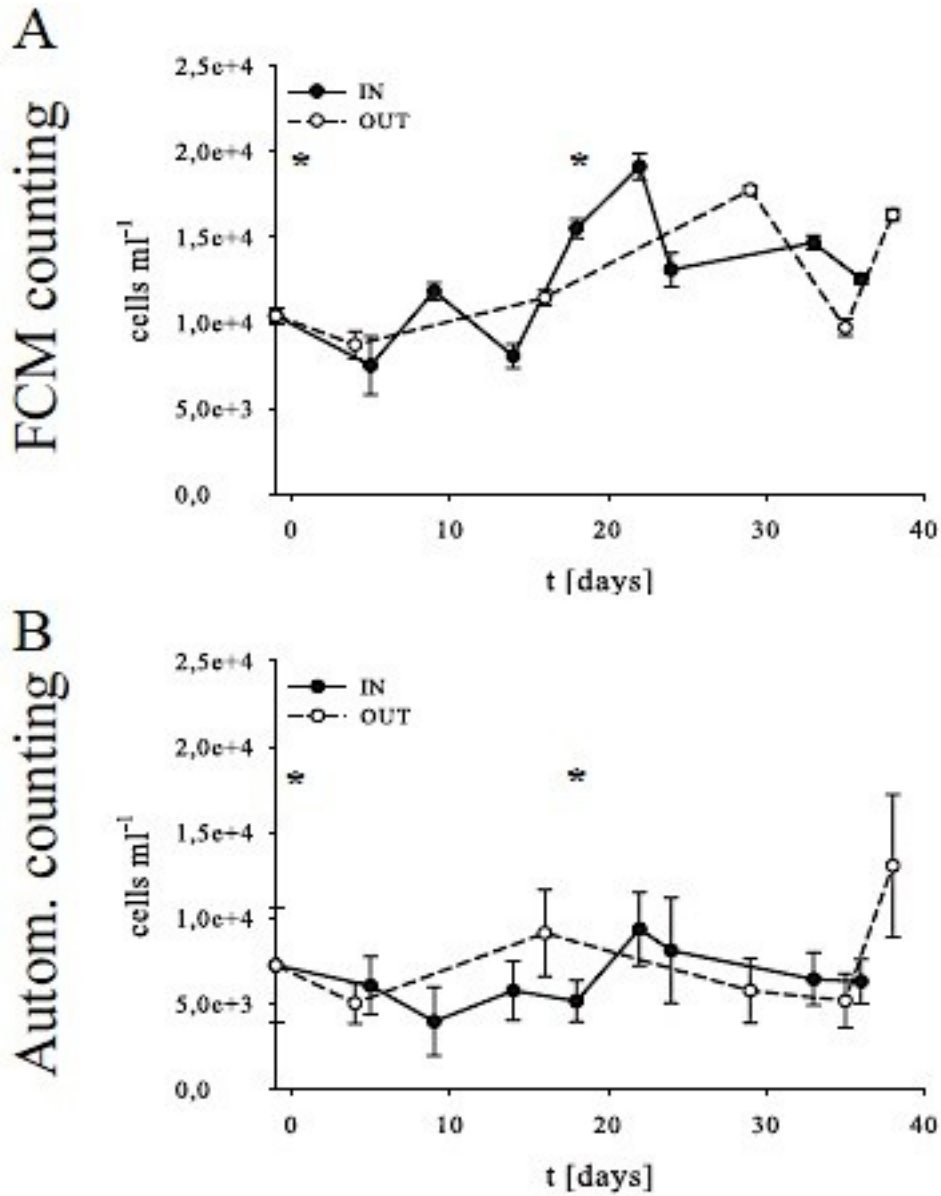


Fig. 2: Total cell counts of all stations inside the fertilized patch achieved by using flow cytometric (FCM) counting and automated microscopic counting after CARD FISH staining. Black spheres with straight lines represent stations inside while white spheres with dashed lines represent stations outside the fertilized patch.

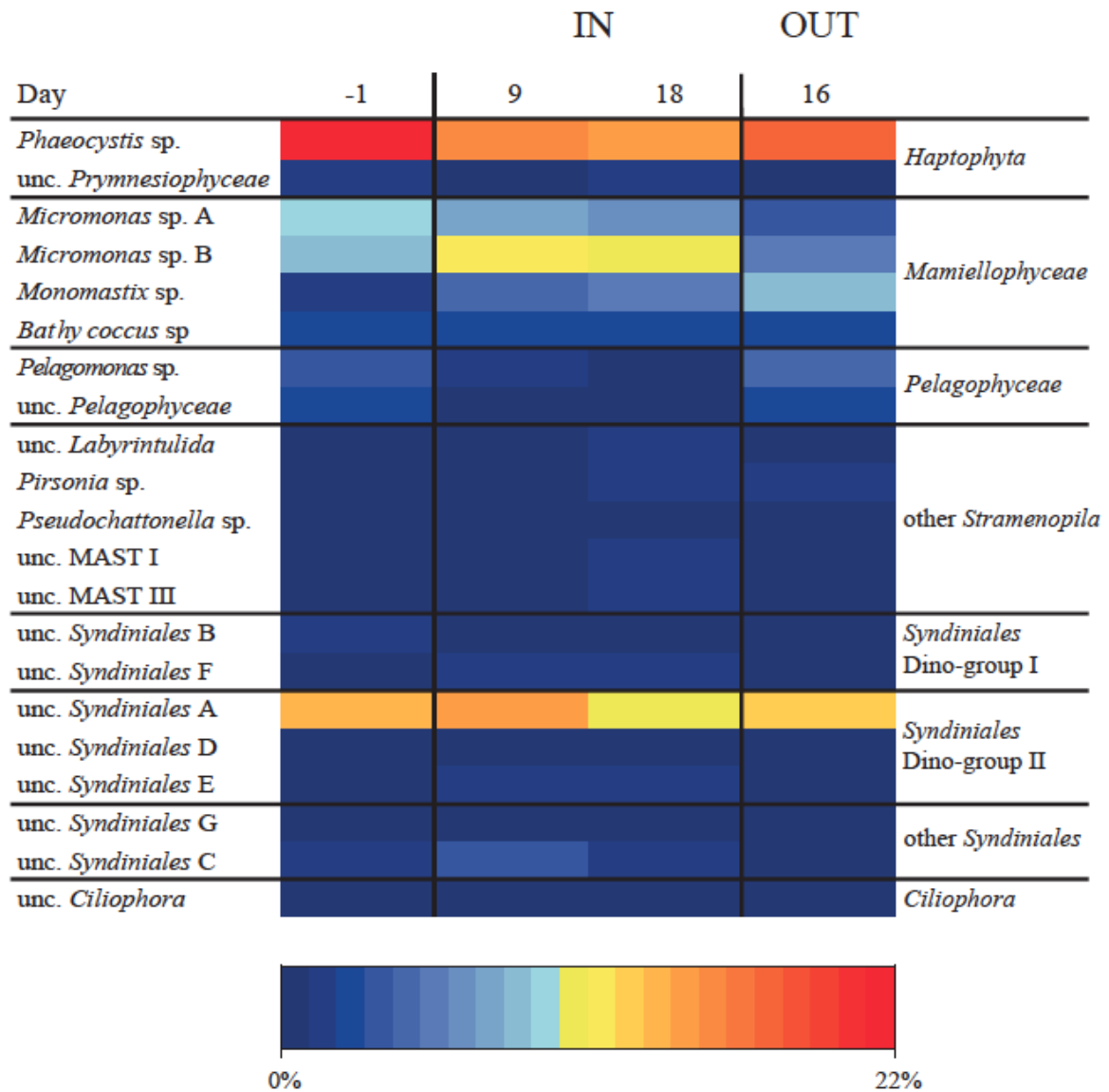


Fig. 3: Relative 18S rRNA gene amplicon frequency revealed by tag pyrosequencing at 20 m depth.

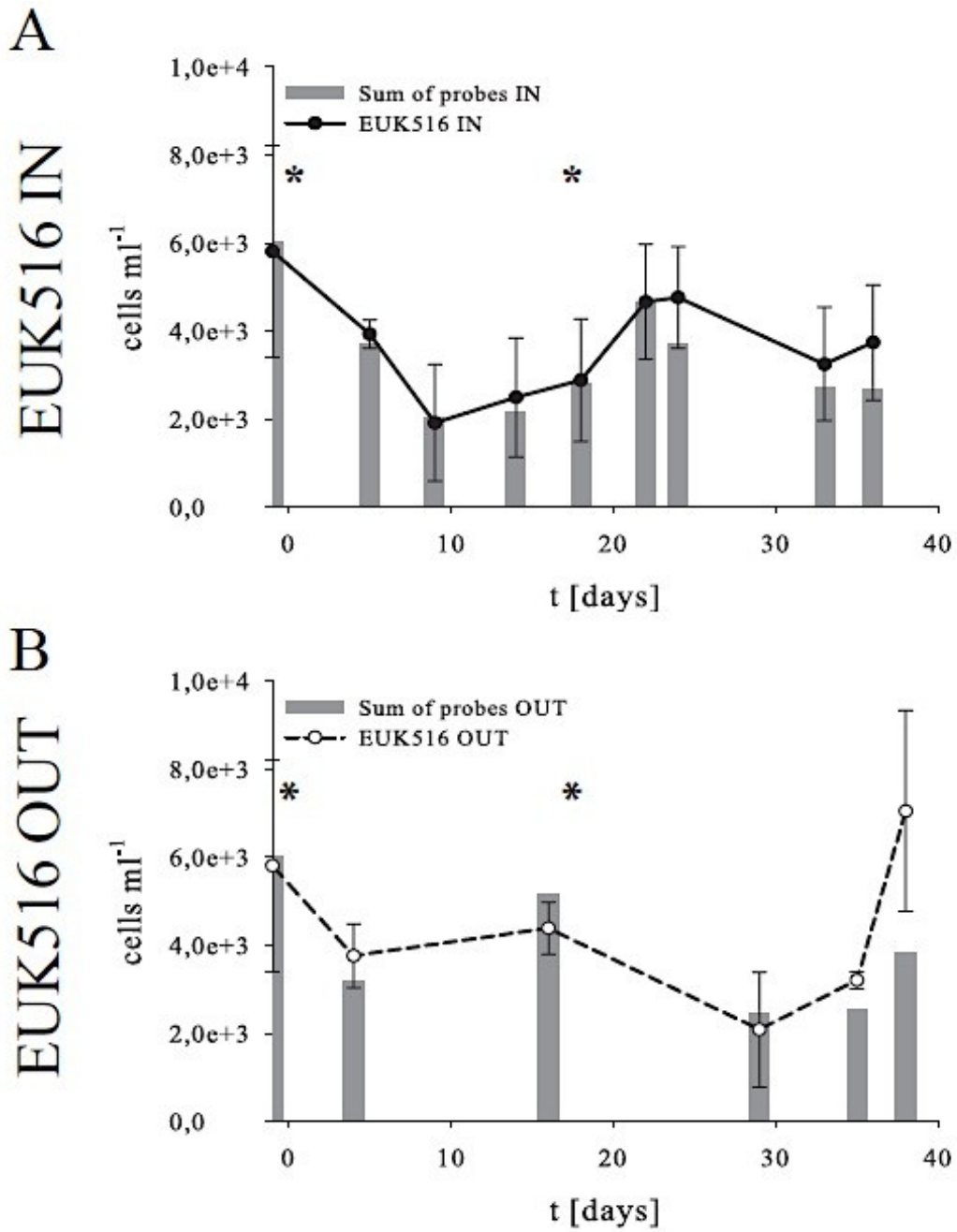


Fig. 4: Total cell numbers of cells stained with the EUK516 probe of the IN (black, A) and OUT (white, B) stations. Bar charts represent the coverage of the EUK516 probe by all other probes used in this study.

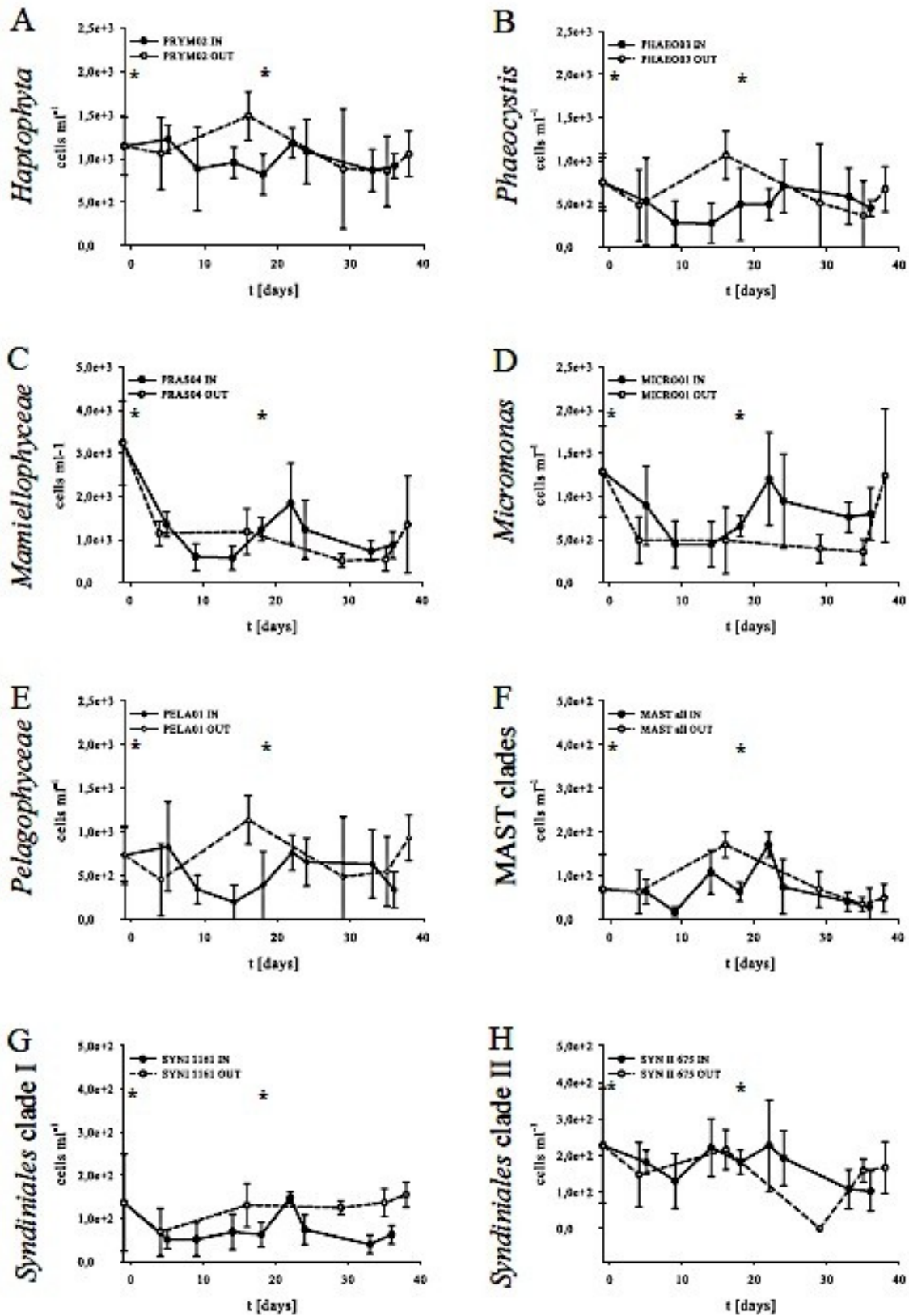


Fig. 5: Total cell numbers of different groups counted using CARD FISH for the IN (black spheres, straight lines) and OUT (white spheres, dashed lines) stations. Please note different scales.

Supplements

SUP 1: Summary of recovered 454-pyrosequencing reads, quality filtering and number of OTUs.

SUP 2 A: Total cell numbers of all probes at 20 m depth. Counts for SYNI 1161 and SYNII 675 were not determined at day 29 OUT (n.d.).

SUP 2 B: Total cell numbers of all probes at 40 m depth. Counts for SYNII 675 were not determined at day 29 OUT (n.d.).

SUP 3: Picture triplets obtained using the macro MPISYS (Zeder unpublished). Three pictures from the same field of view taken in different channels with excitation light of different wavelength (DAPI (365 nm), CARD FISH (470 nm) and autofluorescence (590 nm)), using the probes PRAS04 (Mamiellophyceae) and PHAEO03 (Phaeocystis).

SUP 4: Modified tree of the Syndiniales subgroups including the LOHAFEX sequences. Values in brackets show the total amount of sequences in the consensus sequence. The tree was build using the ARB SILVA ref 108 database (1), calculated using parsimony calculation algorithm and confirmed using neighbour joining and maximum likelihood algorithms.

SUP 5: Modified tree of the Mamiellales subgroups including the LOHAFEX sequences. Values in brackets show the total amount of sequences in the consensus sequence. The tree was build using the ARB SILVA ref 108 database (1), calculated using parsimony calculation algorithm and confirmed using neighbour joining and maximum likelihood algorithms.

References

1. Quast C, Pruesse E, Yilmaz P, Gerken J, Schweer T, Yarza P, Peplies J, Glockner FO. 2012. The SILVA ribosomal RNA gene database project: improved data processing and web-based tools. Nucl. Acids. Res. 41:D590–D596.

SUP 1 Summary of recovered 454-pyrosequencing reads, quality filtering and number of OTUs.

	Sample			
	-1	9	18	16
Total 454-reads	19138	43623	27735	31504
Average length (bp)	326	341	343	344
Acceptable length*	13536	32538	20967	23934
Quality filtering:				
More than one N, chimeras, incorrect forward primer, and non-target organisms	1678	3126	2380	7570
Singletons	341	826	619	714
Total filtered reads	11517	28586	17968	20762
OTUs (97% identity)	459	714	599	702
Abundant OTUs**	12	13	16	12
Rare OTUs**	447	701	583	690

* reads with a minimum length of 300 bp and a maximum length of 670 bp;

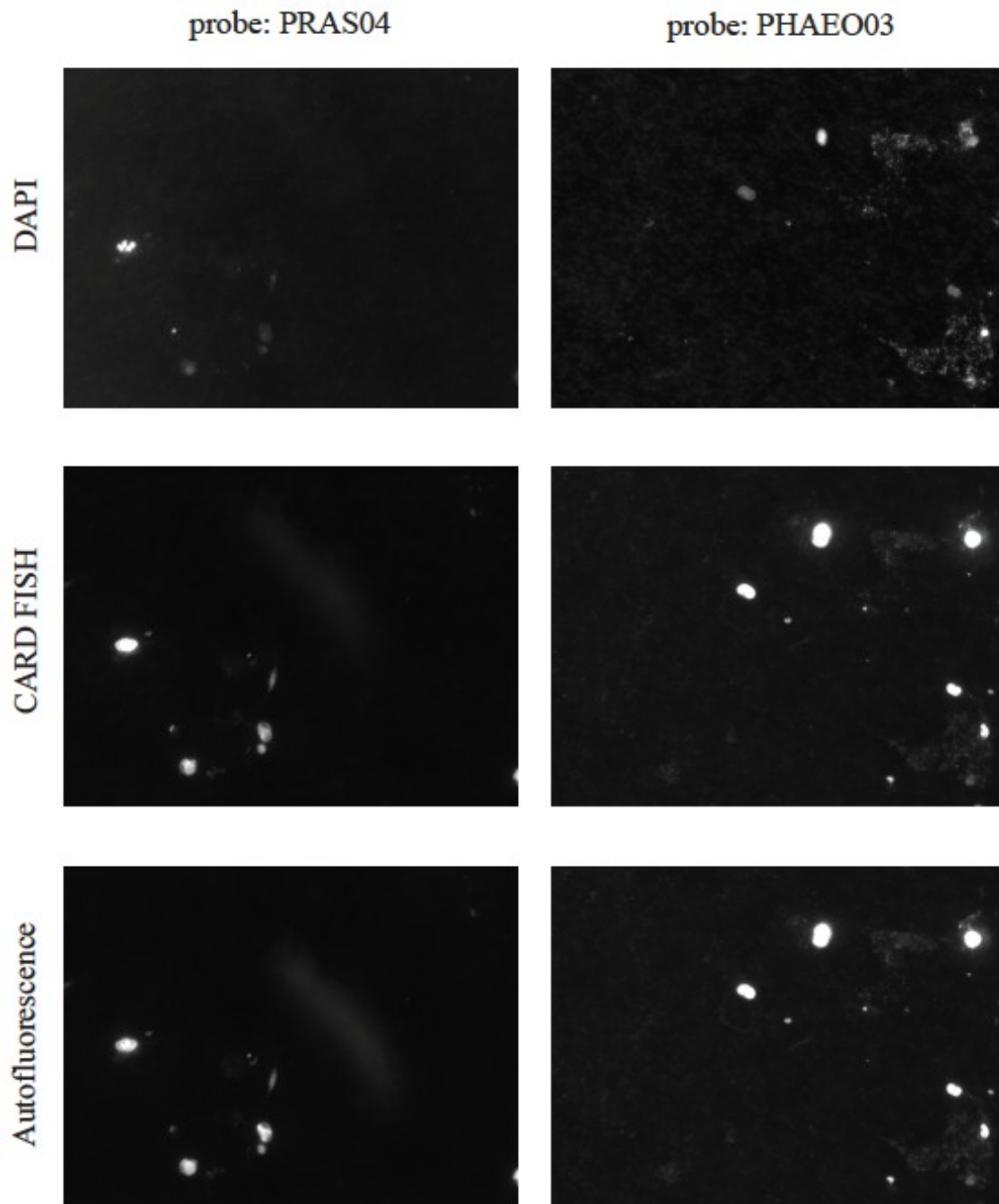
** abundant OTU = number of reads $\geq 1\%$ of total reads, otherwise it is rare

Sup. 2A: Total cell numbers of all probes at 20 m depth. Counts for SYNI 1161 and SYNII 675 were not determined at day 29 OUT (n.d.).

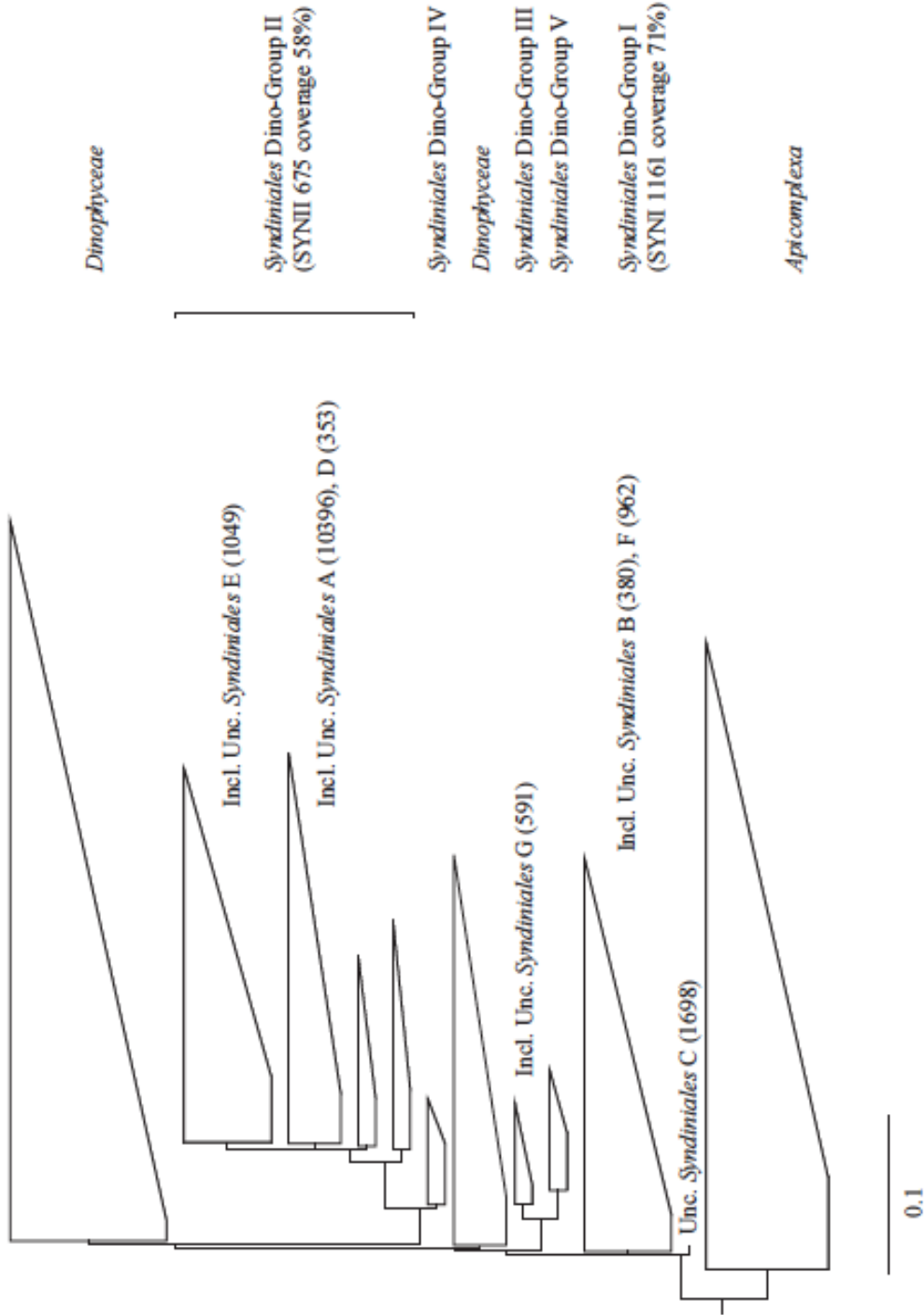
Day	EUKS16	PRAS04	PRYM02	MICRO1	PHAE03	PELA02	MAST 1A	MAST 1B	MAST 1C	MAST 3	MAST 4	SYNI 1161	SYN II 675		
IN Stations	-1	Mean	7.22E+03	3.99E+03	1.27E+03	1.54E+03	1.04E+03	9.08E+02	4.54E+01	4.54E+01	0.00E+00	0.00E+00	2.27E+02	3.63E+02	
		σ	3.02E+03	2.57E+02	5.14E+02	3.21E+02	3.85E+02	6.42E+01	6.42E+01	0.00E+00	0.00E+00	0.00E+00	6.42E+01	0.00E+00	
		5	Mean	3.92E+03	1.55E+03	1.16E+03	9.19E+02	1.35E+03	5.45E+02	2.27E+01	3.40E+01	2.27E+01	0.00E+00	6.81E+01	1.59E+02
		σ	4.81E+01	2.73E+02	6.42E+01	6.26E+02	1.44E+02	4.81E+02	0.00E+00	1.60E+00	0.00E+00	0.00E+00	0.00E+00	3.21E+01	6.81E+01
		9	Mean	8.06E+02	4.99E+02	6.36E+02	3.52E+02	8.30E+02	3.75E+02	0.00E+00	1.13E+01	1.13E+01	0.00E+00	4.16E+01	3.21E+01
		σ	1.44E+02	2.25E+02	5.46E+02	1.60E+01	5.81E+02	1.60E+01	0.00E+00	1.60E+01	0.00E+00	0.00E+00	3.34E+01	3.21E+01	
		14	Mean	3.60E+03	7.72E+02	1.02E+03	6.01E+02	1.09E+03	1.70E+02	1.13E+01	5.67E+01	1.13E+01	4.65E+01	2.61E+02	
		σ	6.26E+02	2.57E+02	9.63E+01	3.05E+02	6.42E+01	1.44E+02	1.60E+01	3.21E+01	0.00E+00	1.60E+01	3.70E+01	1.12E+02	
		18	Mean	3.96E+03	1.03E+03	8.97E+02	7.15E+02	5.79E+02	2.84E+02	0.00E+00	2.27E+01	2.27E+01	0.00E+00	7.94E+01	1.93E+02
		σ	4.33E+02	2.41E+02	3.05E+02	1.60E+01	1.60E+01	3.05E+02	0.00E+00	0.00E+00	0.00E+00	0.00E+00	1.60E+01	1.60E+01	
	22	Mean	3.99E+03	1.13E+03	1.10E+03	8.40E+02	7.83E+02	8.28E+02	3.40E+01	6.81E+01	2.27E+01	1.13E+01	1.36E+02	1.25E+02	
	σ	1.70E+03	3.21E+01	2.41E+02	3.21E+02	1.77E+02	3.05E+02	4.81E+01	3.21E+01	0.00E+00	1.60E+01	0.00E+00	4.81E+01		
	24	Mean	3.99E+03	7.38E+02	1.12E+03	6.01E+02	5.79E+02	6.13E+02	4.54E+01	1.13E+01	0.00E+00	5.67E+01	1.13E+01	1.48E+02	
	σ	8.35E+02	8.02E+01	5.94E+02	2.09E+02	1.60E+01	3.21E+02	3.21E+01	1.60E+01	0.00E+00	4.81E+01	1.60E+01	0.00E+00	8.02E+01	
	33	Mean	3.33E+03	9.31E+02	9.42E+02	8.51E+02	1.26E+03	5.67E+02	4.54E+01	0.00E+00	0.00E+00	0.00E+00	5.67E+01	1.25E+02	
	σ	2.07E+03	6.42E+01	2.41E+02	2.09E+02	2.24E+02	3.53E+02	3.21E+01	0.00E+00	0.00E+00	0.00E+00	1.60E+01	8.02E+01		
	36	Mean	4.72E+03	6.01E+02	1.01E+03	7.04E+02	8.62E+02	4.77E+02	0.00E+00	1.13E+01	0.00E+00	0.00E+00	5.67E+01	5.67E+01	
	σ	8.99E+02	4.81E+01	1.12E+02	9.63E+01	1.93E+02	6.42E+01	0.00E+00	0.00E+00	0.00E+00	0.00E+00	1.60E+01	1.60E+01		
OUT stations	-1	Mean	7.22E+03	3.99E+03	1.27E+03	1.54E+03	1.04E+03	9.08E+02	4.54E+01	4.54E+01	0.00E+00	0.00E+00	2.27E+02	3.63E+02	
		σ	3.02E+03	2.57E+02	5.14E+02	6.42E+02	3.21E+02	3.85E+02	6.42E+01	6.42E+01	0.00E+00	0.00E+00	6.42E+01	0.00E+00	
		4	Mean	4.34E+03	1.35E+03	1.15E+03	3.75E+02	7.04E+02	6.36E+02	2.27E+01	2.27E+01	1.13E+01	1.13E+02	2.04E+02	
		σ	4.69E+02	1.77E+02	4.01E+02	4.81E+01	6.42E+01	1.28E+02	3.21E+01	3.21E+01	1.60E+01	0.00E+00	0.00E+00	3.21E+01	
		16	Mean	3.99E+03	9.42E+02	1.41E+03	4.54E+02	8.85E+02	1.12E+03	2.27E+01	1.13E+01	2.27E+01	1.02E+02	1.82E+02	
		σ	6.74E+02	4.98E+02	6.42E+01	5.14E+02	9.63E+01	1.60E+01	0.00E+00	8.02E+01	1.60E+01	3.21E+01	1.60E+01	6.42E+01	
		29	Mean	1.11E+03	3.97E+02	3.29E+02	3.63E+02	2.60E+03	2.95E+02	0.00E+00	1.13E+01	0.00E+00	nd	nd	
		σ	7.06E+02	1.44E+02	4.81E+01	0.00E+00	1.03E+02	1.28E+02	0.00E+00	3.21E+01	1.60E+01	0.00E+00	nd	nd	
		38	Mean	8.93E+03	2.19E+03	9.40E+02	1.84E+03	4.38E+02	1.26E+03	0.00E+00	1.62E+01	2.27E+01	1.62E+02	1.30E+02	
		σ	9.86E+02	8.94E+02	9.17E+01	5.46E+02	4.36E+02	4.13E+02	0.00E+00	0.00E+00	2.29E+01	0.00E+00	0.00E+00	9.17E+01	

Sup. 2B: Total cell numbers of all probes at 40 m depth. Counts for SYNII 675 were not determined at day 29 OUT (n.d.).

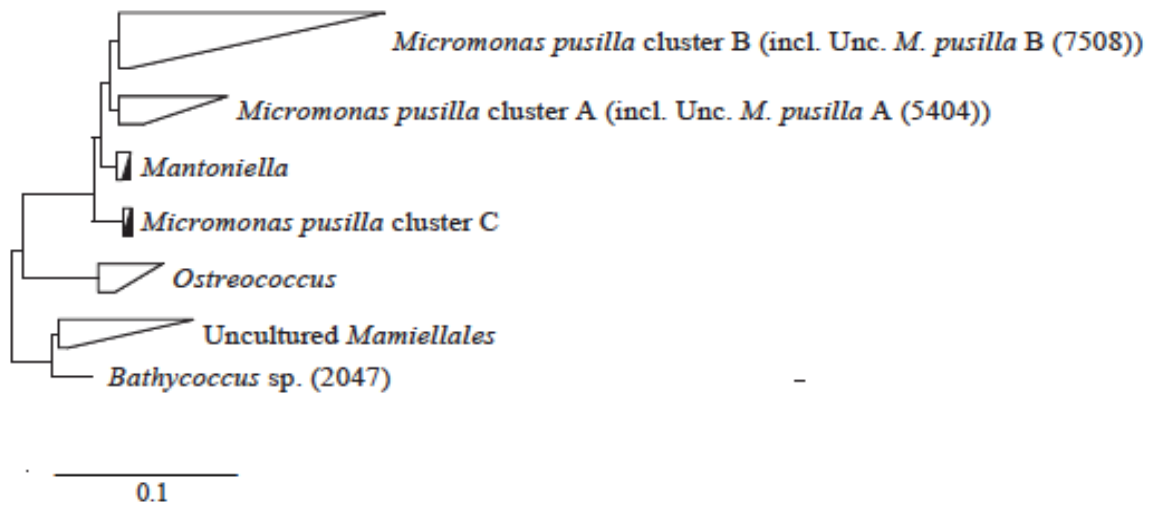
Day	EUK516	PRAS04	PRYM02	MICRO1	PHAE03	PELA02	MAST 1A	MAST 1B	MAST 1C	MAST 3	MAST 4	SYNI 1161	SYN II 675	
IN Stations	-1 Mean	4.39E+03	2.47E+03	1.01E+03	1.02E+03	7.83E+02	1.13E+01	0.00E+00	1.13E+01	0.00E+00	2.27E+01	4.54E+01	9.08E+01	
	σ	4.98E+02	7.06E+02	4.81E+01	3.85E+02	8.02E+01	1.12E+02	0.00E+00	1.60E+01	0.00E+00	3.21E+01	3.21E+01	0.00E+00	
	5 Mean	3.94E+03	1.13E+03	9.65E+02	8.62E+02	1.11E+03	2.27E+01	2.27E+01	0.00E+00	0.00E+00	0.00E+00	3.40E+01	2.04E+02	
	σ	5.62E+02	9.63E+01	5.62E+02	4.81E+02	2.66E+02	4.81E+02	3.21E+01	0.00E+00	0.00E+00	0.00E+00	1.60E+01	0.00E+00	
	9 Mean	3.01E+03	6.81E+02	1.12E+03	5.33E+02	6.47E+02	3.06E+02	1.13E+01	0.00E+00	0.00E+00	0.00E+00	7.94E+01	1.93E+02	
	σ	6.26E+02	4.49E+02	4.01E+02	4.33E+02	4.81E+01	2.73E+02	1.60E+01	0.00E+00	0.00E+00	0.00E+00	1.60E+01	1.60E+01	
	14 Mean	1.38E+03	3.63E+02	4.01E+02	2.84E+02	1.05E+03	2.16E+02	0.00E+00	2.27E+01	1.13E+01	1.13E+01	5.67E+01	1.82E+02	
	σ	4.17E+02	3.21E+01	2.57E+02	1.12E+02	4.36E+02	3.05E+02	0.00E+00	3.21E+01	3.21E+01	1.60E+01	4.81E+01	0.00E+00	
	18 Mean	1.80E+03	1.43E+03	7.38E+02	5.90E+02	5.79E+02	4.88E+02	1.13E+01	2.27E+01	4.54E+01	0.00E+00	0.00E+00	4.54E+01	1.70E+02
	σ	9.79E+02	6.42E+01	2.09E+02	1.60E+02	1.60E+01	5.62E+02	1.60E+01	0.00E+00	0.00E+00	0.00E+00	0.00E+00	3.21E+01	4.81E+01
	22 Mean	5.32E+03	2.53E+03	1.25E+03	1.55E+03	1.01E+03	6.92E+02	3.40E+01	4.54E+01	7.94E+01	0.00E+00	3.40E+01	1.59E+02	3.29E+02
	σ	6.58E+02	7.86E+02	9.63E+01	4.98E+01	3.04E+02	1.12E+02	1.60E+01	3.21E+01	4.81E+01	0.00E+00	4.81E+01	0.00E+00	4.81E+01
	24 Mean	5.52E+03	1.70E+03	1.03E+03	1.28E+03	3.29E+02	6.92E+02	0.00E+00	0.00E+00	1.13E+01	1.13E+01	0.00E+00	1.02E+02	2.38E+02
	σ	9.95E+02	6.74E+02	2.09E+02	6.26E+02	1.60E+01	3.37E+02	0.00E+00	0.00E+00	1.60E+01	1.60E+01	0.00E+00	1.60E+01	4.81E+01
33 Mean	3.17E+03	5.22E+02	7.83E+02	6.58E+02	6.22E+02	6.92E+02	1.13E+01	1.13E+01	0.00E+00	1.13E+01	0.00E+00	2.27E+01	9.08E+01	
σ	8.19E+02	0.00E+00	3.05E+02	9.63E+01	3.62E+02	5.62E+02	1.60E+01	1.60E+01	0.00E+00	1.60E+01	0.00E+00	0.00E+00	3.21E+01	
36 Mean	2.75E+03	1.13E+03	8.17E+02	8.85E+02	1.82E+03	1.93E+02	0.00E+00	0.00E+00	2.27E+01	1.13E+01	1.13E+01	6.81E+01	1.48E+02	
σ	6.42E+02	6.42E+01	9.63E+01	4.81E+02	5.78E+02	2.09E+02	0.00E+00	0.00E+00	3.21E+01	1.60E+01	1.60E+01	3.21E+01	1.60E+01	
OUT Stations	-1 Mean	4.39E+03	2.47E+03	1.01E+03	1.02E+03	7.83E+02	1.13E+01	0.00E+00	1.13E+01	0.00E+00	2.27E+01	4.54E+01	9.08E+01	
	σ	4.98E+02	7.06E+02	4.81E+01	3.85E+02	8.02E+01	1.12E+02	0.00E+00	1.60E+01	0.00E+00	3.21E+01	3.21E+01	0.00E+00	
	4 Mean	3.18E+03	9.19E+02	9.65E+02	6.01E+02	7.90E+02	2.61E+02	0.00E+00	2.27E+01	0.00E+00	2.27E+01	0.00E+00	9.08E+01	
	σ	1.93E+02	1.44E+02	5.62E+02	4.01E+02	5.91E+02	1.60E+01	0.00E+00	0.00E+00	3.21E+01	0.00E+00	3.21E+01	9.63E+01	
	16 Mean	4.77E+03	1.41E+03	1.57E+03	5.22E+02	1.24E+03	1.15E+03	3.40E+01	6.81E+01	5.67E+01	2.27E+01	1.13E+01	1.59E+02	2.50E+02
	σ	9.63E+01	6.10E+02	4.49E+02	4.17E+02	5.42E+01	3.05E+02	1.60E+01	6.42E+01	4.81E+01	0.00E+00	1.60E+01	6.42E+01	0.00E+00
	29 Mean	3.05E+03	6.13E+02	1.43E+03	4.20E+02	4.09E+02	6.70E+02	3.40E+01	1.13E+01	4.54E+01	1.13E+01	0.00E+00	1.25E+02	n.d.
	σ	9.15E+02	6.42E+01	4.49E+02	2.73E+02	9.63E+01	1.60E+01	4.81E+01	6.42E+01	6.42E+01	1.60E+01	0.00E+00	1.60E+01	n.d.
	35 Mean	3.20E+03	5.33E+02	8.51E+02	6.36E+02	4.43E+02	5.45E+02	1.13E+01	1.13E+01	0.00E+00	0.00E+00	1.13E+01	1.36E+02	1.59E+02
	σ	1.93E+02	2.73E+02	4.01E+02	1.93E+02	1.44E+02	6.42E+01	1.60E+01	1.60E+01	0.00E+00	0.00E+00	1.60E+01	3.21E+01	3.21E+01
	38 Mean	5.15E+03	4.88E+02	1.16E+03	6.36E+02	1.12E+03	5.90E+02	0.00E+00	3.40E+01	2.27E+01	0.00E+00	0.00E+00	1.48E+02	2.04E+02
	σ	5.78E+02	3.05E+02	3.85E+02	1.93E+02	5.27E+02	3.53E+02	0.00E+00	4.81E+01	0.00E+00	0.00E+00	0.00E+00	4.81E+01	3.21E+01



SUP 3: Picture triplets obtained using the macro MPISYS (Zeder unpublished). Three pictures from the same field of view taken in different channels with excitation light of different wavelength (DAPI (365 nm), CARD FISH (470 nm) and autofluorescence (590 nm)), using the probes PRAS04 (Mamiellophyceae) and PHAEO03 (Phaeocystis).



SUP 4: Modified tree of the Syndiniales subgroups including the LOHAFEX sequences. Values in brackets show the total amount of sequences in the consensus sequence. The tree was built using the ARB SILVA ref 108 database (64), calculated using parsimony calculation algorithm and confirmed using neighbour joining and maximum likelihood algorithms.



SUP 5: Modified tree of the Mamiellales subgroups including the LOHAFEX sequences. Values in brackets show the total amount of sequences in the consensus sequence. The tree was built using the ARB SILVA ref 108 database (1), calculated using parsimony calculation algorithm and confirmed using neighbour joining and maximum likelihood algorithms.

Manuscript III

**Investigation of the protist plankton (>20 μm) during the iron
fertilization experiment LOHAFEX
in the Southern Ocean**

*Isabelle Schulz^{1,2}, Philipp Assmy³, Sina Wolzenburg¹, Christine Klaas¹, Victor
Smetacek¹*

To be submitted to Deep Sea Research I

¹Alfred-Wegener-Institut Helmholtz-Zentrum für Polar- und Meeresforschung, 27570
Bremerhaven, Germany

²MARUM – Center for Marine Environmental Sciences and Faculty of Geosciences,
University of Bremen, Leobener Str., 28359 Bremen

³Norwegian Polar Institute, Fram Centre, Hjalmar Johansens gt. 14, 9296 Tromsø, Norway

Acknowledgements

We are indebted to the captain and crew of RV *Polarstern*. We thank the co-chief scientist S.W.A. Naqvi for making LOHAFEX a successful experiment. The Council of Scientific and Industrial Research (CSIR), India and the Helmholtz Foundation, Germany equally shared the costs of the experiment. This work was funded through DFG- Research Center / Cluster of Excellence „The Ocean in the Earth System“. This work was also supported by GLOMAR – Bremen International Graduate School for Marine Sciences.

Abstract

The abundance, biomass and vertical distribution of large protozooplankton ($> 20 \mu\text{m}$), including heterotrophic (aplastidic) tintinnid ciliates, aplastidic thecate dinoflagellates and rhizaria (acantharia, radiolaria, foraminifera and the taxopodidan *Sticholonche zancelea*) were measured during the 38-day *in situ* iron fertilization experiment LOHAFEX. The experiment was carried out in a mesoscale cold core eddy in the Polar Frontal Zone of the Southern Ocean from January-March 2009. For the quantitative assessment of protozoa, concentrated seawater samples were collected at 10 discrete depths between 10 – 500 m using Niskin bottles attached to a CTD rosette (SeaBird Electronics, USA). Due to low Si-concentrations within the fertilized patch, diatoms were unable to grow, instead small flagellates ($< 20 \mu\text{m}$) dominated the bloom. Protozoa showed a muted response to iron addition, due to high grazing pressure of copepods, which were highly abundant within the patch. Large protozooplankton standing stocks integrated over the upper 500 m amounted to 0.9 g C m^{-2} at the beginning of the experiment and differed not significantly to the out-patch. Acantharians dominated the protozooplankton community in terms of biomass and were mainly distributed in depths below 80 m. In the upper 100 m tintinnid ciliates accounted for 95 % of protozoan abundance and contributed 22 % to protozoan biomass, while aplastidic thecate dinoflagellates were the most abundant taxon below 100 m. Radiolaria, foraminifera and *Sticholonche zancelea* were less dominant in terms of numbers and biomass.

Copepod fecal pellets obtained many damaged and empty loricae, but also cells of foraminifera, which are usually not a preferred food item of copepods. This indicated that copepods were food limited and resorted to large, armoured protozoans, which they might have otherwise avoided. Hence we suggest that the large protozoa were strongly top-down controlled during LOHAFEX. The addition of iron (Fe) to a mesoscale eddy in the Southern Ocean had a considerable impact on the food chain components and sheds new light on food-web interactions within the pelagic ecosystem.

1. Introduction

The large protozooplankton ($> 20 \mu\text{m}$) is an important component of the pelagic food web (Sieburth et al., 1978; Porter et al., 1985; Stoecker and Capuzzo, 1990). However, this size class tends to be neglected in standard plankton studies, because larger protozoa are under-sampled in small-volume samples examined for phytoplankton and not quantitatively retained in net samples for larger metazooplankton. Most studies pay attention to specific taxa and only few have investigated the diversity and function of the larger protozooplankton community as a whole (Gowing and Garrison, 1991; Nöthig and Gowing, 1991; Gowing and Garrison, 1992; Gowing et al., 2001; Klaas, 2001; Henjes et al., 2007).

Protozoa are a phylogenetically diverse group with a wide size-range and the ability to reach standing stocks in the range of metazooplankton, which highlights their ecological importance in pelagic food webs (Alder and Boltovskoy, 1993).

The role and importance of protozooplankton in structuring the pelagic ecosystem of the Southern Ocean has been mentioned in previous studies (Gonzales, 1992; Burkill et al. 1995; Becquevort 1997; Klaas, 1997; Caron et al. 2000). They can be fairly abundant in this region (Dieckmann et al., 1991; Gowing and Garrison, 1992; Abelman and Gowing, 1996; Klaas 2001) and many species appear to have relatively rapid reproductive rates (Sherr and Sherr, 2002).

Protozoa are grazers of phyto- and microzooplankton and are themselves food for higher trophic levels (Sherr and Sherr, 2009; Irigoien et al., 2005). Gowing (1989) showed that *Salpa thompsoni* fed on phaeodarians and studies by Atkinson (1996) and Lonsdale (2000) showed that ciliates but also dinoflagellates can be preferred prey for small copepods (e.g. *Oithona* spp.) consuming up to 57 % of daily ciliate production. Thecate dinoflagellates have quite diverse mechanisms to capture and ingest their prey, which enables them to feed on prey much larger than themselves. Dinoflagellates of the genus *Protooperidinium* can extrude a large feeding veil, a pseudopod called the pallium, to capture and digest prey extracellularly (Smetacek 1981, Jacobson and Anderson, 1986). Others use a feeding tube, a peduncle, to suck up the cytoplasm from their prey (Hansen 1991; Jacobson and Anderson, 1986; Jacobson, 1999).

Members of the Rhizaria, in particular foraminifera and polycystine radiolaria, are widely used as paleo-proxies to reconstruct past climate conditions (Morley and Stepien, 1985; Boltovskoy and Alder 1992; Abelman and Gowing 1996, 1997; Boltovskoy et al., 1996,

Abelmann und Nimmergut, 2005) because their mineral tests and skeletons preserve well in sediments.

Despite their role as paleo-proxies, live Rhizaria and their remains but also other larger protozoa (tintinnid ciliates and dinoflagellates) play an important role in vertical flux of organic matter and mineral elements. Sinking events of live radiolaria (Gowing, 1986) and cysts (Spindler and Beyer, 1990; Boltovskoy and Uliana, 1996) were shown to contribute to the vertical flux of organic matter. Acantharian skeletons, foraminifera tests and tintinnid loricae have contributed to the flux of barium (Ba) and strontium (Sr), calcium carbonate and organic carbon, respectively (Bernstein et al., 1987, Boltovskoy et al., 1993; Schiebel, 2002). Acantharia play a unique role in the Ba and Sr cycle (Bernstein et al., 1987, 1992, 1998) because they have a Ba-enriched celestite (Ba/SrSO_4) skeleton implicating their role in Barite deposition in the sediments which has been used as paleoproxy for ocean productivity. However, the mechanisms leading to Barite formation are under debate (Dehairs et al., 1991, 1992, 1997; Dymond et al., 1992; Dymond and Collier, 1996; Francois et al., 1995; Esser and Volge 2002; Bernstein and Byrne, 2004).

Although radiolarians contribute relatively little to the ocean's silicon cycle (DeMaster, 2002) their silica skeletons, especially those of the polycystine radiolarians, preserve well in the sediment record and Klaas (1997) suggested that even though their contribution to silica deposits in the Southern Ocean is small they might be important agents in the redistribution of silica to deeper water layers. Calcareous tests of foraminifera instead might contribute significantly to pelagic calcareous flux and CO_2 flux of the ocean (Honjo and Manganini, 1993; Thunell et al., 1994; Ziveri et al., 1995) due to their relatively large size, high density and sinking rates (Takahashi and Bé, 1984).

In summary, large protozoans differ widely in their ecology and in their impact on biogeochemical cycles. Iron fertilization experiments are the perfect tool to follow the responses of the major protozoan groups and their interrelationships under natural conditions. In this study we followed the response of larger protozoa ($> 20 \mu\text{m}$), including acantharia, foraminifera, radiolarian, the taxopodidan *Sticholonche zanclea*, tintinnid ciliates and aplastidic thecate dinoflagellates over 38 days during the iron fertilization experiment LOHAFEX, carried out in the Atlantic sector of the Southern Ocean during RV Polarstern cruise ANT-XXV/3 (27 January to 6 March 2009).

2. Materials and Methods

2.1. Study site and tracking of the fertilized patch

Sampling took place during the joint Indo-German in situ mesoscale iron (LOHA is the Hindi word for iron) fertilization (FEX) experiment (LOHAFEX) conducted in the Atlantic sector of the Southern Ocean (48° S 16°W) during late austral summer (27 January to 6 March 2009). The stable cyclonic eddy provided a coherent water mass over the course of the experiment, and the wind mixed layer (WML) depth varied between 50 and 80 m (Martin et al., 2013). The response of large protozooplankton to an iron-induced phytoplankton bloom dominated by flagellates (Schulz et al., in prep., manuscript I) was observed over 38 days. An initial patch of 300 km² was fertilized with 10t of dissolved iron (II) sulphate (FeSO₄) inside the eddy. A second fertilization with 10t of FeSO₄ was carried out on day 18 of the experiment. Four different ways of tracking the patch were used: 1. trajectories of GPS drifters placed in the centre of the fertilized patch, 2. labelling with the inert tracer sulfurhexafluoride (SF₆) released together with the FeSO₄ solution, 3. online measurements of photosynthetic efficiency (Fv/Fm), and 4. underway Chl *a* sampling and continuous pCO₂ measurements. The “in-patch stations” were placed at the highest observed photosynthetic efficiency (Fv/Fm) and highest Chl *a* concentrations. Out-patch stations were located in adjacent waters with background SF₆ concentrations, low Fv/Fm ratios and Chl *a* concentrations. Protozooplankton was sampled at six in-patch and two out-patch stations (Table 1). The station sampled prior to the first iron addition (day -0.6) is used as the starting point for both in- and out-patch trends. Due to the limited number of stations temporal trends outside the patch need to be treated with caution.

2.2. Sampling

For the quantitative assessment of Rhizaria (acantharia, radiolaria, foraminifera and the taxopodidan *Sticholonche zanclea*), tintinnid ciliates and aplastidic thecate dinoflagellates, concentrated seawater samples were collected at 10 discrete depths (Table 1) between 10 – 500 m using Niskin bottles attached to a CTD (Conductivity, Temperature, Depth) rosette (SeaBird Electronics, USA). The volume of a Niskin bottle (12 L) was gently passed over 20 µm mesh gauze for samples taken from 10-100 m and two Niskin bottles (24 L) for depth intervals from 200-500 m. The concentrated samples, with a final volume of 50 ml, were fixed with hexamethylenetetramine-buffered formaldehyde (2 % final concentration). Strontium chloride (SrCl₂) was added to prevent dissolution of acantharian skeletons.

Unfortunately acantharian data are unavailable for in-patch day 9.7 because SrCl_2 was not added to the samples.

2.3. Abundance

Large protozoa were identified and enumerated using inverted light microscopy (Axiovert 135, Zeiss, Oberkochen) according to the method of Thronson (1995). Water samples were settled in 50 mL sedimentation chambers (Hydrobios, Kiel, Germany) at 4 °C for 48 hours. Depending on their size and abundance, organisms were counted at 50-200 x magnification in one to four transects, a quarter, half or entire Utermöhl chamber. In order to obtain statistically robust results, samples have been analyzed until at least 50 cells of the most abundant species and at least 500 cells in total were counted.

Prior to counting, 250 μL SYBR Green I was added to each sample and incubated for 15 minutes in the dark at 4 °C to stain the nucleus of the cells. SYBR Green stock solution was diluted using MOPS (3-(N-morpholino)propanesulfonic acid) buffer (1:5000) to yield a working solution at near neutral pH (Good et al, 1966). Alive cells with stained nuclei were counted via epifluorescence microscopy. Besides live cells, intact, empty and damaged loricae were enumerated. Our fixation and concentration procedure might have resulted in some of the empty loricae, but we consider the impact to be minor. In comparison to other commonly used zooplankton sampling methods, our concentration method and preservative concentrations are gentle and low, respectively. Copepod grazing is the most likely cause of damaged loricae because they are endowed with mandibles capable of crushing and biting off pieces from the stiff tintinnid lorica. Aloricate ciliates and athecate dinoflagellates were not included in this study because they are not quantitatively retained by our concentration procedure.

As far as possible all large protozoa were identified to species or genus level (Table 2). Radiolaria were differentiated into phaeodaria and polycystines, with the latter further divided into nassellaria and spumellaria. Foraminifera were differentiated into juvenile and adult specimens according to size and number of chambers.

2.4. Volume measurements and biomass conversion

The cell size of each tintinnid and aplastidic thecate dinoflagellate species was measured on 20 randomly picked cells and their cell volume calculated from equivalent geometrical formulas (Hillebrand et al., 1999). The biovolume of foraminifera was determined by assuming a spherical shape and using the longest dimension across the calcite test as the diameter (Bè et al.,1977). Biovolumes of acantharia and adult radiolaria were calculated

assuming a sphere in case of the former and the diameter of the spherical central capsule in case of the latter (Michaels et al., 1995).

Cell volume of tintinnids and thecate dinoflagellates was converted into cellular carbon content using recommended carbon conversion factors (Table 3) (Menden-Deuer and Lessard, 2000). Biovolumes of acantharia, foraminifera and radiolaria were converted to biomass using measured carbon:volume ratio estimates (Michaels et al., 1995) (Table 3). The carbon estimates should be conservative, as protozoan cytoplasm tends to shrink during fixation (Gowing and Garrison, 1991, 1992; Michaels et al., 1995).

Abundance (individuals m^{-2}) and biomass (mg C m^{-2}) of all species described in this study are trapezoidal depth-integrated values (equation 1), calculated from 10 depth intervals between the surface and 500 m.

$$N_t = \left(\int_{500}^0 N dz \right) / z \quad (1)$$

N_t : is the average abundance at time t

$\int_{0-500} N$: the depth integral and

z : depth

2.5. Statistical data analysis

Mann-Whitney U-test was applied to test differences between in-patch and out-patch station data sets. All data were tested for equality of variances. Abundance of foraminifera was tested for equality of variances and a two sample T-test was applied. Statistical analyses were conducted using Genstat (7. Edition, VSN Int. Ltd.).

3. Results

3.1 Standing stocks, community composition and temporal trends

Large protozooplankton standing stocks integrated over the upper 500 m amounted to 0.9 g C m^{-2} at the beginning of the experiment. Mean standing stocks inside the patch were 0.6 g C m^{-2} (± 0.25) with a maximum of 1.0 g C m^{-2} on day 33.4. Standing stocks outside the patch remained relatively constant at 0.7 g C m^{-2} (± 0.19) and differed not significantly ($p > 0.05$; Mann-Whitney U-test) from values inside the patch (Fig. 1).

Acantharians dominated the protozooplankton community and accounted for 61 % and 73 % of large protozoan standing stocks inside and outside the patch. Tintinnid ciliates were the group which contributed the second most to protozoan standing stocks with 22 % inside and 15 % outside the patch while foraminifera contributed 11 % inside and 9 % outside the patch. Aplastic thecate dinoflagellates contributed 5 % inside and 3 % outside the patch while the contribution of radiolarians was less than 1 % both inside and outside the patch.

3.1.1 Tintinnid ciliates

Standing stocks of tintinnids inside the patch increased from 65 mg C m^{-2} to 274 mg C m^{-2} on day 9.7 and declined steadily thereafter to values recorded at the beginning of the experiment (Fig. 2 H). Peak standing stocks outside the patch were observed on day 16.5 with 137 mg C m^{-2} . Standing stocks inside and outside the patch differed not significantly ($p > 0.05$ Mann-Whitney U-test).

Over the course of the experiment intact empty tintinnid loricae, converted to carbon equivalents for direct comparison with full loricae, contributed 20-25 % to total tintinnid standing stocks, with exception on day -0.6 where they contributed 36 % to total tintinnid standing stocks (Fig. 4 A). The contribution of empty loricae outside the patch decreased steadily from 36 % to 19 % at the end of the experiment (Fig. 4 B). There was no significant difference between in and out patch ($p > 0.05$ Mann-Whitney U-test). When converted to carbon damaged loricae contributed most (50-70 %) to total tintinnid standing stocks (Fig. 4) and increased both inside and outside the patch but differed significantly ($p < 0.05$ Mann-Whitney U-test). The ratio of full to empty and damaged loricae (F:ED) and the ratio of empty to damaged loricae (E:D) inside and outside the patch was always below one (Fig. 4). In terms of standing stocks the most dominant tintinnid species were *Cymatocylis antarctica*, *Acanthastomella norvegica* and *Codonellopsis pusilla*.

3.1.2 Acantharia

Acantharia were almost equally abundant inside and outside the patch. In terms of standing stocks a marked decline could be observed within as well as out of the patch from initially 734 mg C m⁻² to 318 mg C m⁻² and 280 mg C m⁻² respectively (Fig 2 B). Within the patch a maximum was reached on day 33 with 817 mg C m⁻². The difference between in- and out-patch stations in abundance and biomass was not significant ($P > 0.05$; Mann-Whitney U-test). The group of acantharia comprised species of the genera *Acanthometra* spp., *Acanthostaurus* spp., *Amphistaurus* spp., *Gigartacon* spp. and *Stauracon* spp.. The latter two were the most dominant and contributed most to acantharian standing stocks inside and outside the patch. *Acanthostaurus* spp. and unidentified acantharians came next in importance.

3.1.3 Foraminifera

Standing stocks of adult foraminifera remained relatively stable over the course of the experiment with mean values of 58.8 (± 12.0) mg C m⁻² inside and 51.1 (± 14.7) mg C m⁻² outside the patch (Fig. 2 A). Out-patch standing stocks followed the trend of the in-patch standing stocks. There was no significant difference between in and out-patch stations ($p > 0.05$; Mann-Whitney U-test). Juvenile foraminifera standing stocks were 4.8-fold lower compared to those of adult foraminifera. Juvenile stocks inside the patch increased from 7.7 mg C m⁻² to 17.3 mg C m⁻² on day 24.8 and decreased thereafter. Mean standing stocks outside the patch amounted to 10.6 (± 3.6) mg C m⁻² with highest stocks of 14.3 mg C m⁻² on day 35. The ratio of full to empty and damaged foraminifera ranged from 50 to 400 with the highest ratio recorded at the end of the experiment (Fig. 6).

3.1.4 Aplastidic thecate dinoflagellates

From day -0.6 to day 9.4 thecate dinoflagellate standing stocks within the patch varied between 17-19 mg C m⁻² and increased steadily thereafter to 57 mg C m⁻² on day 33.4. At the end of the experiment, standing stocks decreased on day 36 to initial values (Fig. 2 F). Out-patch standing stocks were generally lower compared to in-patch and had mean stocks of 17.5 mg C m⁻² (± 2.2) (Fig. 2 F).

Protoperidinium spp. dominated both in terms of integrated abundances and standing stocks and reached up to 22 mg C m⁻² within the patch. Mean standing stocks outside the patch reached 9.1 mg C m⁻² (± 0.8). *Dinophysis* spp. and *Diplosalis* spp. accounted for only a minor fraction of thecate dinoflagellate standing stocks both inside and outside the patch. While *Dinophysis* spp. steadily increased from the beginning of the experiment from initially 1.1 to

3.5 mg C m⁻², *Diplosalis* spp. decreased from initially 1.5 to 0.6 mg C m⁻² on day 24.8 and increased slightly again towards the end of the experiment to 1.6 mg C m⁻².

3.1.5 Radiolaria and heliozoa

The contribution of radiolaria to total protozoan biomass was relatively low with < 2.6 mg C m⁻² at the beginning of the experiment, increased only slightly to 6.4 mg C m⁻² on day 9 and declined thereafter. Mean standing stocks outside the patch were 2.8 mg C m⁻² (\pm 0.6). Standing stocks inside and outside the patch were not significantly different ($p > 0.05$; Mann-Whitney U-test). The group of phaeodaria dominated radiolarian standing stocks and comprised the species: *Protocystis* cf. *swirei*, *P.* cf. *sloggettii*, *P.* cf. *harstoni*, *P.* cf. *tridens*, *P.* cf. *varians*, *Lirella melo*, *Lirella bullata* *Euphysetta elegans* and *Borgertella caudata* (Table 2). Phaeodaria contributed up to 4.15 mg C m⁻² on day 9.7 and stayed relatively stable over the course of the experiment, with mean values of 2.26 (\pm 0.9) mg C m⁻² inside the patch and mean values of 1.5 (\pm 0.5) mg C m⁻² outside the patch (Fig. 2 C).

Nassellaria contributed 0.6-2.0 mg C m⁻² to total protozoan biomass and showed increasing trends both inside and outside the patch but out-patch stations were generally lower compared to in-patch (Fig. 2 D). Spumellarian standing stocks were similar inside and outside the patch (Fig. 2 G). Identification of nassellaria and spumellaria to species level was not possible.

The taxopodidan *Sticholonche zanclea* accounted for only a minor contribution (0.2 – 2.1 mg C m⁻²) to total protozoan biomass. Standing stocks increased at the beginning, inside and out of the patch until day 14 and 16 to 1.6 mg C m⁻² and 2.1 mg C m⁻², respectively, and declined thereafter. Another increase was recorded inside the patch after day 25 reaching 1.3 mg C m⁻² (Fig. 3). There was no significant difference between in- and out-patch ($p > 0.05$; Mann-Whitney U-test).

3.2 Vertical distribution

In the upper 100 m tintinnid ciliates accounted for 95 % of protozoan abundance, both inside and outside the patch while aplastidic thecate dinoflagellates were the most abundant taxon below 100 m. Radiolaria increased below 100 m inside and outside the patch and contributed 20-30 % to total protozoan abundance. Acantharia and foraminifera contributed < 2 % in the upper 80 m and about 8-10 % below 80 m to total protozoan abundance (Fig. 7 A and C).

In terms of biomass tintinnid ciliates dominated in the upper 80 m inside the patch and contributed 40-70 % to total protozoan biomass. The relative contribution of tintinnid ciliates decreased inside the patch below 80 m while the relative contribution of acantharia increased

from 30 to 90 % (Fig. 7 B and D). Inside the patch aplastidic thecate dinoflagellates and radiolaria contributed only minor to total protozoan biomass, the former 2-8 % with increasing contribution below 80 m and the latter less than 1 %. Foraminifera contributed 19 % to total protozoan biomass inside and 17 % outside the patch in the upper 100 m while their contribution decreased below 100 m (Fig. 7 C and D).

3.2.1 Tintinnid ciliates

Full tintinnid ciliates were abundant only in the upper 100 m both inside and outside the patch and declined below (Fig. 8 A). While empty tintinnids were abundant in the upper 100 m damaged tintinnids were abundant in depths from 80-200 m (Fig. 8 B and C).

3.2.2 Acantharia

In terms of abundance total acantharia dominated in the surface layer throughout the experiment and declined below 150 m depth inside and outside the patch. Two peaks in abundance reaching up to 15 cells L⁻¹ were recorded on day 14 and at the end of the experiment on day 36 (Fig. 9 A). *Gigartacon* spp. was abundant at the beginning of the experiment but declined thereafter. Out patch stations showed elevated abundances of *Gigartacon* spp. on day -0.6, 16.3 and 35.3 each in 100 m depths. While *Gigartacon* spp. was abundant in surface waters (0-100 m) *Stauracon* spp. showed elevated abundances well below 100 m (Fig. 9 B and C). Out patch stations showed elevated abundances of *Stauracon* spp. on day -0.6 in 300 m and on day 16.3 in 200 m depth.

3.2.3 Foraminifera

Elevated abundances of adult foraminifera were restricted to the upper 100 m of the water column both inside and outside the patch and sharply declined below (Fig. 10 A). Juvenile foraminifera were more abundant between 80-150 m (Fig. 10 B).

3.2.4 Aplastidic thecate dinoflagellates

Dinophysis spp. showed a clear subsurface peak centred at 200 m depth both inside and outside the patch (Fig. 11 A). *Diplopsalis* spp. showed a similar vertical distribution to *Dinophysis* spp., however, with some abundance maxima below 200 m depth (Fig. 11 B). While *Protoperidinium* spp. showed a more patchy vertical distribution than species of the former two genera, abundance peaks were allocated below 100 m depth, except at two stations on day 9.7 and 14.3 at 60 m (Fig. 11 C).

3.2.5 Radiolaria and heliozoa

Radiolaria were largely restricted to depths below 50 m both inside and outside the patch. Nassellaria, phaeodaria and spumellaria showed a patchy vertical distribution with peaks generally occurring between 100 and 300 m (Fig. 12 A, B and C). *Sticholonche zancelea* showed a distinct subsurface maximum at 100 m depth both inside and outside the patch (Fig. 13 A).

4. Discussion

4.1.1 Tintinnid ciliates

Tintinnid standing stocks were highest on days 9 and 15 with $>270 \text{ mg C m}^{-2}$, considerably higher compared to earlier studies from the Southern Ocean (Klaas, 2001; Henjes et al., 2007) but in the same range as those observed during EIFEX (Assmy et al., in preparation). The dominance of small flagellates and coccoid cells during LOHAFEX likely facilitated biomass built-up in tintinnid grazers as tintinnids generally prefer prey not larger than 45 % the oral diameter of their lorica (Caron et al., 2012) and the ingestion rate increases when the size of the prey only takes up 25 % of the loricae diameter (Dolan et al., 2002). Numerically the protist community was dominated by cells $<6 \mu\text{m}$ in diameter, thus in the optimal size window for tintinnid grazers. Hence the initial increase of tintinnids in the euphotic zone might be due to the iron-induced increase of flagellate biomass while the decline thereafter can be attributed to copepod grazing. Indeed, empty and damaged loricae were frequently observed in fecal pellets (Fig. 14). We cannot rule out that some empty loricae might have been caused by cell lyses but suspect this effect to be minor as it has been shown to be very species specific (Leakey et al., 1994; Karayanni et al., 2004; Henjes et al., 2007). While both full and empty loricae showed a similar vertical distribution with peaks in the upper 60 m, damaged loricae generally peaked at around 100 m depth. As only crustacean grazers are able to crush and damage the stiff, leathery loricae, fragmentation and retention of fecal pellets are the most likely source of damaged loricae at subsurface depths. This is in line with carbon flux estimates that have shown that most of the iron-induced production was retained in the surface layer (Martin et al., 2013). We attribute the increase of intact empty and damaged loricae during LOHAFEX to the high grazing pressure by the dominant copepod species. Standing stocks of damaged loricae increased inside and outside the patch but differed significantly ($P < 0.05$ Mann-Whitney U-test) indicating higher grazing pressure on tintinnids within the patch. The ratio of full to empty and damaged (F:ED) loricae also confirmed high grazing pressure on tintinnids as for every full lorica two empty and four damaged loricae were recorded (Fig. 5).

Ciliates, including tintinnids, are quantitatively important in the diet of copepods especially when abundances of large cell-size phytoplankton are scarce (Ohmann and Runge, 1994; Gifford and Dragg, 1991) which was clearly the case during LOHAFEX (Schulz et al., in preparation, manuscript I). Thus, despite optimal food conditions and potentially high growth rates tintinnids were kept in check by copepod predation, indicating a high turn-over in this

protozoan group. In addition our findings support previous observations that ciliates are preferred food of copepod grazers (Calbet and Saiz, 2005).

4.1.2 Acantharia

Even though acantharian standing stocks were very variable inside the patch and showed no significant difference to outside waters, they by far accounted for the largest contribution to total large protozoan standing stocks. Peak acantharian stocks inside the patch were considerably higher than those recorded during two previous Southern Ocean iron fertilization experiments (Henjes et al., 2007; Assmy et al., in prep.). Maintenance of large standing stocks indicates that acantharians fared better than the other groups, possibly due to a combination of lower grazer-induced mortality and hosting of symbiotic algae in their endoplasm (Fig. 15 A-F). Indeed, the vertical distribution in the sunlit part of the water column supports their symbiotic life style. About 40 % of acantharia in the Equatorial Pacific and Gulf of Mexico were found to host symbionts, contributing up to 80 % of acantharian biomass (Stoecker et al., 1996) and acantharian symbionts accounted for up to 20 % of the total primary production in surface waters in the Sargasso Sea and Pacific Ocean (Michaels, 1988). The majority of acantharians were hosting autotrophic symbionts during LOHAFEX, suggesting that the symbiont's contribution to the host's metabolic demand might be substantial which is supported by the observations made during EIFEX, where two symbiont-bearing genera *Acanthostaurus* and *Gigartacon* responded rapidly to the iron addition (Assmy et al., in preparation). However, these two genera showed no pronounced increase in abundance during LOHAFEX. Henjes et al. (2007) argued that the increase in food availability during EisenEx played an important role for the increase in acantharian abundance. Acantharia are known to be active predators using their axopods to capture a wide variety of prey ranging from bacteria, small algae, ciliates, to small crustaceans such as copepods, which are rapidly digested in their ectoplasm (Swanberg and Caron, 1991). The flagellate dominated bloom during LOHAFEX apparently constituted a good food source for acantharia.

Acantharian skeletons were rarely observed in fecal pellets suggesting avoidance of the long and stiff spines by copepod grazer. However the grazing pressure on acantharians might have been higher during LOHAFEX compared to EisenEx and EIFEX, because copepods were food limited, as the bloom forming species were mainly small flagellates which were at the lower end of the handling capacity of the dominant large copepod species, in particular *Calanus simillimus*. Hence to ensure the copepods energy demand even large, bulky food items such as acantharians might have served as an alternative food source to meet their energy demand.

4.1.3 Foraminifera

Adult foraminifera were frequently hosting algal symbionts which could explain that they were largely restricted to the upper 100 m of the water column. Interestingly, juvenile foraminifera which were not hosting algal symbionts were generally situated deeper in the water column. Standing stocks of foraminifera contributed 11 % to large protozoan standing stocks and were comparable to foraminifera standing stocks recorded during EisenEx (Henjes et al., 2007), EIFEX (Asmy et al., in preparation) and a transect study in the same region (Klaas, 2001).

Standing stocks of juvenile foraminifera increased steadily from the beginning of the experiment until day 24.8, indicating enhanced reproduction. Adult foraminifera on the other hand decreased until day 14, when a full-moon event happened, and levelled off thereafter. Previous studies suggested that the reproductive cycle of some species of foraminifera might be influenced by the lunar cycle (Spindler et al., 1979; Hemleben et al., 1989; Bijma et al., 1990). This could be recorded for EisenEx (Henjes et al., 2007) but was neither observed during EIFEX (Assmy et al., in preparation) nor during LOHAFEX. Bijma et al. (1990) suggested that adult foraminifera decrease approximately four days after a full moon event, instead, adult foraminifera during LOHAFEX increased.

In previous studies foraminifera were observed in faecal pellets of copepods and in stomachs of salps (Caron and Swanberg, 1990). During LOHAFEX whole foraminifera shells were occasionally seen in the copepod faeces but rarely broken ones, indicating that they might be resistant to crushing by copepods (Fig. 16 A and B). Interestingly several individuals had their spines reduced to stumps (Fig. 16 C-E). However copepod fecal pellets contained bundles of intact spines (Fig. 16 F) indicating that copepods were a.) indeed capable of biting off the spines and swallowing them whole, b.) preferred spines instead of whole cells and c.) must have been food limited to resort to such bulky prey items. Nevertheless the overall grazing pressure on foraminifera was low as indicated by the high ratio of full to empty and damaged foraminifera.

4.1.4 Aplastidic thecate dinoflagellates

Inside and outside the patch aplastidic thecate dinoflagellate standing stocks contributed only 5 % and 3 % respectively, to total large protozoan standing stocks. *Protoberdidinium* spp. was the dominant genus followed by *Dinophysis* spp. and *Diplosalis* spp.. These species use various feeding modes (Epstein, 1992; Jacobson, 1999; Hansen and Calado, 1999) not necessarily adapted to capture small-sized prey. Indeed, the pallium-feeding mode of *Protoberdidinium* spp. and *Diplosalis* spp. enables them to capture large prey like diatoms

while the peduncle-feeding mode of *Dinophysis* spp. is tailored to pierce larger prey items and suck out their contents. The dominance of small sized flagellates during LOHAFEX might have thus not represented the ideal food source for the dominant dinoflagellate species. Suboptimal food size spectra in combination with avoidance of surface feeding copepods might explain the deep abundance maxima (generally below 100 m) of these genera. This contrasts with the diatom dominated blooms during EisenEx and EIFEX where *Protoperdinium* spp. were the dominant dinoflagellate grazers, showed significantly higher abundances in the surface mixed layer and contributed a much larger fraction to large protozoan biomass than during LOHAFEX. During EisenEx *Protoperdinium* spp. showed a significant correlation with Chl *a*, primary production and diatom abundance, which supported their preference for diatom prey (Henjes et al., 2007). During LOHAFEX surface maxima in *Protoperdinium* spp. could only be observed until day 18 while they were restricted to depths of 200 m towards the end of the experiment. The low diatom standing stocks during LOHAFEX as compared to EisenEx and EIFEX were likely not sufficient to sustain food demands of pallium-feeding dinoflagellates against the grazing pressure by copepods on them. Species of the genera *Diplopsalis* spp. and *Dinophysis* spp. were nearly absent in the surface layer and showed distinct subsurface maxima at 200 m depth. Subsurface maxima in *Dinophysis* spp. were also observed during EIFEX indicating that species of this genus spend a considerable portion of their life cycle at greater depths. Although we cannot rule out that these deep-dwelling taxa were feeding on the particle flux emanating from the surface layer their contribution to flux feeding was likely minor as most of the particle transformation occurred between the base of the mixed layer and 150 m (Martin et al., 2013), above the depth horizon where the bulk of these genera was situated. A recent study by Jeong and others (2010) showed that heterotrophic dinoflagellates are important predators of other dinoflagellates. This predator-prey relationship could explain why all deep dwelling dinoflagellate genera were mainly recorded at 200 m depth if they were feeding at each other. An alternative explanation is that species of these genera remain largely inactive at subsurface depths during periods of unfavourable food conditions which is supported by their persistent behaviour at low food concentrations (Sherr and Sherr, 2007).

4.1.5 Radiolaria and *Sticholonche zancelea*

In general radiolaria were a minor component of large protozoa during LOHAFEX. Within the radiolaria, spumellaria were most abundant and contributed most to radiolarian standing stocks (0.5 mg C m^{-2}). Phaeodaria, spumellaria and nassellaria showed subsurface maxima centred at 100 and 200 m depth, whereas the latter showed a wider vertical distribution down

to 450 m. Subsurface maxima of radiolarian were also observed during EisenEx (Henjes et al., 2007) and EIFEX (Assmy et al., in prep.). Klaas (1997) suggested that phaeodaria retain and repackage particles and material sinking out of the surface layers. This is supported in the EIFEX study from where phaeodaria intercepted particles emanating from the continuous background flux measured underneath the patch and outside of it (Assmy et al. in prep.). However, the low export flux recorded during LOHAFEX (Martin et al., 2013; Ebersbach et al., in review) likely accounted for their low subsurface abundances underneath the patch and outside of it. Different feeding modes, flux versus suspension feeders, are most likely explaining the vertical segregation amongst the different radiolarian groups (Abelmann and Nimmergut, 2005).

During LOHAFEX *Sticholonche zancelea* showed maxima below the WML, which is in good agreement with previous observations (Gowing and Garrison, 1992; Klaas, 2001; Henjes et al., 2007) but stands in contrast to observations during EIFEX (Assmy et al. in prep.) where *S. zancelea* appeared also in the WML. Assmy et al. (in prep.) observed a positive relationship between *S. zancelea* and tintinnid biomass suggesting a predator-prey relationship. However, despite the high abundances of tintinnid ciliates during LOHAFEX *S. zancelea* showed no relationship with tintinnid standing stocks. Maxima of tintinnids appeared in the WML on day 14 and maxima of *S. zancelea* at depth from 100 m onwards on day 14 and at the end of the experiment.

5. Conclusions

None of the groups investigated, apart from damaged tintinnid loricae, showed a pronounced increase or a significant difference between in and out-patch. Possible explanations for the lack of response of larger protozoa during LOHAFEX might be due to the flagellate dominated community during LOHAFEX compared to previous Southern Ocean OIF experiments that were dominated by diatoms. One of the driving forces during LOHAFEX but also during EisenEx and EIFEX was the exceedingly high abundances of copepods. Due to their high abundances and suboptimal food availability, copepods were food limited and resorted to large, armoured protozoans which they might have otherwise avoided. Our study indicates for the group of foraminifera that mineral armour does not necessarily mean absolute grazer protection. Copepod grazing pressure seems to be the driving force for the muted response of thecate dinoflagellates inside the patch. Tintinnid ciliates were kept in check by copepod predation albeit optimal food conditions and potentially high growth rates, indicating a high-turn over in this group and confirming the importance of this group as preferred prey for copepods consequently as link to higher trophic levels. The feeding behaviour of tintinnids but also of the protozoan community in general, are important factors determining grazing impact of the protozoa on pico- and nanoplankton in pelagic ecosystems. Thus, the iron-mediated increase in flagellate biomass during LOHAFEX might have been partly due top-down control of protozoan grazers by copepods. Hence it is of major importance to investigate the taxonomic composition of the whole protozoan assemblage to deepen our understanding of the complex relationships within the pelagic food webs.

References

- Abelmann, A., and Gowing, M. M., 1996, Horizontal and vertical distribution pattern of living radiolarians along a transect from the Southern Ocean to the South Atlantic subtropical region: *Deep Sea Research Part I*, v. 43, no. 3, p. 361-382.
- , 1997, Spatial distribution pattern of living polycystine radiolarian taxa -- baseline study for paleoenvironmental reconstructions in the Southern Ocean (Atlantic sector): *Marine Micropaleontology*, v. 30, no. 1-3, p. 3-28.
- Abelmann, A., and Nimmergut, A.-P., 2005, Radiolarians in the Sea of Okhotsk and their ecological implication for paleoenvironmental reconstructions: *Deep Sea Research Part II: Topical Studies in Oceanography*, v. 52, no. 16-18, p. 2302-2331.
- Alder, V. A., and Boltovskoy, D., 1993, The ecology of larger microzooplankton in the Weddell-Scotia confluence area: Horizontal and vertical distribution patterns.: *Journal of Marine Research*, v. 51, no. 2, p. 323-344.
- Assmy, P., Smetacek, V., Montresor, M., Klaas, C., Henjes, J., Strass, V. H., Arrieta, J. M., Bathmann, U., Berg, M. G., Breitbarth, E., Cisewski, B., Friedrichs, L., Fuchs, N., Herndl, G. J., Jansen, S., , Krägefsky, S., Latasa, N., Passow, U., Peeken, I., Röttgers, R., Scharek, R., Schüller, S. E., Steigenberger, S., and Webb, A., IN REVISION, 2013, Grazer-protected diatoms decouple ocean carbon and silicon cycles around Antarctica: *PNAS*.
- Atkinson, A., 1996, Subantarctic copepods in an oceanic, low chlorophyll environment: ciliate predation, food selectivity and impact on prey populations: *Marine Ecology Progress Series*, v. 130, p. 85-96.
- Becquevort, S., 1997, Nanoprotozooplankton in the Atlantic sector of the Southern Ocean during early spring: Biomass and feeding activities: *Deep-Sea Research II*, v. 44, no. 1-2, p. 355-373.
- Bernstein, R. E., Betzer, P. R., Feely, R. A., Byrne, R. H., Lamb, M. F., and Michaels, A. F., 1987, Acantharian fluxes and strontium to chlorinity ratios in the North Pacific Ocean.: *Science*, v. 237, no. 4821, p. 1490-1494.
- Bernstein, R. E., and Byrne, R. H., 2004, Acantharians and marine barite: *Marine Chemistry*, v. 86, no. 1-2, p. 45-50.
- Bernstein, R. E., Byrne, R. H., Betzer, P. R., and Greco, A. M., 1992, Morphologies and transformations of celestite in seawater: The role of acantharians in strontium and barium geochemistry: *Geochimica et Cosmochimica Acta*, v. 56, no. 8, p. 3273-3279.
- Bijma, J., Erez, J., and Hemleben, C., 1990, Lunar and semi-lunar reproductive cycles in some spinose planktonic foraminifers: *Journal of Foraminiferal Research*, v. 20, no. 2, p. 117-127.
- Boltovskoy, D., and Alder, V. A., 1992, Paleocological implications of radiolarian distribution and standing stocks versus accumulation rates in the Weddell Sea: Kennett, J. P. and Warnke, D. A.
- Boltovskoy, D., Alder, V. A., and Abelmann, A., 1993, Radiolarian sedimentary imprint in Atlantic equatorial sediments: Comparison with the yearly flux at 853 m: *Marine Micropaleontology*, v. 23, no. 1, p. 1-12.
- Boltovskoy, D., and Uliana, E., 1996, Seasonal variation in the flux of microplankton and radiolarian assemblage compositions in the northeastern Tropical Atlantic at 2,195 m: *Limnology and Oceanography*, v. 41, no. 4, p. 615-635.
- Boltovskoy, E., Boltovskoy, D., Correa, N., and Brandini, F., 1996, Planktic foraminifera from the southwestern Atlantic (30 degree -60 degree S): Species-specific patterns in the upper 50 m: *Marine Micropaleontology*, v. 28, no. 1, p. 53-72.

- Burkill, P. H., Edwards, E. S., and Sleigh, M. A., 1995, Microzooplankton and their role in controlling phytoplankton growth in the marginal ice zone of the Bellingshausen Sea: Deep Sea Research Part II, v. 42, no. 4-5, p. 1277-1290.
- Calbet, A., and Saiz, E., 2005, The ciliate-copepod link in marine ecosystems: Aquatic Microbial Ecology, v. 38, no. 2, p. 157-167.
- Caron, D., Dennett, M., Lonsdale, D., Moran, D., and Shalapyonok, L., 2000, Microzooplankton herbivory in the Ross Sea, Antarctica: Deep-Sea Research II, v. 47, no. 15-16, p. 3249-3272.
- Caron, D. A., Countway, P. D., Jones, A. C., Kim, D. Y., and Schnetzer, A., 2012, Marine Protistan Diversity: Annual Review of Marine Science, v. 4, p. 467-493.
- Caron, D. A., and Swanberg, N. R., 1990, The ecology of planktonic sarcodines: Rev. Aquat. Sci., v. 3, p. 147-180.
- Dehairs, F., Baeyens, W., and Goeyens, L., 1992, Accumulation of suspended barite at mesopelagic depths and export production in the Southern Ocean: Science (Washington), v. 258, no. 5086, p. 1332-1335.
- Dehairs, F., Shopova, D., Ober, S., Veth, C., and Goeyens, L., 1997, Particulate barium stocks and oxygen consumption in the Southern Ocean mesopelagic water column during spring and early summer: relationship with export production: Deep Sea Research Part II, v. 44, no. 1-2, p. 497-516.
- Dehairs, F., Stroobants, N., and Goeyens, L., 1991, Suspended barite as a tracer of biological activity in the Southern Ocean: Marine Chemistry, v. 35, no. 1-4, p. 399-410.
- DeMaster, D. J., 2002, The accumulation and cycling of biogenic silica in the Southern Ocean: revisiting the marine silica budget: Deep Sea Research Part II: Topical Studies in Oceanography, v. 49, no. 16, p. 3155-3167.
- Dieckmann, G., S., Spindler, M., Lange, M., A., Ackley, S., F., and Eicken, H., 1991, Antarctic Sea Ice: A habitat for the foraminifer *Neogloboquadrina pachyderma*: Journal of Foraminiferal Research, v. 21, no. 2, p. 182-189.
- Dolan, J. R., Claustre, H., Carlotti, F., Plounevez, S., and Moutin, T., 2002, Microzooplankton diversity: relationships of tintinnid ciliates with resources, competitors and predators from the Atlantic Coast of Morocco to the Eastern Mediterranean: Deep Sea Research Part I: Oceanographic Research Papers, v. 49, no. 7, p. 1217-1232.
- Dymond, J., and Collier, R. W., 1996, Particulate barium fluxes and their relationships to biological productivity: Deep Sea Research Part II: Topical Studies in Oceanography, v. 43, no. 4-6, p. 1283-1308.
- Dymond, J., Suess, E., and Lyle, M., 1992, Barium in deep-sea sediment: A geochemical proxy for paleoproductivity: Paleoceanography, v. 7, no. 2, p. 163-181.
- Ebersbach, F., Assmy, P., Martin, P., Schulz, I. K., Wolzenburg, S., and Nöthig, E.-M., IN REVISION, Sedimentation patterns of phyto- and protozooplankton and sinking particle assemblage during the iron fertilisation experiment LOHAFEX in the Southern Ocean: Deep Sea Research Part I: Oceanographic Research Papers.
- Epstein, S. S., Burkovsky, I. V., and Shiaris, M. P., 1992, Ciliate grazing on bacteria, flagellates, and microalgae in a temperate zone sandy tidal flat: Ingestion rates and food niche partitioning: Journal of Experimental Marine Biology and Ecology, v. 165, no. 1, p. 103-123.
- Esser, B. K., and Volpe, A. M., 2002, At-sea high-resolution chemical mapping: extreme barium depletion in North Pacific surface water: Marine Chemistry, v. 79, no. 2, p. 67-79.
- Francois, R., Honjo, S., Manganini, S. J., and Ravizza, G. E., 1995, Biogenic barium fluxes to the deep sea: Implications for paleoproductivity reconstruction: Global Biogeochem. Cycles, v. 9, no. 2, p. 289-304.
- Gifford, D. J., and Dagg, M. J., 1991, The microzooplankton–mes-ozooplankton link: consumption of planktonic protozoa by the calanoid copepods

- Acartia tonsa Dana and Neocalanus plumchrus Murukawa: Marine Microbial Food Webs, v. 5, p. 161-177.
- Gonzalez, H., 1992, Distribution and abundance of minipellets around the Antarctic peninsula. Implications for protistan feeding behaviour: Marine Ecology Progress Series, v. 90, no. 3, p. 223-236.
- Good, N. E., Winget, G. D., Winter, W., Connolly, T. N., Izawa, S., and M.S., R. M., 1966, Hydrogen Ion Buffers for Biological Research: Biochemistry, v. 5, no. 2, p. 467-477.
- Gowing, M. M., 1986, Trophic biology of phaeodarian radiolarians and flux of living radiolarians in the upper 2000 m of the North Pacific Central Gyre: Deep-Sea Research, v. 33, no. 5A, p. 655-674.
- , 1989, Abundance and feeding ecology of Antarctic phaeodarian radiolarians: Marine Biology, v. 103, no. 1, p. 107-118.
- Gowing, M. M., and Garrison, D. L., 1991, Austral winter distributions of large tintinnid and large sarcodinid protozooplankton in the ice-edge zone of the Weddell/Scotia Seas: Journal of Marine Systems, v. 2, no. 1-2, p. 131-141.
- , 1992, Abundance and feeding ecology of larger protozooplankton in the ice edge zone of the Weddell and Scotia Seas during the austral winter: Deep Sea Research, v. 39, no. 5, p. 893-919.
- Gowing, M. M., Garrison, D. L., Kunze, H. B., and Winchel, C. J., 2001, Biological components of Ross Sea short-term particle fluxes in the austral summer of 1995-1996: Deep Sea Research I, v. 48, no. 12, p. 2645-2671.
- Hansen, P. J., 1991, Quantitative importance and trophic role of heterotrophic dinoflagellates in a coastal pelagial food web: Marine Ecology Progress Series, v. 73, no. 2-3, p. 253-261.
- Hansen, P. J., and Calado, A. J., 1999, Phagotrophic mechanisms and prey selection in free-living dinoflagellates: J. Eukaryot. Microbiol., v. 46, no. 4, p. 382-389.
- Hemleben, C., Spindler, M., and Anderson, O. R., 1989, Modern Planktonic Foraminifera: Springer Verlag, p. 363.
- Henjes, J., Assmy, P., Klaas, C., and Smetacek, V., 2007, Response of the larger protozooplankton to an iron-induced phytoplankton bloom in the Polar Frontal Zone of the Southern Ocean (EisenEx): Deep Sea Research Part I: Oceanographic Research Papers, v. 54, no. 5, p. 774-791.
- Hillebrand, H., Duerselen, C. D., Kirschtel, D., Pollinger, U., and Zohary, T., 1999, Biovolume calculation for pelagic and benthic microalgae: Journal of Phycology [J. Phycol.]. v. 35, no. 2, p. 403-424.
- Honjo, S., and Manganini, S. J., 1993, Annual biogenic particle fluxes to the interior of the North Atlantic Ocean: Deep Sea Research Part II: Topical Studies in Oceanography, v. 40, no. 1-2, p. 587-607.
- Irigoien, X., Flynn, K. J., and Harris, R. P., 2005, Phytoplankton blooms: a 'loophole' in microzooplankton grazing impact?: Journal of Plankton Research, v. 27, no. 4, p. 313-321.
- Jacobson, D. M., 1999, A brief history of dinoflagellate feeding research: J. Eukaryot. Microbiol., v. 46, no. 4, p. 376-381.
- Jacobson, D. M., and Anderson, D. M., 1986, Thecate heterotrophic dinoflagellates: Feeding behavior and mechanisms.: Journal of Phycology, v. 22, no. 3, p. 249-258.
- Jeong, H. J., Yoo, Y. D., Kim, J. S., Seong, K. A., Kang, N. S., and Kim, T. H., 2010, Growth, Feeding and Ecological Roles of the Mixotrophic and Heterotrophic Dinoflagellates in Marine Planktonic Food Webs: Ocean Science Journal, v. 45, p. 65-91.
- Karayanni, H., Christaki, U., Van Wambeke, F., and Dalby, A. P., 2004, Evaluation of double formalin--Lugol's fixation in assessing number and biomass of ciliates: an example of

- estimations at mesoscale in NE Atlantic: *Journal of Microbiological Methods*, v. 56, no. 3, p. 349-358.
- Klaas, C., 1997, Distribution and role of microprotozoa in the Southern Ocean [Dissertation]: Bremen Univ., Bremen (FRG), Fachber. Biologie/Chemie, 119 p.
- Klaas, C., 2001, Spring distribution of larger (>64 μm) protozoans in the Atlantic sector of the Southern Ocean: *Deep-Sea Research I*, v. 48, no. 7, p. 1627-1649.
- Leakey, R., Burkill, P., and Sleight, M., 1994, A comparison of fixatives for the estimation of abundance and biovolume of marine planktonic ciliate populations: *Journal of Plankton Research*, v. 16, no. 4, p. 375-389.
- Lonsdale, D., Caron, D., Dennett, M., and Schaffner, R., 2000, Predation by *Oithona* spp. on protozooplankton in the Ross Sea, Antarctica: *Deep-Sea Research II*, v. 47, no. 15-16, p. 3273-3283.
- Martin, P., Rutgers van der Loeff, M., Cassar, N., Vandromme, P., d'Ovidio, F., Stemmann, L., Rengarajan, R., Soares, M., González, H. E., Ebersbach, F., Lampitt, R. S., Sanders, R., Barnett, B. A., Smetacek, S., and Naqvi, S. W. A., 2013, Iron fertilization enhanced net community production but not downward particle flux during the Southern Ocean iron fertilization experiment LOHAFEX: *Global Biogeochemical Cycles*, v. 27.
- Menden-Deuer, S., and Lessard, E. J., 2000, Carbon to volume relationships for dinoflagellates, diatoms and other protist plankton: *Limnology and Oceanography*, v. 45, no. 3, p. 569-579.
- Michaels, A. F., Caron, D. A., Swanberg, N. R., Howse, F. A., and Michaels, C. M., 1995, Planktonic sarcodines (Acantharia, Radiolaria, Foraminifera) in surface waters near Bermuda: Abundance, biomass and vertical flux: *Journal of Plankton Research*, v. 17, no. 1, p. 131-163.
- Morley, J. J., and Stepien, J. C., 1985, Antarctic Radiolaria in late winter/early spring Weddell Sea waters: *Micropaleontology*, v. 31, no. 4, p. 365-371.
- Nöthig, E.-M., and Gowing, M. M., 1991, Late winter abundance and distribution of phaeodarian radiolarians, other large protozooplankton and copepod nauplii in the Weddell Sea, Antarctica.: *Marine biology*, v. 111, no. 3, p. 473-484.
- Ohmann, M. D., and Runge, J. A., 1994, Sustained fecundity when phytoplankton resources are in short supply: omnivory by *Calanus finmarchicus* in the Gulf of St. Lawrence: *Limnology and Oceanography*, v. 39, p. 21-36.
- Porter, K. G., Sherr, E. B., Sherr, B. F., Pace, M., and Sanders, R. W., 1985, Protozoa in planktonic food webs: *J. Protozool.*, v. 32, no. 3, p. 409-415.
- Schiebel, R., 2002, Planktic foraminiferal sedimentation and the marine calcite budget: *Global Biogeochemical Cycles*, v. 16, no. 4, p. 13-11-13-21.
- Schiebel, R., Hiller, B., and Hemleben, C., 1995, Impacts of storms on recent planktonic foraminiferal test production and CaCO_3 flux in the North Atlantic at 47 degree N, 20 degree W (JGOFS): *Marine Micropaleontology*, v. 26, no. 1-4, p. 115-129.
- Schulz, I. K., Assmy, P., Montresor, M., Ebersbach, F., Gauns, M., Klaas, C., Mazzocchi, G. M., Roy, R., Sarkar, A., Thiele, S., Wolf, C., Wolzenburg, S., and Smetacek, S., TO BE SUBMITTED, Response of a flagellate-dominated plankton community to artificial iron fertilization in the Southern Ocean: *PLOS ONE*.
- Sherr, E. B., and Sherr, B. F., 2002, Significance of predation by protists in aquatic microbial food webs: *Antonie Van Leeuwenhoek; International Journal Gen. Molecular Microbiology*, v. 81, no. (1-4), p. 293-308.
- , 2007, Heterotrophic dinoflagellates: a significant component of microzooplankton biomass and major grazers of diatoms in the sea: *Marine Ecological Progress Series*, v. 352, p. 187-197.

- Sherr, E. B., and Sherr, B. F., 2009, Capacity of herbivorous protists to control initiation and development of mass phytoplankton blooms: *AQUATIC MICROBIAL ECOLOGY*, v. 57, no. 3, p. 253-262.
- Sieburth, J. M., Smetacek, V., and Lenz, J., 1978, Pelagic ecosystem structure: Heterotrophic compartments of the plankton and their relationship to plankton size fractions: *Limnol. and Oceanogr.*, v. 23, no. 6, p. 1256-1263.
- Smetacek, V., 1981, The annual cycle of protozooplankton in the Kiel Bight: *Marine Biology*, v. 63, no. 1, p. 1-11.
- Spindler, M., and Beyer, K., 1990, Distribution, abundance and diversity of Antarctic acantharian cysts: *Mar. Micropaleontol.*, v. 15, no. 3-4, p. 209-218.
- Spindler, M., Hemleben, C., Bayer, U., Be, A. W. H., and Anderson, O. R., 1979, Lunar Periodicity of Reproduction in the Planktonic Foraminifer *Hastigerina pelagica*: *Marine Ecological Progress Series.*, v. 1, p. 61-64.
- Stoecker, D., Gustafson, D., and Verity, P., 1996, Micro- and mesoprotozooplankton at 140 degree W in the Equatorial Pacific: Heterotrophs and mixotrophs: *Aquatic Microbial Ecology*, v. 10, no. 3, p. 273-282.
- Stoecker, D. K., and Capuzzo, J. M., 1990, Predation on Protozoa: Its importance to zooplankton: *Journal of Plankton Research*, v. 12, no. 5, p. 891-908.
- Swanberg, N. R., and Caron, D. A., 1991, Patterns of sarcodine feeding in epipelagic oceanic plankton: *Journal of Plankton Research*, v. 13, no. 2, p. 287-312.
- Takahashi, K., and Be, A. W. H., 1984, Planktonic foraminifera: Factors controlling sinking speeds: *Deep-Sea Research*, v. 31, no. 12A, p. 1477-1500.
- Thronsen, J., 1995, Chapter "Estimating cell numbers: In: *Manual on Harmful Marine Microalgae*. (eds. Hallegraeff, G. M., Anderson, D. M. & Cembella, A. D.) v. 33, no. UNESCO, Paris,, p. 63-80.
- Thunell, R. C., Pride, C. J., Tappa, E., and Muller-Karger, F. E., 1994, Biogenic silica fluxes and accumulation rates in the Gulf of California: *Geology*, v. 22, p. 303-306.
- Ziveri, P., Thunell, R. C., and Rio, D., 1995, Export production of coccolithophores in an upwelling region: Results from San Pedro Basin, Southern California Borderlands.: *Marine Micropaleontology*, v. 24, p. 335-358.

Tables

Table 1: Sampling overview during LOHAFEX for large protozoa.

Table 2: List of identified species and groups of large protozoa during LOHAFEX.

Table 3: The cellular carbon content (C , pg C cell^{-1}) for different plankton groups can be determined through cell volume (V , μm^3) using specific carbon conversion factors (Menden-Deuer and Lessard, 2000; Michaels et al., 1995).

Figures

Figure 1: Standing stocks (mg C m^{-2}) of large protozoa inside (A) and outside (B) the patch.

Figure 2: Standing stocks (mg C m^{-2}) of adult and juvenile foraminifera, acantharia, aplastidic thecate dinoflagellates, phaeodaria, spumellaria, nassellaria and tintinnid ciliates, inside (black circles) and outside (red circles) the patch. The thin lines represent running averages over three temporally adjacent stations.

Figure 3: Standing stocks (mg C m^{-2}) of *Sticholonche zanclea* inside (black circles) and outside (red circles) the patch. The thin lines represent running averages over three temporally adjacent stations.

Figure 4: Relative contribution (%) of full, empty and damaged loricae inside (A) and outside (B) the patch.

Figure 5: Ratio of tintinnid ciliates full (F) to empty (E) and damaged (D) (grey triangles) and empty to damaged (purple diamonds).

Figure 6: Foraminifera ratio of full (F) to empty (E) and damaged (D) shells.

Figure 7: Protozoa community composition of abundance and biomass integrated over 500 m given in percentage, inside (A+B) and outside (C+D) the patch.

Figure 8: Vertical distribution of tintinnid ciliates (A), empty (B) and damaged tintinnids (C) inside the patch (cells L^{-1}).

Figure 9: Vertical distribution of Acantharia (A), *Gigartacon* spp. (B) and *Stauracon* spp. (C) inside the patch (cells L⁻¹).

Figure 10: Vertical distribution of adult (A) and juvenile (B) foraminifera inside the patch (cells L⁻¹).

Figure 11: Vertical distribution of *Dinophysis* spp. (A), *Diplosalis* spp. (B) and *Protoperidinium* spp. (C) inside the patch (cells L⁻¹).

Figure 12: Vertical distribution of Phaeodaria (A), Spumellaria (B) and Nassellaria (C) inside the patch (cells L⁻¹).

Figure 13: Vertical distribution *Sticholonche zanzlea* (A) inside the patch (cells L⁻¹).

Figure 14: Light (A, C) and epifluorescence (B, D) micrographs showing tintinnid loricae inside the pellets (A, B, D; red arrows) and a damaged loricae (C).

Figure 15: Each pair of images shows acantharia of the genus *Acanthostaurus* sp under light (A, C, E) and under epifluorescence microcopy (B, D, F) with autotrophic symbionts illuminated in red.

Figure 16: Pictures of foraminifera under light (A, C-F) and epifluorescence microscopy (B) showing foraminifera inside a copepod fecal pellet (red arrows, A, B, F); note autofluorescence of algal symbionts in picture B and pictures of individual foraminifera (*Turborotalita quinquiloba*) with intact spines (C) and spines bitten off (D-E).

Table 1: Sampling overview during LOHAFEX for large protozoa.

Date (d/m/yr)	Station	Day since first Fe-release	Latitude (Degree decimal)	Longitude (Degree decimal)	IN or OUT patch	Sampling depth (m)
26.01.09	114	-0.6	-47,99989	-15,80677	IN/OUT	10; 20; 40; 60; 80; 100; 200; 300; 400; 500
31.01.09	132	5.0	-47,61603	-15,74679	IN	10; 20; 40; 60; 80; 100; 200; 300; 400; 500
05.02.09	135	9.7	-47,71383	-15,10737	IN	10; 20; 40; 60; 80; 100; 200; 300; 400; 500
09.02.09	139	14.3	-47,94621	-15,14766	IN	10; 20; 40; 60; 80; 100; 200; 300; 400; 500
20.02.09	162	24.8	-47,39253	-14,61561	IN	10; 20; 40; 60; 80; 100; 200; 300; 400; 500
01.03.09	192	33.4	-48,82138	-15,25705	IN	10; 20; 40; 60; 80; 100; 200; 300; 400; 500
04.03.09	204	36.7	-49,01781	-15,3160	IN	10; 20; 40; 60; 80; 100; 200; 300; 400; 500
12.02.09	146	16.5	-47,50081	-15,42622	OUT	10; 20; 40; 60; 80; 100; 200; 300; 400; 500
03.03.09	199	35.3	-48,03436	-15,26251	OUT	10; 20; 40; 60; 80; 100; 200; 300; 400; 500

Table 2: List of identified species and groups of large protozoa during LOHAFEX.

Foraminifera	Acantharia	Radiolaria
<i>Neoglobigerina incompta</i> <i>Neogloboquadrina pachyderma</i> <i>Globigerina bulloides</i> <i>Turborotalita quinquiloba</i> juv. Foraminifera (< 50 µm) mature Foraminifera (> 50 µm)	<i>Acantharia</i> spp. <i>Acanthometra</i> spp. <i>Acanthostaurus</i> spp. <i>Amphistaurus</i> spp. <i>Gigartacon</i> spp. <i>Stauracon</i> spp.	<i>Radiolaria</i> spp. Phaeodaria: <i>Protocystis cf swirei</i> <i>Protocystis cf sloggettii</i> <i>Protocystis cf harstoni</i> <i>Protocystis</i> spp. <i>cf Cornucella maya</i> <i>Euphysette</i> spp. <i>cf Euphysette elegans</i> <i>Borgertella caudata</i> <i>Lirella bullata</i> <i>Lirella melo</i> Phaeodaria (unid. species) Challengeridae
Dinoflagellates	Tintinnid ciliates	Nasselaria: Artostrobiidae Nassellaria (unid. species) <i>Antarctissa</i> spp. Spumellaria: Spumellaria (unid. species) Heliozoa: <i>Sticholonche zanclea</i>
<i>Amphisolenia globifera</i> <i>Protoperidinium cf antarcticum</i> <i>Protoperidinium cf elegantissimum</i> <i>Protoperidinium cf oceanicum</i> <i>Protoperidinium cf pseudoantarcticum</i> <i>Protoperidinium penitum</i> <i>Protoperidinium cf rosaceum</i> <i>Protoperidinium</i> spp.(20-50 µm) <i>Protoperidinium</i> spp.(> 50 µm) <i>Dinophysis cf cornuta</i> <i>Dinophysis cf punctata</i> <i>Dinophysis cf tuberculata</i> <i>Dinophysis</i> spp. (20-50 µm) <i>Dinophysis</i> spp. (>50 µm) <i>Diplopsalis cf minor</i> <i>Diplopsalis</i> spp. (20-50 µm) <i>Diplopsalis</i> spp. (> 50 µm) <i>Podolampas cf palmipes</i> <i>Podolampas cf antarctica</i>	<i>Acanthostomella norvegica</i> <i>Amphorides</i> spp. <i>Amphorellopsis</i> spp. <i>Codonellopsis cf gausii</i> <i>Codonellopsis cf pusilla</i> <i>Cymatocylis antartica</i> <i>Cymatocylis calyciformis</i> <i>Cymatocylis nobilis</i> <i>Cymatocylis vanhoffeni</i> <i>Dictyocysta elegans</i> <i>Laackmanniella naviculaefera</i> <i>Ormosella acantharus</i> <i>Parundella cf caudata</i> <i>Salpingella cf acuminata</i> <i>Salpingella</i> spp. <i>Stenosomella avellana</i>	

Table 3: The cellular carbon content (C, pg C cell⁻¹) for different plankton groups can be determined through cell volume (V, μm³) using specific carbon conversion factors (Menden-Deuer and Lessard, 2000; Michaels et al., 1995).

Group	Menden-Deuer & Lessard	Michaels
aplastidic thecate Dinoflagellates	$C \text{ cell}^{-1} = 0.444 \times V^{0.864}$	
Tintinnid ciliates	$C \text{ cell}^{-1} = 0.679 \times V^{0.841}$	
Foraminifera		$C = V \times 0.089$
Acantharia		$C = V \times 0.08$
Radiolaria		$C = V \times 0.01$

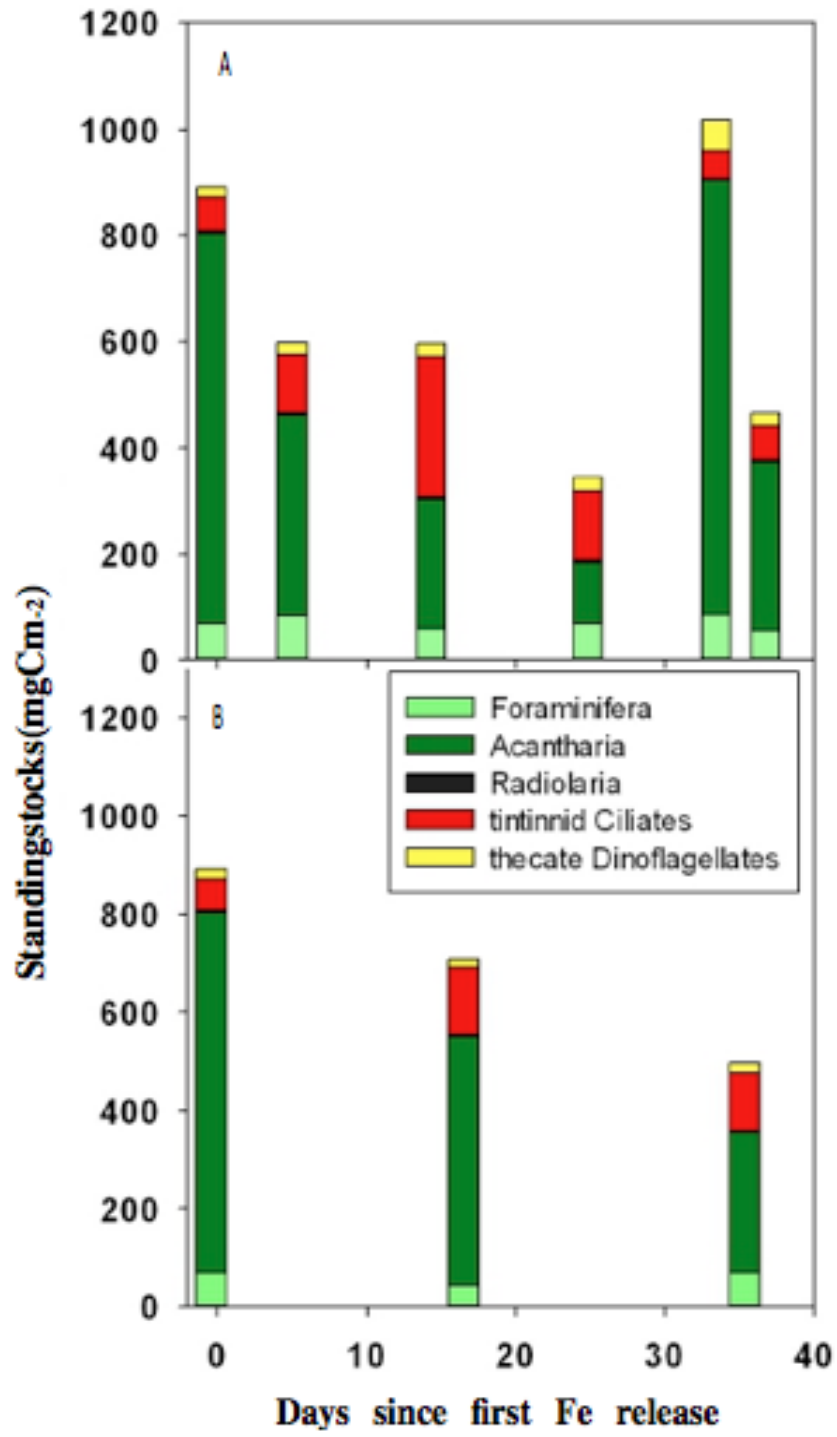


Figure 1: Standing stocks (mg C m⁻²) of large protozoa inside (A) and outside (B) the patch.

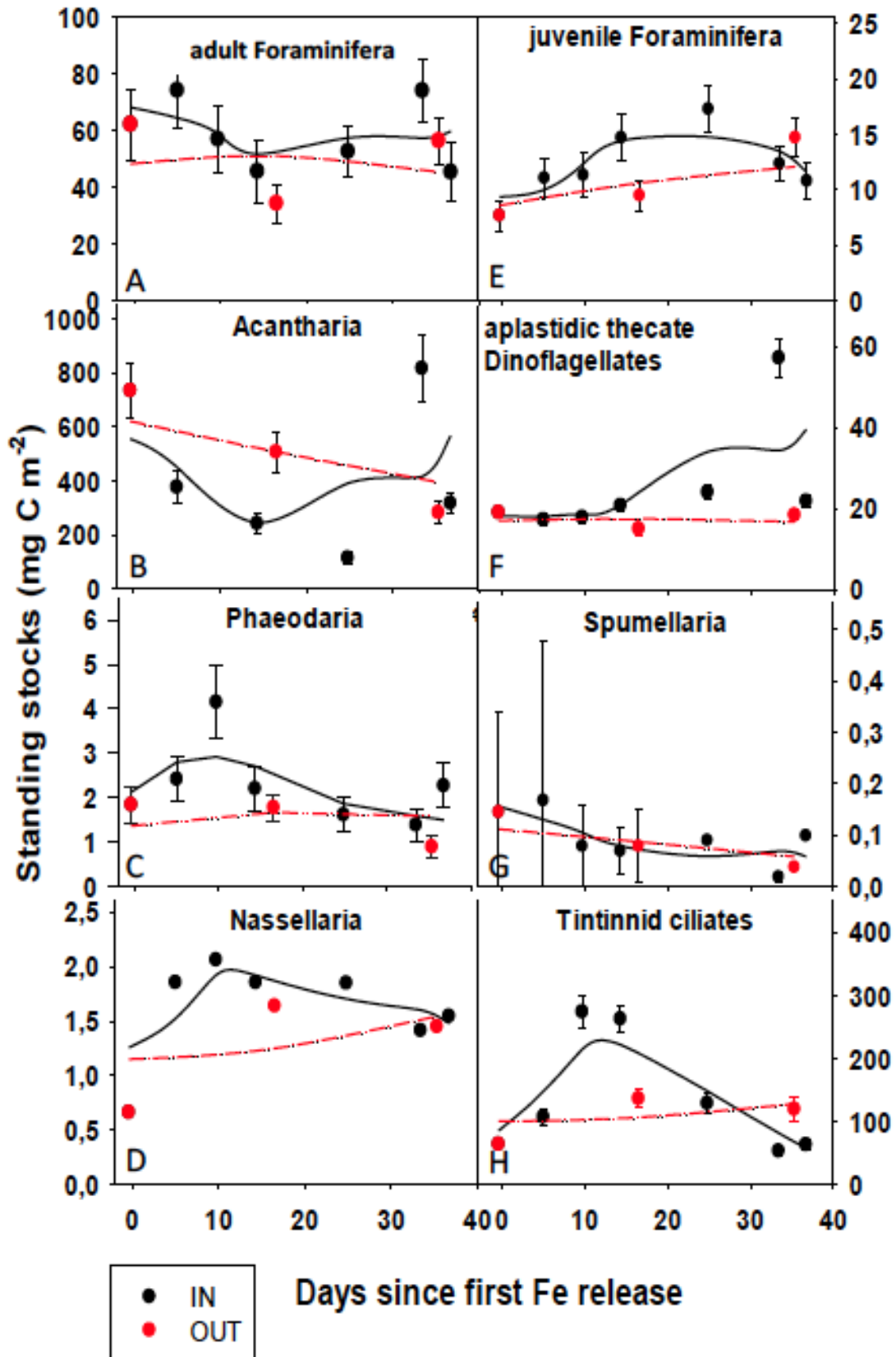


Figure 2: Standing stocks (mg C m⁻²) of adult and juvenile foraminifera, acantharia, aplastidic thecate dinoflagellates, phaeodaria, spumellaria, nassellaria and tintinnid ciliates, inside (black circles) and outside (red circles) the patch. The thin lines represent running averages over three temporally adjacent stations.

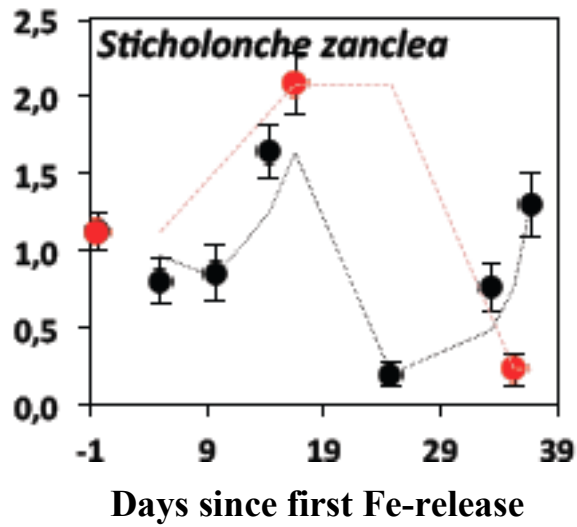


Figure 3: Standing stocks (mg C m⁻²) of *Sticholonche zanclea* inside (black circles) and outside (red circles) the patch. The thin lines represent running averages over three temporally adjacent stations.

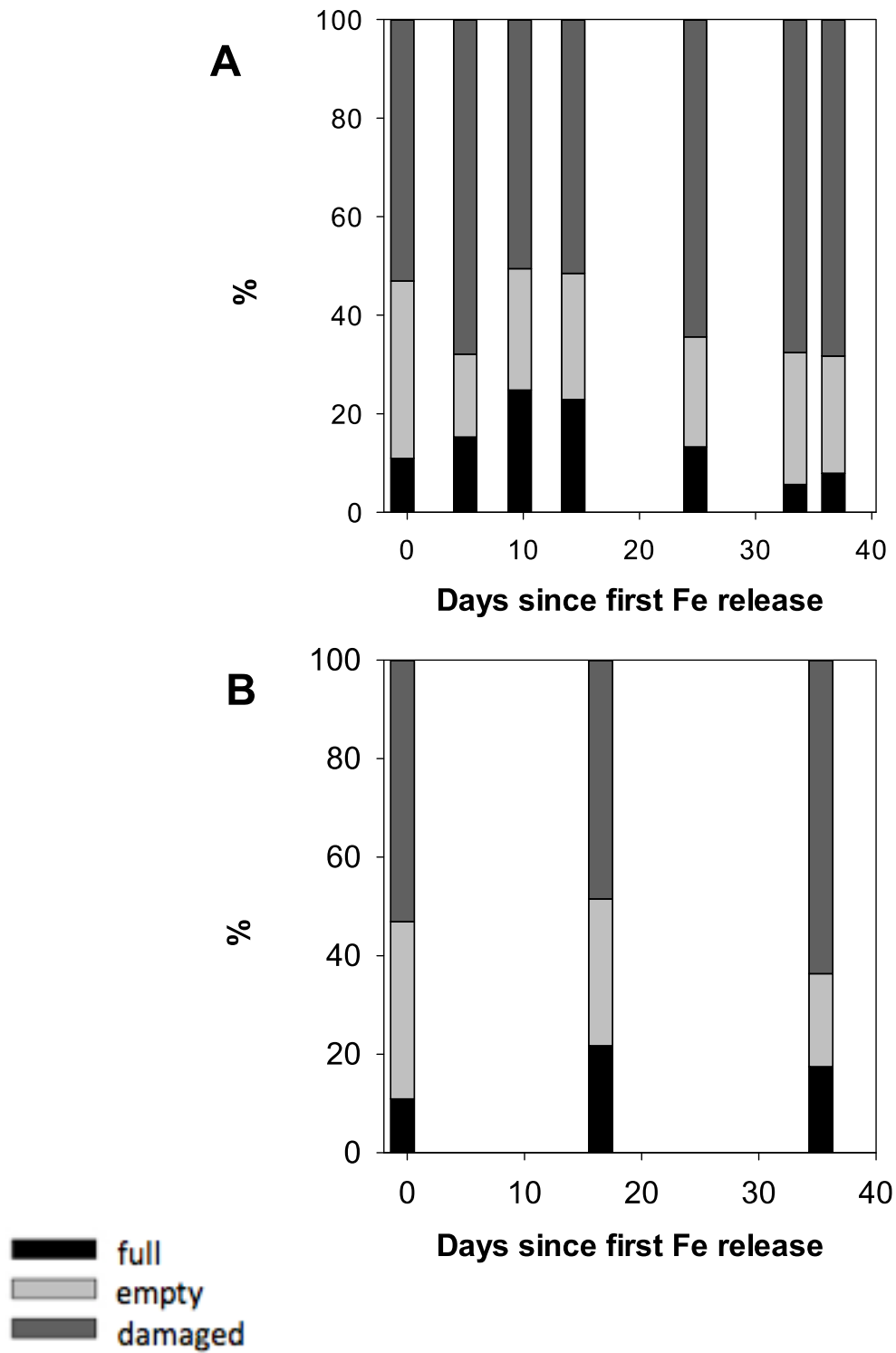


Figure 4: Relative contribution (%) of full, empty and damaged loricae inside (A) and outside (B) the patch integrated over 80 m WML.

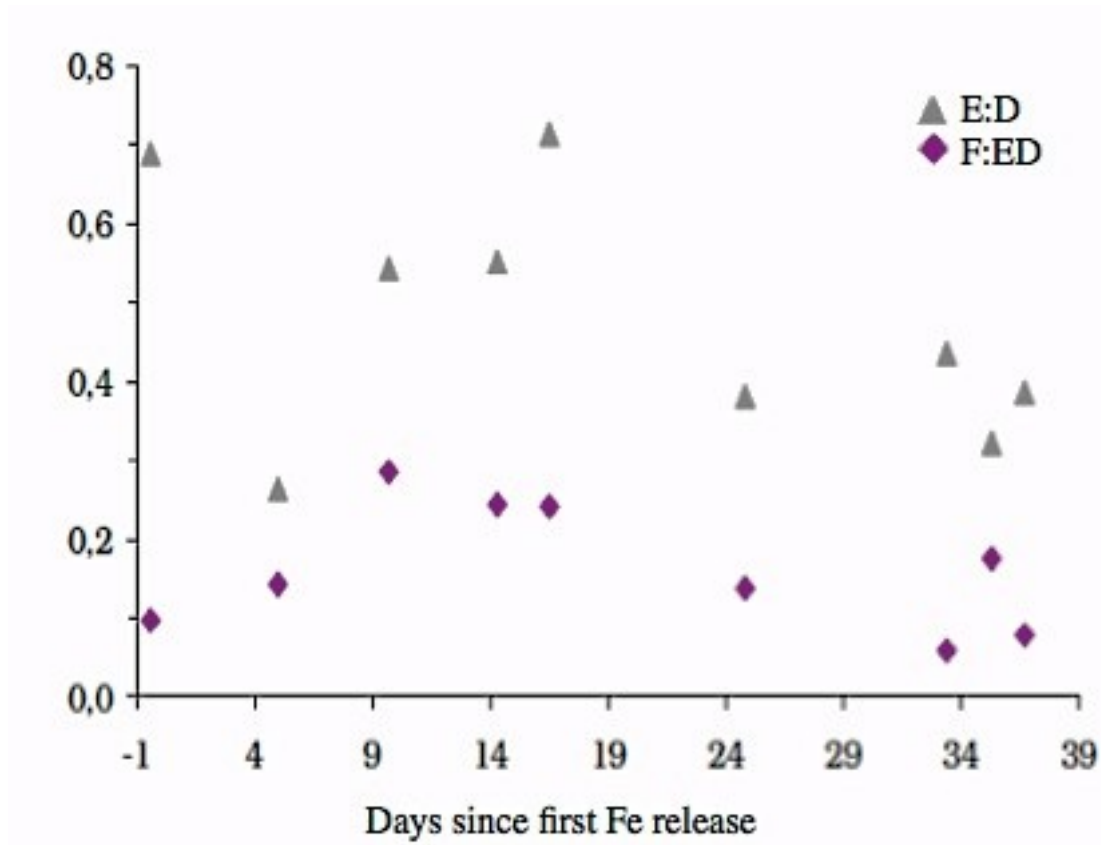


Figure 5: Ratio of tintinnid ciliates full (F) to empty (E) and damaged (D) (grey triangles) and empty to damaged (purple diamonds).

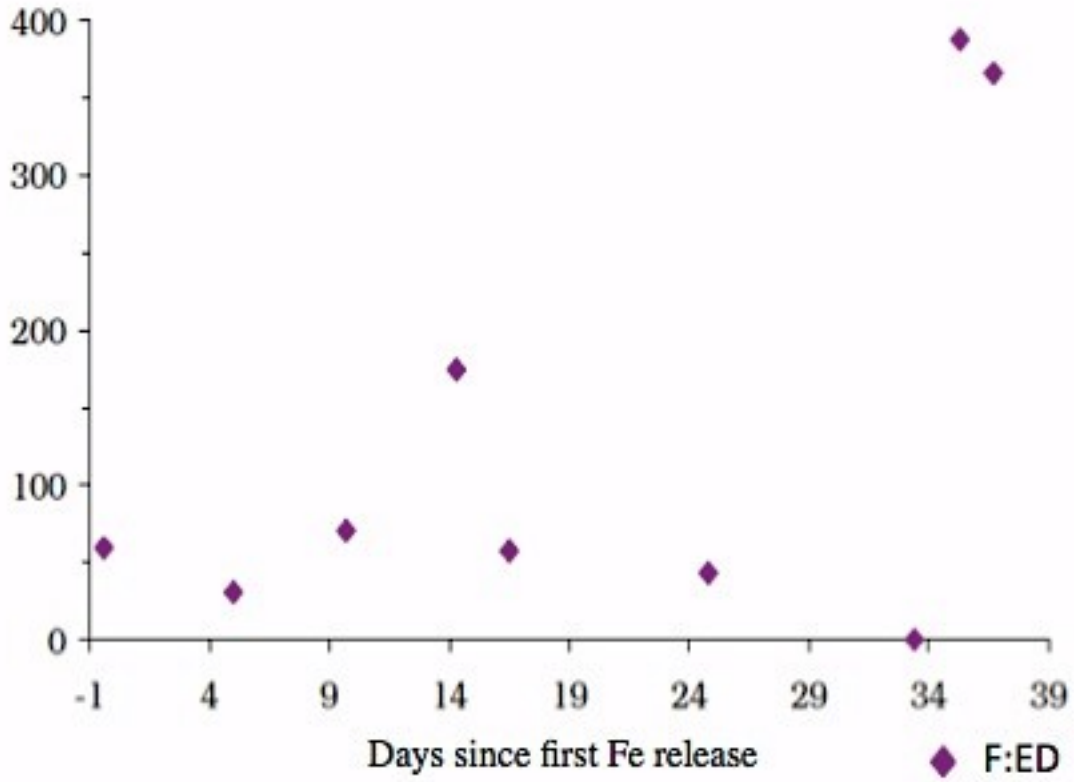


Figure 6: Foraminifera ratio of full (F) to empty (E) and damaged (D) shells.

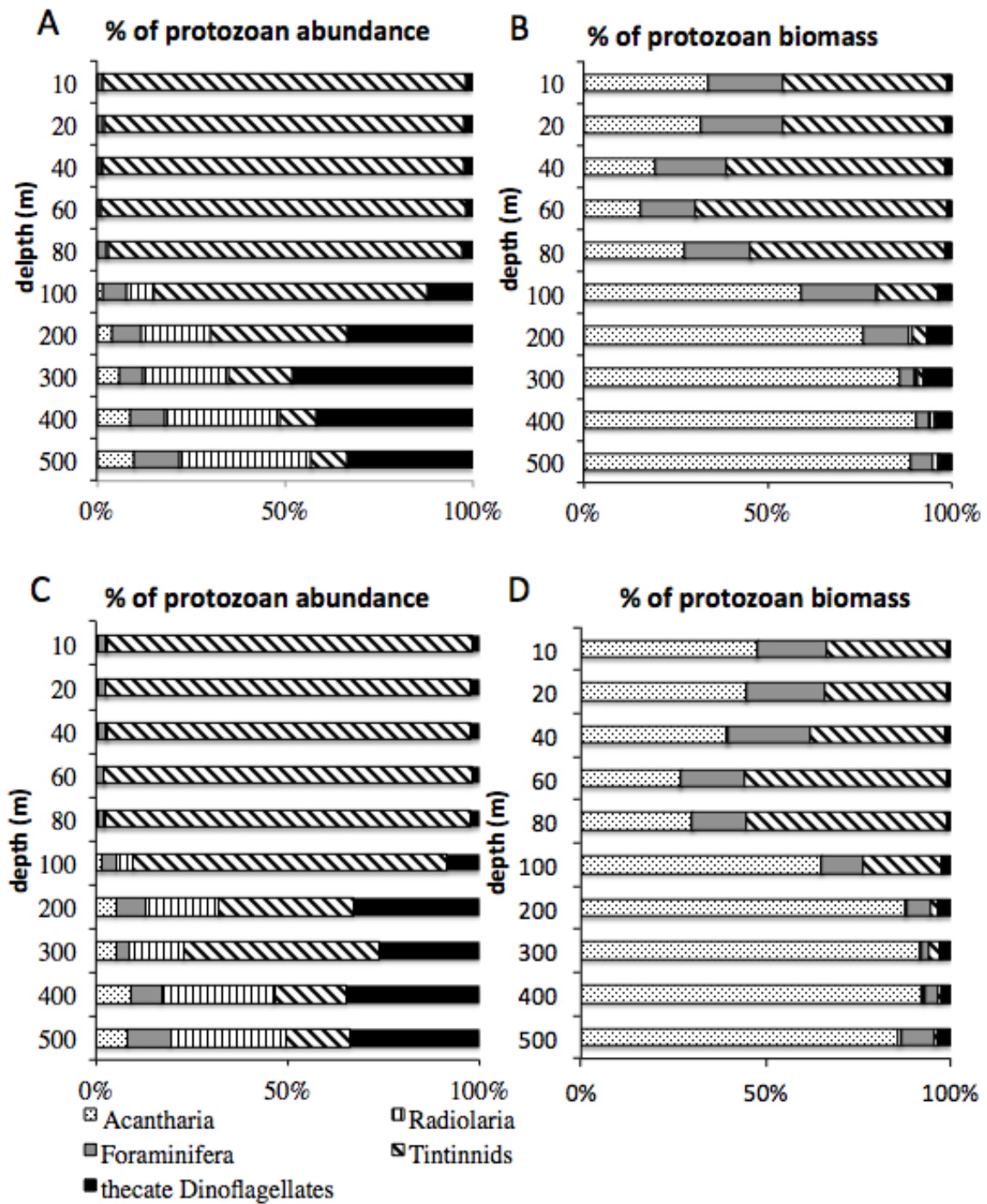


Figure 7: Protozoa community composition of abundance and biomass integrated over 500 m given in percentage, inside (A+B) and outside (C+D) the patch.

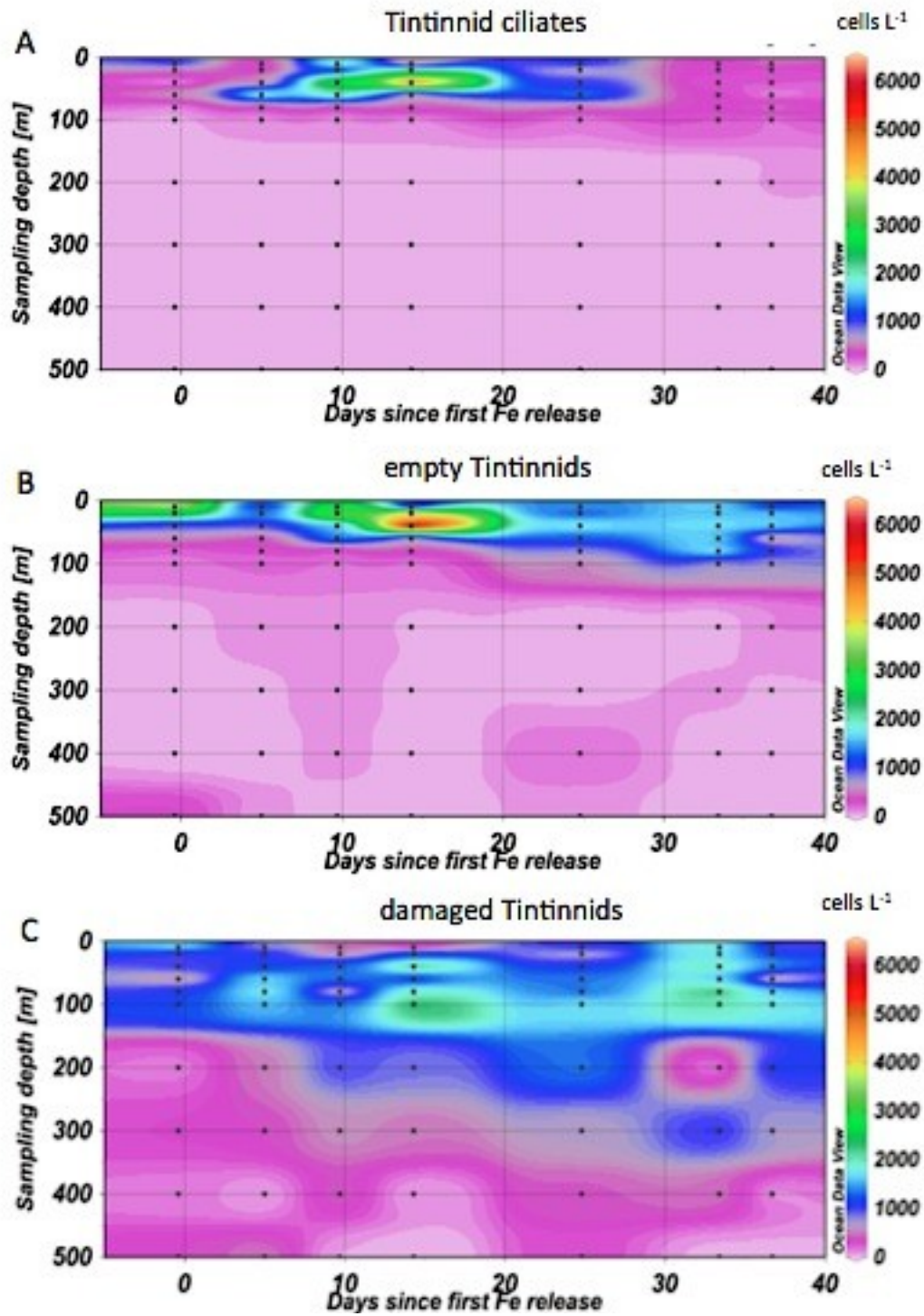


Figure 8: Vertical distribution of tintinnid ciliates (A), empty (B) and damaged tintinnids (C) inside the patch (cells L⁻¹).

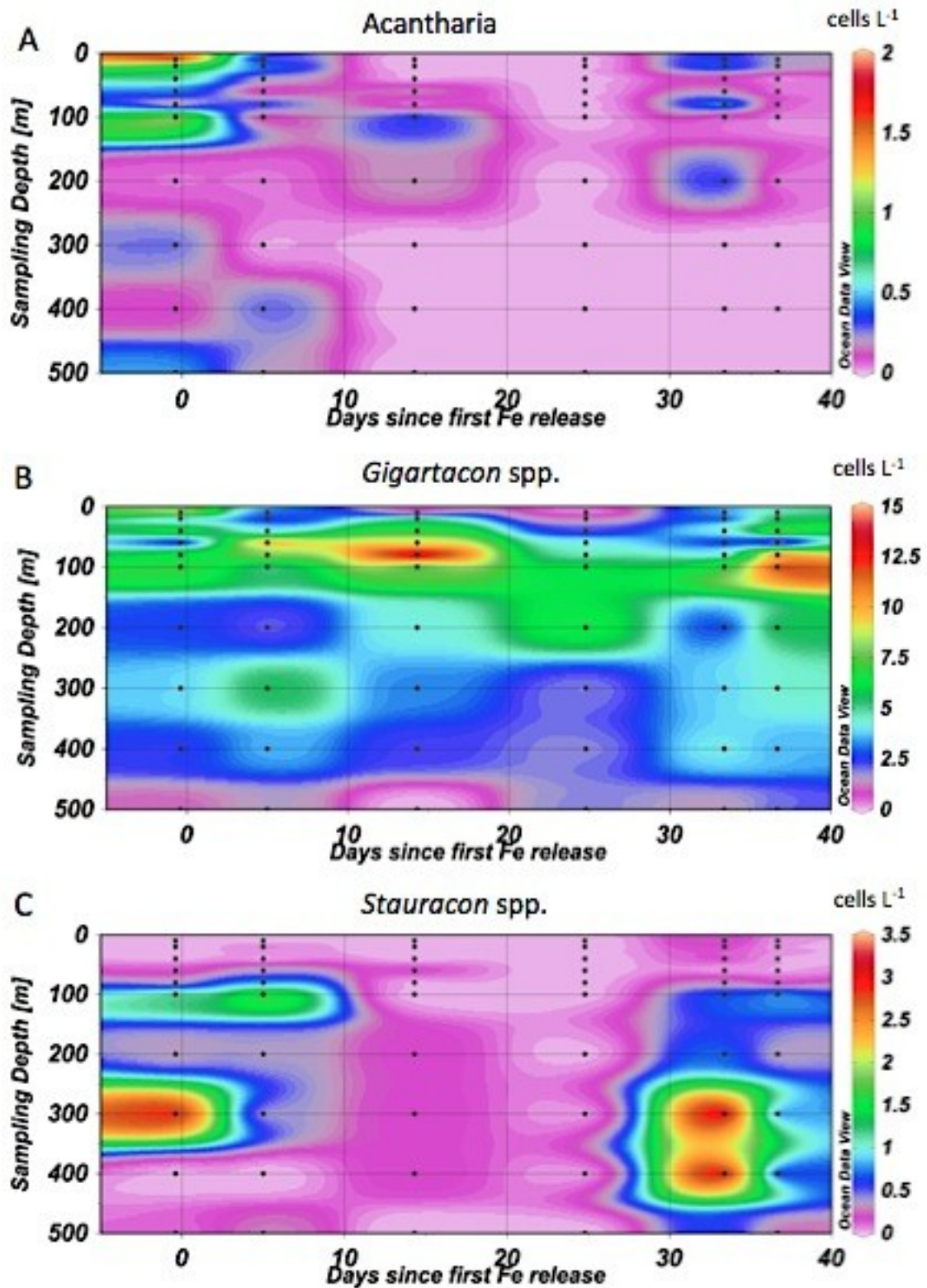


Figure 9: Vertical distribution of *Acantharia* (A), *Gigartacon* spp. (B) and *Stauracon* spp. (C) inside the patch (cells L⁻¹).

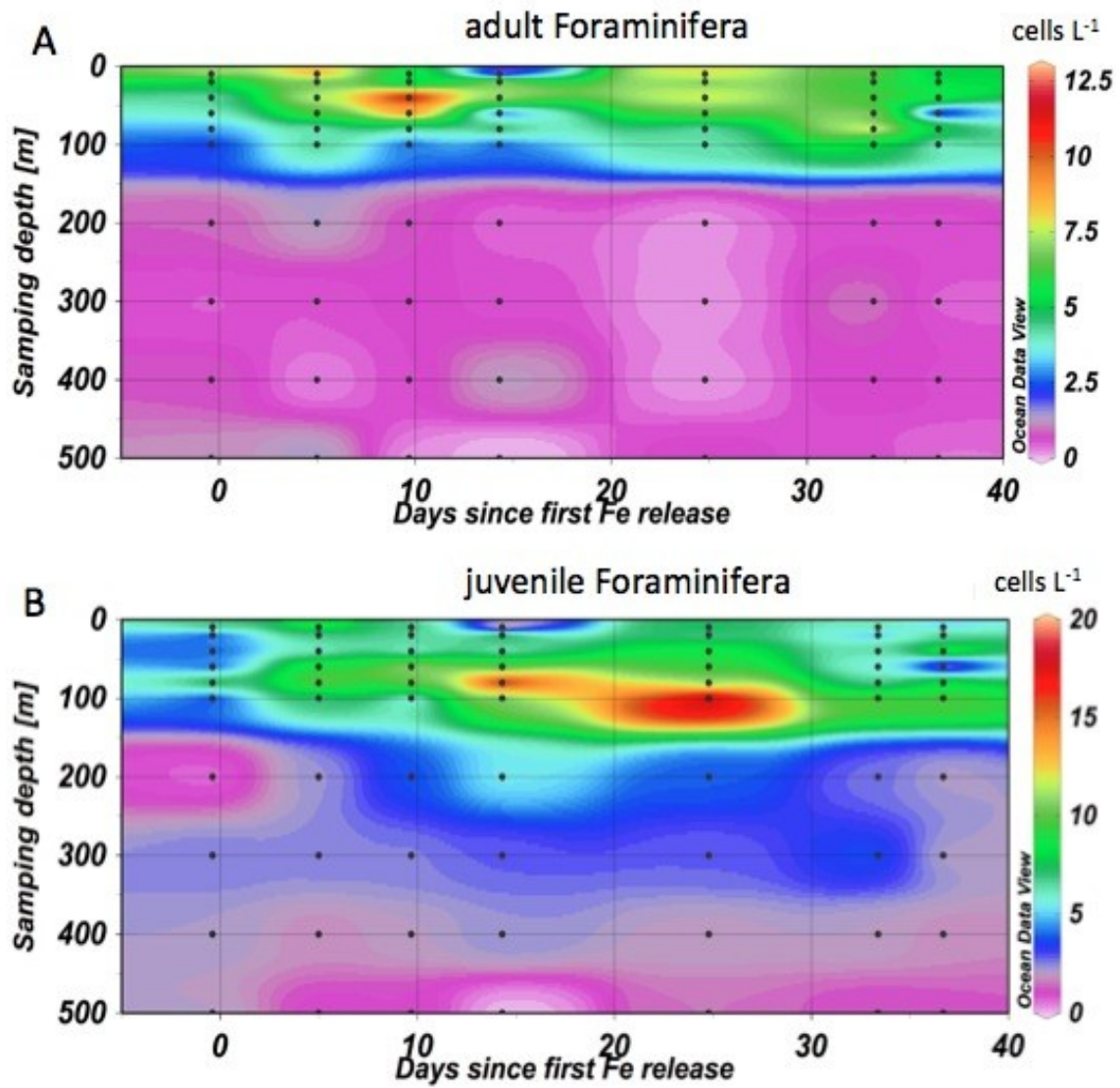


Figure 10: Vertical distribution of adult (A) and juvenile (B) foraminifera inside the patch (cells L⁻¹).

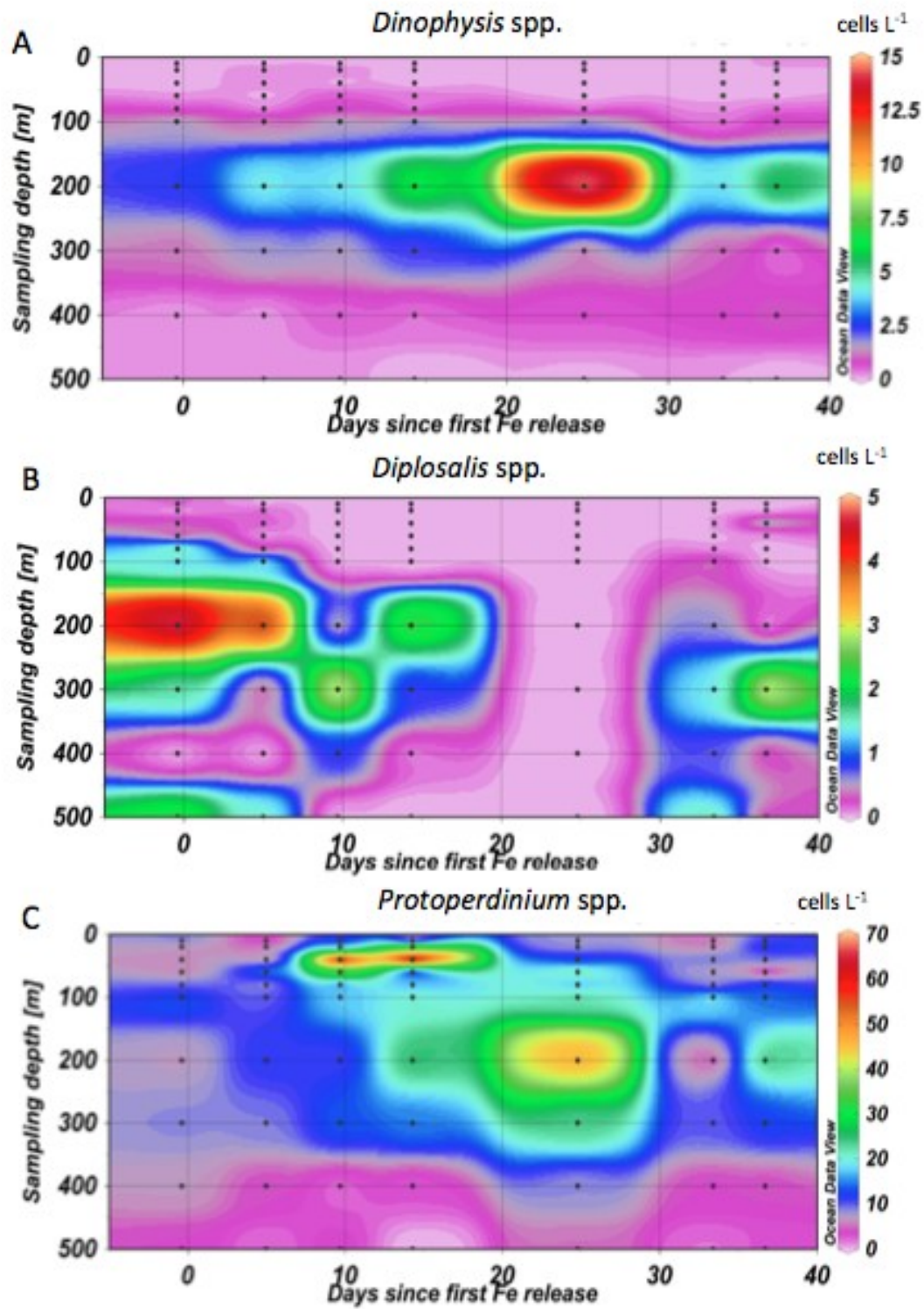


Figure 11: Vertical distribution of *Dinophysis* spp. (A), *Diplosalis* spp. (B) and *Protoperdinium* spp. (C) inside the patch (cells L⁻¹).

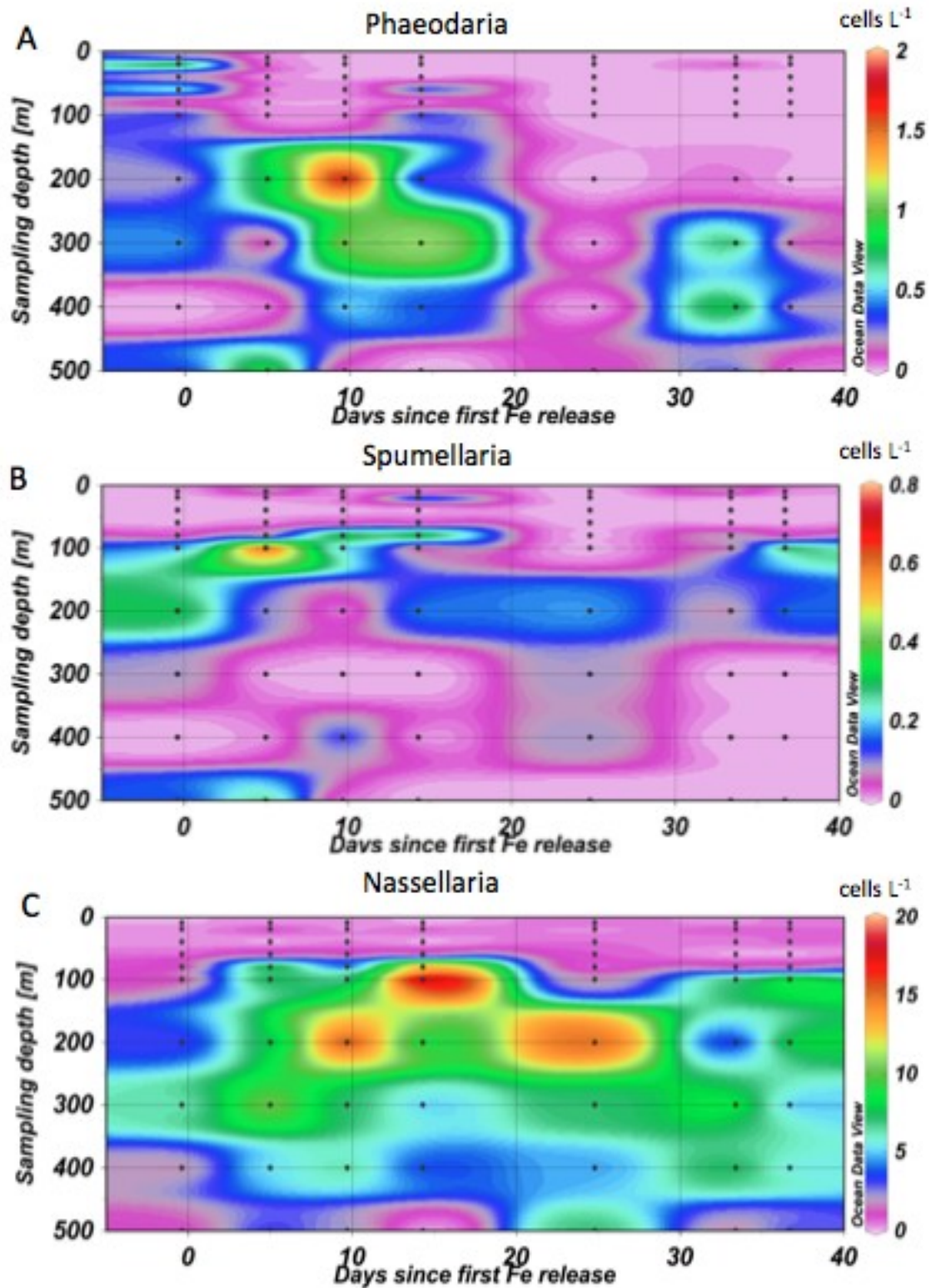


Figure 12: Vertical distribution of Phaeodaria (A), Spumellaria (B), and Nassellaria (C) and *Sticholonche zanlea* (D) inside the patch (cells L⁻¹).

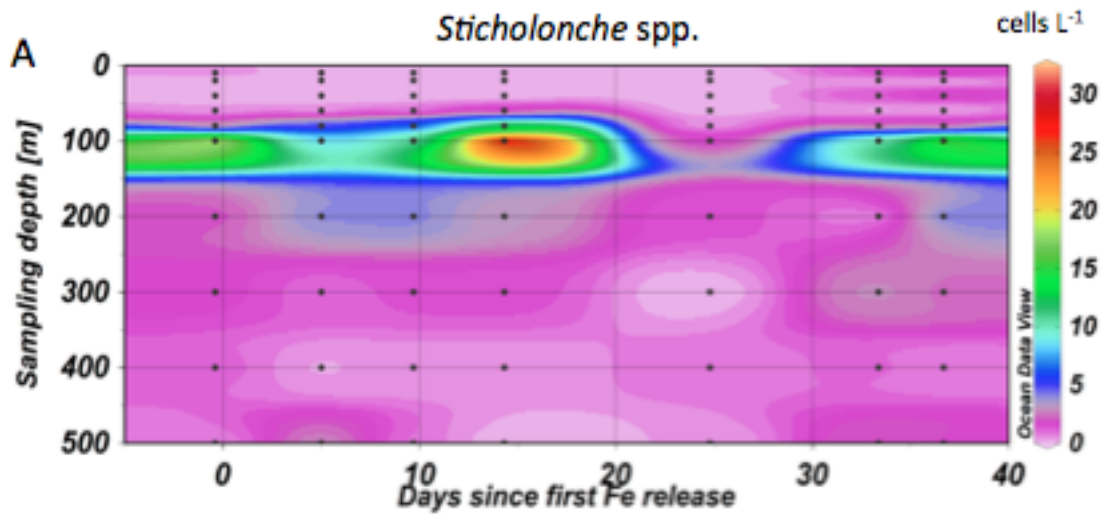


Figure 13: Vertical distribution *Sticholonche zancelea* (A) inside the patch (cells L⁻¹).

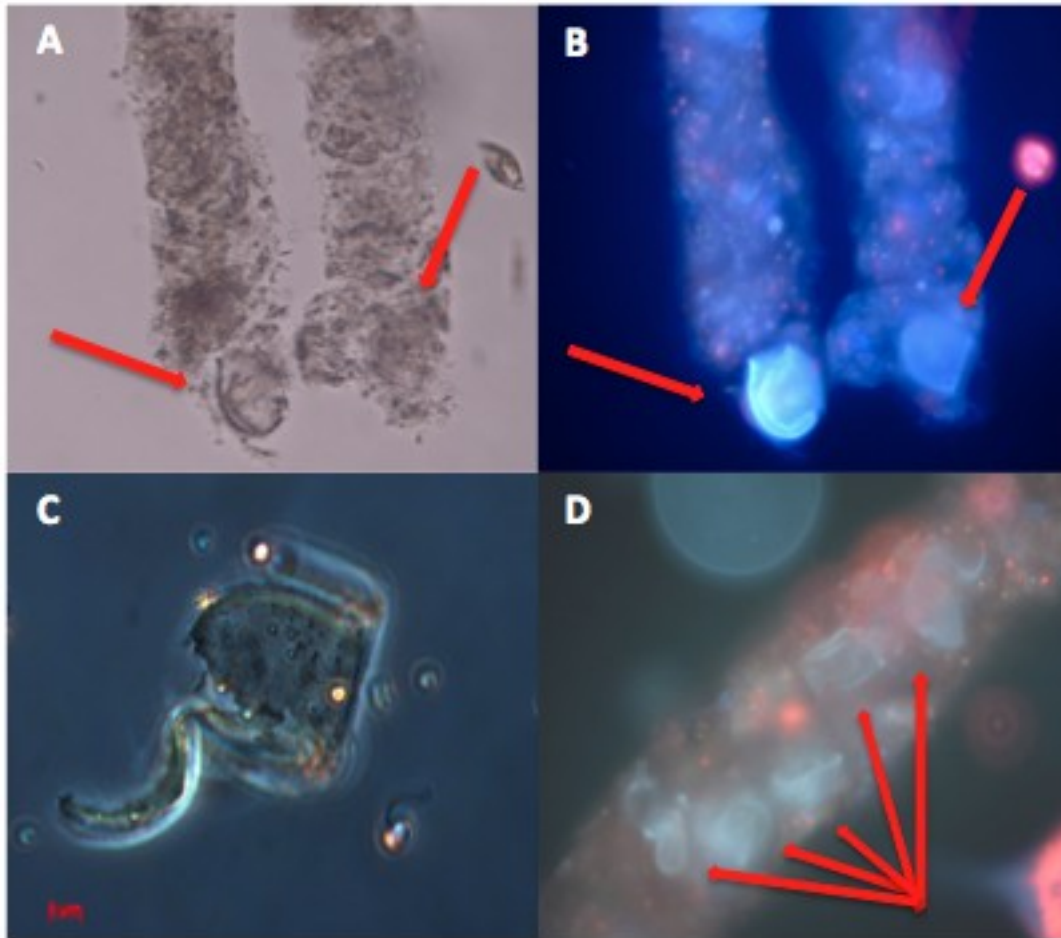


Figure 14: Light (A, C) and epifluorescence (B, D) micrographs showing tintinnid loricae inside the pellets (A, B, D; red arrows) and a damaged loricae (C).

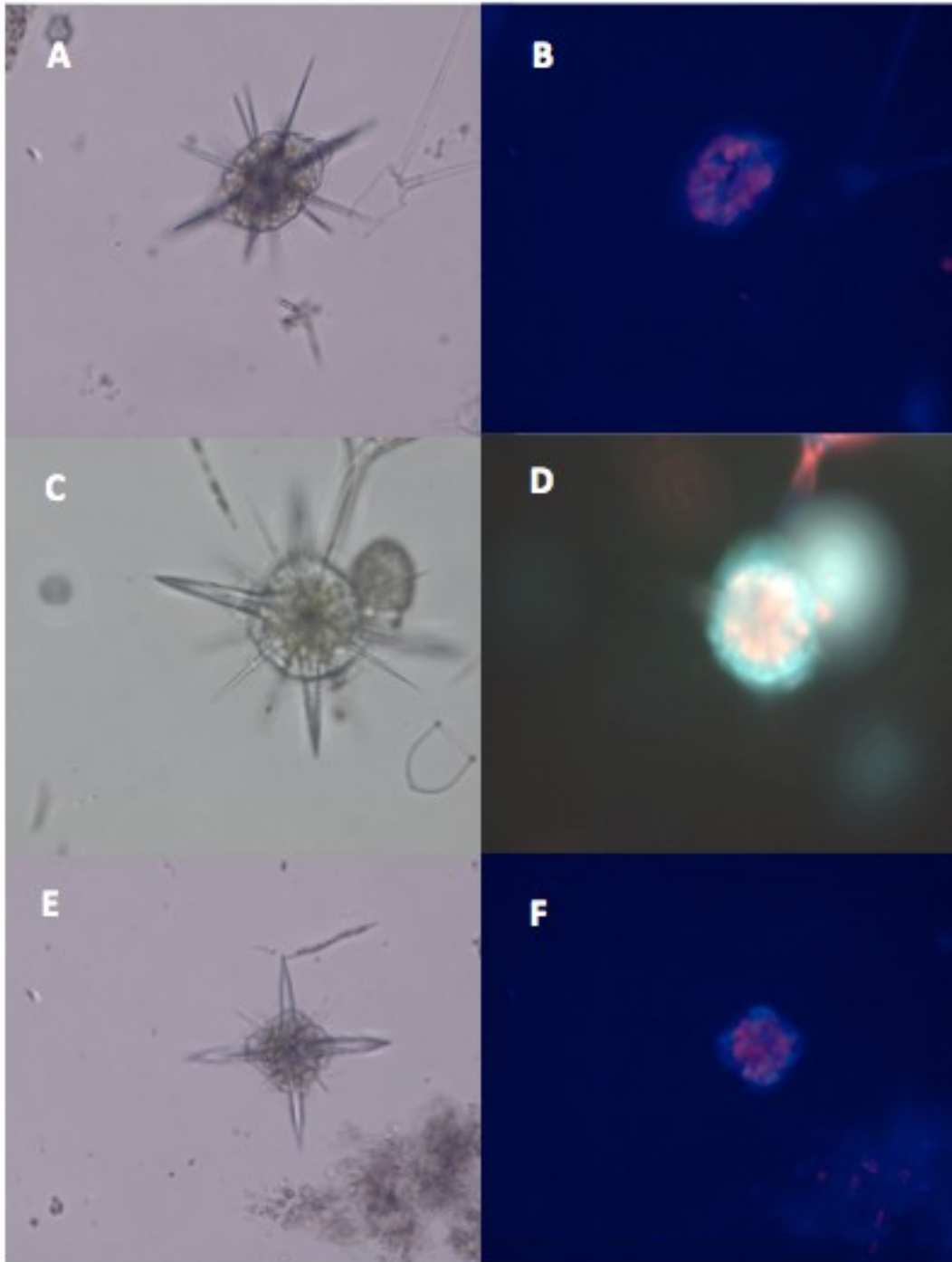


Figure 15: Each pair of images shows acantharia of the genus *Acanthostaurus sp* under light (A, C, E) and under epifluorescence microscopy (B, D, F) with autotrophic symbionts illuminated in red.

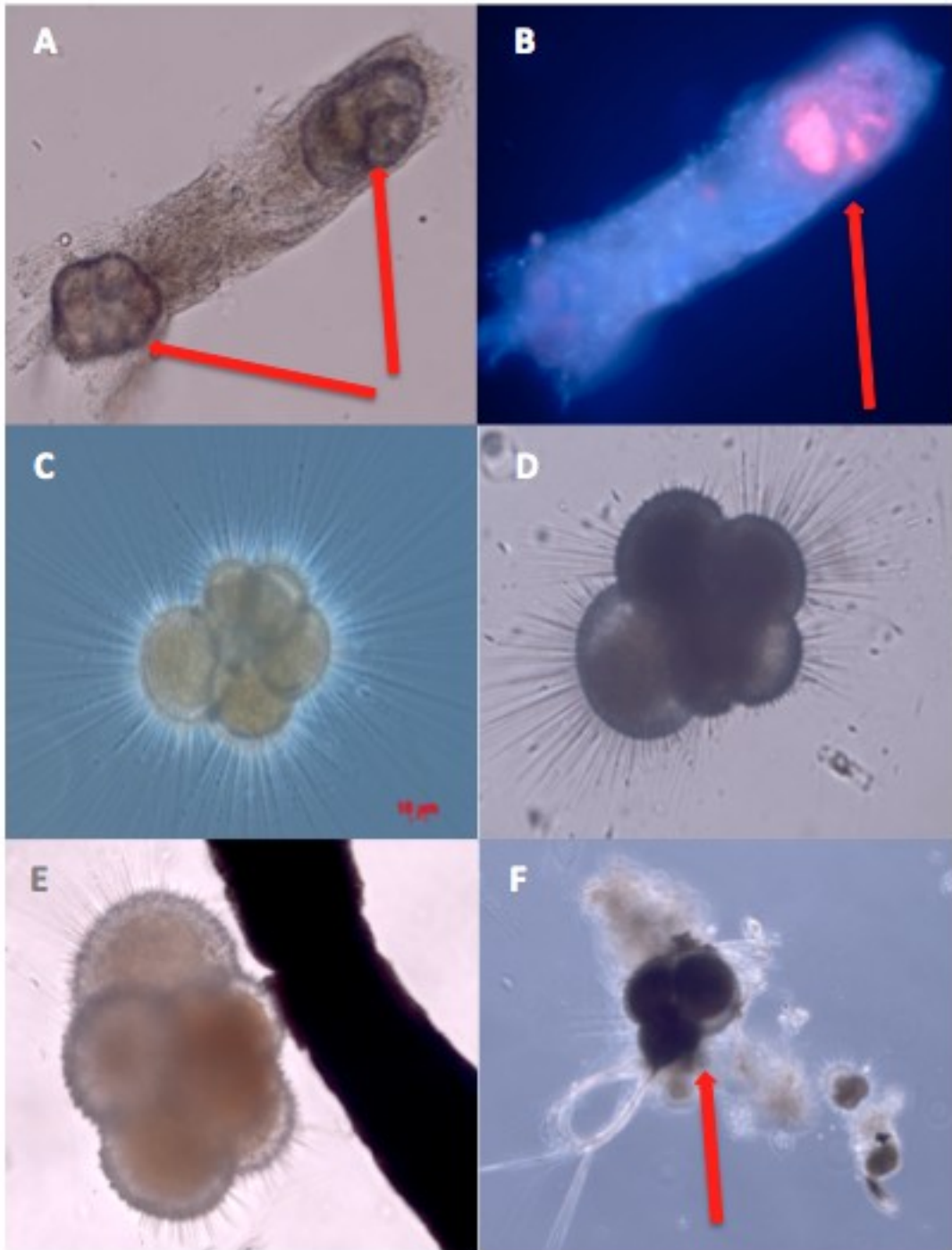


Figure 16: Pictures of foraminifera under light (A, C-F) and epifluorescence microscopy (B) showing foraminifera inside a copepod fecal pellet (red arrows, A, B, F); note autofluorescence of algal symbionts in picture B and pictures of individual foraminifera (*Turborotalita quinquiloba*) with intact spines (C) and spines bitten off (D-E).

Manuscript IV

**Copepod grazing during the LOHAFEX Experiment:
natural diets and impact on phytoplankton communities**

(preliminary title)

*Maria Grazia Mazzocchi^{1#}, Isabelle Schulz^{2,3}, Humberto González⁴, Ines
Borrione², Mangesh Gauns⁵, Marina Montresor¹, Diana Sarno¹*

in preparation

¹ Stazione Zoologica Anton Dohrn, Villa Comunale, 80121 Naples, Italy

² Alfred Wegener Institute Helmholtz Center for Polar and Marine Research, 27570
Bremerhaven, Germany

³ MARUM – Center for Marine Environmental Sciences, University of Bremen, Leobener
Str., 28359 Bremen

⁴ Institute of Marine and Limnological Sciences, Universidad Austral de Chile,
Independencia 641, Valdivia, Chile

⁵ National Institute of Oceanography, Dona Paula-Goa, 403 004 India

corresponding authors

contact: Stazione Zoologica Anton Dohrn, Villa Comunale, 80121 Naples, Italy

e-mail: grazia.mazzocchi@szn.it

Acknowledgements

We are indebted to the captain and crew of RV *Polarstern*. We thank the co-chief scientist S.W.A. Naqvi for making LOHAFEX a successful experiment. The Council of Scientific and Industrial Research (CSIR), India and the Helmholtz Foundation, Germany equally shared the costs of the experiment. This work was partly funded through DFG Research Center / Cluster of Excellence „The Ocean in the Earth System“.

Abstract

The results achieved so far in various chemical and biological compartments suggest that zooplankton was responsible of phytoplankton biomass retention in the epipelagic layer. Mesozooplankton were by far dominated by copepods, which were mostly represented by four species, the most important being the large *Calanus simillimus*, which dominated in biomass, and the small *Oithona similis*, which dominated in abundance; they were followed by *Ctenocalanus citer* and *Oithona atlantica*. The zooplankton communities did not change significantly in abundance with time and were not significantly different inside and outside the patch. Therefore, they did not seem to respond to the fertilization with their structural parameters but rather in terms of functional properties. Grazing experiments conducted on board with the food removal method showed that *C. simillimus* fed on natural particle assemblages had higher ingestion rates inside than outside the patch. This was confirmed by the grazing rates estimated by fecal pellet production, which was higher inside than outside the patch (Gonzalez et al., in preparation). From the microscopic examinations of fecal pellets onboard, we could estimate that copepod grazing was the most prominent cause of mortality for diatoms, large dinoflagellates and foraminifera.

1. Introduction

Trophic interactions are fundamental processes in the functioning of communities in all marine ecosystems. Grazing, i.e. the food intake by zooplankton, shapes the structure of the pelagic food webs, since zooplankters are the primary link between protists and secondary consumers in the water column (Banse, 1995). Zooplankton feeding and metabolic processes are major elements of biological pumps in the oceans. The high diversity of zooplankton in terms of size, groups and species characteristics and feeding behaviours, lead to a remarkably complexity of trophic interactions at sea. In marine zooplankton communities, copepods represent the numerically dominant component and their grazing activities have a considerable influence on the dynamics of phytoplankton assemblages and fate of particle flux in epipelagic waters.

The daily removal rates of phytoplankton by copepods can vary over a very wide range according to the species involved and the characteristics of the phytoplankton assemblages. In fact, copepods can discriminate between different food items on the basis of particle size and nutritional features (e.g., Poulet and Marsot, 1980). Moreover, the feeding strategies and prey intake can change in response to environmental variability (e.g., Kiørboe et al., 1996).

The bulk of phytoplankton biomass after blooms can either sink or be consumed and enter into microbial food webs (Bode and Varela, 1994). Copepods can substantially affect the fate of the blooms with their particle removal and production of fecal pellets that sink out of the layer, thus contributing to the vertical flux of particulate carbon and nitrogen in the water column.

The importance of copepods in the plankton food web and ecosystem dynamics in the Southern ocean has been widely established (e.g., Razouls et al., 2000), with a key role of the small-sized component (e.g., Dubiscar et al., 2002). During the LOHAFEX iron fertilization experiments in the Atlantic sector of the Southern Ocean, the mesozooplankton communities were characterized by a few copepod species, with the predominance of small representatives (*Oithona similis*, *O. atlantica*, *Ctenocalanus vanus*) in terms of abundance and of the large calanoid *Calanus simillimus* in terms of biomass (Mazzocchi et al., in preparation). We aimed at investigating the grazing activity of *C. simillimus* in different phases of the fertilization experiment to elucidate the role of primary consumers on the evolution of the bloom. The results shown in this thesis represent a still preliminary and partial view of this work still in progress.

2. Materials and Methods

2.1. Study site and tracking of the fertilized patch

LOHAFEX was carried out in the Atlantic sector of the Southern Ocean during RV Polarstern cruise ANT-XXV/3 (27 January to 6 March 2009). A stable cyclonic eddy, located at approximately 48° S 16°W and originating from the Polar Frontal Zone (PFZ), was chosen as the experimental site. The chosen eddy provided a coherent water mass over the course of the experiment, and the wind mixed layer (WML) depth varied between 50 and 80 m (Martin et al, 2013).

With 39 days, LOHAFEX was the longest Ocean Iron Fertilization experiment (OIF) experiment carried out so far. Two fertilization steps on day 1 and 18, each releasing 10t of dissolved iron (II) sulphate (FeSO_4), were applied to a 300 km² patch. The final iron concentration reached ~ 1.2 nmol L⁻¹.

Four different ways of tracking the patch were used: 1. Trajectories of GPS drifters, 2. Labeling with the inert tracer sulfurhexafluoride (SF_6) released together with the FeSO_4 solution, 3. Online measurements of photosynthetic efficiency (F_v/F_m), 4. Underway Chl *a* sampling and continuous pCO₂ measurements.

2.2 Zooplankton sampling and copepod acclimatization

Copepod grazing experiments were conducted in five occasions starting from the day before the fertilization (-0.6) until day 24.6 after the fertilization, which included four stations inside the patch and only one outside the patch (Table.1). The feeding performances were investigated in the large calanoid *Calanus simillimus* and the small cyclopoid *Oithona* spp. (dominated by *O. similis*), which were the most important zooplankters during LOHAFEX in terms of biomass and abundance, respectively (Fig. 1). However, since only two data points are available for *Oithona* spp., the results regarding these cyclopoids should be considered only indicative and need to be treated with caution.

At the selected stations, zooplankton samples were gently collected by slow vertical hauls in the upper 100 m water column with a WP2 net (60 cm mouth diameter, 200 µm mesh) equipped with a 10 L plastic bin as non-filtering cod-end to prevent damaging the organisms. The samples were diluted in 25 L coolers that had been previously half filled with water pumped from the surface and immediately transported in the laboratory. Within 5-10 min, dead animals and detritus that had sunk and accumulated at the bottom of the coolers were siphoned off.

The target copepod species were sorted by picking active individuals with a wide bore pipette from aliquots taken with large glass beakers from the original diluted samples. After a check under the dissecting microscope, only intact and healthy individuals were selected and transferred into 2130 ml glass jars with large-mouth screw-cup that had been filled with surface sea water containing natural particle assemblages. The jars were sealed with cling film under the screw-cup to prevent air bubble formation. The jars were placed, end over end, on a plankton wheel at 0.2 rotations per minutes (r.p.m) for the acclimatization period that lasted a few hours.

All procedures during the acclimatization and the experimental phases were conducted in a light and temperature controlled room. The photoperiod of 8 light: 16 dark hours was similar to the natural one and the temperature of 5.5 °C represented the depth-averaged value in the upper 100 m water column.

2.3 Grazing experiments

The natural plankton assemblages for grazing experiments were collected with a rosette sampler equipped with Niskin bottles and a CTD (conductivity, temperature, depth) (SeaBird Electronics, USA), at the depth of chlorophyll maximum (~20 m). The water was drained into a 50 L plastic bin by using a long large-mouth silicone tube to prevent bubble formation and cell damage. For each experiment, 2 L glass jars were filled in parallel by carefully pouring the water from the 50 L bin with a plastic carafe after gentle mixing and left to settle while a visual inspection allowed removing the few animals that were present. The experimental water was not pre-screened through gauze to remove extraneous metazoans in order to avoid cell damaging. Nutrients were not added to exclude altering of the natural assemblage. Start (2 replicates), controls without copepods (3 replicates), and experimental jars with copepods (2-4 replicates) were prepared (Fig. 2).

Copepods were transferred from the acclimatization jars to the experimental ones (2130 ml for *C. simillimus* and 1000 ml for *Oithona* spp.) by rapidly picking the individuals with a wide bore glass pipette. All the control and experimental jars were sealed with cling film, closed and placed end over end on the plankton wheel at 0.2 r.p.m. The experiments lasted for 24 hour and at the end copepods were recovered with a wide bore glass pipette and kept in small beakers for successive size and dry weight measurements.

2.4 Plankton cell counts and biomass estimation

To assess the change in abundance and composition of the plankton community during the experiments, subsamples were siphoned at the beginning from the start jars and at the end from the control and experimental jars, with a silicone tube after careful mixing. Two

subsamples of 200 ml and 100 ml were taken and fixed, respectively, with hexamethylenetetramine-buffered formaldehyde (2 %) and Lugol's iodine solution (2 %) for taxonomic identification and counts of phytoplankton and ciliates; they were kept in darkness (formaldehyde samples at 4° C) until they were analysed in the home laboratory.

Cells were identified and enumerated using inverted light and epifluorescence microscopy (Axiovert 200 and Axio Observer 1.0, Oberkochen, Germany) according to the method of Thronson (1995). To determine pico- and nanoplankton abundance and biomass, Lugol preserved water samples were settled in 25 mL sedimentation chambers (Hydrobios, Kiel, Germany) for 24 hours. Due to the lack of distinctive morphological features, size differentiation was the main classification tool for most flagellates and coccoid cells. Flagellates have been classified in two size categories: < 10 µm, > 10 µm and coccoid cells in the size category < 10 µm. The prymnesiophyte *Phaeocystis antarctica* has been classified in the size categories 2-4 µm and 4-6 µm.

For estimating the species composition and abundance of microplankton, samples were settled in 50 ml sedimentation chambers for 48 hours. Diatoms, dinoflagellates, other flagellates, ciliates and tintinnids were identified at species or genus level and counted according to their abundance in fields of view, in transects, in half or the whole chamber. Broken and empty tintinnids were also counted but not considered for calculating the grazing rates. According to the size of the organisms examined, they were counted at magnifications of 320-640x. Starting from the detailed taxonomic counts, phytoplankton and ciliate taxa were grouped in food categories mainly established on the basis of size (Table 2). Abundances of pico, nano and microplankton were calculated in cells mL⁻¹.

Length and width measurements from at least 4-20 randomly selected cells of each species/category were measured and cell volume calculated from equivalent geometrical shapes (Hillebrand et al., 1999). To convert cell volume (V) into cellular carbon content (C) the C:V relationships for the specific groups were used (Table 3) (Menden-Deuer and Lessard, 2000).

2.5 Copepod biomass and grazing rates

Copepods recovered from the experiments were examined and sized under the dissecting microscope, checked for their conditions and the presence of gut content. The copepod biomass was measured from conspecific individuals sorted from the same zooplankton sample. A variable number of individuals depending on species size were pooled on a slide and the interstitial water was removed with a thin Pasteur pipette. The animal pellet was transferred in a tin capsule (10x10 mm) and dried in the oven at 60 °C for 24 hours.

Thereafter, each capsule was closed and sealed in a vial and stored. In the lab in the home laboratory, the tin capsule was again placed in the oven at 60 °C for 24 hours; the copepod pellet was then carefully removed, weighted on a microbalance for measuring the dry mass, and successively analyzed at a Carbon-Hydrogen-Nitrogen- (CHN) analyzer (Thermo CHN Flash EA112).

Copepod daily grazing rates (F, clearance, ml ind.⁻¹ d⁻¹; I, ingestion, cells ind.⁻¹ d⁻¹) were calculated for each food category according to the Frost's equations (Frost, 1972). Negative clearance rates were considered as zero feeding. The individual ingestion rates were calculated by multiplying the positive clearance rates of a given food category with its average cell concentration <C> in each experimental jar during the incubation time. The ingestion rates in terms of carbon were calculated by multiplying the daily ingestion rates on each food item by its estimated cell carbon content. The total ingestion for each replicate jar was calculated as the sum of all ingestion rates.

The trophic cascade effect due to the grazing of microzooplankton (Nejstgaard et al., 2001) has not been considered in the present work and probably led to an underestimation of the copepod grazing rates on prey also grazed by ciliates and heterotrophic dinoflagellates.

The impact exerted by *C. simillimus* and *Oithona* spp. on phytoplankton and ciliates in the upper 100 m water column was determined by multiplying the individual ingestion rates by the copepod depth- integrated abundance, assuming the same ingestion rates for all components of the respective populations (females, males and juveniles).

3. Results

3.1 Initial conditions

The natural particle assemblages available as potential food offered to copepods at the beginning of the experiments presented small differences among stations in terms of concentration (6445.9-7460.5 cells ml⁻¹; 280.1 - 426.3 ng C ml⁻¹) (Fig. 3).

In terms of cell composition, the potential food was mostly represented by flagellates (61.2-69.6 %) and *Phaeocystis antarctica* (solitary cells) (26.2-31.9 %). In terms of carbon concentration, a major contribution was due to athecate dinoflagellates and flagellates, followed by thecate dinoflagellate, aloricate ciliates, *Phaeocystis antarctica* and tintinnid ciliates. Diatoms and the coccolitophore *Emiliana huxleyi* accounted for negligible percentages to the total carbon available to copepods (0.6-1.9 %) (Fig. 4).

3.2 Grazing rates

Before fertilization, *C. simillimus* cleared total particle assemblage at a rate of 55.2 ml ind.⁻¹ h⁻¹. Thereafter, inside the patch the clearance rate halved to 20.7 ml ind.⁻¹ h⁻¹ on day 9.5 but increased to 72.9 ml ind.⁻¹ h⁻¹ on day 24.6. The clearance rate outside the patch was 25.0 ml ind.⁻¹ h⁻¹. The clearance rate of *Oithona* spp. decreased almost three fold from day -0.6 to day 9.5 within the patch (Table 4). The daily carbon ingestion rates of *C. simillimus* showed a similar decreasing pattern as the clearance rates, from 11.3 µg C ind.⁻¹ d⁻¹ before fertilization to about 3-4 µg C ind.⁻¹ d⁻¹ both inside and outside of the patch. A peak was reached on day 24.6 with 21.8 µg C ind.⁻¹ d⁻¹. *Oithona* spp. ingested three times more carbon before fertilization (4.2 µg C ind.⁻¹ d⁻¹) than 4.6 days after (1.5 µg C ind.⁻¹ d⁻¹) (Fig. 5).

The comparison of natural diets between the two copepod species showed that, on average, the carbon ingested by *C. simillimus* was mainly represented by athecate dinoflagellates, followed by thecate dinoflagellates, flagellates and naked ciliates (Table 5A), while *Oithona* spp. ingested prevalently athecate dinoflagellates and flagellates (Table 5 B). However, the copepod diet changed with time inside the patch and differed from the unfertilized patch, as indicated by the relative contribution of the prey categories to the total carbon ingested (Fig. 6). The day before fertilization *C. simillimus* ingested prevalently athecate dinoflagellates (70 %), and a lower amount of flagellates (11 %) and thecate dinoflagellates (9 %) (Fig. 6 A). Within the fertilized patch, the calanoid fed mostly on flagellates (52 %) and aloricate ciliates (31 %) and partly on thecate dinoflagellates (10 %) (Fig. 6 B). The contribution of the latter group increased almost four fold (39 %) on day 9.5, while aloricate ciliates almost disappeared (0.04 %) and were replaced by tintinnid ciliates (13 %) (Fig. 6 C). On day 24.6

inside the patch, athecate dinoflagellates prevailed again (39 %) as before fertilization but the diet was overall more diversified (Fig.6 D). Conversely, the carbon ingested by *C. simillimus* outside the patch was mainly represented by thecate dinoflagellates (67 %), followed by athecate dinoflagellates (20 %) and flagellates (10 %) (Fig. 6 E).

Before fertilization, *Oithona* spp. acquired most of the carbon from athecate dinoflagellates (61 %), and a lower percentage from flagellates (19 %) and thecate dinoflagellates (8 %) (Fig. 7 A). On day 9.5, the diet of these copepods changed and it was composed mainly by flagellates (62%), tintinnids (19%), *Phaeocystis antarctica* (13 %) and athecate dinoflagellates (5 %) (Fig. 7 B).

C. simillimus ingested more carbon from the largest (> 15 μm) than the small items within each of the non-diatom prey categories considered in the present study (Fig. 8 A-F). Small dinoflagellates, flagellates and aloricate ciliates (< 10 μm), coccoid cells (< 5 μm), and solitary *P. antarctica* (< 6 μm), when present in the diet, did contribute with negligible amount to the carbon ingested, while tintinnids < 15 μm did not even appear in the diet (Fig. 8 A-F). Larger cell categories also accounted for most of the carbon ingested by *Oithona* spp. when fed on non-diatoms categories (Fig. 9 A-F). However, small flagellates < 10 μm also contributed to the diet of these small cycloids (Fig. 9 E). The amount of carbon acquired from diatoms was very low for both copepod species and mainly due to large species such as *Corethron pennatum* (40 μm), *Ephemera* sp. (50-60 μm), *Pseudo-nitzschia turgidula* (30-40 μm), and *Thalassionema* (~ 30 μm) (Fig. 10 A,B). The diet of *C. simillimus* included also small *Thalassiosira* < 15 μm (Fig. 10 A).

3.3 Grazing impact

The populations of *Calanus simillimus* and *Oithona* spp. accounted, altogether, from 67.0 % (on day 9.5) to 94.8 % (on day 24.6) of total copepod abundance in the upper 100 m water column at the stations where the grazing experiments were conducted (Fig. 11). Both species showed higher abundances during night than day hours, with the exception of *Oithona* spp. on day 24.6 inside the fertilized patch (Fig. 11). The small cyclopid species prevailed over the large calanoid in terms of abundance (Fig. 11) but the opposite occurred in terms of biomass (Fig. 12).

The grazing impact exerted by *C. simillimus* and *Oithona* spp. populations in the upper 100 m water column was highest before fertilization and decreased thereafter (Fig. 13). The amount of total carbon ingested by *C. simillimus* inside the patch, decreased from 141 to 67 $\text{mg C m}^{-2} \text{d}^{-1}$ from day 4.6 to day 9.5 after Fe release and increased to 218 on day 24. The grazing impact differed among different food categories and varied in time (Fig. 14). The

impact exerted by *C. simillimus* on athecate dinoflagellates was remarkable only before the Fe release and on day 24.6, that on thecate dinoflagellates was more frequent and less variable, while it was negligible on diatoms (Fig. 14 A). Before fertilization, the population of *Oithona* spp. removed the food categories in similar proportions as that of *C. simillimus* (Fig. 14 B).

4. Discussion

During the LOHAFEX experiment, the mesozooplankton community in the epipelagic layer (0-200 m) did not show large variability in abundance around a general mean of $\sim 150 \times 10^3$ Ind. m^{-2} in the top 200 m water column (Mazzocchi et al., in preparation). A peak in abundance (359×10^3 Ind. m^{-2}) occurred 18 days after the first Fe release, while a low (27×10^3 Ind. m^{-2}) occurred at day 39. No significant differences appeared between inside and outside the fertilized patch, with slightly higher variability within the fertilized area likely due to highly patchy distribution. The structure of mesozooplankton community was very simple, dominated by four copepod species, the calanoids *Calanus simillimus* and *Ctenocalanus citer*, and the cyclopoids *Oithona similis* and *O. atlantica*, each of them with different patterns in temporal and vertical distribution (Mazzocchi et al., in preparation). *C. simillimus*, consisting almost entirely of late juvenile stages (CIV and CV copepodites), dominated mesozooplankton in terms of biomass, while the tiny *O. similis* dominated in numbers (Mazzocchi et al., 2009) These two copepods, reported as key species in the region also by other studies, were chosen as target consumers to evaluate the role of grazers on plankton assemblages during LOHAFEX. Abundant representatives of large (~ 3 mm) and small (≤ 1 mm) grazers were expected to feed on different food items and have different impact on the qualitative composition of the bloom.

A major conclusion from preliminary LOHAFEX analyses conducted on board was that, despite high growth rates, biomass of non-diatom phytoplankton was kept in check by grazing pressure of copepods (Mazzocchi et al., 2009). This was suggested by the rates of faecal pellet production (expressed as volume of faecal pellets egested by incubated copepods), which were double inside as compared outside the fertilized patch (Mazzocchi et al., 2009) and indicated a similar spatial disparity in the derived estimates of grazing rates (González et al., in preparation). A more intense copepod feeding activity inside than outside the patch did not, however, appear from the results of grazing experiments presented here.

The direct investigation of feeding performances of dominant copepods species during LOHAFEX was addressed with a limited number of experiments that cannot alone explain exhaustively the trophic role of grazers inside and outside the fertilized patch. In particular, the feeding responses outside the patch were examined only at a single site and only for *C. simillimus*. The results presented here must be therefore taken with caution and must be necessarily further and deeper analysed in conjunction with other quantitative and qualitative aspects of zoo- and phytoplankton communities (Mazzocchi et al., in preparation). Before presenting a few preliminary points for discussion, we will comment on some methodological limits.

Among the numerous methods applied to investigate feeding in zooplankton, the food removal method is the one longest in use to estimate grazing under conditions that mimic the natural environment as closely as possible. Potential limitations of this method include the stress of capture and volume constraint, crowding of grazers and multiple trophic interactions within the prey assemblages. Despite these problems and the laborious analysis involved, this is the only method currently available that allows direct quantification of natural diets and feeding rates in mixed plankton assemblages including non-phytoplankton cells (Båmstedt et al., 2000). The “trophic cascade” effects due to the growth and feeding of micrograzers in the community (Nejstgaard et al., 2001) has not been evaluated in the present study and it will be considered successively when the results of the dilution experiments will be available (C. Klaas, S. Patil et al., unpublished data).

The present results highlight a large variability in the feeding rates and in the composition of natural diets for both *Calanus simillimus* and *Oithona* spp. at different times since the first Fe release, despite the low variability in the initial food conditions. Feeding of microzooplankton in the unscreened particle assemblages might have been a possible source of the large variability observed among experiments in the present study. Another possible source might have been the high and variable number of copepods incubated in the bottles, which was up to 8- or 15-fold the highest abundance of *Oithona* spp. and *C. simillimus*, respectively, in our field samples. Our present results should be considered

C. simillimus was actively feeding during the entire period, though with different intensity, and this also appeared as visible gut content in specimens counted for abundance in fixed samples collected with a multinet sampler (Mazzocchi et al., in preparation). In the abundant last developmental stages (CV, CIV), which dominated by far the population of this species, large oil drops were also visible, suggesting that food was presumably being converted into lipid reserves before entering diapause for likely overwintering. *C. simillimus* is reported among epipelagic copepods in the Southern Ocean that have a predominantly omnivorous /

detritivorous diet, an extended period of feeding, growth and reproduction and less reliance on diapause at depth in comparison with other large calanoids (Atkinson, 1998). This species was the dominant copepod in the > 2 mm size class during another iron fertilization experiments (EisenEx) conducted in the Atlantic Sector of the Southern Ocean during the austral spring of year 2000, where it occurred with similar abundances (Schultze et al., 2006) as recorded during LOHAFEX. The diet of *C. simillimus* during LOHAFEX differed remarkably from what observed during EisenEx, when this species fed predominantly on diatoms (Schultes et al., 2006). The amount of carbon ingested by *C. simillimus* during Lohafex inside and outside the patch was in the range of what measured during EisenEx (Schultes et al., 2006). However, during LOHAFEX *C. simillimus* did not seem to respond to the iron fertilization by enhancing its feeding activity, while during EisenEx the ingestion rates were double inside ($5.0 \mu\text{g C ind.}^{-1} \text{d}^{-1}$) than outside ($2.7 \mu\text{g C ind.}^{-1} \text{d}^{-1}$) the fertilized patch (Schultes et al., 2006). The occurrence of high temporal and spatial variability in food acquisition even within the same species does emerge from numerous studies on copepod feeding and may indicate the ample plasticity of copepods in responding to different environmental conditions, both in terms of food quantity and quality.

Oithona spp., which are reported as abundant component of the copepod assemblages in the Southern Ocean (Atkinson, 1998 and references therein) and major grazers (e.g. Atkinson, 1995), had much higher individual clearance rates during LOHAFEX than in other areas of the Southern Ocean and other seasons (e.g., 5-7 ml copepod⁻¹ day⁻¹, Atkinson 1995). Our results, though based on a limited dataset, suggest that these small cyclopoids played an important functional role in the trophic webs during LOHAFEX, which was further enhanced by their high abundance. *Oithona* is reported to feed preferentially on small nano- or dinoflagellates and ciliates (Atkinson, 1996) or faecal materials (González and Smetacek, 1994) and not on large diatoms. During our study, small flagellates (< 10 μm) contributed to the diet of *Oithona* spp.; however, larger cells in non-diatom food categories accounted for most of the carbon ingested by these cyclopoids, which ingested also large diatoms though in small quantities. It is most likely that, in the mixed assemblages used in our experiments, the larger *O. atlantica* (~ 1-1.2 mm total length) had easier access to these larger food items than the co-occurring small *O. similis* (~ 0.7 mm).

Albeit our results are based on a limited dataset, a comparison between the two investigated copepod species can be attempted. The daily carbon ingested by *C. simillimus* doubled that of *Oithona* spp. and this quantitative difference remain consistent in the two parallel experiments. Before fertilization, the two species acquired most of the carbon from the same food categories and in similar proportion. However, their food items differed on day 9.5

after the Fe release because in the diet of *Oithona* spp. appeared *Phaeocystis antarctica* and disappeared the thecate dinoflagellates, differently from *C. simillimus*.

The impact of copepod grazing on the plankton assemblages in terms of carbon removed by the consumers changed in space and time as a combined effect of two components, i.e., the abundance of grazers and their feeding performances. The amount of total carbon ingested by *C. simillimus* in the top 100 m water column showed a progressive decreasing pattern inside the patch from day -0.6 to day 9.5 and a threefold increase on day 24.6. This increase was due to an increase in feeding activity and not in copepod abundance, which had halved in about two weeks. Conversely, the lowest impact of *C. simillimus* impact on plankton assemblages outside the patch was mainly due to low population abundance because the ingestion rates had not changed from the previous days and sites within the patch.

Overall, the intense feeding of dominant copepod species on plankton assemblages (present study) and the abundant occurrence of faecal pellets in the upper layers (Morten, personal communication) should have resulted in high turnover of material within the top 100 m layer and in low vertical flux. This seems to be confirmed by the low sedimentation rates out of the surface layer as measured by the sedimentation traps (Martin et al., 2013). It was observed in fresh samples on board that copepod faecal pellets contained cells still viable and able to grow once the peritrophic membrane was disrupted (Montesor and Assmy, personal communication), so that faecal pellets likely represented hot spots of biological activity and sources of recycled and new production in the upper layer. *Oithona* spp. have been suggested to contribute to the retention of faecal material in the upper layer with their coprophagous feeding behaviour (González and Smetacek, 1994). Results from mesocosms experiments have shown a retarded vertical flux of carbon in presence of abundant *Oithona* spp. (Svensen and Nejstgaard, 2003), and a similar process might have been occurred in the surface layer during the LOHAFEX experiment. However, the regulative role of these small cyclopoids in the vertical flux of biogenic matter remains controversial, as suggested by Reigstad et al. (2005) who proposed that *Oithona* spp. may be indicator species of a “retention ecosystem”, but they are probably not the single factor explaining pellet recycling.

References

- Atkinson, A., 1995, Omnivory and feeding selectivity in five copepod species during spring in the Bellingshausen Sea, Antarctica: ICES Journal of Marine Science, v. 52, no. 3-4, p. 385-396.
- , 1998, Life cycle strategies of epipelagic copepods in the Southern Ocean: Journal of Marine Systems, v. 15, no. 1-4, p. 289-311.
- Båmstedt, U., Gifford, D. J., Irigoien, X., Atkinson, A., and Roman, M., 2000, Feeding.: In: Harris, R.P., Wiebe, P.H., Lenz, J., Skjoldal, H.R., Huntley, M. (Eds), ICES Zooplankton Methodology Manual, v. Academic Press, p. 297-399.
- Banse, K., 1995, Zooplankton: Pivotal role in the control of ocean production: ICES Journal of Marine Science, v. 52, no. 3-4, p. 265-277.
- Bode, A., and M. Varela 1994, Plankton carbon and nitrogen budgets for the N-NW Spanish shelf: The role of pelagic nutrient regeneration during upwelling events: Scientia Marina, v. 58, p. 221-231.
- Dubischar, C. D., Lopes, R. M., and Bathmann, U. V., 2002, High summer abundances of small pelagic copepods at the Antarctic Polar Front--implications for ecosystem dynamics: Deep Sea Research Part II: Topical Studies in Oceanography, v. 49, no. 18, p. 3871-3887.
- Frost, B. W., 1972, Effects of size and concentration of food particles on the feeding behaviour of the marine planktonic copepods *Calanus pacificus*: Limnology and Oceanography, v. 17, no. 6, p. 805-815.
- González H.E., Mazzocchi M.G., Giesecke R., Borrione I., Mahadik G., Martin P., V., andromme P., Ribera d'Alcalà M., Assmy, P., Iversen M., Naqvi W., and V, S., IN PREPARATION, In situ evidence of zooplankton control on phytoplankton growth and carbon export during the iron fertilization experiment LOHAFEX in SW Atlantic Ocean.
- Gonzalez, H. E., and Smetacek, V., 1994, The possible role of the cyclopoid copepod *Oithona* in retarding vertical flux of zooplankton faecal material: Marine ecology progress series., v. 113, no. 3, p. 233-246.
- Hillebrand, H., Duerselen, C. D., Kirschtel, D., Pollingher, U., and Zohary, T., 1999, Biovolume calculation for pelagic and benthic microalgae: Journal of Phycology [J. Phycol.]. v. 35, no. 2, p. 403-424.
- Kioerboe, T., Saiz, E., and Viitasalo, M., 1996, Prey switching behaviour in the planktonic copepod *Acartia tonsa*: Mar. Ecol. Progr. Ser., v. 143, p. 65-75.
- Martin, P., Rutgers van der Loeff, M., Cassar, N., Vandromme, P., d'Ovidio, F., Stemmann, L., Rengarajan, R., Soares, M., González, H. E., Ebersbach, F., Lampitt, R. S., Sanders, R., Barnett, B. A., Smetacek, S., and Naqvi, S. W. A., 2013, Iron fertilization enhanced net community production but not downward particle flux during the Southern Ocean iron fertilization experiment LOHAFEX: Global Biogeochemical Cycles, v. 27.
- Mazzocchi, G. M., González, H. E., Vandromme, P., Borrione, I., Ribera d'Alcala, M., Gauns, M., Assmy, P., Fuchs, B. M., Klaas, C., Martin, P., Montresor, M., Ramaiah, N., Naqvi, S. W. A., and Smetacek, V., 2009, A non-diatom plankton bloom controlled by copepod grazing and amphipod predation: Preliminary results from the LOHAFEX iron-fertilisation experiment: GLOBEC International Newsletter, v. 15, no. 2, p. 3-6.
- Mazzocchi, M. G., González, H. E., Mahadick, G., Schulz, I. K., Vandromme, P., Borrione, I., Gauns, M., Ribera d'Alcalà, M., N., W., , and Smetacek, V., IN PREPARATION, Mesozooplankton communities during the Lohafex iron fertilization experiment: Structural and functional responses in the epipelagic layer.

- Menden-Deuer, S., and Lessard, E. J., 2000, Carbon to volume relationships for dinoflagellates, diatoms and other protist plankton: *Limnology and Oceanography*, v. 45, no. 3, p. 569-579.
- Nejstgaard, J. C., Naustvoll, L. J., and Sazhin, A., 2001, Correcting for underestimation of microzooplankton grazing in bottle incubation experiments with mesozooplankton: *Marine Ecology Progress Series [Mar. Ecol. Prog. Ser.]*. v. 221, p. 59-75.
- Poulet, S., and Marsot, P. , 1980, Chemosensory feeding and food-gathering by omnivorous marine copepods. In: Kerfoot W.C. (ed)) *Evolution and ecology of zooplankton communities*. : University Press of New England, p. 198-218.
- Razouls, S., Razouls, C., and De Bovee, F., 2000, Biodiversity and biogeography of Antarctic copepods. : *Antarctic Science* v. 12, no. 3, p. 343-362.
- Reigstad, M., Riser, C. W., and Svensen, C., 2005, Fate of copepod faecal pellets and the role of *Oithona* spp: *Marine Ecology Progress Series [Mar. Ecol. Prog. Ser.]*. v. 304, p. 265-270.
- Schultes, S., Verity, P. G., and Bathmann, U., 2006, Copepod grazing during an iron-induced diatom bloom in the Antarctic Circumpolar Current (EisenEx): I. Feeding patterns and grazing impact on prey populations: *Journal of Experimental Marine Biology and Ecology*, v. 338, no. 1, p. 16-34.
- Svensen, C., and Nejstgaard, J. C., 2003, Is sedimentation of copepod faecal pellets determined by cyclopoids? Evidence from enclosed ecosystems: *Journal of Plankton Research*, v. 25, no. 8, p. 917-926.
- Thronsen, J., 1995, Chapter "Estimating cell numbers: In: *Manual on Harmful Marine Microalgae*. (eds. Hallegraeff, G. M., Anderson, D. M. & Cembella, A. D.) v. 33, no. UNESCO, Paris,, p. 63–80.

Tables

Table 1: Sampling overview for grazing experiments during LOHAFEX (Individuals = Ind.).

Table 2: Overview of plankton categories counted in the samples including biovolume (μm^3), carbon content per cell (pg C) and equivalent spherical diameter ESD (μm).

Table 3: Carbon conversion equations to calculate cellular carbon content (pg C) through cell volume (V in μm^3). To convert cell Volume into biomass, the C:volume relationships for the specific groups were used (Menden_Deuer and Lessard 2000).

Table 4: Clearance rates ($\text{ml ind.}^{-1} \text{h}^{-1}$) on total particles before the fertilization, inside and outside the patch.

Table 5: Daily ingestion rates ($\mu\text{g C ind.}^{-1} \text{d}^{-1}$) of *C. simillimus* (A) and *Oithona* spp. (B) on the different plankton categories considered as prey in the natural particle assemblages.

Figures

Fig. 1: The copepod species *Calanus simillimus*. Mostly copepodites CIV-CV were used for the experiments.

Fig. 2: Scheme of the experimental jars prepared for each grazing experiment (S, start; C, control without copepods; T, test with copepods; 1,2,3,4 replicates).

Fig. 3: Concentration of natural particles (in cells mL^{-1} and ng C mL^{-1}) at the beginning of the five grazing experiments.

Fig. 4: Relative plankton composition available to copepods at the beginning of the grazing experiments.

Fig. 5: Daily carbon ingestion rates ($\mu\text{g C ind.}^{-1} \text{d}^{-1}$) of *Calanus simillimus* and *Oithona* spp..

Fig. 6: Relative prey contribution to total carbon ingested by *Calanus simillimus* within the patch (A-D) and outside the patch (E).

Fig. 7: Relative prey contribution to total carbon ingested by *Oithona* spp. before fertilization (A) and on day 9,5 within the patch (B).

Fig. 8: Non-diatom prey (A-F) ingested by *Calanus simillimus* ($\mu\text{g C ind.}^{-1} \text{d}^{-1}$).

Fig. 9: Non-diatom prey (A-F) ingested by *Oithona* spp. ($\mu\text{g C ind.}^{-1} \text{d}^{-1}$).

Fig. 10: Diatom prey ingested by *Calanus simillimus* (A) and *Oithona* spp. (B) ($\mu\text{g C ind.}^{-1} \text{d}^{-1}$).

Fig. 11: Abundance of *Calanus simillimus* (green) and *Oithona* spp. (red) in the upper 100 m water column and percentage contribution of their summed populations to total copepod abundance (blue). D, day; N, night samples.

Fig. 12: Biomass ($\mu\text{g C m}^{-2}$) of *Calanus simillimus* (green) and *Oithona* spp. (red) in the upper 100 m water column (D, day; N, night).

Fig. 13: Total carbon ingested by *Calanus simillimus* and *Oithona* spp. populations in the upper 100 m water column before (day -0.6) and after Fe release inside and outside the fertilized patch. Data for days 9.5, 16.3, 24.6 are averaged from day and night copepod samples.

Fig. 14: Grazing impact of (A) *Calanus simillimus* and (B) *Oithona* spp. population on different food categories in the upper 100 m water column.

Table 1: Sampling overview for grazing experiments during LOHAFEX (Individuals = Ind.).

Date	Station	Day since first Fe release	Latitude (Degree decimal)	Longitude (Degree decimal)	IN or OUT patch	Copepod species	No. Ind.	Ind. L ⁻¹
26.01.09	114	-0,6	-47,99793	-15,80336	IN/OUT	<i>Calanus similininus</i> (CIV-CV) <i>Oithona</i> spp.	13-15 30-40	6-7 25-33
31.01.09	132	4,6	-47,65656	-15,73177	IN	<i>Calanus similininus</i> (CV)	20-25	9-12
05.02.09	135	9,5	-47,69418	-15,09783	IN	<i>Calanus similininus</i> (CIV-CV) <i>Oithona</i> spp.	30-33 35-46	14-15 29-38
12.02.09	146	16,3	-47,49086	-15,41995	OUT	<i>Calanus similininus</i> (CIV-CV)	15-25	7-12
20.02.09	162	24,6	-47,35543	-14,7156	IN	<i>Calanus similininus</i> (CV)	6-7	2-3

Table 2: Overview of plankton categories counted in the samples including biovolume (μm^3), carbon content per cell (pg C) and equivalent spherical diameter ESD (μm).

	Biovolume (μm^3)	ESD (μm)	Menden-Deuer (pg cell ⁻¹)
Diatoms:			
<i>Chaetoceros</i> spp.	2975	18	189
<i>Corethron pennatum</i> (> 40 μm)	310321	84	8041
<i>Corethron pennatum</i> (~ 40 μm)	2.631	17	170,90
<i>Cylindrotheca</i> spp.	146	7	16
<i>Ephemera</i> sp.	2805	17	180
<i>Fragilariopsis kergulensis</i> (~ 30 μm)	487	10	44
<i>Fragilariopsis kergulensis</i> (30-40 μm)	1014	12	79
<i>Haslea trompeii</i> (~ 70 μm)	2431	17	160
<i>Lennoxia</i> spp. (30-40 μm)	21	3	3
<i>Navicula</i> sp.	993	12	78
<i>Pseudo-nitzchie</i> spp. (30-40 μm)	392	9	36
<i>Pseudo-nitzschia</i> spp. (40-60 μm)	645	11	55
<i>Rhizosolenia</i> spp.	472405	97	11643
<i>Thalassionema nitzschioides</i> (~30 μm)	273	8	27
<i>Thalassiosira</i> spp. (< 15 μm)	928	12	73
<i>Thalassiosira</i> sp. (> 15 μm)	4160	20	180
unidentified Diatom	389	9	36
Prymnesiophytes:			
<i>Phaeocstis antarctica</i> (3-4 μm)	20	3	4
<i>Phaeocstis antarctica</i> (4-6 μm)	86	5	14
<i>Emiliana huxleyi</i>	161	7	25
Flagellates:			
coccoid cells (< 5 μm)	38	4	7
Flagellates (< 10 μm)	137	6	22
Flagellates (10-20 μm)	718	7	104
Dinoflagellates:			
Dinos < 10 μm thecate	276	8	42
Dinos 10-15 μm thecate	1173	13	165
Dinos > 15 μm thecate	59752	49	6607
Dinos < 10 μm athecate	285	8	44
Dinos 10-15 μm athecate	1157	13	163
Dinos > 15 μm athecate	59752	49	6607
Ciliates:			
aloriccate ciliates (10-15 μm)	1439	14	200
aloriccate ciliates (> 15 μm)	72661	52	7939
Tintinnid ciliates (10-15 μm)	10983	28	1347
Tintinnid ciliates (> 15 μm)	252404	78	25560

Table 3: Carbon conversion equations to calculate cellular carbon content (pg C) through cell volume (V in μm^3). To convert cell Volume into biomass, the C:volume relationships for the specific groups were used (Menden_Deuer and Lessard 2000).

Group	Menden-Deuer & Lessard
diatoms (<3000 μm^3)	$C \text{ cell}^{-1} = 0.288 \times V^{0.811}$
diatoms (>3000 μm^3)	$C \text{ cell}^{-1} = 0.177 \times V^{0.881}$
all protists except diatoms	$C \text{ cell}^{-1} = 0.216 \times V^{0.939}$
dinoflagellates	$C \text{ cell}^{-1} = 0.444 \times V^{0.864}$
ciliates (athecate)	$C \text{ cell}^{-1} = 0.23 \times V^{0.984}$
tintinnid ciliates	$C \text{ cell}^{-1} = 0.679 \times V^{0.841}$

Table 4: Clearance rates ($\text{ml ind.}^{-1} \text{ h}^{-1}$) on total particles before the fertilization, inside and outside the patch.

Days since first Fe release	<i>Calanus simillimus</i>	<i>Oithona</i> spp.
-0,6 (IN)	55.2 (\pm 13.2)	14.2 (\pm 4.2)
4,6 (IN)	26.4 (\pm 12.6)	
9,5 (IN)	20.7 (\pm 6.3)	5.4 (\pm 3.0)
16,3 (OUT)	25.0 (\pm 15.0)	
24,6 (IN)	72.9 (\pm 35.4)	

Table 5: Daily ingestion rates ($\mu\text{g C ind.}^{-1}\text{d}^{-1}$) of *C. similimus* (A) and *Oithona* spp. (B) on the different plankton categories considered as prey in the natural particle assemblages.

<i>Calanus similimus</i>					
Days since first Fe release	-0,6 (IN/OUT)	4,6 (IN)	9,5 (IN)	16,3 (OUT)	24,6 (IN)
athecate Dinoflagellates	7,87 ($\pm 6,29$)	0,05 ($\pm 0,09$)	0,00 ($\pm 0,00$)	0,75 ($\pm 0,85$)	8,49 ($\pm 9,04$)
thecate Dinoflagellates	0,98 ($\pm 1,14$)	0,34 ($\pm 0,29$)	1,32 ($\pm 1,52$)	2,57 ($\pm 1,90$)	4,30 ($\pm 3,61$)
aloricate Ciliates	0,72 ($\pm 1,01$)	1,03 ($\pm 0,42$)	0,00 ($\pm 0,002$)	0,00 ($\pm 0,002$)	2,54 ($\pm 1,05$)
Tintinnid Ciliates	0,36 ($\pm 0,04$)	0,00 ($\pm 0,00$)	0,45 ($\pm 0,25$)	0,00 ($\pm 0,00$)	3,17 ($\pm 0,47$)
Flagellates	1,23 ($\pm 0,28$)	1,72 ($\pm 0,44$)	1,41 ($\pm 0,10$)	0,37 ($\pm 0,731$)	2,70 ($\pm 2,51$)
<i>Phaeocystis antarctica</i>	0,06 ($\pm 0,01$)	0,06 ($\pm 0,09$)	0,05 ($\pm 0,04$)	0,08 ($\pm 0,135$)	0,47 ($\pm 0,68$)
<i>Emiliania huxleyi</i>	0,00 ($\pm 0,0$)	0,03 ($\pm 0,04$)	0,07 ($\pm 0,01$)	0,00 ($\pm 0,00$)	0,00 ($\pm 0,00$)
Diatoms	0,04 ($\pm 0,01$)	0,08 ($\pm 0,04$)	0,09 ($\pm 0,02$)	0,06 ($\pm 0,025$)	0,13 ($\pm 0,11$)
<i>Oithona</i> spp.					
Days since first Fe release	-0,6 (IN/OUT)	9,5 (IN)			
athecate Dinoflagellates	2,85 ($\pm 0,01$)	0,07 ($\pm 0,013$)			
thecate Dinoflagellates	0,39 ($\pm 0,30$)	0,00 ($\pm 0,002$)			
aloricate Ciliates	0,24 ($\pm 0,14$)	0,00 ($\pm 0,001$)			
Tintinnid Ciliates	0,14 ($\pm 0,19$)	0,30 ($\pm 0,223$)			
Flagellates	0,88 ($\pm 0,24$)	0,96 ($\pm 0,609$)			
<i>Phaeocystis antarctica</i>	0,20 ($\pm 0,20$)	0,20 ($\pm 0,005$)			
<i>Emiliania huxleyi</i>	0,00 ($\pm 0,00$)	0,00 ($\pm 0,00$)			
Diatoms	0,01 ($\pm 0,006$)	0,01 ($\pm 0,00$)			

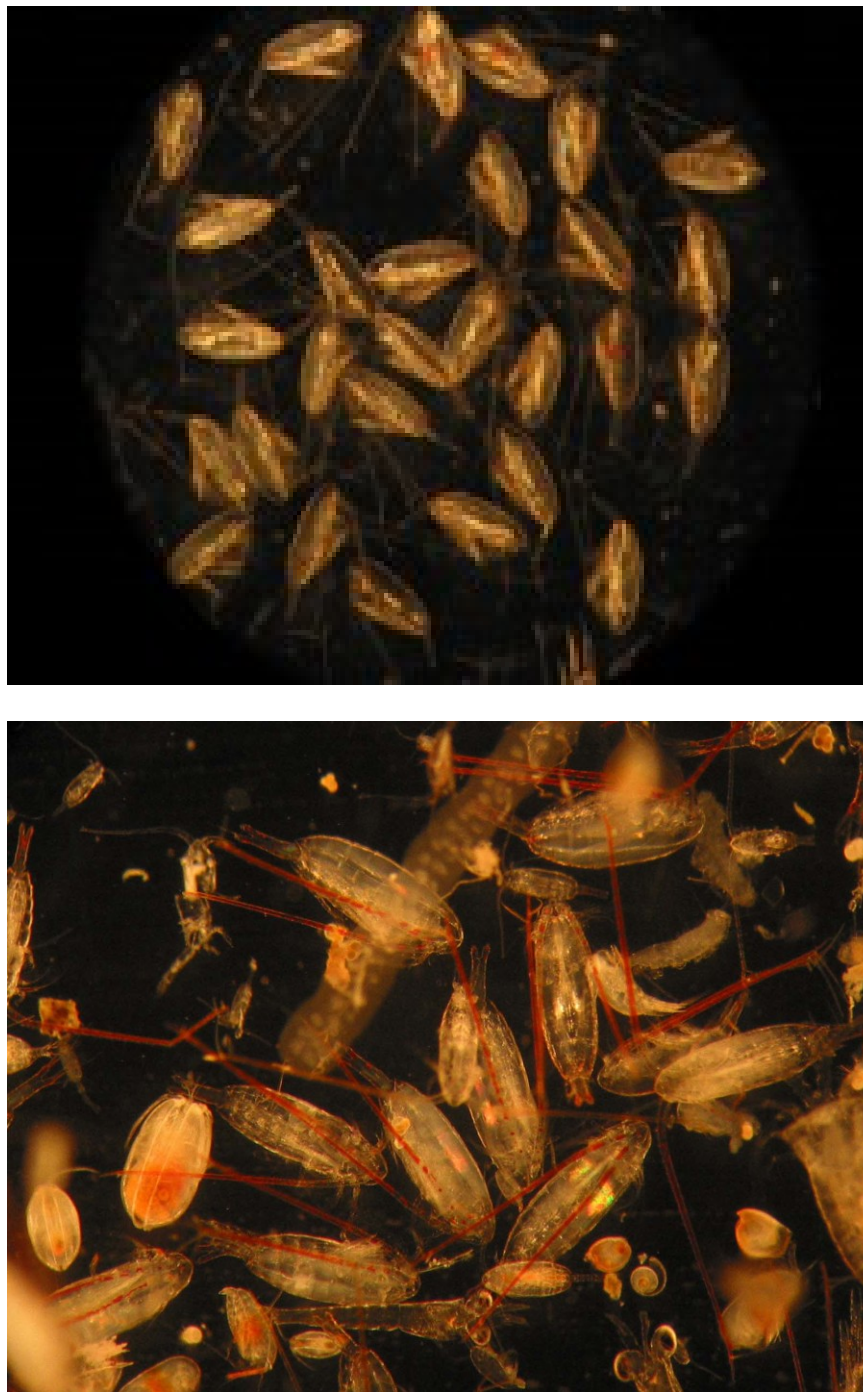


Fig. 1: The copepod species *Calanus simillimus*. Mostly copepodites CIV-CV were used for the experiments.

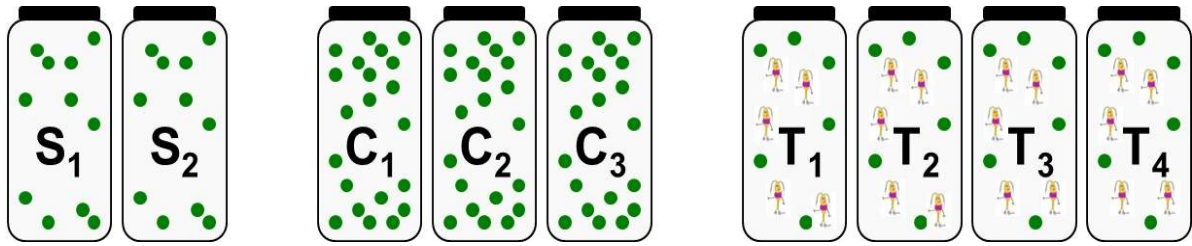


Fig. 2: Scheme of the experimental jars prepared for each grazing experiment (S, start; C, control without copepods; T, test with copepods; 1,2,3,4 replicates).

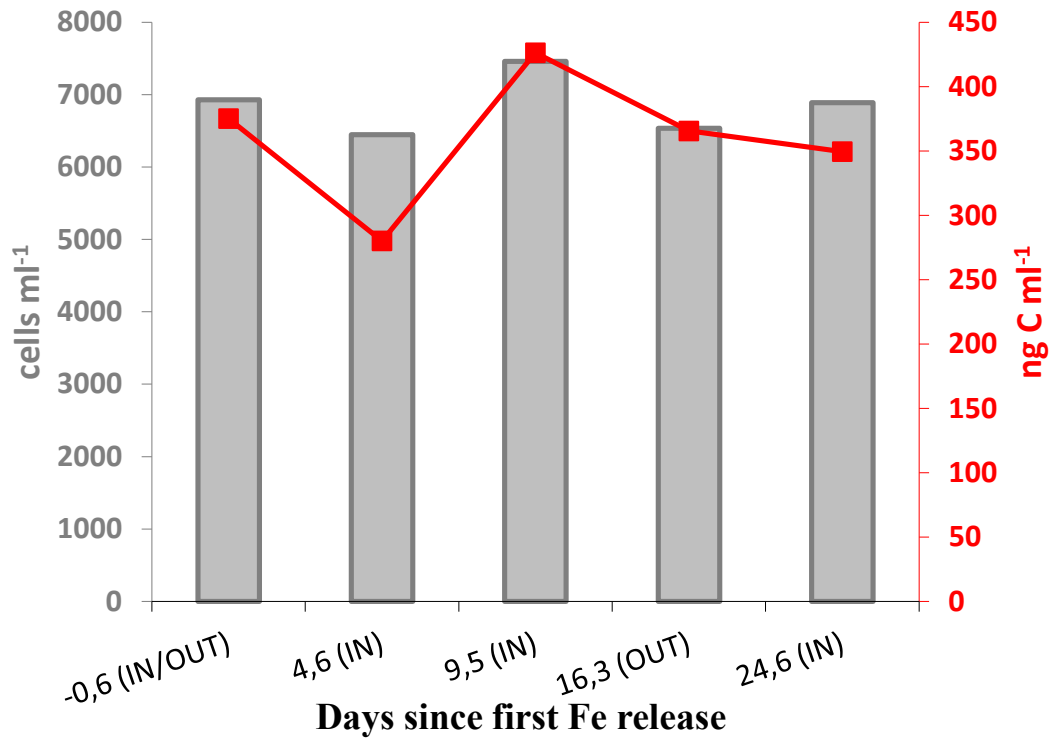


Fig. 3: Concentration of natural particles (in cells mL⁻¹ and ng C mL⁻¹) at the beginning of the five grazing experiments.

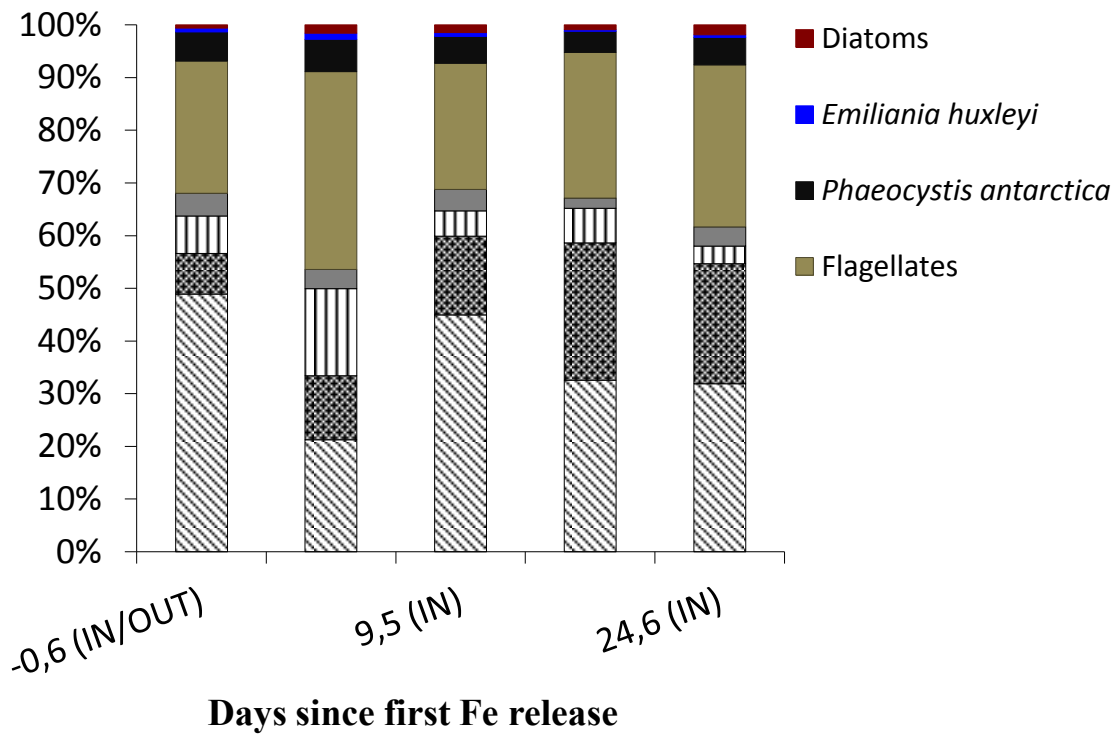


Fig. 4: Relative plankton composition available to copepods at the beginning of the grazing experiments.

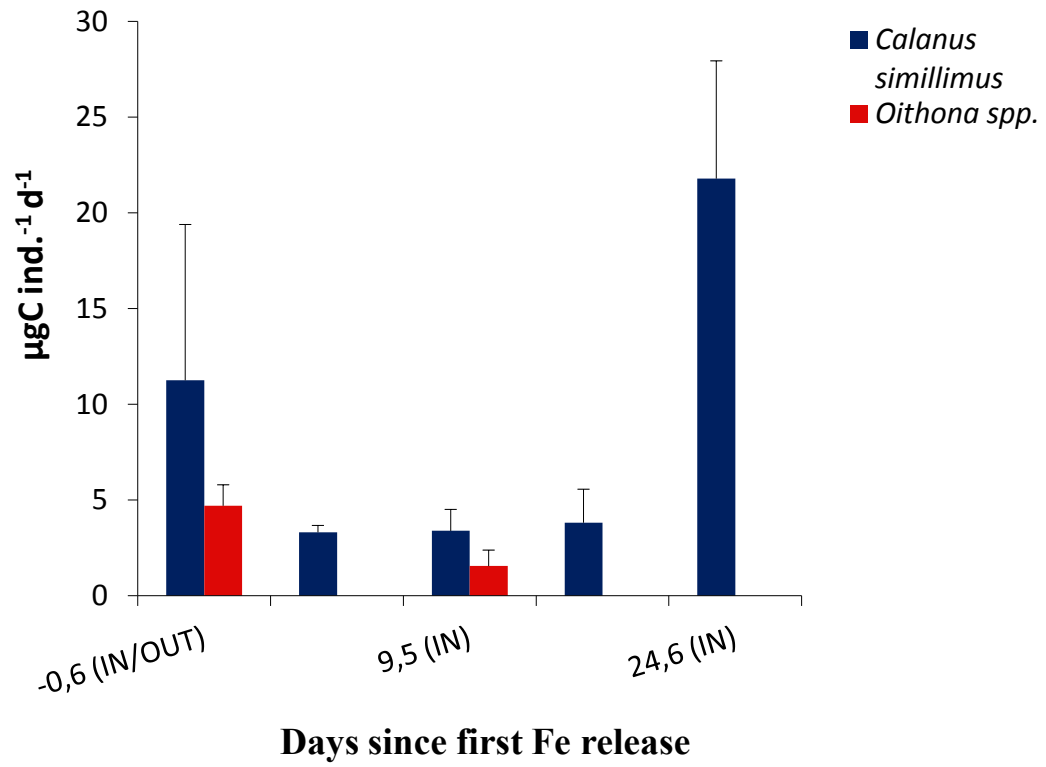


Fig. 5: Daily carbon ingestion rates ($\mu\text{g C ind.}^{-1} \text{d}^{-1}$) of *Calanus simillimus* and *Oithona* spp..

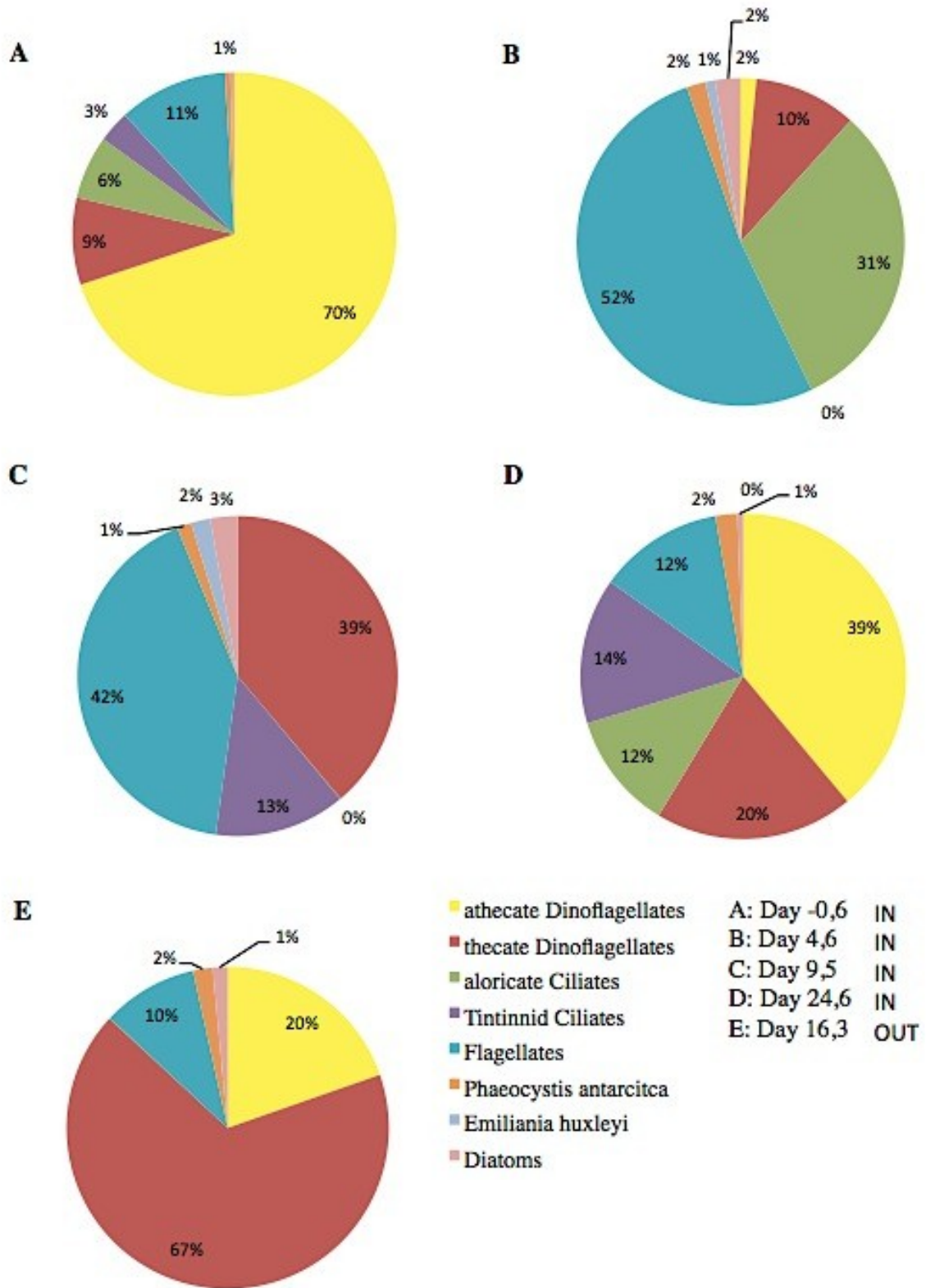


Fig. 6: Relative prey contribution to total carbon ingested by *Calanus simillimus* within the patch (A-D) and outside the patch (E).

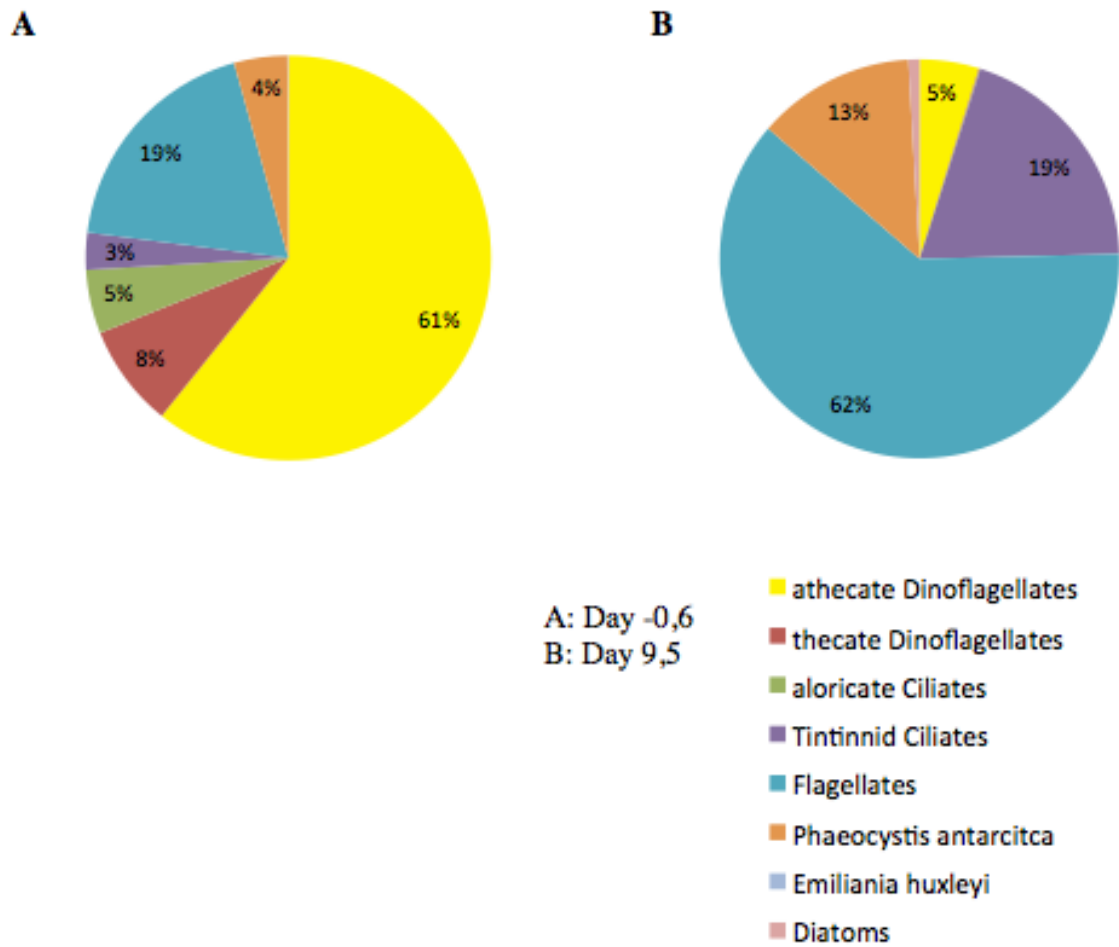


Fig. 7: Relative prey contribution to total carbon ingested by *Oithona* spp. before fertilization (A) and on day 9,5 within the patch (B).

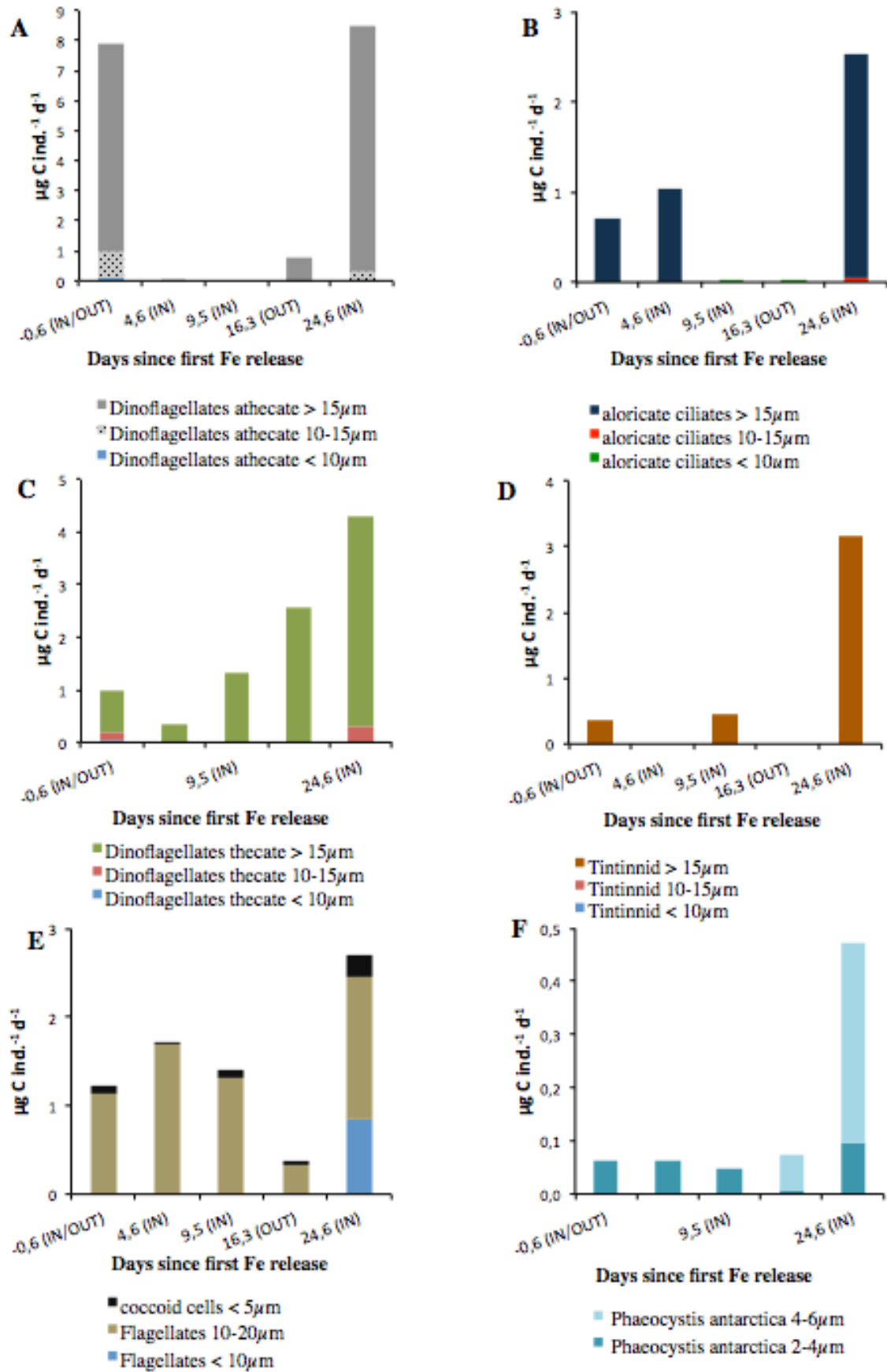


Fig. 8: Non-diatom prey (A-F) ingested by *Calanus simillimus* ($\mu\text{g C ind.}^{-1} \text{d}^{-1}$).

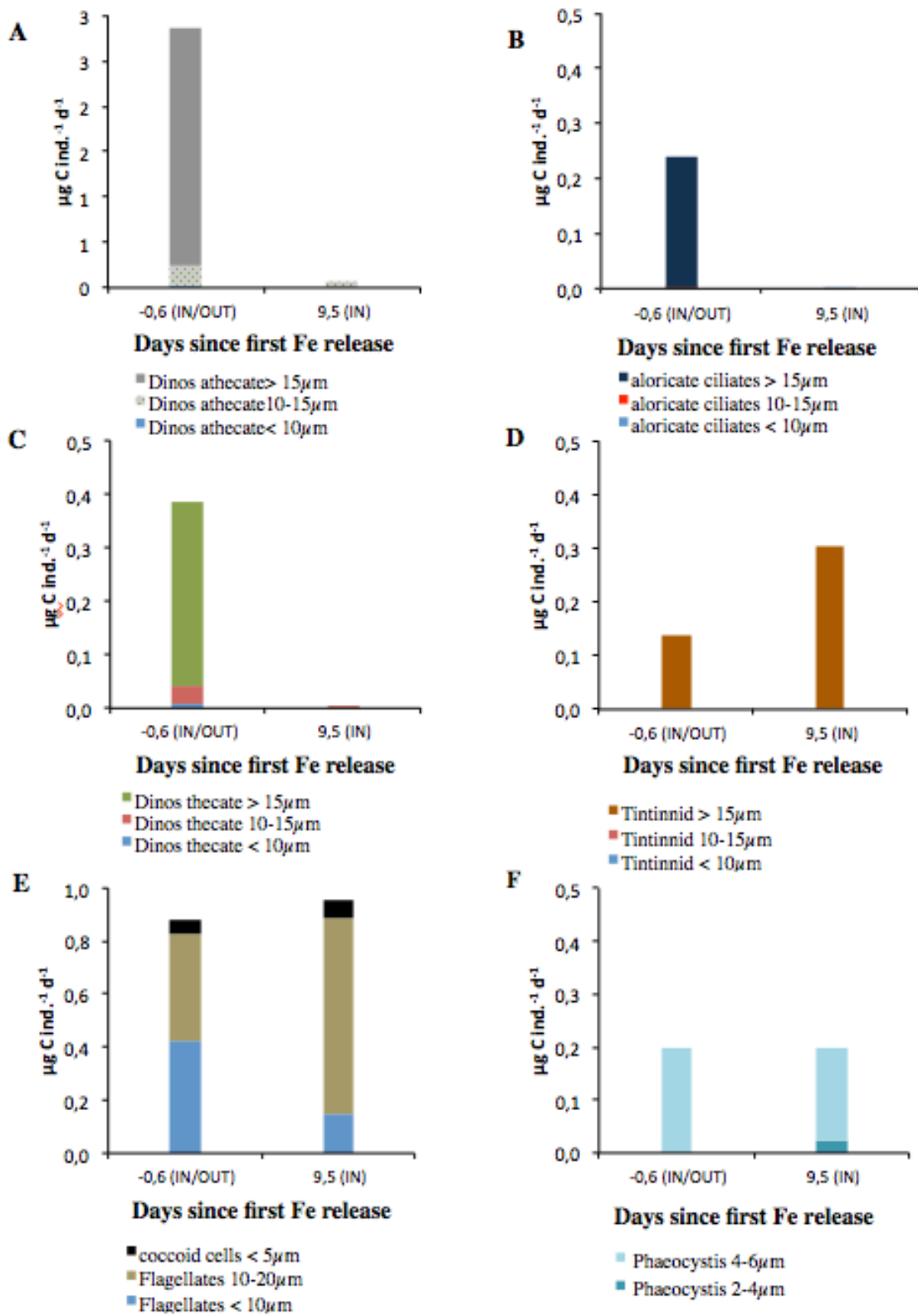


Fig. 9: Non-diatom prey (A-F) ingested by *Oithona* spp. ($\mu\text{g C ind.}^{-1} \text{d}^{-1}$).

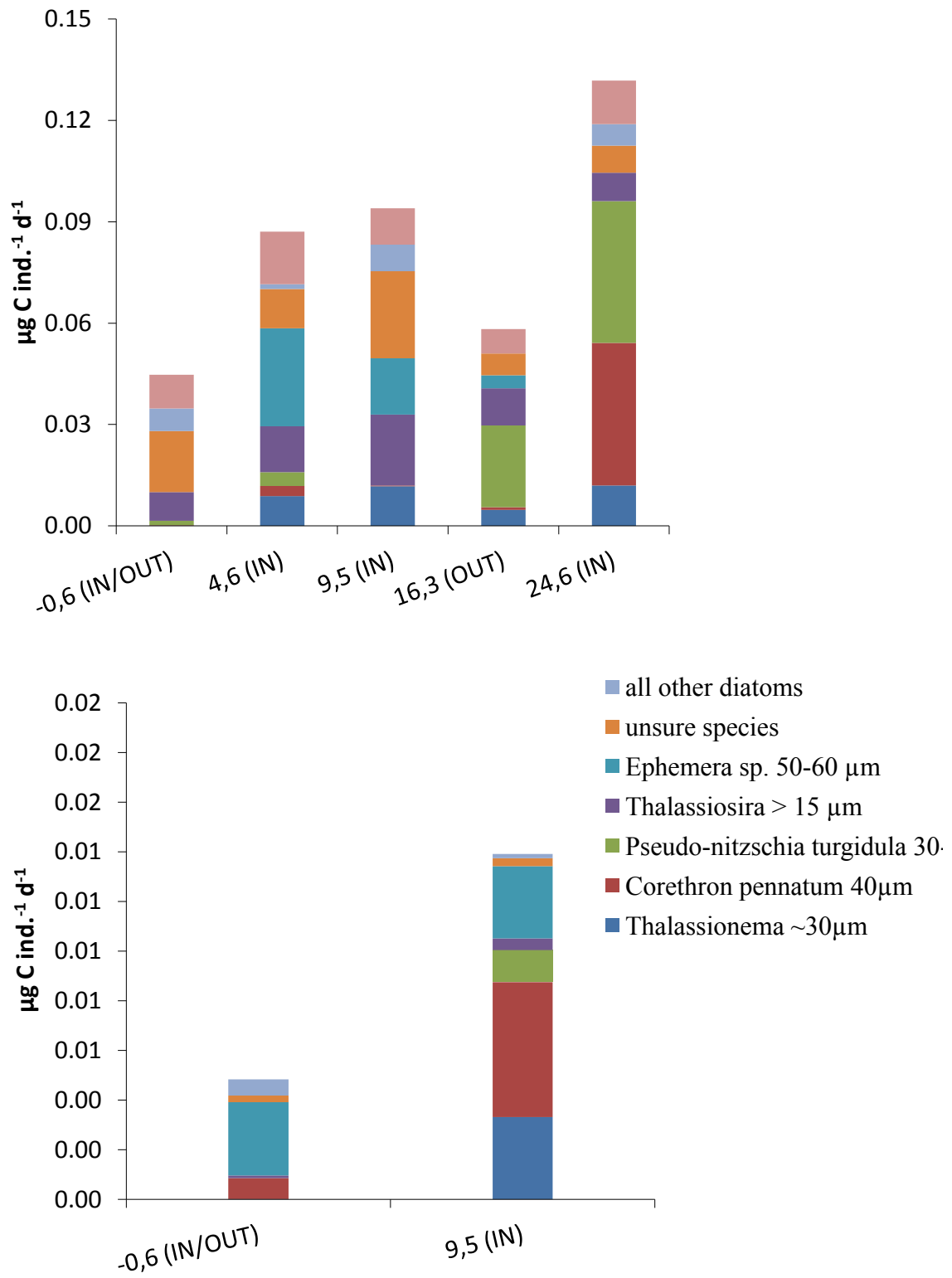


Fig. 10: Diatom prey ingested by *Calanus simillimus* (A) and *Oithona* spp. (B) ($\mu\text{g C ind.}^{-1} \text{d}^{-1}$).

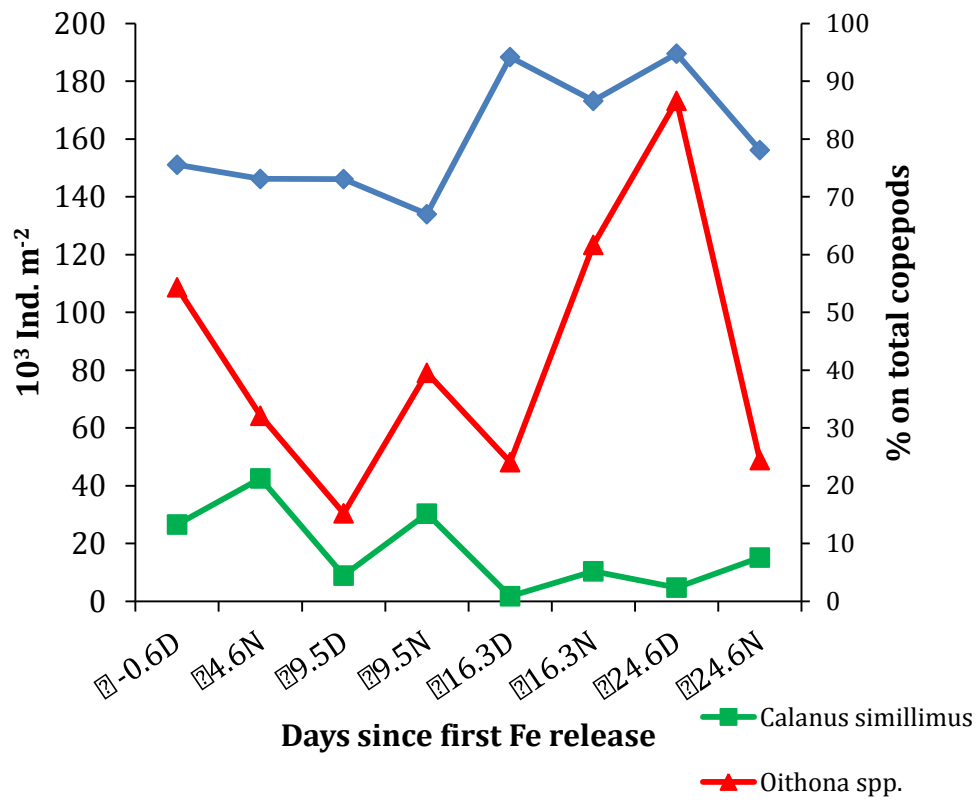


Fig. 11: Abundance of *Calanus simillimus* (green) and *Oithona* spp. (red) in the upper 100 m water column and percentage contribution of their summed populations to total copepod abundance (blue). D, day; N, night samples.

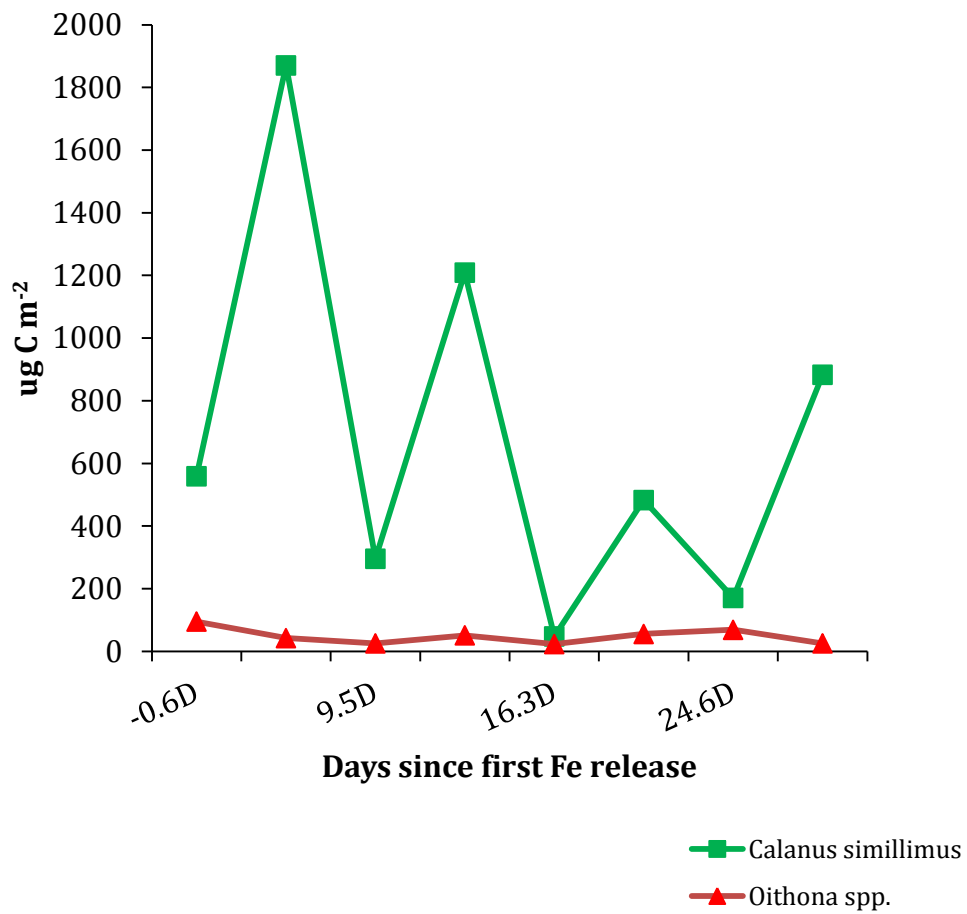


Fig. 12: Biomass ($\mu\text{g C m}^{-2}$) of *Calanus simillimus* (green) and *Oithona* spp. (red) in the upper 100 m water column (D, day; N, night).

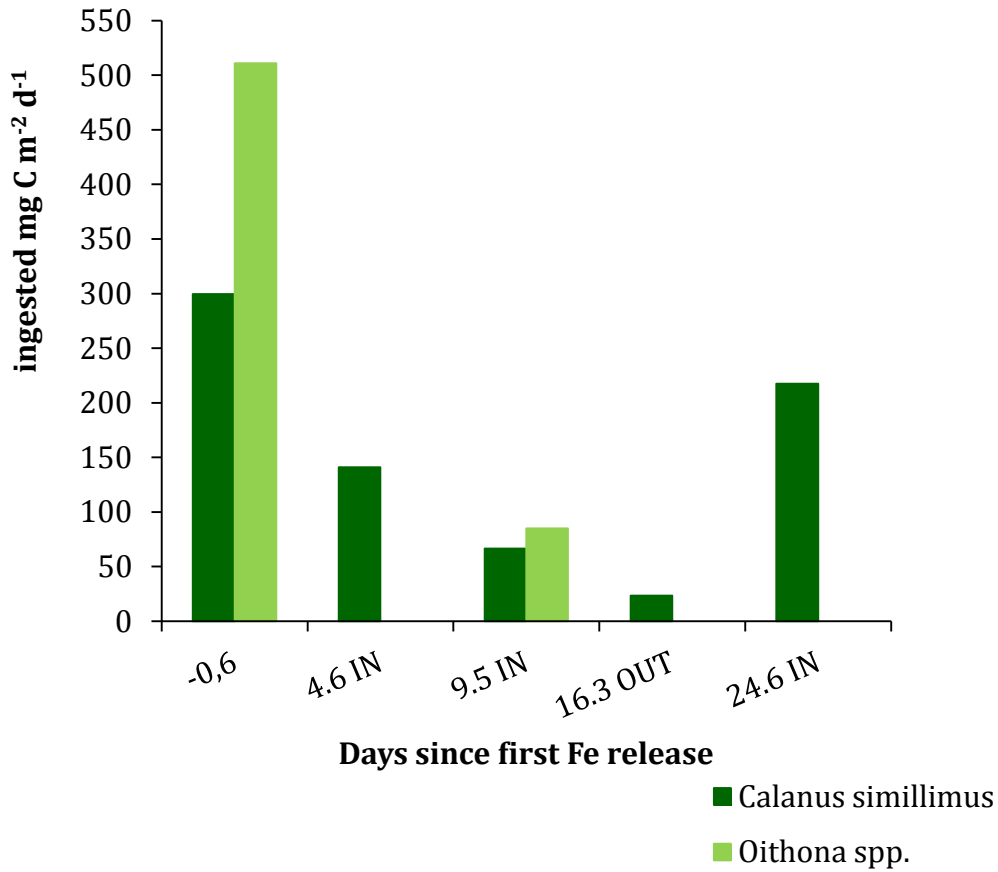


Fig. 13: Total carbon ingested by *Calanus simillimus* and *Oithona* spp. populations in the upper 100 m water column before (day -0.6) and after Fe release inside and outside the fertilized patch. Data for days 9.5, 16.3, 24.6 are averaged from day and night copepod samples.

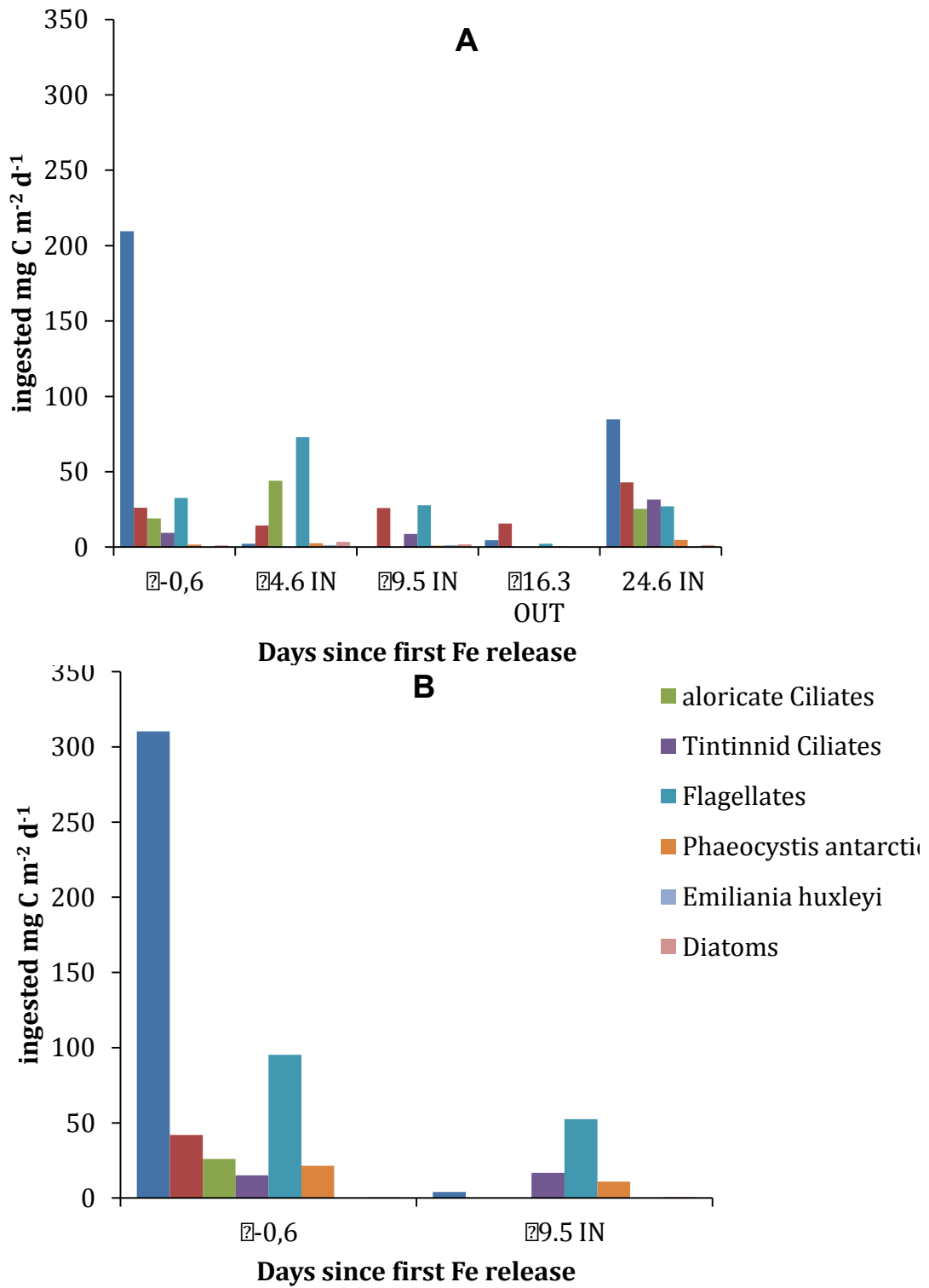


Figure 14: Grazing impact of (A) *Calanus simillimus* and (B) *Oithona* spp. population on different food categories in the upper 100 m water column.

Manuscript V

**Sedimentation patterns of phyto- and protozooplankton and
sinking particle assemblage during the iron fertilisation
experiment LOHAFEX in the Southern Ocean**

Friederike Ebersbach^{a,b,}, Philipp Assmy^{a,b,1}, Patrick Martin^{c,2}, Isabelle Schulz^{a,b},
Sina Wolzenburg^a, Eva-Maria Nöthig^b*

submitted to Deep Sea Research I

a Center for Marine Environmental Sciences, University of Bremen

b Alfred Wegener Institute for Polar and Marine Research, Am Handelshafen 12, 27570
Bremerhaven, Germany

c National Oceanography Centre, Southampton, SO14 3ZH, UK

1 Present address: Norwegian Polar Institute, Fram Centre, 9296 Tromsø, Norway

2 Present address: Department of Marine Chemistry & Geochemistry, Woods Hole
Oceanographic Institution, Woods Hole, MA 02543, USA

* Corresponding author. Tel. +49(0)42169316181, friederike.ebersbach@gmx.net

Abstract

The meso-scale iron fertilisation experiment LOHAFEX, conducted in low-silicate waters of the Atlantic Sector of the Southern Ocean during austral summer (January – March 2009), examined the response and fate of the plankton community to iron addition as compared to surrounding waters. Sinking particles were collected using i) bulk samples of neutrally buoyant sediment traps (NBSTs) for biogeochemical fluxes and microscopic investigations, and ii) polyacrylamide (PA) gel equipped NBSTs in order to preserve the shape and structure of intact particles. Furthermore, transparent exopolymer particles (TEP) were analysed in the water column and in trap samples as TEP might act as a binding agent for small particles and thereby impact aggregation and the export process.

The LOHAFEX bloom was dominated by flagellates and characterised by low export fluxes throughout the experiment. The dominance of re-processed faecal material and intact faecal pellets and the minor contribution of TEP-rich phyto-detrital aggregates to the export flux indicate that most of the iron-induced increase in biological carbon fixation was retained in the upper 100 m by a highly efficient grazer/recycling community. Although diatoms were a minor component of the surface community, they contributed disproportionately to downward particle flux (albeit mostly as empty and broken frustules), indicating selective export of silica associated with the sinking frustules.

Research Highlights

- very low deep export followed the iron-induced bloom during LOHAFEX
- particle assemblage was dominated by re-processed faecal material and faecal pellets
- phyto-detritus played a minor role for export processes
- diatom flux was disproportionately higher than their surface contribution
- this selective export was in account of flagellates

Keywords

export flux, mesopelagic, iron fertilization, sediment trap, sinking particles, Southern Ocean

Abbreviations

BCP: biological carbon pump

NBST: neutrally buoyant sediment trap

PA gel: polyacrylamide gel

PC: protist carbon

POC: particulate organic carbon

TEP: transparent exopolymer particles

Acknowledgements

We thank LOHAFEX co-chief scientists Victor Smetacek and Wajih Naqvi and the captain and crew of *RV Polarstern*. Kevin Saw prepared and deployed the PELAGRA traps. We are grateful to Uta Passow, Dieter Wolf-Gladrow and Ulrich Bathmann for thoughtful discussions. F. E., I. S. and P. A. were funded through DFG- Research Center / Cluster of Excellence „The Ocean in the Earth System“ and supported by GLOMAR – Bremen International Graduate School for Marine Sciences.

1. Introduction

The downward transport of organic carbon from the surface ocean to the deep ocean, the biological carbon pump (BCP; Volk and Hoffert, 1985; De La Rocha, 2007), exerts an important control on atmospheric CO₂ concentrations (Parekh et al., 2006; Kwon et al., 2009). The mesopelagic (100 – 1000 m depth) and the deep ocean (>1000 m depth) are coupled through processes in the euphotic zone (e.g. primary production (PP)) via sinking particles (e.g. Boyd and Trull, 2007). Most of the organic carbon is remineralised in the upper few hundred meters, but some sinks below the permanent thermocline and is removed from contact with the atmosphere for climatically-relevant time-scales (Lutz et al., 2002; Buesseler and Boyd, 2009; Kwon et al., 2009). The magnitude of the BCP is strongly dependent on the nature of the particles that are exported from the surface, which is governed by the structure of the prevailing phytoplankton community and the food web in surface and the mesopelagic layers (Boyd and Trull 2007; Buesseler and Boyd, 2009). Moreover, transparent exopolymer particles (TEP) are known to stimulate formation of marine snow and facilitate incorporation of small particles into larger aggregates that would otherwise be too small to sink on their own (Passow et al., 2001; Passow, 2002).

However, even basic questions remain unanswered, such as which types of particles, and which phytoplankton taxa, contribute most to the flux, and which have a greater tendency to pass through the mesopelagic zone without being remineralized (Turner 2002; François et al., 2002; Richardson and Jackson, 2007; Buesseler and Boyd, 2009). This poor understanding of the BCP limits our ability to predict responses to environmental changes (Taucher and Oschlies, 2011).

In this context, the Southern Ocean is of particular interest, as it consists largely of High-Nitrate-Low-Chlorophyll (HNLC) areas, where PP is limited by the availability of the micronutrient iron (Fe) – according to the ‘iron-hypothesis’ (Martin, 1990), and clearly illustrated by 11 scientific *in situ* mesoscale iron fertilisation experiments (Boyd et al., 2007). This has raised the question of whether enhancing iron supply to the Southern Ocean would stimulate the BCP and sequester anthropogenic CO₂ (Lampitt et al., 2008a; Smetacek and Naqvi, 2008).

Five artificial iron fertilisation experiments have been carried out in the Southern Ocean: SOIREE (Boyd et al., 2000), SOFeX-N and -S (Coale et al., 2004), EisenEx (Assmy et al., 2007), EIFEX (Smetacek et al., 2012), and SAGE (Harvey et al., 2011). Moreover, two studies have examined the biogeochemistry and ecosystem functioning in natural iron fertilised waters downstream of Southern Ocean islands, CROZEX (Pollard et al., 2007) and

KEOPS (Blain et al., 2007). Although carbon export out of the surface ocean (>200 m) was enhanced during SOFeX, EIFEX, CROZEX and KEOPS, deep export (>1000 m) was enhanced during EIFEX, CROZEX and KEOPS (Coale et al., 2004; Salter et al., 2007; Blain et al., 2007; Smetacek et al., 2012). The lack of an export signal at depth during most artificial iron fertilisation experiments can be partly explained by the fact that most experiments were too short to follow the demise phase of the iron-induced blooms (Smetacek and Naqvi, 2008). The latest iron fertilisation experiment, LOHAFEX ('loha' is the Hindi word for iron), was hence designed to follow the build-up and demise of the bloom, and to cover a large enough area to minimise the effects of dilution with unfertilised waters (Smetacek and Naqvi, 2008). Given the uncertainty regarding export processes in general and in the mesopelagic zone in particular, the direct examination of the particle assemblage is useful. This manuscript focuses on the contribution of phytoplankton and protozooplankton (protist carbon (PC) flux) to the downward carbon flux during LOHAFEX. Therefore, we deployed NBSTs, partly equipped with PA gels to preserve intact sinking particles, and investigated the collected material microscopically. Thus, species composition was determined, converted into carbon fluxes, and compared with the particulate matter as collected with the PA gels. The combination of both approaches provides insights into particle dynamics that regulated export flux during LOHAFEX. In addition, the analysis of TEP distribution in the water column and in the trap material allows for assumptions on particle formation.

2. Material and Methods

2.1 Study area

LOHAFEX was conducted during austral summer within a meso-scale eddy in the Antarctic Circumpolar Current (ACC) in the Atlantic Sector of the Southern Ocean (Fig. 1). Over the course of the experiment, a mean surface mixed layer depth of 62 ± 19 m was observed. The chosen eddy provided a horizontally and vertically coherent water mass (Martin et al., *subm.*), enabling us to link the carbon fluxes measured at the trap deployment depths (see below) with surface processes. The centre of the eddy was fertilised with 2 t of iron (as $\text{FeSO}_4 \cdot 7 \text{H}_2\text{O}$) in acidified solution on January 27 (d0) creating a patch of $\sim 300 \text{ km}^2$. Another 2 t of iron were applied 18 days later on February 14. The fertilised patch was marked with two surface-tethered buoys equipped with GPS-receivers. Stations inside the patch (IN-stations) were distinguished from control stations outside the patch (OUT-stations) on the basis of the photosynthetic quantum efficiency (F_v/F_m ratio) of surface phytoplankton, and concentrations of chlorophyll, $p\text{CO}_2$, and the inert tracer SF_6 . The fertilised patch was studied for 39 days

(27 January to 6 March 2009), making LOHAFEX the longest iron fertilisation experiment to date.

2.2 Sediment traps

Funnel-shaped neutrally buoyant sediment traps (PELAGRA-traps, Lampitt et al., 2008b) were deployed at 200 and 450 m depth. Each trap has four separate collection funnels, each leading to a 500 mL Nalgene collection cup. Collection cups were programmed to open 18-24 h after deployment (by sliding under the funnel), and to close again minutes before ascending to the surface.

Splits of trap samples for plankton counts were preserved with 2% borate- buffered formaldehyde in filtered (0.2 μ m) seawater, split on board using a rotary splitter identical to that described by Lamborg et al. (2008), and stored at 4° C.

PA gels were prepared prior to the cruise following the method described in Ebersbach and Trull (2008), and were deployed on a subset of the traps. Unfortunately, several of the trap deployments equipped with PA gels failed due to technical problems. Hence, PA gel samples are only available from the beginning and the end of the experiment (Table 1). Successful PA gels were photographed on board following Ebersbach and Trull (2008) to document the state of the freshly collected material. Particles identified in PA gels were divided into (intact) faecal pellets, re-processed faecal material and phyto-detritus – as illustrated in Appendix 1). Most faecal pellets were of cylindrical shapes and a few pellets were oval (fp in Appendix 1). The re-processed faecal material (fm in Appendix 1) consisted of more compact, denser and somewhat more clearly shaped/formed aggregates than the fluffy phyto-detritus (pd in Appendix 1).

2.3 Microscopic analyses and data processing

The composition of the sedimented plankton material collected with the PELAGRA traps was examined using inverted light and epifluorescence microscopy (Axiovert 135, 200; Zeiss, Oberkochen, Germany) following the method of Throndsen (1995). Subsamples of 10 or 50 mL from each split, depending on the density of the material, were settled in sedimentation chambers (Hydrobios; Kiel, Germany) for 48 h. Unicellular organisms were identified and counted at either 100, 200, and 400 \times , depending on the size of the cells. According to their abundance, cells were counted in transects, quarter, half or whole chambers, and identified to species level where possible.

Taxon-specific biovolumes were estimated according to Hillebrand et al. (1999) by measuring 10-20 individuals per taxon at $400 \times$ magnification. Biovolumes were converted into carbon content after Menden-Deuer and Lessard (2000), with $C \text{ cell}^{-1}$ in pg and V in μm^3 .

$$\log C \text{ cell}^{-1} = \log a + b * \log V \quad (1)$$

Different a and b values were used for different types of protists and for two size classes of diatoms (smaller or larger than $3000 \mu m^3$) (Menden-Deuer and Lessard, 2000). Using the taxon-specific carbon content per cell, and the abundance of each taxon in the sediment trap samples, we calculated the carbon flux contributed by each taxon (in $mg \text{ C m}^{-2} \text{ d}^{-1}$). This is referred to below as protist carbon (PC) flux.

PC comprised both phyto- and protozooplankton. Phytoplankton was divided into diatoms, flagellates, silicoflagellates, coccoid cells, and plastidic dinoflagellates. Within the flagellates, there was no distinction made between auto- and heterotrophic but between size classes (2.5-5, 5-10, and 10-20 μm); all flagellates possessed a flagellum. Coccoid cells were defined as circular autotrophic cells up to 2 μm in size that were lacking flagella. Protozooplankton was divided into heterotrophic dinoflagellates, ciliates, foraminifera, radiolaria, and heliozoa. All taxa are listed in Appendix 2.

For diatoms, we also enumerated intact empty and broken frustules according to Assmy et al. (2007). While empty frustules can result from mortality factors ranging from natural cell death, viral infection, parasite infestation, protozoan to metazoan grazing, broken frustules are mainly due to handling by copepods. Their equivalent C flux of intact empty and broken diatom frustules was calculated for direct comparison with full cells.

For comparison with re-processed faecal material, PC and the carbon associated with phyto-detrital aggregates quantified in PA gels were summarized under phyto-detritus.

2.4 TEP analyses

TEP were measured both in the sediment trap samples and in the water column. Water samples of 250 mL were collected with Niskin bottles attached to a CTD rosette at discrete depth in the upper 500 m, and were processed in duplicate within a few hours of collection following the protocol of Passow and Alldredge (1995). Samples were filtered onto 0.4 μm polycarbonate filters, stained with Alcian blue and stored at -20°C in sealed polycarbonate tubes. TEP in sediment trap samples were stained according to an adapted method described by Passow et al. (2001).

The amount of Alcian blue stain on each filter was then measured colorimetrically after dissolution in 80% H_2SO_4 on a Pharma Spec UV-1700 spectrophotometer. The Alcian blue

solution was calibrated against Gum Xanthan and TEP concentration expressed as Gum Xanthan equivalents (GX eq., $\mu\text{g L}^{-1}$).

Depth-integrated TEP inventories in the water column were from zero to 100, 200 and 500 m, respectively. TEP content of the trap samples was converted into TEP flux.

3. Results

3.1 Flux characteristics from PA gels

Particle flux at 450 m qualitatively consisted predominantly of large and relatively compact particles (faecal pellets and/or re-processed faecal material), while fragile phyto-detrital aggregates were rare (Fig. 2). However, only small differences were noted between the gels at the beginning and the end of the experiment, as well as between IN and OUT gels (Fig. 3). Prior to iron addition, the sinking material seems to be somewhat more re-worked and several proto-zooplankton were collected (Fig. 3a). Towards the end, slightly more intact faecal pellets and distinct aggregates were present IN and OUT (Fig. 3b, c; respectively), while zooplankton had almost disappeared. But since only few gel samples were available, temporal trends cannot be properly resolved.

3.2 Protist carbon (PC) fluxes

PC fluxes were very low IN and OUT throughout the experiment, mostly $<400 \mu\text{g m}^{-2} \text{d}^{-1}$, with lowest fluxes around Days 15-33 (Fig. 4; Table 2). Due to the limited number of deployments at 200 m (Table 1), flux dynamics over the course of the experiment were not well captured at this depth and are therefore not considered in detail.

PC fluxes were composed of diatoms, flagellates, autotrophic coccoid cells, and autotrophic and heterotrophic dinoflagellates (Fig. 5). All other taxa were present as either just empty and/or broken individuals, or at very low abundance (see below for details).

Dinoflagellates, dominated by *Ceratium pentagonum*, generally contributed more than half of the PC flux, but their dominance decreased over time (Fig. 5; Table 2). However, dinoflagellates were disproportionally represented in the traps as compared to their surface contribution of 15% at the most. Flagellates usually contributed 30-40% of PC flux with an increasing contribution over time (Fig. 5). Diatoms contributed little to PC flux, never more than 16%, but, like the flagellates, their relative contribution seemed to increase over time at the expense of the dinoflagellates. This increase of diatoms and flagellates was even more pronounced in absolute fluxes (Table 2). In terms of C flux, the weekly silicified diatom *Ephemera cf. planamembranacea* played the most important role, followed by *Fragilariopsis*

kerguelensis and *Thalassionema nitzschioides*. Far more numerous than intact diatoms were empty and/or broken frustules and their presence in the traps increased markedly after Day 20 (Fig. 6). Generally, most diatoms encountered during LOHAFEX were present in the lower size-range reported in the literature for the respective species (Hasle and Syvertsen, 1996).

The absolute C flux of coccooid cells (2 μm in diameter) at 450 m increased with time (Table 3), reflected in an increasing relative C flux of these small cells (Fig. 5).

Amongst ciliates, only tintinnids, ciliates living within a rigid structure called the lorica, were found (Appendix 2) and their flux consisted entirely of empty and damaged loricae (Fig. 7). The abundance of tintinnid loricae inside the patch increased throughout the experiment and was always somewhat lower outside the patch (Table 3).

The vast majority of foraminifera tests were empty (Table 4). Some of the empty individuals also showed explicit signs of grazing, such as broken spines and/or tests (Fig. 7).

Radiolaria and Heliozoa played a minor role in the protozoan flux and were thus neglected for PC flux considerations.

3.3 TEP concentrations in the water column and TEP flux

TEP concentrations were highest in the surface layer (upper 20 m) and strongly decreased with depth (Fig. 8a, b). Inside the patch, water column TEP increased over the first two weeks and slightly decreased towards the end again (Fig. 8a; Table 5). Unfortunately, OUT-TEP profiles are only available for the second half of the experiment, but they are very similar to IN-TEP profiles (Fig. 8a, b). Depth-integrated TEP reflects the highest TEP concentrations between Days 14-25 (Fig. 8c). Moreover, the concentrations of TEP and Chl*a* in the surface layer were not correlated ($R^2 = 0.15$, $p = 0.28$).

TEP fluxes throughout the experiment were very low (always $\leq 5 \text{ mg GX eq. m}^{-2} \text{ d}^{-1}$), and showed no marked temporal trends or IN *versus* OUT patch differences (Table 5; Fig. 9).

4. Discussion

4.1 Trap accuracy

Although traps are referred to as either IN or OUT traps, it cannot be ruled out that they collected particles emanating from outside waters and the fertilised patch, respectively. However, the trajectories of the traps were in all cases completely consistent with the surface circulation determined by a ship-board ADCP, which itself was homogenous as deep down as the ADCP could measure (200 m, Martin et al., *subm.*). Given such a consistent circulation from the surface down to the depth of the traps, it is most likely that the traps will have collected particles derived from a relatively small area of the surface water not far removed from the location of the trap. That would suggest that our designation is accurate.

The initial particle assemblage from the PA gels was rather similar in appearance to those collected well after iron enrichment (Fig. 3; see 4.2). This might either reflect the fact that flux characteristics were not influenced by iron fertilisation (see 4.5) or indicate a heavy impact of the trap design on the samples (e.g. Gardner, 2000), or both. The collected particles were not undisturbed as observed in previous studies (Ebersbach and Trull, 2008; Ebersbach et al., 2011; Waite et al., 2000; 2005) and were probably altered in the trap funnel before they settled into the PA gel (Fig. 2, 3). Undisturbed settling is expected to result in more or less evenly and randomly distributed particles across the gel surface, with also fragile shapes of individual particles being well preserved. In contrast, our PA gels revealed particle accumulations presumably derived from individual particles that clogged together as they rolled along the collection funnel when sinking into the sediment trap. The circular alignment of the particulate matter further supports this assumption. Identification of individual particles was thus very difficult (Fig. 3), especially of those that appear to be heavily reworked and may be attributed to re-processed faecal material. These particles might also partly consist of phyto-detritus and/or faecal pellets that were modified during sampling.

4.2 Composition of the flux

Under initial conditions (#1 and #3), PC flux made the highest contribution to particulate organic carbon (POC) flux (14% at 200 m and 6% at 450 m depth, Table 2) during this study. This might possibly be a residual signal from a previous natural bloom that occurred in the eddy prior to our arrival – and is consistent with the evident ^{234}Th -derived POC fluxes in the beginning of the experiment (Martin et al., *subm.*). The slight increase in PC (and POC) towards the end of the experiment (Table 2, Fig. 4) probably reflects the sinking particulate material from the iron-induced bloom. However, PC flux remained very low, playing a minor

role in export. Instead, most of the POC flux consisted of re-processed faecal material and only some phyto-detrital aggregates (see below).

Species contribution within the PC flux differed considerably from that of the surface phytoplankton community. PC flux reflected the phytoplankton composition of the surface layer inasmuch as *Phaeocystis antarctica* and unidentified flagellates dominated PC flux. *P. antarctica* always contributed more than 10% to the biomass in the surface bloom (Schulz et al., in prep.), which is mirrored in its contribution to the flux at 200 and 450 m depth (Table 2). However, while flagellate biomass at the surface exceeded diatom biomass by more than an order of magnitude, flagellate flux into the traps was mostly just 2–4-fold higher than diatom flux (Fig. 10). Even the highest flagellate:diatom flux ratio was 9 (trap #11), still lower than at the surface, where diatoms were almost absent at this time (3%) and flagellates made up 50% of the standing stock. However, this statement has to be regarded with caution because there are several possibilities for errors. Firstly, most flagellates were smaller than diatoms and their shapes are not as distinct as diatom frustules. Secondly, flagellates rather entered the traps embedded in larger particles (compare 4.5). This made it difficult to distinguish between different taxa of flagellates in the trap samples under the microscope, which were loaded with re-processed faecal and phyto-detrital material that might cover individual flagellates. Contrariwise, during sampling (compare 4.1) and during splitting of the trap samples large particles might have been broken up and released their content such as flagellates so that they were nonetheless counted for the most part. This reduces the bias towards diatoms. However, as the same bias applies to the surface community a comparison between surface and trap PC composition is nevertheless valid. Our data thus point to preferential export of diatoms even when they comprise just a very minor fraction of the phytoplankton community (compare 4.5).

The marked increase in the number of intact empty and broken diatom frustules (Fig. 6) as well as empty and damaged tintinnid loricae is indicative of high grazing activity at the surface. While empty loricae can be partly explained by the detachment of the ciliate cell from its lorica during sample fixation damaged loricae can be only explained by deformation of the tough lorica through crustacean grazing. The absence of “naked” tintinnid cells detached from their loricae in the trap material further points to selective removal of the refractory loricae while the inhabiting ciliates were grazed at the surface. Similarly, broken radiolaria, silicoflagellates and foraminifera (partly with bitten off spines) outnumbered intact individuals in the trap samples by a wide margin (20-fold and more for foraminifera; Table 4). The high amount of recognisable remains of the aforementioned taxa in faecal pellets and re-processed faecal material further points to heavy grazing pressure by the local copepod community.

While phyto-detritus (PC and phyto-detrital aggregates) did not contribute to POC flux to a large extent, export flux was dominated by heavily processed particulate matter (Fig. 2 and 3). Most of it appears to be of faecal origin (compare also 4.1), indicative of grazing as described above. The intact faecal pellets were probably derived from copepods and they contributed around 45% to POC flux as determined from sediment traps (Martin et al., *subm.*) The somewhat looser material (re-processed faecal material) might be due to coprorhexy, the disintegration of faecal pellets (Lampitt et al., 1990). Thus retention played an important role in channelling carbon through the pelagic food web and eventually led to an export flux dominated by faecal material as evidenced by the PA gels (Fig. 2 and 3).

4.3. The role of TEP for export processes

Water column TEP profiles (Fig. 8a, b) showed the usual pattern of high surface concentrations and a strong decrease with depth (Passow, 2002). However, TEP concentrations were about one order of magnitude lower than in previous Southern Ocean studies (Passow et al., 1995; Hong et al., 1997). Furthermore, TEP fluxes were very low at 200 and at 450 m (Fig. 9). Due to the limited number of other TEP flux studies, the results from this study can only be compared to a diatom bloom in the North Atlantic (Martin et al., 2011) and a study in the Santa Barbara Channel (Passow et al., 2001). Both studies reported TEP fluxes of about $100 \text{ mg GX eq. m}^{-2} \text{ d}^{-1}$, far higher than the $\leq 5 \text{ mg GX eq. m}^{-2} \text{ d}^{-1}$ found during LOHAFEX.

At a first look this seems to stand in contrast to the observation that flagellate dominated blooms (like the LOHAFEX bloom) were observed to correlate with TEP production (Riebesell et al., 1995; Hong et al., 1997; Reigstad and Wassmann 2007). However, the sinking particulate material during LOHAFEX consisted predominantly of re-processed faecal material (not of TEP rich phyto-detritus). Thus, the low TEP fluxes seem reasonable. However, these low fluxes still constitute a large fraction of water column TEP (up to $12\% \text{ d}^{-1}$; Table 5), compared to the $2\% \text{ d}^{-1}$ from the Santa Barbara Channel, where water column TEP was much higher (Passow et al., 2001).

Furthermore, neither POC and TEP fluxes, nor PC and TEP fluxes were correlated ($R^2 = 0.01$, $p = 0.80$ and $R^2 = 0.01$, $p = 0.82$, respectively), suggesting an export process other than the formation of TEP-containing aggregates. TEP loss due to grazing has been examined in previous studies (e.g. Passow and Alldredge, 1999; Ling and Alldredge, 2003) and is presumably responsible for the low TEP concentration during LOHAFEX. Nevertheless, it appears as though TEP formation during LOHAFEX was of low importance for downward POC flux.

4.4 Comparison to previous iron fertilisation studies

LOHAFEX was carried out in the northern part of the ACC in waters strongly depleted in silicic acid ($<2 \mu\text{mol L}^{-1}$) and the iron-induced phytoplankton bloom was dominated by flagellates. While, most previous iron fertilisation experiments resulted in diatom blooms (Boyd et al., 2007), two other experiments under low silicic acid concentrations have been conducted: SOFEX-N (Coale et al., 2004), and SAGE (Harvey et al., 2011).

Silicic acid concentrations during SOFEX-N were initially close to $3 \mu\text{mol L}^{-1}$ and declined during the experiment due to the growth of *Pseudo-nitzschia* spp. Flagellates and diatoms had a roughly equal share to bloom biomass by the end of the experiment (Coale et al., 2004). During SAGE silicic acid concentrations were $<1 \mu\text{mol L}^{-1}$ and the surface phytoplankton community was dominated by picoplankton ($<2 \mu\text{m}$) with very few diatoms present (Peloquin et al., 2011). In terms of phytoplankton community composition, LOHAFEX is more similar to SAGE despite a larger contribution of diatoms and the majority of flagellates associated with the nano-size fraction.

Iron addition during SOFEX-N led to enhanced export flux in the upper 100 m (Bishop et al., 2004; Coale et al., 2004). During SAGE, particle export was unfortunately not measured, but remineralisation in the surface was intense (Harvey et al., 2011). Neither of the two studies (nor any other artificial iron fertilisation experiment except EIFEX) revealed enhanced carbon export to the deep ocean (Boyd et al., 2007; Harvey et al., 2011; Smetacek et al., 2012). The EIFEX study, on the other hand, showed the clearest response in terms of sequestering carbon through iron fertilisation: A massive sinking event of the senescent bloom was observed at the end of the experiment and followed to a depth of more than 1000 m (Smetacek et al., 2012). During LOHAFEX, neither shallow export flux nor deeper carbon fluxes were enhanced, and most of the algal biomass that was built up at the surface upon iron addition was retained in the upper 100 m (Martin et al., *subm.*).

During EIFEX and SOIREE diatom-aggregates dominated the flux (Smetacek et al., 2012; Waite and Nodder, 2001), and export flux of the natural CROZEX bloom consisted of phyto-detrital aggregates (Salter et al., 2007). SOFEX export flux was probably also regulated through phyto-detritus and aggregated diatoms were found in the surface (Coale et al., 2004). In the initial phase of the SOFEX-N bloom Lam and Bishop (2007) found the flux below 200 m to be dominated by various faecal aggregates and inferred that grazing activities determined export flux characteristics. However, they did not examine the demise of the bloom. Nevertheless, the majority of the iron fertilisation studies identified phyto-detritus as the main export flux driver. Diatoms played the major role for the formation of phyto-detritus in these studies and therefore provided a pool of non-digested phytoplankton aggregates that

result from physical aggregation. These findings stand in contrast to LOHAFEX, where the sinking particle assemblage predominantly consisted of re-processed faecal material (see 4.2) and intact faecal pellets contributed around 45% of total POC (Martin et al., *subm.*), which indicates biological re-processing (in contrast to physical aggregation). A somewhat similar composition of the particulate matter was detected during the natural iron fertilisation study KEOPS (Blain et al., 2007). Faecal aggregates and intact faecal pellets made up for most of the export flux during KEOPS (Ebersbach and Trull, 2008), although the surface community was dominated by diatoms (Armand et al., 2008). Thus, not only species composition of a bloom is relevant for export fluxes (as repeatedly shown in models (e.g. Jackson, 1990; Riebesell and Wolf-Gladrow, 1992)), but also the reprocessing by the grazer community. This is illustrated by the fact that both diatom- and flagellate-dominated blooms (KEOPS and LOHAFEX, respectively) were regulated by grazers.

4.5 Mechanisms of export flux

Thus the very low export flux during LOHAFEX appears to have been regulated through grazing. What can be a possible mechanism for the downward transport, keeping in mind that the surface phytoplankton composition is qualitatively (in terms of species present) but not quantitatively (in terms of relative composition) displayed in the sinking particles? Despite the vast dominance of flagellates over diatoms in the water column, diatoms contributed relatively more to the flux. This was also observed during CROZEX, where export flux was mainly carried by diatoms, although flagellates contributed most to the surface bloom (Poulton et al., 2007; Salter et al., 2007) and SOFEX-N, where the communities driving export fluxes shifted towards diatoms, while flagellates were important for surface biomass built up (Coale et al., 2004). However, in both of these cases diatoms comprised a large portion of total phytoplankton biomass in the surface. Our data suggest that diatoms are preferentially exported even when they form a very minor component of the community, and do not sink out in mass sedimentation events initiated by TEP-mediated coagulation. Especially the silica-ballast associated with the empty cells and chains of the heavily silicified diatoms typical for the Southern Ocean (e.g. *F. kerguelensis*) facilitates sedimentation.

Furthermore, a study in the Barents Sea revealed a similar pattern and suggested that the contribution of flagellates (especially *Phaeocystis*) to export flux is not of importance, whereas diatoms always sink out of surface waters (Reigstad and Wassmann, 2007). The explanation is that un-grazed diatoms form rapidly sinking aggregates (Beaulieu, 2002 and references therein), a strategy embedded in their life history cycles (Smetacek 1985). In contrast, most flagellates are retained in the surface layer by selective grazing pressure on

them and only a small fraction of the surface population actually reaches deep waters, probably integrated in re-processed faecal aggregates and phyto-detrital aggregates (as seen during LOHAFEX; Fig. 9). According to Richardson and Jackson (2007) small phytoplankton can be exported directly from the surface – incorporated in larger aggregates – which is in agreement with our findings.

5. Conclusions

Deep export fluxes during the iron fertilisation experiment LOHAFEX were very low. The bulk of the iron-induced biomass built up at the surface was remineralised within the upper 100 m. The particulate matter predominantly consisted of re-processed faecal material, while phyto-detritus (PC and phyto-detrital aggregates) played only a minor role in overall export. This fact illustrates the strong grazing pressure in the surface layer.

Remarkably, diatom export was disproportionately high. Whereas diatoms made up less than 3% to the surface bloom consisting almost entirely of flagellates (more than 95%), their contribution to export flux was as high as 12%. This selective export is an important finding, as it demonstrates that the ability of a pelagic ecosystem to sequester CO₂ is impacted not only by surface composition but also by export process.

References

- Armand, L.K., Cornet-Barthaux, V., Mosseri, J., Quéguiner, B., 2008. Late summer diatom biomass and community structure on and around the naturally iron-fertilised Kerguelen Plateau in the Southern Ocean. *Deep Sea Research Part II: Topical Studies in Oceanography* 55 (5-7), 653-676.
- Assmy, P., Henjes, J., Klaas, C., Smetacek, V., 2007. Mechanisms determining species dominance in a phytoplankton bloom induced by the iron fertilization experiment EisenEx in the Southern Ocean. *Deep Sea Research I* 54, 340-362.
- Beaulieu, S.E., 2002. Accumulation and fate of phytodetritus on the sea floor. *Oceanography and Marine Biology: an Annual Review* 40, 171-232.
- Bishop, J.K.B., Wood, T.J., Davis, R.E., Sherman, J.T., 2004. Robotic Observations of Enhanced Biomass and Export at 55°S During SOFex. *Science* 304, 417-420.
- Blain, S., Quéguiner, B., Armand, L., Belviso, S., Bombled, B., Bopp, L., Bowie, A., Brunet, C., Brussaard, C., Carlotti, F., Christaki, U., Corbiere, A., Durand, I., Ebersbach, F., Fuda, J.-L., Garcia, N., Gerringa, L., Griffiths, B., Guige, C., Guillerm, C., Jacquet, S.H.M., Jeandel, C., Laan, P., Lefevre, D., Lo Monaco, C., Malits, A., Mosseri, J., Obernosterer, I., Park, Y.-H., Picheral, M., Pondaven, P., Remenyi, T., Sandroni, V., Sarthou, G., Savoye, N., Scouarnec, L., Souhaut, M., Thuiller, D., Timmermans, K., Trull, T., Uitz, J., van Beek, P., Veldhuis, M., Vincent, D., Viollier, E., Vong, L., Wagener, T., 2007. Effect of natural iron fertilization on carbon sequestration in the Southern Ocean. *Nature* 446, 1070-1075.
- Boyd, P.W., Jickells, T., Law, C., Blain, S., Boyle, E.A., Buesseler, K.O., Coale, K.H., Cullen, J.J., de Baar, H.J.W., Follows, M., Harvey, M., Lancelot, C., Levasseur, M., Owens, N.P.J., Pollard, R., Rivkin, R.B., Sarmiento, J., Schoemann, V., Smetacek, V., Takeda, S., Tsuda, A., Turner, S., Watson, A.J., 2007. Mesoscale Iron Enrichment Experiments 1993-2005: Synthesis and Future Directions. *Science* 315, 612-617.
- Boyd, P.W., Trull, T.W., 2007. Understanding the export of biogenic particles in oceanic waters: Is there consensus? *Progress in Oceanography* 72 (4), 276-312.
- Boyd, P.W., Watson, A.J., Law, C.S., Abraham, E.R., Trull, T., Murdoch, R., Bakker, D.C.E., Bowie, A.R., Buesseler, K.O., Chang, H., Charette, M., Croot, P., Downing, K., Frew, R., Gall, M., Hadfield, M., Hall, J., Harvey, M., Jameson, G., LaRoche, J., Liddicoat, M., Ling, R., Maldonado, M.T., McKay, R.M., Nodder, S., Pickmere, S., Pridmore, R., Rintoul, S., Safi, K., Sutton, P., Strzepek, R., Tanneberger, K., Turner, S., Waite, A., Zeldis, J., 2000. A mesoscale phytoplankton bloom in the polar Southern Ocean stimulated by iron fertilization. *Nature* 407 (6805), 695-702.
- Buesseler, K.O., Boyd, P.W., 2009. Shedding light on processes that control particle export and flux attenuation in the twilight zone of the open ocean. *Limnology and Oceanography* 54 (4), 1210-1232.
- Coale, K.H., Johnson, K.S., Chavez, F.P., Buesseler, K.O., Barber, R.T., Brzezinski, M.A., Cochlan, W.P., Millero, F.J., Falkowski, P.G., Bauer, J.E., Wanninkhof, R.H., Kudela, R.M., Altabet, M.A., Hales, B.E., Takahashi, T., Landrey, M.R., Bidigare, R.R., Wang, X., Chase, Z., Strutton, P.G., Friederich, G.E., Gorbunov, M.Y., Lance, V.P., Hilting, A.K., Hiscock, M.R., Demarest, M., Hiscock, W.T., Sullivan, K.F., Tanner, S.J., Gordon, R.M., Hunter, C.N.,

Elrod, V.A., Fitzwater, S.E., Jones, J.L., Tozzi, S., Koblizek, M., Roberts, A.E., Herndon, J., Brewster, J., Ladizinsky, N., Smith, G., Cooper, D., Timothy, D., Brown, S.L., Selph, K.E., Sheridan, C.C., Twining, B.S., Johnson, Z.I., 2004. Southern Ocean Iron Enrichment Experiment: Carbon Cycling on High- and Low-Si Waters. *Science* 304, 408-414.

De La Rocha, C.L., 2007. The Biological Pump. In: Heinrich, D.H., Karl, K.T. (Eds.), *Treatise on Geochemistry*. Pergamon, Oxford, pp. 1-29.

Ebersbach, F., Trull, T., 2008. Sinking particle properties from polyacrylamide gels during the Kerguelen Ocean and Plateau compared Study (KEOPS): Zooplankton control of carbon export in an area of persistent natural iron inputs in the Southern Ocean. *Limnology and Oceanography* 53 (1), 212-224.

Ebersbach, F., Trull, T.W., Davies, D.M., Bray, S.G., 2011. Controls on mesopelagic particle fluxes in the Sub-Antarctic and Polar Frontal Zones in the Southern Ocean south of Australia in summer - perspectives from free-drifting sediment traps. *Deep-Sea Research II* 58 (21-22), 2260-2276.

Francois, R., Honjo, S., Krishfield, R., Manganini, S., 2002. Factors controlling the flux of the organic carbon to the bathypelagic zone of the ocean. *Global Biogeochemical Cycles* 16 (4, 1087), 34, 31-20.

Gardner, W.D., 2000. Sediment trap sampling in surface waters. In: Hanson, R.B., Ducklow, H.W., Field, J.G. (Eds.), *The Changing Ocean Carbon Cycle, A midterm synthesis of the Joint Global Ocean Flux Study*. Cambridge University Press, Cambridge, pp. 240-280.

Harvey, M.J., Law, C.S., Smith, M.J., Hall, J.A., Abraham, E.R., Stevens, C.L., Hadfield, M.G., Ho, D.T., Ward, B., Archer, S.D., Caine, J.M., Currie, K.I., Devries, D., Ellwood, M.J., Hill, P., Jones, G.B., Katz, D., Kuparinen, J., Macaskill, B., Main, W., Marriner, A., McGregor, J., McNeil, C., Minnett, P.J., Nodder, S.D., Peloquin, J., Pickmere, S., Pinkerton, M.H., Safi, K.A., Thompson, R., Walkington, M., Wright, S.W., Ziolkowski, L.A., 2011. The SOLAS air-sea gas exchange experiment (SAGE) 2004. *Deep Sea Research Part II: Topical Studies in Oceanography* 58 (6), 753-763.

Hasle, G.R., Syvertsen, E.E., 1996. Marine diatoms. In: Tomas, C.R. (Ed.), *Identifying Marine Diatoms and Dinoflagellates*. Academic Press, Inc., New York, pp. 5-385.

Hillebrand, H., Dürselen, C.-D., Kirschtel, D., Pollinger, U., Tamar, Z., 1999. Biovolume calculation for pelagic and benthic microalgae. *J. Phycol.* 35, 403-424.

Hong, Y., Smith, W.O.J., White, A.-M., 1997. Studies on transparent exopolymer particles (TEP) produced in the Ross Sea (Antarctica) and by *Phaeocystis Antarctica* (Prymnesiophyceae). *Journal of Phycology* 33, 368-376.

Jackson, G.A., 1990. A model of the formation of marine algal flocs by physical coagulation processes. *Deep Sea Research I* 37, 1197-1211.

Kwon, E.Y., Primeau, F., Sarmiento, J.L., 2009. The impact of remineralization depth on the air-sea carbon balance. *Nature Geoscience* 2, 630-635.

Lam, P.J., Bishop, J.K.B., 2007. High biomass, low export regimes in the Southern Ocean. *Deep Sea Research II* 54, 601-638.

Lamborg, C.H., Buesseler, K.O., Valdes, J., Bertrand, C.H., Bidigare, R.R., Manganini, S.J., Pike, S., Steinberg, D.K., Trull, T.W., Wilson, S., 2008. The flux of bio- and lithogenic material associated with sinking particles in the mesopelagic 'twilight zone' of the northwest and North Central Pacific Ocean. *Deep Sea Research II* 55, 1540-1562.

Lampitt, R.S., Achterberg, E.P., Andersom, T.H., Hughes, J.A., Iglesias-Rodriguez, M.D., Kelly-Gerreyn, B.A., Lucas, M.I., Popova, E.E., Sanders, R., Shepherd, J.G., Smythe-Wright, D., Yool, A., 2008a. Ocean fertilization: a potential means of geoengineering? *Philosophical Transactions of the Royal Society A* published online, 1-27.

Lampitt, R.S., Boorman, B., Brown, L., Lucas, M., Salter, I., Sanders, R., Saw, K., Seeyave, S., Thomalla, S.J., Turnewitsch, R., 2008b. Particle export from the euphotic zone: Estimates using a novel drifting sediment trap, 234Th and new production. *Deep Sea Research Part I: Oceanographic Research Papers* 55 (11), 1484-1502.

Lampitt, R.S., Noji, T., von Bodungen, B., 1990. What happens to zooplankton faecal pellets? Implications for material flux. *Marine Biology* 104, 15-23.

Ling, S.C., Alldredge, A.L., 2003. Does the marine copepod *Calanus pacificus* consume transparent exopolymers (TEP). *Journal of Plankton Research* 25 (5), 507-515.

Lutz, M., Dunbar, R., Caldeira, K., 2002. Regional variability in the vertical flux of particulate organic carbon in the ocean interior. *Global Biogeochemical Cycles* 16 (3), 1037, 11/11-18.

Martin, J.H., 1990. Glacial-Interglacial CO₂ Change: The Iron Hypothesis. *Paleoceanography* 5 (1), 1-13.

Martin, P., Lampitt, R.S., Perry, M.J., Sanders, R., Lee, C., D'Asaro, E., 2011. Export and mesopelagic particle flux during a North Atlantic spring diatom bloom. *Deep-Sea Research I* 58, 338-349.

Martin, P., Rutgers van der Loeff, M.M., Cassar, N., Vandromme, P., d'Ovidio, F., Rengarajan, R., Soares, M., Gonzalez, H.E., Ebersbach, F., Lampitt, R.S., Sanders, R., Barnett, B.A., Smetacek, V., Naqvi, S.W.A., subm. Iron fertilization enhanced net community production but not downward particle flux during LOHAFEX. *Global Biogeochemical Cycles*.

Menden-Deuer, S., Lessard, E.J., 2000. Carbon to volume relationship for dinoflagellates, diatoms, and other protist plankton. *Limnology and Oceanography* 45 (3), 569-579.

Parekh, P., Dutkiewicz, P., Follows, M.J., Ito, T., 2006. Atmospheric carbon dioxide in a less dusty world. *Geophysical Research Letter* 33 (L03610).

Passow, U., 2002. Transparent exopolymer particles (TEP) in aquatic environments. *Progress in Oceanography* 55, 287-333.

Passow, U., Alldredge, A.L., 1995. A dye-binding assay for the spectrophotometric measurement of transparent exopolymer particles (TEP). *Limnology and Oceanography* 40 (7), 1326-1335.

Passow, U., Alldredge, A., 1999. Do transparent exopolymer particles (TEP) inhibit grazing by the euphausiid *Euphausia pacifica*? *Journal of Plankton Research* 21, 2203-2217.

Passow, U., Kozłowski, W., Vernet, M., 1995. Palmer LTER: Temporal variability of transparent exopolymer particles in Arthur Harbor during the 1994-1995 growth season. *Antarctic Journal of the United States* 30, 265-266.

Passow, U., Shipe, R.F., Murray, A., Pak, D.K., Brzezinski, M.A., Alldredge, A.L., 2001. The origin of transparent exopolymer particles (TEP) and their role in the sedimentation of particulate matter. *Continental Shelf Research* 21, 327-346.

Peloquin, J., Hall, J., Safi, K., Smith Jr, W.O., Wright, S., van den Enden, R., 2011. The response of phytoplankton to iron enrichment in Sub-Antarctic HNLCLS waters: Results from the SAGE experiment. *Deep Sea Research Part II: Topical Studies in Oceanography* 58 (6), 808-823.

Pollard, R., Sanders, R., Lucas, M., Statham, P., 2007. The Crozet Natural Iron Bloom and Export Experiment (CROZEX). *Deep Sea Research II* 54 (18-20), 1905-1914.

Poulton, A.J., Moore, C.M., Seeyave, S., Lucas, M.I., Fielding, S., Ward, P., 2007. Phytoplankton community composition around the Crozet Plateau, with emphasis on diatoms and Phaeocystis. *Deep-Sea Research II* 54, 2085-2105.

Reigstad, M., Wassmann, P., 2007. Does Phaeocystis spp. contribute significantly to vertical export of organic carbon? *Biogeochemistry*, 1-18.

Richardson, T.L., Jackson, G.A., 2007. Small Phytoplankton and Carbon Export from the Surface Ocean. *Science* 315, 838-840.

Riebesell, U., Reigstad, M., Wassmann, P., Noji, T., Passow, U., 1995. On the trophic fate of Phaeocystis pouchetii (Hariot): VI. Significance of Phaeocystis-derived mucus for vertical flux. *Netherlands Journal of Sea Research* 33, 193-203.

Riebesell, U., Wolf-Gladrow, D., 1992. The relationship between physical aggregation of phytoplankton and particle flux: a numerical model. *Deep-Sea Research* 39 (7/8), 1085-1102.

Salter, I., Lampitt, R.S., Sanders, R., Poulton, A., Kemp, A.E.S., Boorman, B., Saw, K., Pearce, R., 2007. Estimating carbon, silica and diatom export from a naturally fertilised phytoplankton bloom in the Southern Ocean using PELAGRA: A novel drifting sediment trap. *Deep Sea Research Part II: Topical Studies in Oceanography* 54 (18-20), 2233-2259.

Schulz, I., Assmy, P., Ebersbach, F., Gauns, M., Klaas, C., Mazzocchi, M.G., Roy, R., Sakar, A., Thiele, S., Wolf, C., Wolzenburg, S., Smetacek, V., in prep. Response of a flagellate-dominated plankton community to artificial iron fertilization in the Southern Ocean. *Deep Sea Research Part II: Topical Studies in Oceanography*.

Smetacek, V., 1985. Role of sinking in diatom life-history cycles: ecological, evolutionary and geological significance. *Marine Biology* 84, 239-251.

Smetacek, V., Klaas, C., Strass, V.H., Assmy, P., Montresor, M., Cisewski, B., Savoye, N., Webb, A., d'Ovidio, F., Arrieta, J.M., Bathmann, U., Bellerby, R., Berg, G.M., Croot, P.L., Gonzalez, S., Henjes, J., Herndl, G.J., Hoffmann, L.J., Leach, H., Losch, M., Mills, M.M., Neill, C., Peeken, I., Röttgers, R., Sachs, O., Sauter, E., Schmidt, M.M., Schwarz, J., Terbrüggen, A., Wolf-Gladrow, D., 2012. Deep carbon export from a Southern Ocean iron-fertilized diatom bloom. *Nature* 487, 313-319.

Smetacek, V., Naqvi, S.W.A., 2008. The next generation of iron fertilisation experiments in the Southern Ocean. *Philosophical Transactions of the Royal Society London A*. 366, 3947-3967.

Taucher, J., Oschlies, A., 2011. Can we predict the direction of marine primary production change under global warming? *Geophysical Research Letter* 38 (L02603).

Thronsen, J., 1995. Estimating cell numbers. In: Hallegraeff, G.M., M., A.D., Cembella, A.D. (Eds.), *Manual on Harmful Marine Microalgae*. UNESCO, Paris, pp. 63-80.

Turner, J.T., 2002. Zooplankton fecal pellets, marine snow and sinking phytoplankton blooms. *Aquatic Microbial Ecology* 27 (1), 57-102.

Volk, T., Hoffert, M.I., 1985. Ocean carbon pumps: analysis of relative strengths and efficiencies in ocean-driven atmospheric CO₂ changes. *Geophysical Monographs* 32, 99-110.

Waite, A.M., Gustafsson, Ö., Lindahl, O., Tiselius, P., 2005. Linking ecosystem dynamics and biogeochemistry: Sinking fractionation of organic carbon in a Swedish fjord. *Limnology and Oceanography* 50 (2), 658-671.

Waite, A.M., Nodder, S.D., 2001. The effect of in situ iron addition on the sinking rates and export flux of Southern Ocean diatoms. *Deep-Sea Research II* 48, 2635-2654.

Waite, A.M., Safi, K.A., Hall, J.A., Nodder, S.D., 2000. Mass sedimentation of picoplankton embedded in organic aggregates. *Limnology and Oceanography* 45 (1), 87-97.

Figures

Fig. 1. Composite MODIS image of the LOHAFEX study area showing Chl a surface concentrations in the period 12 to 14 February. The iron-induced bloom is encircled (its elongated form is just an “illusion” because the “circular” patch had moved over the three days the MODIS image was assembled). Note the size of the much larger natural phytoplankton blooms in the northeast of the (artificial) LOHAFEX bloom for comparison. (Source: <http://modis.gsfc.nasa.gov/>)

Fig. 2. Image of entire PA gel (Gel 6; see Table 1 for deployment time), in which particulate flux of a 24 h sampling period, IN, from the second half of the LOHAFEX study is preserved. The uneven distribution of the particulate matter points to a strong impact of the trap design on the collection procedure (see 4.1.2 for a detailed discussion). The diameter of the gel is 10 cm.

Fig. 3. Detailed images of PA gels as they were obtained during LOHAFEX: a) Gel 1-3 (IN, parallel samples, d0-d2), b) Gel 4/5 (OUT, parallel samples, d26), c) Gel 6 (IN, d34). See Table 1 for deployment details. The majority of the collected particles appear to be of faecal origin; in the beginning the material seems to be more re-worked (a)), while at the end more intact faecal pellets and thus fresher material was found (b), c)). Note that the protozooplankton almost disappeared in Gel 4-6 from the second half of the experiment. (Scale bar: 1 cm)

Fig. 4. Total Unicellular Planktonic Carbon (PC) flux determined from PELAGRA trap samples: Development of IN and OUT fluxes at 200 and 450 m, respectively.

Fig. 5. Relative Unicellular Plankton Carbon (UPC) flux of the C flux carrying groups i) diatoms, ii) flagellates, iii) coccoid cells, and iv) dinoflagellates: Development over the course of the experiment a) at 200 m (IN and OUT), b) at 450 m IN, and c) at 450 m OUT.

Fig. 6. Contribution of diatoms to the flux at 450 m inside the patch (IN) throughout the course of the experiment: C flux (full frustules) and C flux equivalent (empty and broken frustules), total diatom flux.

Fig. 7. Images showing the flux composition as examined with the microscope (from bulk sediment trap samples; a, b, c, f: 450 m; e, d: 200 m): a) dinoflagellate *Gyrodinium* spec. and

aggregates (re-processed faecal material and (loose) phyto-detritus), b) broken radiolaria embedded in re-processed faecal matter, c) shells of probably protozoan origin (for instance empty tintinnid loricae) integrated in re-processed faecal material and phyto-detrital aggregates, d) foraminifera with broken spines and dinoflagellate *C. pentagonum* incorporated in re-processed faecal material, e) broken diatoms *Rhizosolenia* spec., *C. pentagonum*, and aggregates of re-processed faecal matter and phyto-detritus, f) re-processed faecal material, phyto-detrital aggregates and recognisable individual faecal pellets.

Fig. 8. TEP distribution in the upper 500 m of the water column: profiles a) IN, and b) OUT, c) integrated TEP over the water column.

Fig. 9. TEP flux at 200 m and 450 m over the course of the experiment,

Fig. 10. Ratio of diatom flux : flagellate flux, surface composition and trap

Tables

Table 1. PELAGRA trap deployments.

Table 2. PC flux, separated into diatoms, flagellates, coccoid cells and dinoflagellates.

Table 3. Abundance of tintinnid ciliates from PELAGRA traps: abundance of empty and crashed loricae together is presented (and the damaged loricae as a fraction thereof is given in brackets). Note: no full tintinnids were present.

Table 4. Abundances of foraminifera: distinction between full, empty and broken individuals ($10^3 \# m^{-2} d^{-1}$). For the total abundance fractions are given in brackets.

Table 5. TEP concentration in the water column and TEP flux.

Appendix

Appendix 1. Particle types found in the PA gels: fm: re-processed faecal material, pd: phyto-detritus, fp: intact faecal pellet. Scale bar: 1 mm.

Appendix 2. Plankton groups present in the PELAGRA traps.

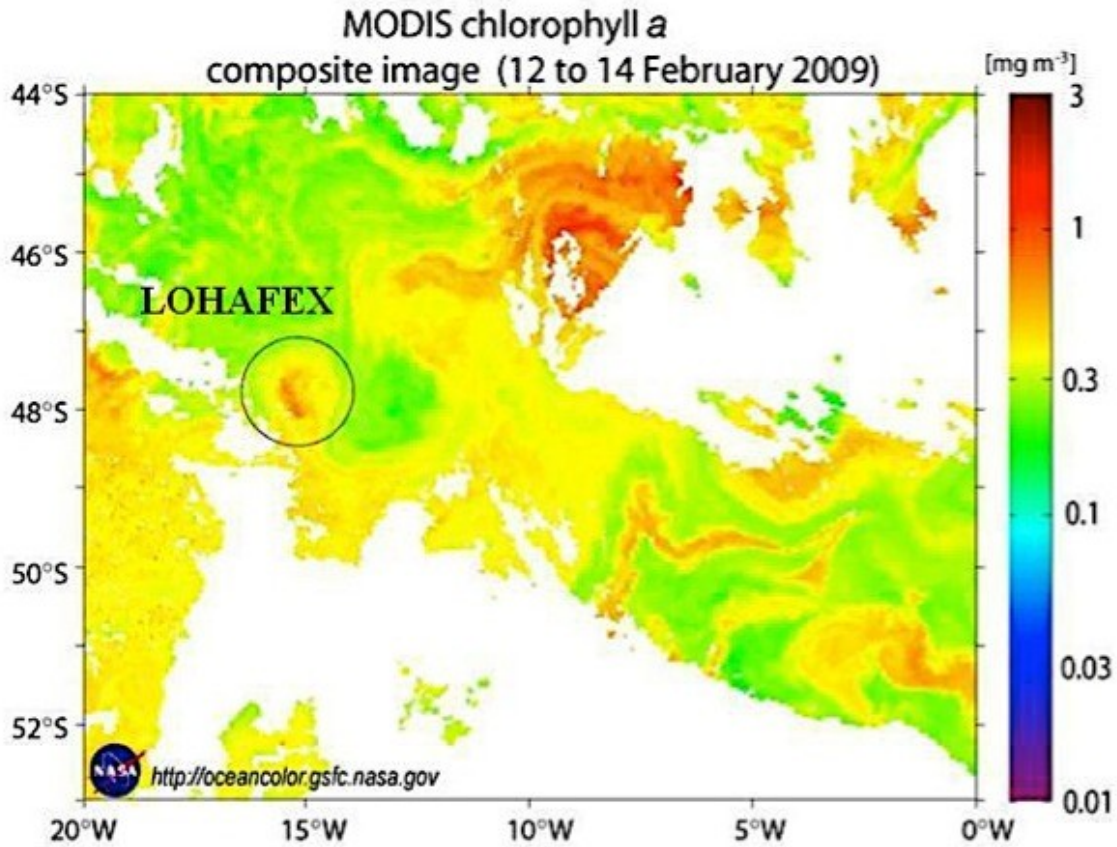


Fig. 1. Composite MODIS image of the LOHAFEX study area showing Chl*a* surface concentrations in the period 12 to 14 February. The iron-induced bloom is encircled (its elongated form is just an “illusion” because the “circular” patch had moved over the three days the MODIS image was assembled). Note the size of the much larger natural phytoplankton blooms in the northeast of the (artificial) LOHAFEX bloom for comparison. (Source: <http://modis.gsfc.nasa.gov/>).

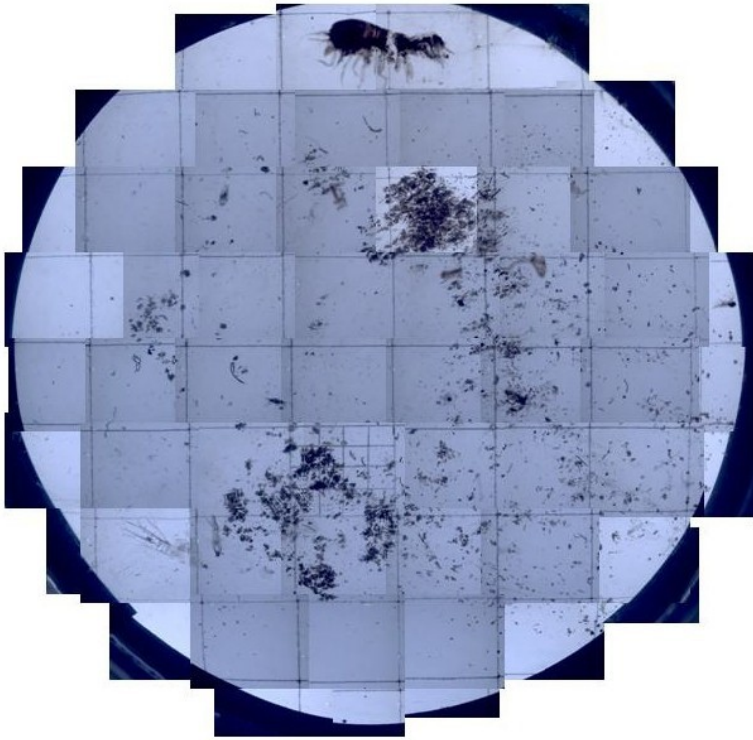


Fig. 2. Image of entire PA gel (Gel 6; see Table 1 for deployment time), in which particulate flux of a 24 h sampling period, IN, from the second half of the LOHAFEX study is preserved. The uneven distribution of the particulate matter points to a strong impact of the trap design on the collection procedure (see 4.1.2 for a detailed discussion). The diameter of the gel is 10 cm.

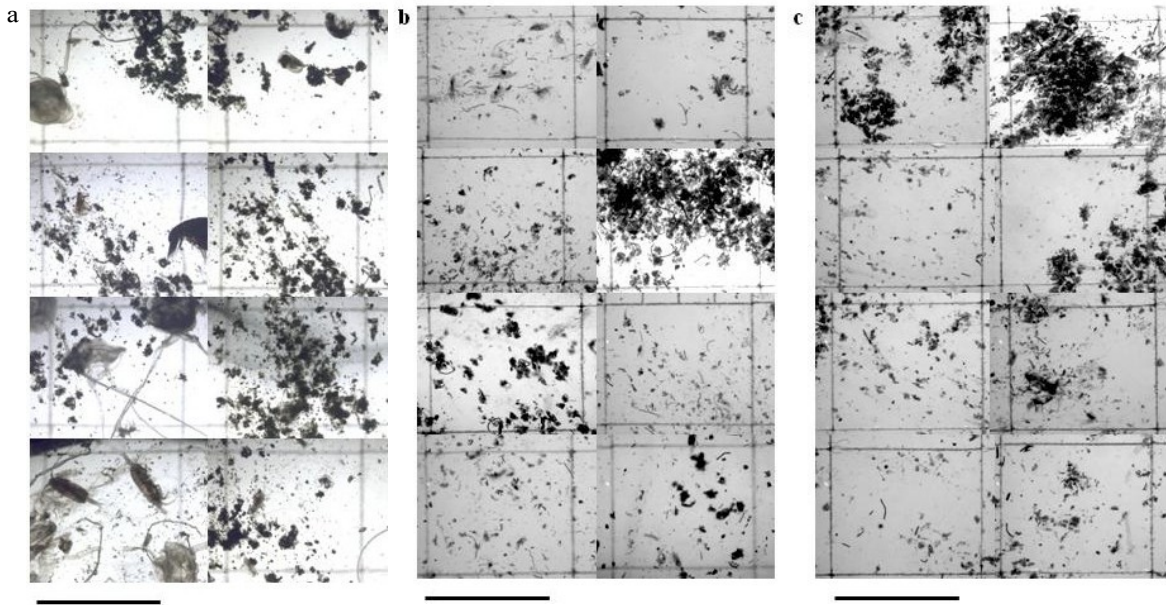


Fig. 3. Detailed images of PA gels as they were obtained during LOHAFEX: a) Gel 1-3 (IN, parallel samples, d0-d2), b) Gel 4/5 (OUT, parallel samples, d26), c) Gel 6 (IN, d34). See Table 1 for deployment details. The majority of the collected particles appear to be of faecal origin; in the beginning the material seems to be more re-worked (a)), while at the end more intact faecal pellets and thus fresher material was found (b), c)). Note that the protozooplankton almost disappeared in Gel 4-6 from the second half of the experiment. (Scale bar: 1 cm).

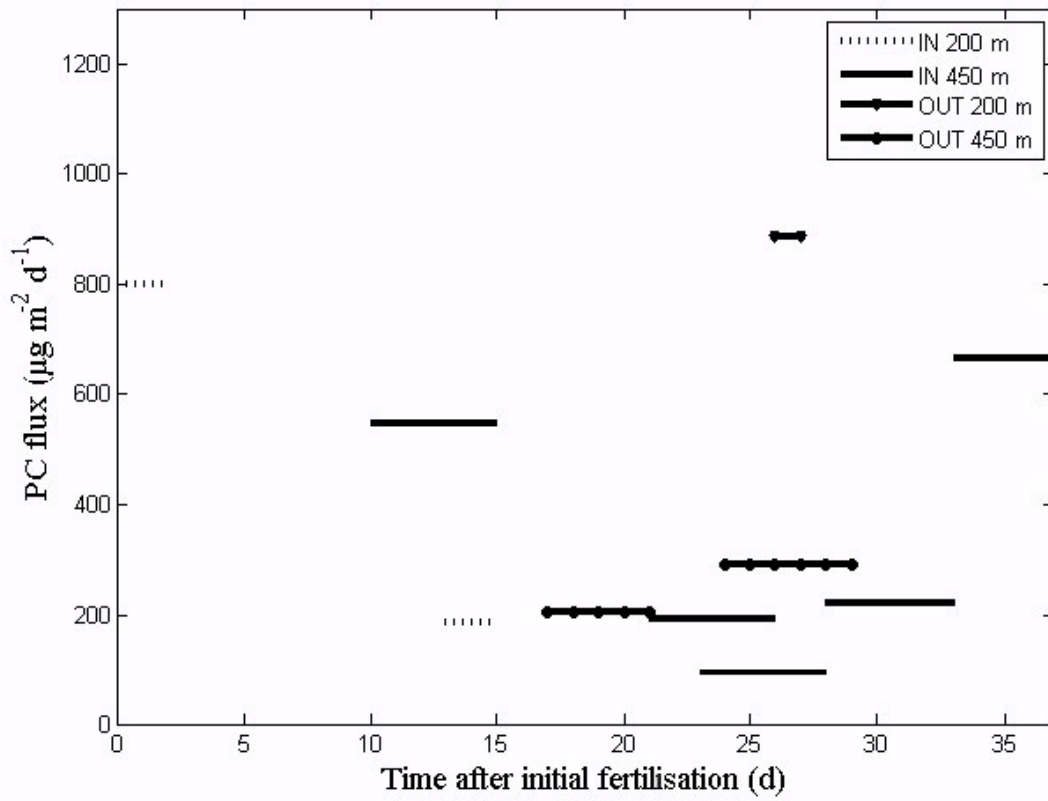


Fig. 4. Total Unicellular Planktonic Carbon (PC) flux determined from PELAGRA trap samples: Development of IN and OUT fluxes at 200 and 450 m, respectively.

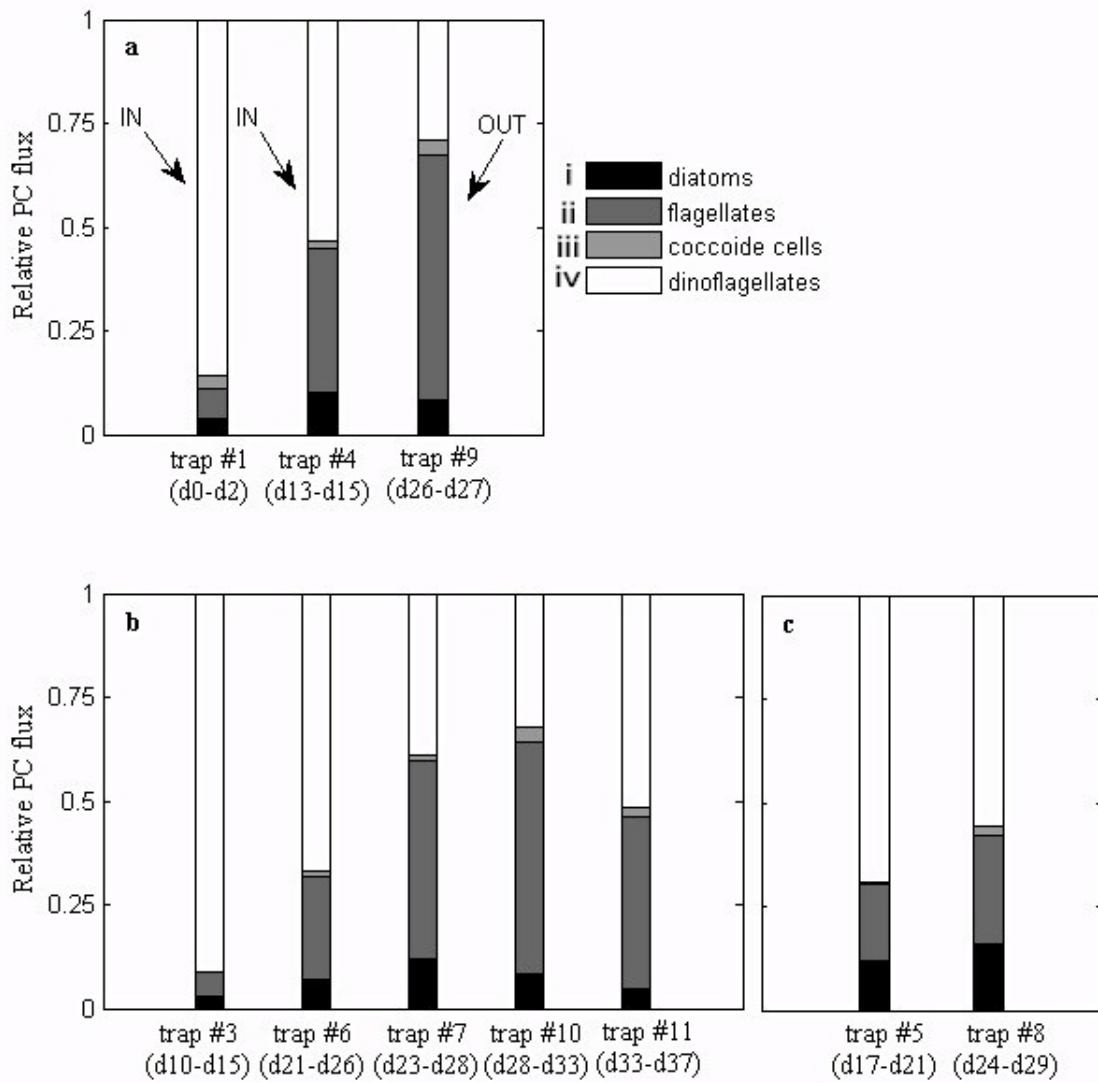


Fig. 5. Relative Unicellular Plankton Carbon (UPC) flux of the C flux carrying groups i) diatoms, ii) flagellates, iii) coccoide cells, and iv) dinoflagellates: Development over the course of the experiment a) at 200 m (IN and OUT), b) at 450 m IN, and c) at 450 m OUT.

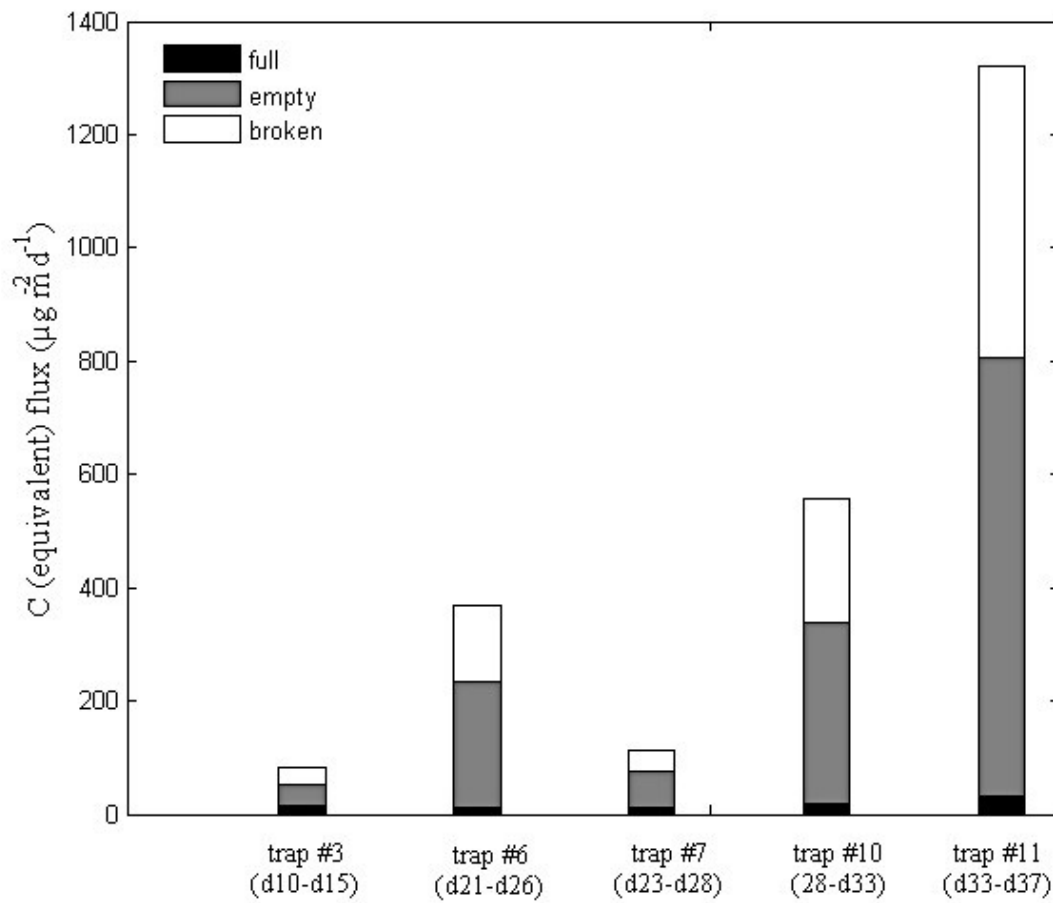


Fig. 6. Contribution of diatoms to the flux at 450 m inside the patch (IN) throughout the course of the experiment: C flux (full frustules) and C flux equivalent (empty and broken frustules), total diatom flux.

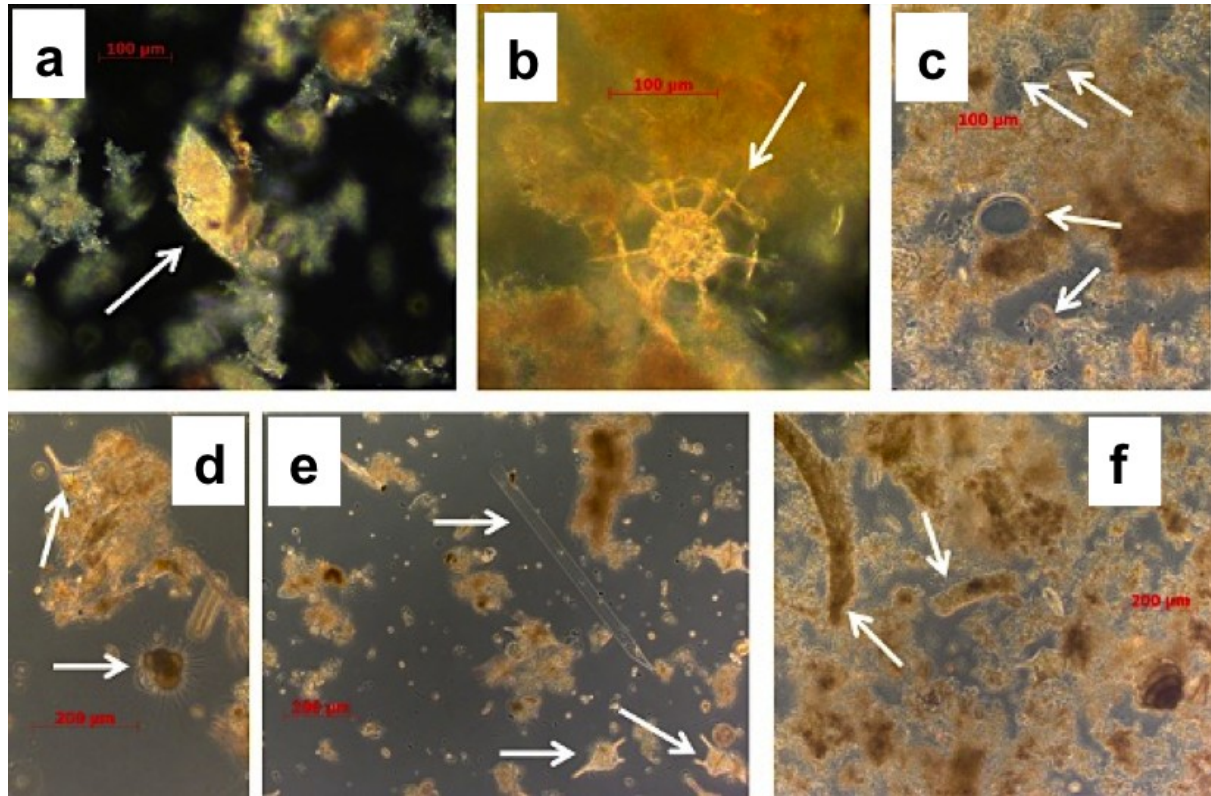


Fig. 7. Images showing the flux composition as examined with the microscope (from bulk sediment trap samples; a, b, c, f: 450 m; e, d: 200 m): a) dinoflagellate *Gyrodinium* spec. and aggregates (re-processed faecal material and (loose) phyto-detritus), b) broken radiolaria embedded in re-processed faecal matter, c) shells of probably protozoan origin (for instance empty tintinnid loricae) integrated in re-processed faecal matter and phyto-detrital aggregates, d) foraminifera with broken spines and dinoflagellate *C. pentagonum* incorporated in re-processed faecal material, e) broken diatoms *Rhizosolenia* spec., *C. pentagonum*, and aggregates of re-processed faecal matter and phyto-detritus, f) re-processed faecal material, phyto-detrital aggregates and recognisable individual faecal pellets.

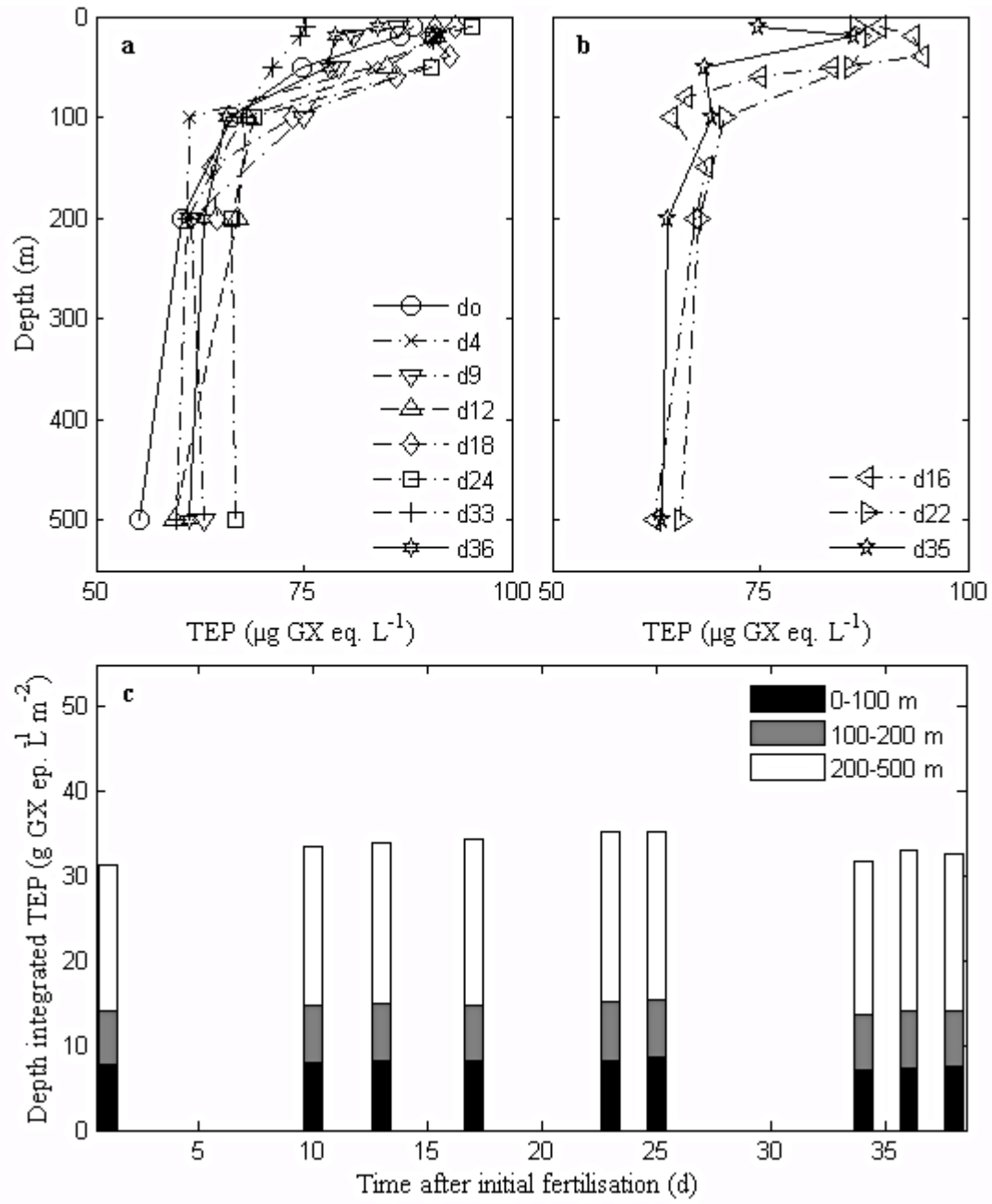


Fig. 8. TEP ($\mu\text{g GX eq. L}^{-1}$) distribution in the upper 500 m of the water column: profiles a) IN, and b) OUT, c) integrated TEP over the water column.

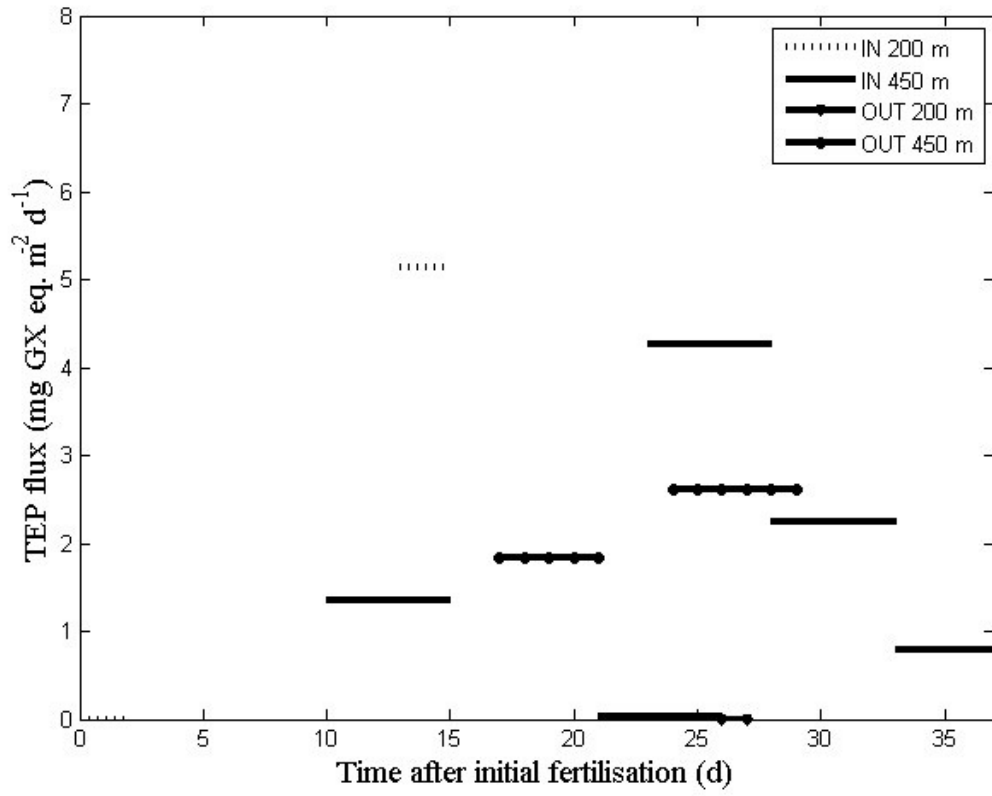


Fig. 9. TEP (mg GX eq. m⁻² d⁻¹) flux at 200 m and 450 m over the course of the experiment,

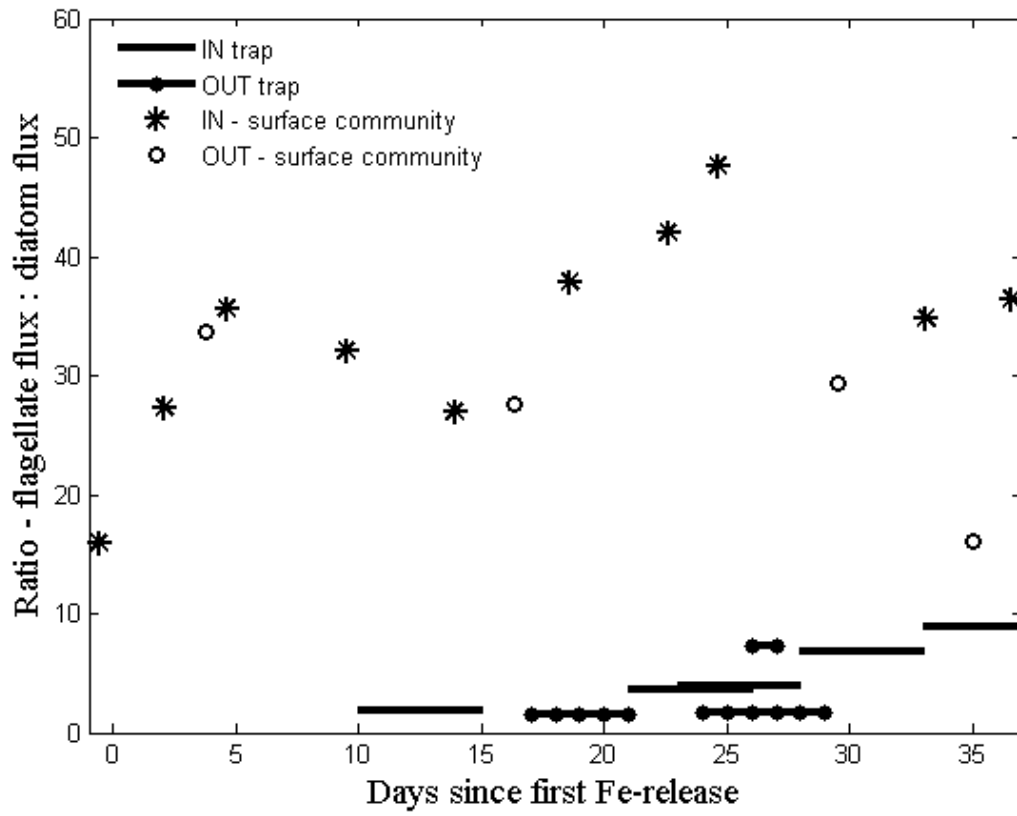


Fig. 10. Ratio of diatom flux: flagellate flux, surface composition and trap

Table 1. PELAGRA trap deployments.

#	Days	Time* (h)	Depth (m)	Patch	Application	Start position	End position
1	d0 - d2	48	210	IN	biogeochemical fluxes	48°02.39'S, 15°81.07'W	47°87.17'S, 15°88.06'W
2	d0 - d2	48	450	IN	Gel 1 - 3	48°02.74'S, 15°80.20'W	47°88.45'S, 15°88.42'W
3	d10 - d15	121	440	prob. IN	biogeochemical fluxes	47°73.20'S, 15°12.53'W	47°84.89'S, 15°46.95'W
4	d13 - d15	48	200	prob. IN	biogeochemical fluxes	47°89.45'S, 15°26.48'W	47°79.95'S, 15°51.89'W
5	d17 - d21	99	470	OUT	biogeochemical fluxes	47°50.27'S, 15°44.10'W	47°47.90'S, 14°88.60'W
6	d22 - d26	123	440	IN	biogeochemical fluxes	47°65.52'S, 15°59.53'W	47°58.60'S, 14°56.11'W
7	d23 - d28	126	440	IN	biogeochemical fluxes	47°35.10'S, 15°41.68'W	47°89.36'S, 14°42.47'W
8	d24 - d29	132	430	OUT	biogeochemical fluxes	47°30.00'S, 15°55.60'W	48°38.47'S, 14°62.64'W
9	d26 - d27	24	230	OUT	biogeochemical fluxes	47°51.38'S, 15°45.07'W	48°37.31'S, 14°75.42'W
10	d29 - d33	120	460	IN	Gel 4, 5 biogeochemical fluxes	48°08.60'S, 14°46.70'W	48°97.89'S, 15°13.47'W
11	d34 - d37	86	440	IN	biogeochemical fluxes	48°79.57'S, 15°23.70'W	49°04.06'S, 15°28.53'W
		18			Gel 6		

* Collection time (Cups open)

Table 2. PC flux, separated into diatoms, flagellates, coccooid cells and dinoflagellates.

<i>PELAGRA</i> trap	Days after Fe addition	diatoms $\mu\text{g C m}^{-2} \text{d}^{-1}$	F:EB*	flagellates $\mu\text{g C m}^{-2} \text{d}^{-1}$	P.a.** $\mu\text{g C m}^{-2} \text{d}^{-1}$ (%)	coccoide cells $\mu\text{g C m}^{-2} \text{d}^{-1}$	dinoflagellates $\mu\text{g C m}^{-2} \text{d}^{-1}$	total PC $\mu\text{g C m}^{-2} \text{d}^{-1}$	POC*** $\text{mg C m}^{-2} \text{d}^{-1}$	PC of POC %
200m										
# 1(IN)	d0 -d2	29.06	0.12	59.10	0 (0)	2.47	710.21	800.84	5.56	14.40
# 4 (prob. IN)	d13 -d15	16.97	0.03	58.35	2.75 (4.41)	3.68	89.80	168.81	4.78	3.53
# 9 (OUT)	d26 -d27	71.77	0.06	524.65	18.59 (3.54)	30.45	258.19	885.04	28.39	3.12
450m (IN)										
# 3 (prob. IN)	d10 -d15	16.65	0.25	31.05	4.41 (14.19)	0.63	495.51	543.84	8.44	6.45
# 6	d21 -d26	13.30	0.04	48.38	1.22 (2.53)	1.97	129.83	193.49	9.18	2.11
# 7	d23 -d28	11.26	0.11	44.30	2.43 (5.49)	1.34	36.36	93.26	22.96	0.41
# 10	d28 -d33	18.18	0.03	123.21	7.19 (5.83)	8.14	71.02	220.55	12.82	1.72
# 11	d33 -d37	31.14	0.02	275.65	8.5 (3.08)	14.99	343.75	665.53	12.85	5.18
450 m (OUT)										
# 5	d17 -d21	24.71	0.07	37.29	7.64 (20.48)	1.17	141.05	204.23	2.83	7.22
# 8	d24 -d29	46.80	0.05	76.59	1.16 (1.51)	5.45	162.81	291.65	10.97	2.66

* ratio of full (F) to empty (E) and broken (B) frustules

** absolute POC flux of *Phaeocystis antarctica* spp. (and fraction of flagellate POC flux in brackets)

*** total POC flux from PELAGRA traps (Martin et al. subm.)

Table 3. A bundance of tintinnid ciliates from PELAGRA traps: a bundance of empty and crashed loricae together is presented (and the damaged loricae as a fraction thereof is given in brackets). Note: no full tintinnids were present.

PELAGRA trap	Days after Fe addition	<i>Acanthostomella</i>		<i>Stenosomella</i>		<i>Cymatocyelis</i>		<i>Cymatocyelis</i>		<i>Codonellopsis</i>		<i>Codonellopsis</i>		total	
		<i>norvegica</i>	<i>norvegica</i>	<i>avelkana</i>	<i>avelkana</i>	<i>antarctica</i>	<i>antarctica</i>	<i>vanhoffeni</i>	<i>vanhoffeni</i>	<i>pusilla</i>	<i>pusilla</i>	<i>gaussii</i>	<i>gaussii</i>		<i>other</i>
		# 10 ³ m ⁻² d ⁻¹	# 10 ³ m ⁻² d ⁻¹	# 10 ³ m ⁻² d ⁻¹	# 10 ³ m ⁻² d ⁻¹	# 10 ³ m ⁻² d ⁻¹	# 10 ³ m ⁻² d ⁻¹	# 10 ³ m ⁻² d ⁻¹	# 10 ³ m ⁻² d ⁻¹	# 10 ³ m ⁻² d ⁻¹	# 10 ³ m ⁻² d ⁻¹	# 10 ³ m ⁻² d ⁻¹	# 10 ³ m ⁻² d ⁻¹	# 10 ³ m ⁻² d ⁻¹	
200 m															
# 1 (IN)	d0 - d2	148.8 (1.00)	148.8 (1.00)	17.5 (1.00)	17.5 (1.00)	0 -	0 -	0.3 (0.50)	0.3 (0.50)	0 -	0 -	8.8 (1.00)	8.8 (1.00)	87.5	262.9
# 4 (prob. IN)	d13 - d15	70.5 (0.93)	70.5 (0.93)	16.3 (0.67)	16.3 (0.67)	2.7 (1.00)	2.7 (1.00)	0 -	0 -	0 -	0 -	0 -	0 -	73.2	162.7
# 9 (OUT)	d26 - d27	475.9 (0.96)	475.9 (0.96)	59.4 (0.79)	59.4 (0.79)	33.9 (1.00)	33.9 (1.00)	0.2 (0.00)	0.2 (0.00)	0 -	0 -	0 -	0 -	100.7	670.1
450 m (IN)															
# 3 (prob. IN)	d10 - d15	348.4 (0.87)	348.4 (0.87)	312.7 (0.97)	312.7 (0.97)	0 -	0 -	0.7 (0.38)	0.7 (0.38)	0 -	0 -	0.1 (0.00)	0.1 (0.00)	160.8	822.6
# 6	d21 - d26	337.0 (0.93)	337.0 (0.93)	199.1 (1.00)	199.1 (1.00)	15.3 (1.00)	15.3 (1.00)	0 -	0 -	0 -	0 -	0 -	0 -	650.9	1202.3
# 7	d23 - d28	4867.2 (1.00)	4867.2 (1.00)	413.2 (1.00)	413.2 (1.00)	137.7 (1.00)	137.7 (1.00)	0.4 (1.00)	0.4 (1.00)	0 -	0 -	0 -	0 -	3076.4	8495.0
# 10	d28 - d33	1371.4 (1.00)	1371.4 (1.00)	222.0 (1.00)	222.0 (1.00)	26.1 (1.00)	26.1 (1.00)	0.4 (0.33)	0.4 (0.33)	0 -	0 -	0 -	0 -	509.4	2129.3
# 11	d33 - d37	1578.5 (0.94)	1578.5 (0.94)	1067.8 (1.00)	1067.8 (1.00)	0 -	0 -	1.3 (0.67)	1.3 (0.67)	0 -	0 -	0 -	0 -	603.6	3251.2
450 m (OUT)															
# 5	d17 - d21	147.7 (1.00)	147.7 (1.00)	64.6 (0.43)	64.6 (0.43)	0 -	0 -	0.3 (0.33)	0.3 (0.33)	9.2 (0.00)	9.2 (0.00)	0 -	0 -	387.6	609.4
# 8	d24 - d29	1383.7 (0.95)	1383.7 (0.95)	739.6 (1.00)	739.6 (1.00)	23.9 (1.00)	23.9 (1.00)	0.7 (0.33)	0.7 (0.33)	0 -	0 -	0 -	0 -	107.4	2255.2

Table 4. Abundances of foraminifera: distinction between full, empty and broken individuals ($10^3 \# m^{-2} d^{-1}$). For the total abundance fractions are given in brackets.

<i>PELAGRA trap</i>	<i>non-spinos</i>			<i>spinos</i>			<i>sum</i>		<i>f:eb*</i>	
	<i>full</i>	<i>empty</i>	<i>broken</i>	<i>full</i>	<i>empty</i>	<i>broken</i>	<i>empty</i>	<i>broken</i>		
200 m										
#1 (IN)	0	4.07	0.34	0	1.53	0	0	5.60 (0.94)	0.34 (0.06)	-
#4 (prob. IN)	0.15	3.09	0.23	0.08	0.70	0	0.30 (0.06)	3.79 (0.89)	0.23 (0.05)	1:17
#9 (OUT)	0.08	1.29	0	0	0.16	0	0.08 (0.05)	1.45 (0.95)	0 (0)	1:18
450 m (IN)										
#3	0	0	0	0	0.51	0.08	0 (0)	0.51 (0.86)	0.08 (0.14)	-
#6	0.58	8.08	1.67	0	0.51	0.22	0.58 (0.05)	8.59 (0.78)	1.89 (0.17)	1:18
#7	0.89	38.29	4.01	0	0.89	0	0.89 (0.02)	39.18 (0.89)	4.01 (0.09)	1:49
#10	0.25	10.64	1.39	0	0.38	0.1	0.25 (0.02)	11.02 (0.86)	1.52 (0.12)	1:50
#11	0	19.19	4.41	0	1.10	0	0 (0)	20.29 (0.82)	4.41 (0.18)	-
450 m (OUT)										
#5	0.27	9.13	0.81	0.09	0.45	0.09	0.36 (0.03)	9.58 (0.89)	0.89 (0.08)	1:29
#8	0.45	28.22	4.19	0	1.02	0.34	0.45 (0.01)	29.24 (0.86)	4.53 (0.13)	1:75

*: ratio of full to empty and broken individuals of all foraminifers

Table 5. TEP concentration in the water column and TEP flux.

Day	Chla*		TEP in the water column					TEP flux		
	surface (10 m) $\mu\text{g L}^{-1}$	surface (10 m) mg m^{-3}	100 m mg m^{-3}	500 m mg m^{-3}	200 m (int.)** g m^{-3}	500 m (int.)** g m^{-3}	200 m $\text{mg m}^{-2} \text{d}^{-1}$	450 m $\text{mg m}^{-2} \text{d}^{-1}$	fraction of int. TEP (% d^{-1})	
IN										
d0	0.48	88.06 ± 0.73	66.38 ± 4.40	55.30 ± 2.72	14.04	31.38	0		0	
d0-d2										
d4	0.87	$91.49 \pm 3.88^*$	61.25 ± 5.24	-	14.18	-				
d9	1.20	86.29 ± 9.76	74.93 ± 12.17	62.92 ± 3.02	14.78	33.44		1.358	0.04	
d10-d15										
d12	0.84	90.77 ± 4.08	68.20 ± 5.01	59.42 ± 0.39	15.04	34.02	5.135		0.34	
d13-d15										
d18	1.06	93.31 ± 1.34	73.62 ± 1.85	-	15.31	-				
d21-d26										
d23-d28										
d24	1.20	95.14	69.09 ± 1.22	66.81 ± 2.97	15.35	35.30		0.025	<0.001	
d29-d33								4.260	0.12	
d33	0.94	75.13 ± 15.08	67.73 ± 1.41	59.56 ± 3.35	13.60	31.68		2.237	0.07	
d34-d37										
d36	0.82	83.95 ± 3.76	65.58 ± 5.47	61.32 ± 3.40	14.02	32.68		0.784	<0.001	
OUT										
d16	0.71	89.38 ± 6.76	64.44 ± 2.23	62.36 ± 0.51	14.82	34.27				
d17-d21										
d22	0.62	86.56 ± 7.45	70.81 ± 2.63	65.54 ± 2.06	15.18	35.15		1.826	0.05	
d24-d29								2.611	0.08	

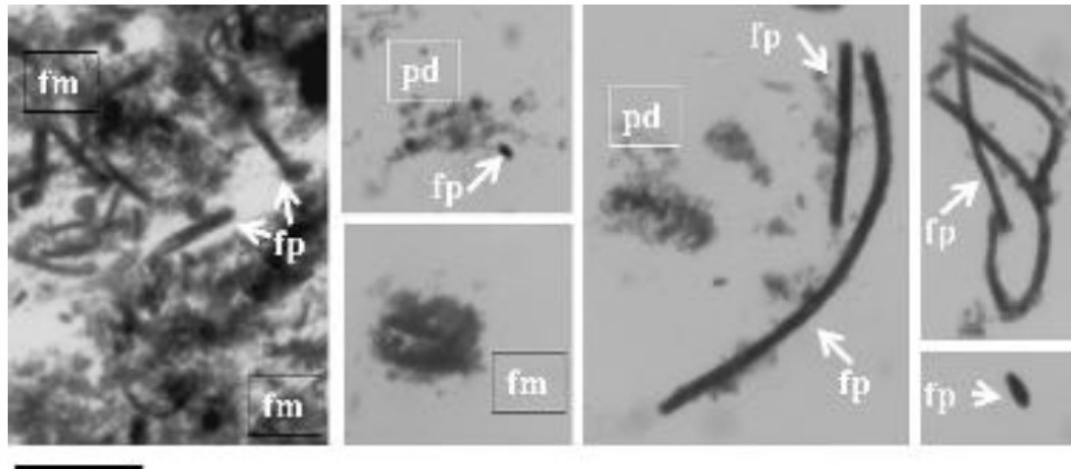
d35 0.53 74.82 ± 0.15 69.28 63.21 ± 3.55 13.98 33.05 |

• *Chla measurement in the water column at 10 m (unpubl. data M. Gauns)*

• *TEP concentration integrated over the water column*

Note: TEP flux at 450 m is estimated as fraction of 500 m, but due to the low TEP concentrations at depth this error is negligible.

Appendix



Appendix 1. Particle types found in the PA gels: fm: re-processed faecal material, pd: phyto-detritus, fp: intact faecal pellet. Scale bar: 1 mm.

Appendix 2. Plankton groups present in the PELAGRA traps

Group (OUT)	200 m (IN)	200 m (OUT)	450 m (IN)	450 m
Diatoms				
pennate diatoms <i>Fragilariopsis</i>				
<i>kerguelensis</i> <i>Fragilariopsis</i>	++	++	++	++
<i>rhombica/seperanda</i>	++	++	++	++
<i>Hasslea</i> sp.	++	++	++	++
<i>Manguinea</i> cf. <i>rigida</i>	++	++	++	++
<i>Lennoxia</i> (large)	-	-	+	-
<i>Lennoxia</i> (small)	++	++	++	++
<i>Pseudo-nitzschia heimii</i>	+	+	+	++
<i>Pseudo-nitzschia linola</i>	++	++	++	+
<i>Pseudo-nitzschia turgidula</i>	++	++	++	++
<i>Thalassionema nitzschioides</i>	++	++	++	++
<i>Thalassionema</i> n. var. <i>lanceolatum</i>	+	+	++	+
centric diatoms				
<i>Actinocyclus</i> sp.	++	+	+	+
<i>Asteromphalus hookeri/parvulus</i>	+	+	++	++
<i>Asteromphalus hyalines</i>	-	-	++	+
<i>Azpeitia</i> sp.	+	+	+	+
<i>Chaetoceros convulata</i>	-	+	+	-
<i>Chaetoceros</i> sp. spore	++	++	++	++
<i>Corethron inerme</i>	+	+	++	+
<i>Corethron pennatum</i> (large)	+	+	+	++
<i>Corethron pennatum</i> (small)	++	++	++	++
<i>Eucampia antarctica</i>	+	+	+	+
<i>Proboscia alata</i>	+	+	++	++
<i>Rhizosilenia curvata</i>	-	-	++	+
<i>Rhizosilenia</i> sp.	-	-	+	+
<i>Thalassiosira gracilis</i>	+	+	+	+
<i>Thalassiosira oestrupii</i>	+	+	+	+
<i>Thalassiosira lentiginosa</i>	++	++	++	++
<i>Thalassiosira</i> spp.	++	++	++	++
Flagellates				
<i>Choanoflagellate</i>	++	++	++	++
<i>Emiliana huxleyi</i>	++	++	++	++
<i>Flagellate</i> sp.	++	++	++	++
<i>Phaeocystis antarctica</i>	++	++	++	++
Coccolid cells				
	++	++	++	++

Dinoflagellates

<i>Ceratium pentagonum</i>	++	++	++	++
<i>Gyrodinium</i>	++	++	++	++
<i>Nematodinium</i>	-	-	++	-
<i>Podolampas sp.</i>	++	++	++	++
<i>Prorocentrum spp.</i>	++	++	++	++
<i>Protoperidinium spp.</i>	++	++	++	++
naked dinoflagellate	++	++	++	++
thecate dinoflagellate	++	++	++	++

Ciliates (tintinnid ciliates)

<i>Acanthostomella norvegica</i>	+	+	+	+
<i>Codonellopsis gausii</i>	+	-	+	-
<i>Codonellopsis pusilla</i>	+	-	+	-
<i>Cymatocyclis antarctica</i>	+	+	+	+
<i>Cymatocyclis vanhoeffeni</i>	+	+	+	+
<i>Stenosonmella avellana</i>	+	+	+	+

Foraminifera

<i>Globigerina buloides /</i>	++	++	++	++
<i>Turborotalita quinqueloba*</i>				
<i>Neogloboquadrina sp.</i>	++	++	++	++

Radiolaria

<i>Nasselaria spp.</i>	+	+	+	+
<i>Spumellaria spp.</i>	+	+	+	+

Heliozoa

<i>Sticholonche zanclea</i>	++	++	++	++
-----------------------------	----	----	----	----

Appendix 1. Particle types found in the PA gels: fm: re-processed faecal material, pd: phyto-detritus, fp: intact faecal pellet. Scale bar: 1 mm.

6. Synthesis

6. Synthesis

The major questions addressed in this thesis were:

1. How will plankton species composition differ in an iron fertilized bloom induced in a Si-limited region of the polar frontal zone of the Atlantic sector of the ACC to previous experiments carried out in high-Si waters? (Chapter **I+II+III**)
2. What are the effects of iron fertilization on higher trophic levels? (Chapter **III+IV**)
3. What is the fate, surface retention versus vertical export, of the iron-induced bloom? (Chapter **V**) → Implications for the carbon pump

The objective of this thesis was to gain a quantitative and qualitative understanding of factors driving the temporal dynamics of the plankton community and ultimately the fate of the produced biomass under iron-replete conditions in the silicic acid poor region of the ACC. The study highlights the differences of diatom-dominated systems with significant vertical export (Smetacek et al., 2012) to flagellate-dominated systems lacking deep carbon export (**Chapter V**, Martin et al., 2013) and sheds light on the controls on phytoplankton structure and function.

In the following I will recapitulate the major questions of my thesis and provide answers and directions for research perspectives.

6.1 Response of a phytoplankton assemblage to iron addition in the silicic acid poor region of the ACC

The phytoplankton community within the LOHAFEX eddy was initially iron-limited illustrated by the immediate increase in F_v/F_m ($0.33 \geq 0.40$) ratios in response to iron addition and tripling of chlorophyll standing stocks from 44 to 94 mg C m⁻². Biomass accumulation was mainly due to nanoflagellates, which is an exceptional finding because, according to the ecumenical hypothesis (Morel et al., 1991; Cullen, 1995), blooms are usually dominated by large cells while nano- and picoplankton is kept in check by grazing. Although diatoms accounted for a negligible fraction of total phytoplankton biomass, there was a considerable turn-over in relative species composition. The range of response patterns within the dominant diatom species was similar to those observed during silicic acid replete OIF experiments and indicates that biomass build-up, but not growth rates were limited at the very

low silicic acid concentrations encountered during LOHAFEX. Despite their dominance during LOHAFEX nanoflagellate composition stayed remarkably stable over the course of the experiment (**Chapter I+II**), illustrating the structural stability of the microbial community based on a network of tight interactions between bacteria and a phylogenetically diverse assemblage of heterotrophic, mixotrophic and autotrophic nanoflagellates.

6.2 Effects of iron fertilization on higher trophic levels: surface retention versus vertical export

The vertical distribution of dead and life organisms can be influenced by various factors such as by turbulent mixing induced by heavy winds, the intensity of radiant energy, advection, deep convection during winter or up-welling of CDW. Furthermore nutrient concentrations and the balance between growth and mortality, the accumulation rate of biomass, determine the survivorship of species populations, and consequently their fate (Banse, 1995; Smetacek et al., 2004). Mortality can be caused through external agents; pathogens (viruses and bacteria), parasitoids and predators or internal processes leading to natural cell death. During LOHAFEX the zooplankton community played a key role in regulating export flux but also in the development of a phytoplankton bloom. The main reason for the steady state of the plankton community was the large copepod population, which exerted high grazing pressure on the community and set an upper limit to bloom biomass (**Chapter I+IV**). Pelagial sediment traps showed evidence for high grazing pressure and low export flux (**Chapter V**). Copepod fecal pellets even contained foraminifera, which are not their preferred food items, hence indicating that they were food limited and exerting on microplankton (**Chapter III**). Despite the heavy grazing pressure and increased production of fecal pellets, the majority of them were recycled in the surface layer (**Chapter V**, Martin et al., 2013). But also the limiting silicic acid concentrations which limited diatom biomass build-up possibly prevented high POC export. However it can not be excluded that OIF in low Si-waters could indeed enhance POC flux, because processes driving export fluxes are highly variable as confirmed by previous studies;

Despite similar environmental conditions during SOFeX-North and LOHAFEX, export flux in the former was characterized by phytodetritus and in the latter partly by fecal pellets (Martin et al., 2013). The SAZ-sense project (Sub-Antarctic Zone sensitivity to global change project) also highlighted how particle flux differs between two regions of the Southern Ocean. One site was characterized by non-silicious phytoplankton, showed low PP and biomass accumulation but high export flux. The other, iron-replete site, showed higher biomass levels

but low POC export due to remineralisation processes (Jacquet et al., 2011). During SAGE, which was located in the Subantarctic zone, silicic acid concentrations were also low resulting in a muted bloom response to iron addition and no appreciable export flux, possibly enhanced due to strong dilution of the patch with surrounding waters. A stable nanoflagellate community, similar to that observed during LOHAFEX, was dominating. .

7. Conclusions

The results of the LOHAFEX demonstrated that the outcome of OIF experiments will strongly depend on the initial composition of the plankton community and the physical-chemical conditions of the experimental site. These pre-conditions need to be considered when predicting the impact of iron fertilization on carbon sequestration. LOHAFEX has shown that OIF in HNLSiLC areas does not boost the strength of the biological carbon pump because build-up of grazer-protected, fast-sinking diatoms is limited.

Instead the microbial community, despite a three-fold increase in biomass, showed only minor changes in community composition due to the tight interactions between its heterotrophic, micotrophic and autotrophic components and their respective predators, resulting in surface retention of the extra carbon generated by iron addition. It can thus be concluded that the suitability of OIF for deep carbon sequestration in silicic acid limited areas of the open ocean is likely very limited.

8. Outlook

Even though several iron fertilization experiments successfully enhanced surface productivity and investigated the phytoplankton community, the results differed either in nutrient concentrations, duration, bloom formation, species composition, fate of the bloom, patch formation or patch dilution (deBaar et al. 2005). Hence the different outcomes indicate the necessity to perform more experiments to study and quantify processes in natural ecosystems. However careful experimental design and examination of the appropriate environmental site is of great importance in this respect.

To answer a broad range of questions one possibility could be to fertilize two eddies simultaneously, which differ only in their Si-concentrations. The response should be followed over a duration of at least 4 weeks. Ideally a diatom-dominated bloom would develop in the eddy with high Si-concentrations and a flagellate-dominated bloom would develop in the eddy with low Si-concentrations. Within the flagellate dominated bloom, it would be essential to differentiate not only between autotrophic and heterotrophic plankton but also in detail between the mixotrophic fraction. Modern molecular methods provide the necessary tools to investigate the microbial community and shed new light into the functional ecology of its composite taxa. Within the diatom dominated bloom it would be necessary to determine particle export and deepen our knowledge about deep-water aggregate processes through sediment traps and in situ plankton recorders.

Large-scale, long-term and multiship OIF experiments conducted over several consecutive years are necessary to quantify the fate of iron-fertilized blooms and determine whether OIF is a suitable carbon sequestration technique. Furthermore these experiments would provide new insights on the reaction of bacteria and zooplankton communities and their predators to enhanced productivity and the response of the deep-sea benthos to enhanced food supply.

References

- Abelmann, A., and Gowing, M. M., 1996, Horizontal and vertical distribution pattern of living radiolarians along a transect from the Southern Ocean to the South Atlantic subtropical region: *Deep Sea Research Part I*, v. 43, no. 3, p. 361-382.
- Abraham, E. R., Law, C. S., Boyd, P. W., Lavender, S. J., Maldonado, M., and Bowie, A. R., 2000, Importance of stirring in the development of an iron-fertilized phytoplankton bloom: *Nature*, v. 407, no. 6508, p. 727-733.
- Alder, V. A., and Boltovskoy, D., 1993, The ecology of larger microzooplankton in the Weddell-Scotia confluence area: Horizontal and vertical distribution patterns.: *Journal of Marine Research*, v. 51, no. 2, p. 323-344.
- Archibald, J. M., and Keeling, P. J., 2002, Recycled plastids: a green movement in eukaryotic evolution: *Trends Genetic*, v. 18, p. 577-584.
- Arrigo, K. R., Robinson, D. H., Worthen, D. L., Dunbar, R. B., DiTullio, G. R., VanWoert, M., and Lizotte, M. P., 1999, Phytoplankton community structure and the drawdown of nutrients and CO₂ in the Southern Ocean: *Science*, v. 283, no. 5400, p. 365-367.
- Assmy, P., Henjes, J., Klaas, C., and Smetacek, V., 2007, Mechanisms determining species dominance in a phytoplankton bloom induced by the iron fertilization experiment EisenEx in the Southern Ocean: *Deep Sea Research Part I*, v. 54, no. 3, p. 340-362.
- Assmy, P., Smetacek, V., Montresor, M., Klaas, C., Henjes, J., Strass, V. H., Arrieta, J. M., Bathmann, U., Berg, M. G., Breitbarth, E., Cisewski, B., Friedrichs, L., Fuchs, N., Herndl, G. J., Jansen, S., , Krägefsky, S., Latasa, N., Passow, U., Peeken, I., Röttgers, R., Scharek, R., Schüller, S. E., Steigenberger, S., and Webb, A., IN REVISION, 2013, Grazer-protected diatoms decouple ocean carbon and silicon cycles around Antarctica: *PNAS*.
- Azam, F., Fenchel, T., Field, J. G., Gray, J. S., Meyer-Reil, L. A., and Thingstad, F., 1983, The ecological role of water-column microbes in the sea: *Marine ecology progress series*, v. 10, no. 3, p. 257-263.
- Banse, K., 1995, Zooplankton: Pivotal role in the control of ocean production: *ICES Journal of Marine Science*, v. 52, no. 3-4, p. 265-277.
- Baumann, K. H., Böckel, B., and Frenz, M., 2004, Coccolith contribution to South Atlantic carbonate sedimentation.: IN: Hans, R., Thierstein, J.R.Y. (Eds.), *Coccolithophores: from molecular processes to global impact.*, v. Springer, Berlin, p. 367-402.
- Becquevort, S., 1997, Nanoprotozooplankton in the Atlantic sector of the Southern Ocean during early spring: Biomass and feeding activities: *Deep-Sea Research II*, v. 44, no. 1-2, p. 355-373.
- Behrenfeld, M., Bale, A., Kolber, Z., Aiken, J., and Falkowski, P., 1996, Confirmation of iron limitation of phytoplankton photosynthesis in the Equatorial Pacific Ocean: *Nature*, v. 383, no. 6600, p. 508-511.
- Bernhard, J. M., and Bowser, S. M., 1999, Benthic Foraminifera of dysoxic sediments: chloroplast sequestration and functional morphology: *Earth Science Reviews*, v. 46, p. 149-165.
- Bernstein, R. E., Betzer, P. R., Feely, R. A., Byrne, R. H., Lamb, M. F., and Michaels, A. F., 1987, Acantharian fluxes and strontium to chlorinity ratios in the North Pacific Ocean.: *Science*, v. 237, no. 4821, p. 1490-1494.
- Bhattacharya, D., Yoon, H. S., and Hackett, J. D., 2003, Photosynthetic eukaryotes unite: Endosymbiosis connects the dots: *Biological Essays*, v. 26, p. 50-60.
- Bidigare, R. R., Hanson, K. L., Buesseler, K. O., Wakeham, S. G., Freeman, K. H., Pancost, R. D., Millero, F. J., Steinberg, P., Popp, P. N., Latasa, N., Landry, M. R., and Laws,

- E. A., 1999, Iron-stimulated changes in ^{13}C fractionation and export by equatorial Pacific Ocean: toward a paleogrowth rate proxy: *Paleoceanography*, v. 14, p. 589-595.
- Blain, S., Queguiner, B., Armand, L., Belviso, S., Bombled, B., Bopp, L., Bowie, A., Brunet, C., Brussaard, C., Carlotti, F., Christaki, U., Corbiere, A., Durand, I., Ebersbach, F., Fuda, J.-L., Garcia, N., Gerringa, L., Griffiths, B., Guigue, C., Guillermin, C., Jacquet, S., Jeandel, C., Laan, P., Lefevre, D., Lo Monaco, C., Malits, A., Mosseri, J., Obernosterer, I., Park, Y.-H., Picheral, M., Pondaven, P., Remenyi, T., Sandroni, V., Sarthou, G., Savoye, N., Scouarnec, L., Souhaut, M., Thuiller, D., Timmermans, K., Trull, T., Uitz, J., van Beek, P., Veldhuis, M., Vincent, D., Viollier, E., Vong, L., and Wagener, T., 2007, Effect of natural iron fertilization on carbon sequestration in the Southern Ocean: *Nature*, v. 446, no. 7139, p. 1070-1074.
- Boyd, P., Berges, J. A., and Harrison, P. J., 1998, In vitro iron enrichment experiments at iron-rich and -poor sites in the NE subarctic Pacific: *Journal of Experimental Marine Biology and Ecology* [*J. Exp. Mar. Biol. Ecol.*] v. 227, no. 1, p. 133-151.
- Boyd, P. W., Jickells, T., Law, C. S., Blain, S., Boyle, E. A., Buesseler, K. O., Coale, K. H., Cullen, J. J., de Baar, H. J. W., Follows, M., Harvey, M., Lancelot, C., Levasseur, M., Owens, N. P. J., Pollard, R., Rivkin, R. B., Sarmiento, J., Schoemann, V., Smetacek, V., Takeda, S., Tsuda, A., Turner, S., and Watson, A. J., 2007, Mesoscale iron enrichment experiments 1993-2005: Synthesis and future directions: *Science*, v. 315, no. 5812, p. 612-617.
- Boyd, P. W., Law, C. S., Wong, C. S., Nojiri, Y., Tsuda, A., Levasseur, M., Takeda, S., Rivkin, R., Harrison, P. J., Strzepek, R., Gower, J., McKay, M., Abraham, E. R., Arychuk, M., Barwell-Clarke, J., Crawford, W., Crawford, D., Hale, M., Harada, K., Johnson, K., Kiyosawa, H., Kudo, I., Marchetti, A., Miller, W., Needoba, J., Nishioka, J., Ogawa, H., Page, J., Robert, M., Saito, H., Sastri, A., Sherry, N., Soutar, T., Sutherland, N., Taira, Y., Whitney, F., Wong, S.-K. E., and Yoshimura, T., 2004, The decline and fate of an iron-induced subarctic phytoplankton bloom: *Nature*, v. 428, no. 6982, p. 549-552.
- Boyd, P. W., Sherry, N. D., Berges, J. A., Bishop, J. K. B., Calvert, S. E., Charette, M. A., Giovannoni, S. J., Goldblatt, R., Harrison, P. J., Moran, S. B., Roy, S., Soon, M., Strom, S., Thibault, D., Vergin, K. L., Whitney, F. A., and Wong, C. S., 1999, Transformations of biogenic particulates from the pelagic to the deep ocean realm: *Deep-Sea Research II*, v. 46, p. 2761-2792.
- Boyd, P. W., Watson, A. J., Law, C. S., Abraham, E. R., Trull, T., Murdoch, R., Bakker, D. C. E., Bowie, A. R., Buesseler, K. O., Chang, H., Charette, M., Croot, P., Downing, K., Frew, R., Gall, M., Hadfield, M., Hall, J. A., Harvey, M., Jameson, G., LaRoche, J., Liddicoat, M., Ling, R., Maldonado, M. T., McKay, R. M., Nodder, S. D., Pickmere, S., Pridmore, R., Rintoul, S., Safi, K. A., Sutton, P., Strzepek, R., Tanneberger, K., Turner, S., Waite, A., and Zeldies, J., 2000, A mesoscale phytoplankton bloom in the polar Southern Ocean stimulated by iron fertilization: *Nature*, v. 407, no. 6805, p. 695-702.
- Broecker, W. S., and Peng, T. H., 1982, *Tracers in the Sea*: Eldigio Press, Palisades, N.Y., U.S.A.
- Brown, M. R., Jeffrey, S. W., Volkman, J. K., and Dunstan, G. A., 1997, Nutritional properties of microalgae for mariculture: *Aquaculture*, v. 151, p. 315-331.
- Bruland, K. W., Rue, E. L., and Smith, G. J., 2001, Iron and macronutrients in California coastal upwelling regimes: Implications for diatom blooms: *Limnology and Oceanography*, v. 46, p. 1661-1674.
- Buesseler, K. O., Andrews, J. E., Pike, S. M., and Charette, M. A., 2004, The effects of iron fertilization on carbon sequestration in the Southern Ocean: *Science*, v. 304, no. 5669, p. 414-417.

- Buesseler, K. O., Andrews, J. E., Pike, S. M., Charette, M. A., Goldson, L. E., Brzezinski, M. A., and Lance, V. P., 2005, Particle export during the Southern Ocean Iron Experiment (SOFEX): *Limnol. and Oceanogr.*, v. 50, no. 1, p. 311-327.
- Buma, A. G. J., de Baar, H. J. W., Nolting, R. F., and van Bennekom, A. J., 1991, Metal enrichment experiments in the Weddell-Scotia Seas: Effects of iron and manganese on various plankton communities: *Limnology and Oceanography*, v. 36, p. 1865-1878.
- Burkholder, J. M. a., and Glasgow, H. B. J., 1995, Interaction of a toxic estuarine dinoflagellate with microbial predators and prey.: *Arch. Protistenked.*, v. 145, p. 177-188.
- Burkill, P. H., Edwards, E. S., John, A. W. G., and Sleigh, M. A., 1993, Microzooplankton and their herbivorous activity in the northeastern Atlantic Ocean: *Deep Sea Research Part II*, v. 40, no. 1-2, p. 479-493.
- Burkill, P. H., Edwards, E. S., and Sleigh, M. A., 1995, Microzooplankton and their role in controlling phytoplankton growth in the marginal ice zone of the Bellingshausen Sea: *Deep Sea Research Part II*, v. 42, no. 4-5, p. 1277-1290.
- Calbet, A., and Landry, M. R., 2004, Phytoplankton growth, microzooplankton grazing, and carbon cycling in marine systems: *Limnol. and Oceanogr.*, v. 49, no. 1, p. 51-57.
- Caron, D., Dennett, M., Lonsdale, D., Moran, D., and Shalapyonok, L., 2000, Microzooplankton herbivory in the Ross Sea, Antarctica: *Deep-Sea Research II*, v. 47, no. 15-16, p. 3249-3272.
- Caron, D. A., Michaels, A. F., Swanberg, N. R., and Howse, F. A., 1995, Primary productivity by symbiont-bearing planktonic sarcodines (Acantharia, Radiolaria, Foraminifera) in surface waters near Bermuda: *Journal of Plankton Research*, v. 17, no. 1, p. 103-129.
- Caron, D. A., and Swanberg, N. R., 1990, The ecology of planktonic sarcodines: *Rev. Aquat. Sci.*, v. 3, p. 147-180.
- Caron, D. A. a., and Goldmann, J. C., 1990, Protozoan nutrient regeneration.: In Capriulo, G. M. (ed.), *Ecology of Marine Protozoa*. Oxford University Press, New York, p. 283-306.
- Cavender-Bares, K. M., EL; Chisholm, SW*; Ondrusek, ME; Bidigare,, and RR, 1999, Differential response of equatorial Pacific phytoplankton to iron fertilization: *Limnology and Oceanography*, v. 44, no. 2, p. 237-246.
- Charlson, R. J., Lovelock, J. E., Andrea, M. O., and Warren, S. G., 1987, Oceanic phytoplankton, atmospheric sulfur, cloud albedo and climate.: *Nature*, v. 326, p. 655-661.
- Chavez, F. P., and Barber, R. T., 1987, An estimate of new production in the equatorial Pacific: *Deep Sea Research Part I: Oceanographic Research Papers*, v. 34, p. 1229-1243.
- Chavez, F. P., Buck, K. R., Serivce, S. K., Newton, J., and Barber, R. T., 1996, Phytoplankton variability in the central and eastern tropical Pacific: *Deep Sea Research Part II: Topical Studies in Oceanography*, v. 43, p. 835-870.
- Chrisholm, S. W., and Morel, F. M. M., 1991, What controls phytoplankton productivity in nutrient-rich areas of the open sea?: *Limnology and Oceanography*, v. 36, no. special volume.
- Coale, K. H., 2004, Open ocean iron enrichment experiments: What they have told us, what they have not, paper presented at the Ocean Research Conference: American society of Limnology and Oceanography, Oceanographic Society, v. Honolulu, Hawaii, p. 15-20.
- Coale, K. H., Johnson, K. S., Chavez, F. P., Buesseler, K. O., Barber, R. T., Brzezinski, M. A., Cochlan, W. P., Millero, F. J., Falkowski, P. G., Bauer, J. E., Wanninkhof, R. H., Kudela, R. M., Altabet, M. A., Hales, B. E., Takahashi, T., Landry, M. R., Bidigare,

References

- R. R., Wang, X. J., Chase, Z., Strutton, P. G., Friederich, G. E., Gorbunov, M. Y., Lance, V. P., Hilting, A. K., Hiscock, M. R., Demarest, M., Hiscock, W. T., Sullivan, K. F., Tanner, S. J., Gordon, R. M., Hunter, C. N., Elrod, V. A., Fitzwater, S. E., Jones, J. L., Tozzi, S., Koblizek, M., Roberts, A. E., Herndon, J., Brewster, J., Ladizinsky, N., Smith, G., Cooper, D., Timothy, D., Brown, S. L., Selph, K. E., Sheridan, C. C., Twining, B. S., and Johnson, Z. I., 2004, Southern ocean iron enrichment experiment: Carbon cycling in high- and low-Si waters: *Science*, v. 304, no. 5669, p. 408-414.
- Coale, K. H., Johnson, K. S., Fitzwater, S. E., Gordon, M. R., Tanner, S., Chavez, F. P., Ferioli, L., Sakamoto, C., Rogers, P., Millero, F., Steinberg, P., Nightingale, P., Cooper, D., Cochlan, W. P., Landry, M. R., Constantinou, J., Rollwagen, G., Trasvina, A., and Kudela, R., 1996, A massive phytoplankton bloom induced by an ecosystem-scale iron fertilization experiment in the equatorial Pacific Ocean: *Nature*, v. 383, p. 495-501.
- Coale, K. H., Johnson, K.S.; Fitzwater, S.E.; Blain, S.P.G.; Stanton, T.P. and Coley, T.L., 1998, Iron Ex I, an in-situ iron-enrichment experiment: Experimental design, implementation and results: *Deep Sea Research Part II: Topical Studies in Oceanography*, v. 45, p. 919-945.
- De Angelis, M., Barkov, N. I., and Petrov, V. N., 1987, Aerosol concentrations over the last climatic cycle (160 kyr) from an Antarctic ice core: *Nature*, v. 325, no. 6102, p. 318-321.
- de Baar, H. J. W., Boyd, P. W., Coale, K. H., Landry, M. R., Tsuda, A., Assmy, P., Bakker, D. C. E., Bozec, Y., Barber, R. T., Brzezinski, M. A., Buesseler, K. O., Boye, M., Croot, P. L., Gervais, F., Gorbunov, M. Y., Harrison, P. J., Hiscock, W. T., Laan, P., Lancelot, C., Law, C. S., Levasseur, M., Marchetti, A., Millero, F. J., Nishioka, J., Nojiri, Y., Oijen, T. v., Riebesell, U., Rijkenberg, M. J. A., Saito, H., Takeda, S., Timmermans, K. R., Marcel J. W. Veldhuis, Waite, A. M., and Wong, C.-S., 2005, Synthesis of iron fertilization experiments: From the Iron Age in the Age of Enlightenment: *Journal of Geophysical Research*, v. 110, p. C09S16.
- De La Rocha, C. L., and Passow, U., 2007, Factors influencing the sinking of POC and the efficiency of the biological carbon pump: *Deep Sea Research Part II: Topical Studies in Oceanography*
- The Role of Marine Organic Carbon and Calcite Fluxes in Driving Global Climate Change, Past and Future, v. 54, no. 5-7, p. 639-658.
- Decelle, J., Martin, P., Paborstava, K., Pond, D. W., Tarling, G., Mahé, F., de Vargas, C., Lampitt, R., and Not, F., 2013, Diversity, Ecology and Biogeochemistry of Cyst-Forming Acantharia (Radiolaria) in the Oceans.: *PLOS ONE*, v. 8(1), no. e53598.
- Detmer, A. E., and Bathmann, U. V., 1997, Distribution patterns of autotrophic pico- and nanoplankton and their relative contribution to algal biomass during spring in the Atlantic sector of the Southern Ocean: *Deep-Sea Research II*, v. 44, no. 1-2, p. 299-320.
- DiTullio, G. R., Grebmeier, J. M., Arrigo, K. R., Lizotte, M. P., Robinson, D. H., Leventer, A., Barry, J. B., VanWoert, M. L., and Dunbar, R. B., 2000, Rapid and early export of *Phaeocystis antarctica* blooms in the Ross Sea, Antarctica: *Nature*, v. 404, no. 6778, p. 595-598.
- Dodge, J. D., and Priddle, J., 1987, Species composition and ecology of dinoflagellates from the Southern Ocean near South Georgia: *Journal of Plankton Research*, v. 9, no. 4, p. 685-697.
- Duce, R. A., and Tindale, N. W., 1991, Atmospheric transport of iron and its deposition in the ocean.: *Limnology and Oceanography*, v. 1715-1726, no. 36.

- Erickson, D. J., Hernandez, J. L., Ginoux, P., Gregg, W. W., McClain, C., and Christian, J., 2003, Atmospheric iron delivery and surface ocean biological activity in the Southern Ocean and Patagonian region: *Geophysical Research Letters*, v. 30, no. 12, p. 11 (11-14).
- Falkowski, P., Scholes, R. J., Boyle, E., Canadell, J., Canfield, D., Elser, J., Gruber, N., Hibbard, K., Hogberg, P., Linder, S., Mackenzie, F. T., Moore, B., Pedersen, T., Rosenthal, Y., Seitzinger, S., Smetacek, V., and Steffen, W., 2000, The global carbon cycle: A test of our knowledge of earth as a system: *Science*, v. 290, no. 5490, p. 291-296.
- Falkowski, P. G., Barber, R. T., and Smetacek, V., 1998, Biogeochemical controls and feedbacks on ocean primary production: *Science*, v. 281, no. 5374, p. 200-206.
- Field, C. B., Behrenfeld, M. J., Randerson, J. T., and Falkowski, P., 1998, Primary production of the biosphere: Integrating terrestrial and oceanic components: *Science*, v. 281, no. 5374, p. 237-240.
- Figueiredo, G. M., Nash, R. D. M., and Montagnes, D. J. S., 2005, The role of the generally unrecognised micro-prey source as food for larval fish in the Irish Sea: *Journal of Marine Biology*, v. 148, p. 394-404.
- Figuères, G., Martin, J. M., and Meybeck, M., 1978, Iron behaviour in the Zaire estuary.: *Neth J. Sea research*, v. 12, p. 329-337.
- Foldvik, A., 2004, Ice shelf water overflow and bottom water formation in the southern Weddell Sea: *Journal of Geophysical Research*, v. 109, no. C02015.
- Gall, M. P., Boyd, P. W., Hall, J., Safi, K. A., and Chang, H., 2001, Phytoplankton processes. Part 1: Community structure during the Southern Ocean Iron RElease Experiment (SOIREE): *Deep Sea Research Part II: Topical Studies in Oceanography*, v. 48, no. 11-12, p. 2551-2570.
- Gantt, E., Edwards, M. R., and Provasoli, L., 1971, Chloroplast structure of the Cryptophyceae.: *Journal of Cell Biology*, v. 48, p. 280-290.
- Gao, Y., Kaufman, Y. J., Tanre, D., Kolber, D., and Falkowski, P. G., 2001, Seasonal Distributions of Aeolian Iron Fluxes to the Global Ocean: *Geophysical Research Letters [Geophys. Res. Lett.]*, v. 28, no. 1, p. 29-32.
- Geider, R. J., and La Roche, J., 1994, The role of iron in phytoplankton photosynthesis and the potential for iron-limitation of primary productivity in the sea.: *Photosynthetical Research*, v. 39, p. 275-301.
- Gervais, F., 1997, Diel vertical migration of *Cryptomonas* and *Chromatium* in the deep chlorophyll maximum of a eutrophic lake: *Journal of Plankton Research*, v. 19, p. 533-550.
- Gervais, F., Riebesell, U., and Gorbunov, M. Y., 2002, Changes in primary productivity and chlorophyll a in response to iron fertilization in the Southern Polar Frontal Zone: *LIMNOLOGY AND OCEANOGRAPHY*, v. 47, no. 5, p. 1324-1335.
- Gold, K., and Morales, E. A., 1976, Studies on the sizes, shapes, and the development of the lorica of agglutinated tintinnida: *Biol. Bull.*, v. 150, p. 377-392.
- , 1977, Studies on the tintinnida of Enewetak Atoll: *J. Protozool.*, v. 24, no. 4, p. 580-587.
- Gonzalez, H., 1992, Distribution and abundance of minipellets around the Antarctic peninsula. Implications for protistan feeding behaviour: *Marine Ecology Progress Series*, v. 90, no. 3, p. 223-236.
- Gordon, A. L., A. H. Orsi, R. Muench, B. A. Huber, E. Zambianchi, M. Visbeck, 2009, Western Ross Sea continental slope gravity currents: *Deep Sea Research Part II: Topical Studies in Oceanography*, v. 56, p. 796-817.
- Gould, S. B., Waller, R. F., and McFadden, G. I., 2008, Plastid evolution: *Annual Review of Plant Biology*, v. 59, p. 491-517.

- Gowing, M. M., 1989, Abundance and feeding ecology of Antarctic phaeodarian radiolarians: *Marine Biology*, v. 103, no. 1, p. 107-118.
- Gowing, M. M., and Garrison, D. L., 1991, Austral winter distributions of large tintinnid and large sarcodiniid protozooplankton in the ice-edge zone of the Weddell/Scotia Seas: *Journal of Marine Systems*, v. 2, no. 1-2, p. 131-141.
- , 1992, Abundance and feeding ecology of larger protozooplankton in the ice edge zone of the Weddell and Scotia Seas during the austral winter: *Deep Sea Research*, v. 39, no. 5, p. 893-919.
- Gowing, M. M., Garrison, D. L., Kunze, H. B., and Winchel, C. J., 2001, Biological components of Ross Sea short-term particle fluxes in the austral summer of 1995-1996: *Deep Sea Research I*, v. 48, no. 12, p. 2645-2671.
- Griffith, E. M., and Paytan, A., 2012, Barite in the ocean – occurrence, geochemistry and palaeoceanographic applications: *Sedimentology*.
- Gustafson, D. E., Stoecker, D. K., Johnson, M. D., Van Heukelem, W. F., and Sneider, K., 2000, Cryptophyte algae are robbed of their organelles by the marine ciliate *Mesodinium rubrum*: *Nature*, v. 405, p. 1049-1052.
- Hamme, R. C., Webley, P. W., Crawford, W. R., Whitney, F. A., DeGrandpre, M. D., Emerson, S. R., Eriksen, C. C., Giesbrecht, E. K., Gower, J. F. R., Kavanaugh, M. T., Peña, M. A., Sabine, L. C., Batten, S. D., Coogan, L. A., Grundle, D. S., and Lockwood, D., 2010, Volcanic ash fiels anomalous plankton bloom in subarctic northeast Pacific: *Geophysical Research Letters*, v. 37.
- Hammer, A., Schumann R., and Schubert, H., 2002, Light and temperature acclimation of *Rhodomonas salina* (Cryptophyceae): photosynthetic performance: *Aquatic Microbial Ecology*, v. 29, p. 287-296.
- Hansen, P. J., 1991, Quantitative importance and trophic role of heterotrophic dinoflagellates in a coastal pelagial food web: *Marine Ecology Progress Series*, v. 73, no. 2-3, p. 253-261.
- Harvey M.J., C. S. L., Murray J. Smith, Julie A. Hall, Edward R. Abraham, Craig L. Stevens,, Mark G. Hadfield, D. T. H., Brian Ward, Stephen D. Archer, Jill M. Caine, Kim I. Currie,, Dawn Devries, M. J. E., Peter Hill, Graham B. Jones, Dave Katz, Jorma Kuparinen,, Burns Macaskill, W. M., Andrew Marriner, John McGregor, Craig McNeil,, Peter J. Minnett, S. D. N., Jill Peloquin, Stuart Pickmere, Matthew H. Pinkerton, Karl A. Safi,, and Rona Thompson, M. W., Simon W. Wright, Lori A. Ziolkowski, 2011, The SOLASair–seagasexchangeexperiment(SAGE)2004: *Deep-Sea Research II*, v. 58, p. 753-763.
- Hasle, G. L., CB; Syvertsen, EE, 1996, A review of Pseudo-nitzschia, with special reference to the Skagerrak, North Atlantic, and adjacent waters: *Helgolander Meeresuntersuchungen*, v. 50, no. 2, p. 131-175.
- Hemleben, C., Spindler, M., and Anderson, O. R., 1989, *Modern Planktonic Foraminifera*: Springer Verlag, p. 363.
- Henjes, J., and Assmy, P., 2008, Particle availability controls agglutination in pelagic tintinnids in the Southern Ocean: *Protist*, v. 159, no. 2, p. 239-250.
- Henjes, J., Assmy, P., Klaas, C., and Smetacek, V., 2007, Response of the larger protozooplankton to an iron-induced phytoplankton bloom in the Polar Frontal Zone of the Southern Ocean (EisenEx): *Deep Sea Research Part I: Oceanographic Research Papers*, v. 54, no. 5, p. 774-791.
- Hillebrand, H., Duerselen, C. D., Kirschtel, D., Pollinger, U., and Zohary, T., 1999, Biovolume calculation for pelagic and benthic microalgae: *Journal of Phycology* [J. Phycol.]. v. 35, no. 2, p. 403-424.

- Hoffmann, L. J., Peeken, I., Lochte, K., Assmy, P., and Veldhuis, M., 2006, Different reactions of Southern Ocean phytoplankton size classes to iron fertilization: *Limnology and Oceanography* [Limnol. Oceanogr.], v. 51, no. 3, p. 1217-1229.
- Holm-Hansen O., and Hewes, C. D., 2004, Deep chlorophyll-a maxima (DCMs) in Antarctic waters. I. Relationships between DCMs and the physical, chemical, and optical conditions in the upper water column: *Polar Biology*, v. 27, p. 699-710.
- Hoppema, M., 2004, Weddell Sea is a globally significant contributor to deep-sea sequestration of natural carbon dioxide: *Deep-Sea Research I*, v. 51, p. 1169–1177.
- Hoppema, M., E. Fahrback, M. Schröder, 1997, On the total carbon dioxide and oxygen signature of the circumpolar deep water in the Weddell Gyre: *Oceanologica Acta*, v. 20, p. 783–798.
- Huhn, O., H. H. Hellmer, M. Rhein, C. Rodehacke, W. Roether, M. P. Schodlok, and Schröder, M., 2008, Evidence of deep- and bottom-water formation in the western Weddell Sea: *Deep Sea Research Part II: Topical Studies in Oceanography*, v. 55, p. 1098–1116.
- Hutchins, D. A., and Bruland, K. W., 1998, Iron-limited diatom growth and Si:N uptake ratios in a coastal upwelling regime: *Nature*, v. 393, no. 6685, p. 561-564.
- Irigoiien, X., Flynn, K. J., and Harris, R. P., 2005, Phytoplankton blooms: a 'loophole' in microzooplankton grazing impact?: *Journal of Plankton Research*, v. 27, no. 4, p. 313-321.
- Irigoiien, X., Huisman, J., and Harris, R. P., 2004, Global biodiversity patterns of marine phytoplankton and zooplankton: *Nature* [Nature], v. 429, no. 6994, p. 863-867.
- Irigoiien, X., Titelman, J., Harris, R. P., Harbour, D., and Castellani, C., 2003, Feeding of *Calanus finmarchicus* nauplii in the Irminger Sea: *Marine Ecological Progress*, v. 262, no. 193-200.
- Jeong, H. J., Yoo, Y. D., Kim, J. S., Seong, K. A., Kang, N. S., and Kim, T. H., 2010, Growth, Feeding and Ecological Roles of the Mixotrophic and Heterotrophic Dinoflagellates in Marine Planktonic Food Webs: *Ocean Science Journal*, v. 45, p. 65-91.
- Jickells, T. D., An, Z. S., Andersen, K. K., Baker, A. R., Bergametti, G., Brooks, N., Cao, J. J., Boyd, P. W., Duce, R. A., Hunter, K. A., Kawahata, H., Kubilay, N., LaRoche, J., Liss, P. S., Mahowald, N., Prospero, J. M., Ridgwell, A. J., Tegen, I., and Torres, R., 2005, Global Iron Connections Between Desert Dust, Ocean Biogeochemistry, and Climate: *Science*, v. 308, no. 5718, p. 67-71.
- Joyce, T. M., and Patterson, S. L., 1977, Cyclonic Ring formation at the Antarctic Polar Front in the Drake Passage: *Nature*, v. 256, p. 131-133.
- Klaas, C., 1997, Distribution and role of microprotozoa in the Southern Ocean [Dissertation]: Bremen Univ., Bremen (FRG), Fachber. Biologie/Chemie, 119 p.
- Klaas, C., 2001, Spring distribution of larger (>64 µm) protozoans in the Atlantic sector of the Southern Ocean: *Deep-Sea Research I*, v. 48, no. 7, p. 1627-1649.
- Kolber, Z. S., Barber, R. T., Coale, K. H., Fitzwater, S. E., Greene, R. M., Johnson, K. S., Lindley, S., and Falkowski, P. G., 1994, Iron limitation of phytoplankton photosynthesis in the Equatorial Pacific Ocean: *Nature*, v. 371, no. 6493, p. 145-149.
- Krainer, K.-H., and Foissner, W., 1990, Revision of the genus *Askenasia* Blochmann, 1895, with proposal of two new species, and description of *Rhabdoaskenasia minima* n. g., n. sp. (Cilophora, Cyclotrichida). *Journal of Protozooplankton*, v. 37, p. 414-427.
- Kudela, R., Pitcher, G., Probyn, T., Figueiridas, F., Moita, T., and Trainer, V., 2005, Harmful algal blooms in coastal upwelling systems: *Oceanography*, v. 18, no. 2, p. 185-197.
- Lampitt, R., Salter, I., and John, D., 2009, Radiolaria: major exporters of organic carbon to the deep ocean.: *Global Biogeochem Cycles*, v. 23, no. GB1010.

- Landry, M., Constantinou, J., Latasa, M., Brown, S., Bidigare, R., and Ondrusek, M., 2000a, Biological response to iron fertilization in the eastern equatorial Pacific (IronEx II). 3. Dynamics of phytoplankton growth and microzooplankton grazing.: *Marine Ecology Progress Series*, v. 201, p. 57-72.
- Landry, M., Ondrusek, M., Tanner, S., Brown, S., Constantinou, J., Bidigare, R., Coale, K., and Fitzwater, S. E., 2000b, Biological response to iron fertilization in the eastern equatorial Pacific (IronEx II). 1. Microplankton community abundances and biomass.: *Marine Ecology Progress Series*, v. 201, p. 17-42.
- Law, C., Smith, M., Stevens, C., Abraham, E., Ellwood, M., Hill, P., Nodder, S., Peloquin, J., Pickmere, S., Safi, K., and Walkington, M., 2011, Did dilution limit the phytoplankton response to iron addition in HNLCLSi Sub-Antartic waters during SAGE?: *Deep Sea Research Part II: Topical Studies in Oceanography*, v. 58 (6), p. 786-799.
- Lea, D. W., 2003, Elemental and Isotopic Proxies of Past Ocean Temperatures. In: Holland, Heinrich D., Turekian, Karl K. (Eds.): *Treatise on Geochemistry*. Pergamon, Oxford, no. 6.14, p. 365-390.
- Legechis, R., 1977, Oceanic Polar Front in the Drake Passage: satellite observations during 1976: *Deep Sea Research* v. 24, p. 701-704.
- Löbl, M., Cockshutt, A. M., Campbell, D., and Finkel, Z. V., 2010, Physiological basis for high resistance to photoinhibition under nitrogen depletion in *Emiliania huxleyi*.: *Limnology and Oceanography*, v. 55, p. 2150-2160.
- Lovelock, J., 2003, *The living earth*: *Nature*, v. 426, p. 769-770.
- Lovelock, J. E., 1979, *Gaia. A new look at life on earth*.: Oxford University Press, Oxford.
- Lund, J. W. G., Kipling, C., and Le Cren, E. D., 1958, The Inverted Microscope Method of Estimating Algal Numbers and the Statistical Basis of Estimations by Counting: *Hydrobiologia*, v. 11, p. 143-170.
- Maier-Reimer, E., Mikolajewicz, U., and Winguth, A., 1996, Future ocean uptake of CO₂: interaction between ocean circulation and biology: *Climate Dynamics*, v. 12, p. 711-721.
- Manton, I., and Parke, M., 1960, Further observations on small green flagellates with special reference to possible relatives of *Chromulina pusilla* Butcher: *Journal of marine Biology Association UK*, no. 39, p. 275-298.
- Martin, J. H., 1990, Glacial-interglacial CO₂ change: The iron hypothesis: *Paleoceanography*, v. 5, no. 1, p. 1-13.
- Martin, J. H., Coale, K. H., Johnson, K. S., Fitzwater, S. E., Gordon, R. M., Tanner, S. J., Hunter, C. N., Elrod, V. A., Nowicki, J. L., Coley, T. L., Barber, R. T., Lindley, S., Watson, A. J., Van Scoy, K., and Law, C. S., 1994, Testing the iron hypothesis in ecosystems of the Equatorial Pacific Ocean: *Nature*, v. 371, no. 6493, p. 123-129.
- Martin, J. H., and Fitzwater, S. E., 1988, Iron deficiency limits phytoplankton growth in the north-east Pacific subarctic: *Nature*, v. 331, p. 341-343.
- Martin, J. H., Fitzwater, S. E., and Gordon, R. M., 1991, We still say iron deficiency limits phytoplankton growth in the subarctic Pacific: *Journal of Geophysical Research. C. Oceans*, v. 96, no. C11, p. 6.
- Martin, P., Allen, J. T., Cooper, M. J., Johns, D. G., Lampitt, R. S., Sanders, R., and Teagle, D. A. H., 2010, Sedimentation of acantharian cysts in the Iceland Basin: Strontium as a ballast for deep ocean particle flux, and implications for acantharian reproductive strategies: *Limnology and Oceanography*, v. 55, no. 2, p. 604-614.
- Martin, P., Rutgers van der Loeff, M., Cassar, N., Vandromme, P., d'Ovidio, F., Stemmann, L., Rengarajan, R., Soares, M., González, H. E., Ebersbach, F., Lampitt, R. S., Sanders, R., Barnett, B. A., Smetacek, S., and Naqvi, S. W. A., 2013, Iron fertilization enhanced net community production but not downward particle flux during the

- Southern Ocean iron fertilization experiment LOHAFEX: *Global Biogeochemical Cycles*, v. 27.
- Menden-Deuer, S., and Lessard, E. J., 2000, Carbon to volume relationships for dinoflagellates, diatoms and other protist plankton: *Limnology and Oceanography*, v. 45, no. 3, p. 569-579.
- Mills, M. M., Ridame, C., Davey, M. S., La Roche, J., and Geider, R. J., 2004, Iron and phosphorus co-limit nitrogen fixation in the eastern tropical North Atlantic: *Nature*, v. 429, no. 7039, p. 292-294.
- Morel, F. M. M., Rueter, J. G., and Price, N. M., 1991, Iron nutrition of phytoplankton and its possible importance in the ecology of ocean regions with high nutrient low biomass: *Oceanography*, v. 4, p. 56-61.
- Morley, J. J., Shemesh, A., and Abelmann, A., 2013, Laboratory analysis of dissolution effects on Southern Ocean polycystine Radiolaria: *Marine Micropaleontology*.
- Müller, J., 1859, Einige neue Polycysten und Acanthometren des Mittelmeers.: *Physic abhandlungen der Königlicher Akademie der Wissenschaften aus der Jahre 1858*, Berlin, p. 1-62.
- Nauwerck, A., 1963, Die Beziehungen zwischen Zooplankton und Phytoplankton im See Erken. *Symp. Bot. Ups*, v. 17, no. 5, p. 1-63.
- Not, F., Latasa, M., Marie, D., Cariou, T., Vaultot, D., and Simon, N., 2004, A single species *Micromonas pusilla* (Prasinophyceae) dominates the eukaryotic picoplankton in the western English Channel.: *Applied Environmental Microbiology*, v. 70, p. 4064–4072.
- Not, F., Massana, R., Latasa, M., and al., e., 2005, Late summer community composition and abundance of photosynthetic picoeukaryotes in Norwegian and Barents: Seas. *Limnol Oceanogr*, v. 50, p. 1677–1686.
- Nöthig, E.-M., and Gowing, M. M., 1991, Late winter abundance and distribution of phaeodarian radiolarians, other large protozooplankton and copepod nauplii in the Weddell Sea, Antarctica.: *Marine biology*, v. 111, no. 3, p. 473-484.
- Orsi, A. H., T. Whitworth, W. D. Nowlin, 1995, On the meridional extent and fronts of the Antarctic Circumpolar Current: *Deep Sea Research Part I: Oceanographic Research Papers*, v. 42, p. 641–673.
- Parsons, T. R., and Whitney, F. A., 2012, Did volcanic ash from Mt.Kasatoshi in 2008 contribute to a phenomenal increase in Fraser River sockeye salmon (*Oncorhynchus nerka*) in 2010?: *Fisheries Oceanography*, v. 21, no. 5, p. 374-377.
- Pastoureaud, A., Dupuy, Chrétiennot-Dinet, M. J., Lantoine, F., and Loret, P., 2003, Red coloration of oysters along the French Atlantic coast during the 1998 winter season: Implication of nanoplanktonic cryptophytes: *Aquaculture*, v. 228, p. 225-235.
- Pedros-Alió, C., Massana, R., Latasa, M., García-Cantizano, J., and Gasol, J. M., 1995, Predation by ciliates on a metalimnetic *Cryptomonas* population – feeding rates, impact and effects of vertical migration.: *Journal of Plankton Research*, v. 17, p. 2131-2154.
- Peloquin, J., Hall, J., Safi, K., Smith, W. O., Wright, S., and van den Enden, R., 2011, The response of phytoplankton to iron enrichment in Sub-Antarctic HNLCLS waters: Results from the SAGE experiment: *Deep-Sea Research Part II-Topical Studies in Oceanography*, v. 58, no. 6, p. 808-823.
- Petit, J. R., et al., 1997, Four climatic cycles in Vostok ice core: *Nature*, v. 387, p. 359–360.
- Petit, J. R., Jouzel, J., Raynaud, D., Barkov, N. I., Barnola, J. M., Basile, I., Bender, M., Chappellaz, J., Davis, M., Delaygue, G., Delmotte, M., Kotiyakov, V. M., Legrand, M., and Stievenard, M., 1999, Climate and atmospheric history of the past 420,000 years from the Vostok ice core, Antarctica: *Nature*, v. 399, no. 6735, p. 429-436.

- Pollard, R., Sanders, R., Lucas, M., and Statham, P., 2007, The crozet natural iron bloom and EXport experiment (CROZEX): Deep-Sea Research Part II-Topical Studies in Oceanography, v. 54, no. 18-20, p. 1905-1914.
- Pollard, R. L., MI; Read, JF, 2002, Physical controls on biogeochemical zonation in the Southern Ocean: DEEP SEA RESEARCH -PART 2-, v. 49, no. 16, p. 3289-3305.
- Pollard, R. T., Salter, I., Sanders, R. J., Lucas, M. I., Moore, C., Mills, R. A., Statham, P. J., Allen, J. T., Baker, A. R., Bakker, D. C. E., Charette, M. A., Fielding, S., Fones, G. R., French, M., Hickman, A. E., Holland, R. J., Hughes, J., Jickells, T. D., Lampitt, R. S., Morris, P. J., Nedelec, F. H., Nielsdottir, M., Planquette, H., Popova, E. E., Poulton, A. J., Read, J. F., Seeyave, S., Smith, T., Stinchcombe, M., Taylor, S., Thomalla, S., Venables, H. J., Williamson, R., and Zubkov, M. V., 2009, Southern Ocean deep-water carbon export enhanced by natural iron fertilization: Nature, v. 457, no. 7229, p. 577-580.
- Raiswell, R., Benning, L. G., Tranter, M., and Tulaczyk, S., 2008, Bioavailable iron in the Southern Ocean: the significance of the iceberg conveyor belt: Geochemical Transactions, v. 9.
- Riegman, R., Stolte, W., Noordeloos, A. A. M., and Slezak, D., 2000, Nutrient uptake and alkaline phosphatase (ec 3:1:3:1) activity of emiliana huxleyi (prymnesiophyceae) during growth under n and p limitation in continuous cultures: Journal of Phycology, v. 36, no. 1, p. 87-96.
- Rintoul, S. R., 1998, On the origin and influence of Ad'elie Land Bottom Water in Ocean, ice and Atmosphere: Interactions at the Antarctic Continental Margin Antarctic Reserach Series edited by S. S. Jacobs and R. F. Weiss AGU, Washington, D.C, v. 75, p. 151-171.
- Rohling, E. J., 2000, Paleosalinity: confidence limits and future applications. : Marine Geology, v. 163, no. (1-4), p. 1-11.
- Ronaghi, M., S. Karamohamed, B. Pettersson, M. Uhlén, a., and Nyrén, P., 1996, Real-Time DNA sequencing using Detection of pyrophosphate release.: Analyt. Biochem., v. 242, p. 84-89.
- Sarmiento JL, R. M., C. LQ, 1995, Air-sea CO₂ transfer and the carbon budget of the North Atlantic: Philos T Roy Soc B, v. 348, p. 211-219.
- Sarnthein, M., Winn, K., and Zahn, R., 1987, Paleoproductivity of oceanic upwelling and the effect of atmospheric CO₂ and climatic change during deglaciation times: in Abrupt climatic change: Evidence and implication, edited by W.H. Berger and L.D. Labeyrie, v. Reidel Dordrecht, p. 311-337.
- Scharek, R., van Leeuwe, M. A., and De Baar, H. J. W., 1997, Responses of Southern Ocean phytoplankton to the addition of trace metals: Deep-Sea Research II, v. 44, no. 1-2, p. 209-227.
- Sciermammano, F. J., 1989, Observations of Antractic Polar Front motions in a deep water expression: Journal of Physical Oceanography, v. 9, p. 221-226.
- Sherr, E. B., and Sherr, B. F., 2002, Significance of predation by protists in aquatic microbial food webs: Antonie Van Leeuwenhoek; International Journal Gen. Molecular Microbiology, v. 81, no. (1-4), p. 293-308.
- Siegenthaler, U., Stocker, T. F., Monnin, E., Lüthi, D., Schwander, J., Stauffer, B., Raynaud, D., Barnola, J.-M., Fischer, H., Masson-Delmotte, V., and J., J., 2005, Stable Carbon Cycle-Climate Relationship During the Late Pleistocene: Science, v. 310 (5752), p. 1313-1317.
- Smetacek, V., 1981, The Annual Cycle of Protozooplankton in the Kiel Bight.: Marine biology, v. 63, no. 1, p. 1-11.
- , 1985, Role of sinking in diatom life-history cycles: ecological, evolutionary and geological significance: Marine Biology, v. 84, p. 239-251.

- Smetacek, V., Klaas, C., Strass, V. H., Montresor, M., Cisewski, B., Savoye, N., Webb, A., d'Ovidio, F., Arrieta, J. M., Bathmann, U., Bellerby, R., Berg, M. G., Croot, P., Gonzalez, S., Henjes, J., Herndl, G. J., Hoffmann, L. J., Leach, H., Losch, M., Mills, M. M., Neill, C., Peeken, I., Röttgers, R., Sachs, O., Sauter, E., Schmidt, M. M., Schwarz, J., Terbrüggen, A., and Wolf-Gladrow, D., 2012, Deep carbon export from a Southern Ocean iron-fertilized diatom bloom: *Nature*, v. 487, p. 313–319.
- Smetacek, V., and Naqvi, S. W. A., 2008, The next generation of iron fertilization experiments in the Southern Ocean: *Philosophical Transactions of the Royal Society a-Mathematical Physical and Engineering Sciences*, v. 366, no. 1882, p. 3947-3967.
- Smetacek, V., Naqvi, S. W. A., and et al., 2010, The Expedition of the Research Vessel "Polarstern" to the Antarctic in 2009 (ANT-XXV/3 - LOHAFEX): *Reports on Polar and Marine Research*, v. 613.
- Smetacek, V., Scharek, R., and Nöthig, E.-M., 1990, Seasonal and regional variation in the pelagial and its relationship to the life history cycle of krill, *in* Kerry, K. R., and Hempel, G., eds., *Antarctic ecosystems. Ecological change and conservation*: Berlin Heidelberg, Springer-Verlag, p. 103-114.
- Spero, H. J., Bijma, J., Lea, D. W., and Bemis, B. E., 1997, Effect of seawater carbonate concentration on foraminiferal carbon and oxygen isotopes.: *Nature*, v. 390, no. 6659, p. 497–500.
- Spivack, A. J., You, C. F., and Smith, H. J., 1993, Foraminiferal boron isotope ratios as a proxy for surface ocean pH over the past 21-Myr.: *Nature*, v. 363, no. 6425, p. 149–151.
- Stefels, J., 2000, Physiological aspects of the production and conversion of DMSP in marine algae and higher plants: *Journal of Sea Research*, v. 43, p. 183-197.
- Sullivan, C. W., Arrigo, K. R., McClain, C. R., Comiso, J. C., and Firestone, J., 1993, Distributions of phytoplankton blooms in the Southern Ocean: *Science (Washington)*, v. 262, no. 5141, p. 1832-1837.
- Sunda, W. G., and Huntsman, S. A., 1995, Iron uptake and growth limitation in oceanic and coastal phytoplankton: *Marine Chemistry The Chemistry of Iron in Seawater and its Interaction with Phytoplankton*, v. 50, no. 1-4, p. 189-206.
- Swanberg, N. R., 1983, The trophic role of colonial radiolaria in oligotrophic oceanic environments: *Limnology and Oceanography*, v. 28, no. 4, p. 655-666.
- Takahashi, K., Hurd, D. C., and Honjo, S., 1983, Phaeodarian skeletons: Their role in silica transport to the deep sea: *Science*, v. 222, no. 4624, p. 616-618.
- Takahashi, K., and Ling, H. Y., 1984, Particle selectivity of pelagic tintinnid agglutination: *Marine Micropaleontology*, v. 9, p. 87-92.
- Takeda, S., 1998, Influence of iron availability on nutrient consumption ratio of diatoms in oceanic waters: *Nature*, v. 393, no. 6687, p. 774-777.
- Taylor, F. J. R., Hoppenrath, M., and Saldarriaga, J. F., 2008, Dinoflagellate diversity and distribution: *Biodiversity Conservation*, v. 17, no. Special Issue: Protist diversity and geographic distribution. Guest editor: W. Foissner., p. 407-418.
- Thiele, S., Fuchs, B. M., and Amann, R., 2011, Identification of Microorganisms Using the Ribosomal RNA Approach and Fluorescence In situ Hybridization: *in* Peter Wilderer (ed.) *Treatise on Water Science Academic Press, Oxford (UK)*. v. 3, p. 171-189.
- Thronsen, J., 1995, Chapter "Estimating cell numbers: *In: Manual on Harmful Marine Microalgae*. (eds. Hallegraeff, G. M., Anderson, D. M. & Cembella, A. D.) v. 33, no. UNESCO, Paris., p. 63–80.
- Thronsen, J., and Kristiansen, S., 1991, *Micromonas pusilla* (Prasinophyceae) as part of the pico- and nanoplankton communities of the Barents Sea: *Polar Research*, v. 10, p. 201-207.

- Timothy, D. A., Wong, C. S., Nojiri, Y., Ianson, D. C., and Whitney, F. A., 2006, The effects of patch expansion on budgets of C, N and Si for the Subarctic Ecosystem Response to Iron Enrichment Study (SERIES): Deep Sea Research Part II: Topical Studies in Oceanography Canadian SOLAS: Subarctic Ecosystem Response to Iron Enrichment (SERIES), v. 53, no. 20-22, p. 2034-2052.
- Tirok, K., and Gaedke, U., 2007, Regulation of planktonic ciliate dynamics and functional composition during spring in Lake Constance.: Aquatic Microbial Ecology, no. 49, p. 87-100.
- Tomas, C. R., 1997, Identifying Marine Phytoplankton: Elsevier Science Oxford, UK, Academic Press.
- Tréguer, P., Nelson, D. M., Van Benkom, A. J., DeMaster, D. J., Leynaert, A., and Quéguiner, B., 1995, The silica balance in the world ocean: a reestimate: Science, v. 268, p. 375-379.
- Trull, T., and Armand, L., 2001, Insights into Southern Ocean carbon export from the delta ^{13}C of particles and dissolved inorganic carbon during the SOIREE iron release experiment: Deep-Sea Research II, v. 48, no. 11-12, p. 2655-2680.
- Trull, T. W., Bray, S. G., Manganini, S. J., Honjo, S., and Francois, R., 2001, Moored sediment trap measurements of carbon export in the Subantarctic and Polar Frontal Zones of the Southern Ocean, south of Australia: J. of Geophysical Research, v. 106, no. C12, p. 31,489-431,509.
- Tsuda, A., Kiyosawa, H., Kuwata, A., Mochizuki, M., Shiga, N., Saito, H., Chiba, S., Imai, K., Nishioka, J., and Ono, T., 2005, Responses of diatoms to iron-enrichment (SEEDS) in the western subarctic Pacific, temporal and spatial comparisons: Progress In Oceanography, v. 64, no. 2-4, p. 189-205.
- Tsuda, A., Takeda, S., Saito, H., Nishioka, J., Kudo, I., Nojiri, Y., Suzuki, K., Uematsu, M., Wells, M. L., Tsumune, D., Yoshimura, T., Aono, T., Aramaki, T., Cochlan, W. P., Hayakawa, M., Imai, K., Isada, T., Iwamoto, Y., Johnson, W. K., Kameyama, S., Kato, S., Kiyosawa, H., Kondo, Y., Levasseur, M., Machida, R. J., Nagao, I., Nakagawa, F., Nakanish, T., Nakatsuka, S., Narita, A., Noiri, Y., Obata, H., Ogawa, H., Oguma, K., Ono, T., Sakuragi, T., Sasakawa, M., Sato, M., Shimamoto, A., Takata, H., Trick, C. G., Watanabe, Y. W., Wong, C. S., and Yoshie, N., 2007, Evidence for the grazing hypothesis: Grazing reduces phytoplankton responses of the HNLC ecosystem to iron enrichment in the western subarctic Pacific (SEEDS II): Journal of Oceanography, v. 63, no. 6, p. 983-994.
- Tsuda, A., Takeda, S., Saito, H., Nishioka, J., Nojiri, Y., Kudo, I., Kiyosawa, H., Shiimoto, A., Imai, K., Ono, T., Shimamoto, A., Tsumune, D., Yoshimura, T., Aono, T., Hinuma, A., Kinugasa, M., Suzuki, K., Sohrin, Y., Noiri, Y., Tani, H., Deguchi, Y., Tsurushima, N., Ogawa, H., Fukami, K., Kuma, K., and Saino, T., 2003, A Mesoscale Iron Enrichment in the Western Subarctic Pacific Induces a Large Centric Diatom Bloom: Science, v. 300, no. 5621, p. 958-961.
- Turner, S. M., Harvey, M. J., Law, C. S., Nightingale, P. D., and Liss, P. S., 2004, Iron induced changes in oceanic sulfur biogeochemistry: Geophysical Research Letter, v. 31.
- Utermöhl, H., 1958, Zur Vervollkommnung der quantitativen Phytoplankton-Methodik: Mitt. Int. Ver. Limnol., v. 9, p. 1-38.
- Vaulot, D., Eikrem, W., Viprey, M., and Moreau, H., 2008, The diversity of small eukaryotic phytoplankton ($< 3 \mu\text{m}$) in marine ecosystems: Federation of European Microbiological Societies, v. 32, p. 795-820.
- Verity, P. G., and Smetacek, V., 1996, Organism life cycles, predation, and the structure of marine pelagic ecosystems: Marine Ecology Progress Series, v. 130, p. 277-293.

References

- Vesk, M., Dwarte, D., Fowler, S., and Hiller, R. G., 1992, Freeze fracture immunocytochemistry of light-harvesting pigment complexes in a cryptophyte.: *Protoplasma*, v. 170, p. 166-176.
- Volk, T., and Hoffert, M. I., 1985, Ocean carbon pumps: Analysis of relative strengths and efficiencies in ocean driven atmospheric CO₂ changes: in *The carbon cycle and atmospheric CO₂: natural variations, Archean to present*, v. edited by E. T. Sundquist and W. S. Broecker, no. Geophysical Monograph 32, American Geophysical Union., p. 99-110.
- Waite, A. M., and Nodder, S. D., 2001, The effect of *in situ* iron addition on the sinking rates and export flux of Southern Ocean diatoms: *Deep Sea Research Part II: Topical Studies in Oceanography*, v. 48, no. 11-12, p. 2635-2654.
- Wasik, A., Mikolajczyk, E., and Ligowski, R., 1996, Agglutinated loricae of some Baltic and Antarctic Tintinnina species (Ciliophora): *Journal of Plankton Research*, v. 18, no. 10, p. 1931-1940.
- Watson, A. J., Law, C. S., van Scoy, K. A., Millero, F. J., Yao, W., Friedrich, G. E., Liddicoat, M. I., Wanninkhof, R. H., Barber, R. T., and Coale, K. H., 1994, Minimal effect of iron fertilization on sea-surface carbon dioxide concentrations: *Nature*, v. 371, p. 143-145.
- Whitworth, T., 1983, Monitoring the transport of the Antarctic Circumpolar Current at Drake Passage: *Journal of Physical Oceanography*, v. 13, p. 2045–2057.
- Whitworth, T., and Nowlin, W. D., 1987, Water masses and currents of the Southern Ocean at the Greenwich Meridian: *Journal of Geophysical Research*, v. 92, p. 6462–6476.
- Whitworth, T., and Peterson, R. G., 1985, Volume transport of the Antarctic Circumpolar Current from bottom pressure measurements: *Journal of Physical Oceanography*, v. 15, p. 810–816.
- Xu, Y., Boucher, J. M., and Morel, F. M. M., 2010, Expression and diversity of alkaline phosphatase EHAP1 in *Emiliana huxleyi* (Prymnesiophyceae): *Journal of Phycology*, v. 46, p. 85-92.
- Zeebe, R., and Wolf-Gladrow, D., 2007, *CO₂ in seawater: equilibrium, kinetics, isotopes*: Elsevier Science B.V., Amsterdam.
- Zielinski, U., and Gersonde, R., 1997, Diatom distribution in Southern Ocean surface sediments (Atlantic sector): implications for paleoenvironmental reconstructions: *Palaeogeography, Palaeoclimatology, Palaeoecology*, v. 129, no. 3-4, p. 213-250.

Acknowledgements

First of all and especially, I would like to thank my supervisor Prof. Dr. Victor Smetacek for the opportunity to work on such an intriguing topic and for his supervision of the thesis. Through his vivid tours in his garden or discussions in the office, my ecological understanding has deepened. His pictorial explanations were of great help to me to always consider the “big picture”. I thank him for his suggestions and comments which have enriched my work.

I would also like to thank Prof. Dr. Kai Bischof, for his willingness to review my work.

This work was funded through the DFG- Research Center: MARUM- Center for Marine environmental Sciences, Bremen / Cluster of Excellence „The Ocean in the Earth System“. Within this framework I would like to thank GLOMAR – Bremen International Graduate School for Marine Sciences, University of Bremen, for numerous opportunities to further educate in valuable workshops and training for young scientists and for giving financial funding to attend international conferences and stays abroad.

I would like to highlight the support and supervision through Dr. Philipp Assmy, without him I would not be where I am now. Even though the supervision was difficult considering the distance from Tromsø to Bremen, he was always available and tried to give advice and assistance whenever he could. Philipp you were of great support to me, especially through many e-mails, skype conferences, where you appeased and encouraged me, thank you! I hope we stay in contact.

I would like to thank the employees of the Alfred Wegener Institute for their support in every way: Dr. Christine Klaas, Dr. Claudia Hanfland, Dr. Sara Besteri, Sina Wolzenburg, Friederike Ebersbach, Nina Keul, Nike Fuchs, Dr. Sandra Heinrich. Especially last three, for their great support and encouragement in the last months, while finishing the thesis.

I would also like to thank for the cooperation with the staff of the Stazione Zoologica Anton Dohrn in Naples, Italy. My special thanks go to Dr. Grazia Mazzocchi, Dr. Marina Montresor, Dr. Diana Sarno and Dr. Adriana Zingone, who supported me during my 3 months stay in Naples, wherever and whenever they could.

Acknowledgements

My thanks goes also to the members of the AWI cooking group; Nina Keul, Nike Fuchs, Dorothee Kottmeier, Clara Hoppe, Mirja Hoins, Meri Eichner, Judith Hauck and Ella Howes, who saved me from the canteen food and thus have made the lunch time a daily highlight.

Many thanks to all my dear friends, Julia, Linda, Henne, Britta, who accompany me for a lifetime and went with me through a lot of up and downs, but never have gone from my side. Thank you for your support and for always believing in me. Finally, I got the "Pokal"! ☺

Judith, Nike and Dominique you were my Bremen girls and you have brightened up my life here in the north in soo many ways. I really loved our girls-evenings with a lot of discussions (and champaign). Judith and Nike, I could call you whenever I needed to, I could be how I am. Nike you were a wonderful office mate, thanks for teaching me to be more communicative. You all have contributed to my self-confidence in many ways and to my encouragement in the last months.

Mama und Papa, es ist geschafft und ihr habt niemals daran gezweifelt. Eure Fürsorge und Zuversicht hat mich immer wieder angetrieben aber vor allem eure bedingungslose Liebe. Dafür möchte ich mich bei euch bedanken! Stets habt ihr mir beigebracht, wie wichtig es ist, sorgfältig und präzise zu arbeiten, ein wichtiges Merkmal für eine(n) WissenschaftlerIn. Auch dafür bin ich euch sehr dankbar, denn ohne diese Eigenschaft, ist eine Doktorarbeit nicht möglich. Es lebe mein „Horoskop“ ☺

Meine lieben Geschwister; Timo und Miriam (+Familie), euch gilt besonderer Dank, denn ohne eure motivierenden Worte und Unterstützung in den letzten Monaten, hätte ich so manches Mal den Mut verloren. Euer Rückhalt bedeutet mir immer viel. Auf euch kann ich zählen, in jeder Lebenslage. Vielen Dank!

Name: Isabelle Katharina Schulz..... Ort, Datum.....

Anschrift: Kulenkampffallee 144, 28213 Bremen.....

ERKLÄRUNG

Hiermit erkläre ich, dass ich die Arbeit mit dem Titel:

“Mechanisms determining species succession and dominance during an
iron-induced Phytoplankton bloom in the Southern Ocean (LOHAFEX)“

selbstständig verfasst und geschrieben habe und außer den angegebenen Quellen keine weiteren Hilfsmittel verwendet habe.

Ebenfalls erkläre ich hiermit eidesstattlich, dass es sich bei den von mir abgegebenen Arbeiten um 3 identische Exemplare handelt.

.....
(Unterschrift)